UNIVERSITÉ DE NEUCHÂTEL

The functions of RMR proteins in the *Physcomitrella patens* secretory pathway

A dissertation submitted to the University of Neuchâtel

For the degree of Doctor in Sciences by

Noémie FAHR

Institute of Biology - Laboratory of Cell and Molecular Biology

Accepted on the recommendation of

Prof. Jean-Marc NEUHAUS, thesis director, University of Neuchâtel, CH

Dr. Sébastien THOMINE, CNRS – Gif-sur-Yvette, FR

Dr. Shanmugabalaji VENKATASALAM, University of Neuchâtel, CH

Dr. Didier SCHAEFER, University of Neuchâtel, CH

Thesis defended on the 29th of August 2017

UNIVERSITÉ DE NEUCHÂTEL

Faculté des Sciences
Secrétariat-décanat de Faculté
Rue Emile-Argand 11
2000 Neuchâtel – Suisse
Tél : + 41 (0)32 718 21 00
E-mail : secretariat.sciences@unine.ch

IMPRIMATUR POUR THESE DE DOCTORAT

La Faculté des sciences de l'Université de Neuchâtel autorise l'impression de la présente thèse soutenue par

Madame Noémie FAHR

Titre:

"Function of RMR proteins in *Physcomitrella patens* secretory pathway"

sur le rapport des membres du jury composé comme suit:

- Prof. Jean-Marc Neuhaus, directeur de thèse, UniNE
- Dr Shanmugabalaji Venkatasalam, UniNE
- Dr Didier Schaerer, UniNE
- Dr Sébastien Thomine, CNRS, Paris-Saclay, France

Neuchâtel, le 11 septembre 2017 Le Doyen, Prof. R. Bshary

Keywords: Vacuole, RMR, Vacuolar Sorting Determinant, *Physcomitrella patens*, E3 ligase, Confocal microscopy

Mots-clés: Vacuole, RMR, Déterminant d'adressage vacuolaire, *Physcomitrella patens*, E3 ligase, Microscopie confocale

Table of Contents

Abstract **13**

Résumé **15**

List of abbreviations **17**

Chapter 1 General Introduction **21**

A. Generalities about the plant secretory pathway and the endomembrane system **21**

A.1 Early secretory pathway 22

A.2 Late secretory pathway 30

A.3 Vesicular traffic 32

A.4 Endocytosis 35

A.5. Protein secretion 38

B. Vacuole types and protein targeting to vacuole **39**

B.1 Vacuole types 39

B.2.Vacuolar sorting determinants 40

B.3 Vacuolar sorting receptors in plant cells 41

The VSR family 41

The RMR family 43

Protease-Associated domain 45

C. C-terminal VSD used in this work **46**

C.1 Ct-VSD of tobacco Chitinase A 46

C.2 Ct-VSD of barley lectin (BL) 46

C.3 Ct-VSD of Phaseolin 47

C.4. Ct-VSD and PSI of Cardosins 47

Generalities about Aspartic proteinases (APs) 47

Plant APs 48

Plant AP domain structure 48

Cardosin A 48

Cardosin B 49

C.5 Ct-VSD and PSI of moss Aspartic proteinase 49

D. RMR homologues **50**

D.1 GRAIL (mammals) 51
D.2 Goliath and Godzilla 52
D.3 RING Finger protein 13 52
D.4 Other PA-TM-RING proteins 53
E. RMR proteins and ubiquitylation activity: a key role for the RING domain? 54
E.1 Ubiquitylation mechanism 54
E.2 Different ubiquitin tags for diverse purposes 56
E.3 RING domain and ubiquitylation: the E3 ligases family 57
RING E3 ligases 57
HECT E3 ligases 58
U-box E3 ligases 59
F. The moss *Physcomitrella patens* 60
F.1 *P. patens* as an experimental model 60
F.1.a Life cycle 60
F.1.b Genome 62
F.1.c Homologous recombination and gene targeting in *P. patens* 63
F.1.d RNAi in moss 64
F.1.e Abiotic stress tolerance in moss 65
F.2 The moss vacuole 65
F.2.a Different kind of vacuoles 65
F.2.b Vacuole structure and dynamics 66
F.3 Quintuple RMR Knock-Out lines 67
G. Aim of this thesis 68

Chapter 2

Study of the secretory system in moss: fluorescent reporters library 69

A. General secretory system markers 70
A.1 Reporter for the endoplasmic reticulum 70
A.2 Reporter for the acidic vacuole 72
A.3 Secreted reporter 74
A.3.a Citrine with just a signal peptide 74
A.3.b Secreted chitinase from *P. patens* 76
B. Reporters for the neutral vacuole (ctVSD) 78
B.1 CtVSD of tobacco chitinase A 78

B.2 CtVSD of cardosin A 78
B.3 CtVSD of moss aspartic proteinase 1 81
C. Plant Specific Insert reporters 83
C.1 PSI domain from Cardosin A 83
C.2 PSI domain of the cardosin B 83
D. Discussion 86

Chapter 3

Characterization of RMR Knock-out mutants 89

A. Phenotypic characterization of RMR mutants with fluorescent reporters 90
A.1 CtVSD reporters 90
A.1.a CtVSD of tobacco chitinase I 90
A.1.b CtVSD of cardosin A 91
A.1.c CtVSD of PpAP1 95
A.2 PSI reporters 96
A.2.a PSI from cardosin A 96
A.2.b PSI domain from cardosin B 96
A.3 Further vacuolar markers 99
A.3.a Secreted Citrine (*SP-Citrine*) 99
A.3.b Acidic vacuole reporter 99
A.3.c Secreted moss chitinase 100
A.3.d ER-retained reporter 100
A.4 Discussion 102
B. Vacuolar routes studies: secretory pathway inhibitors effects 104
B.1 Results 105
B.2 Discussion 110
C. Localization of *Pp*RMR2 111
C.1 *Pp*RMR2 localization in *Physcomitrella patens* 113
C.1.a Preliminary observations 113
C.1.b Control of transgene insertion and expression 114
C.2 Proteasome inhibitors 116
C.3 Discussion 118
D. Phenotypic study of RMR mutants 119
D.1 Results 119

D.2 Discussion 122

Chapter 4

Identification of RMR2 partners: clues to the role of RMRs in moss? 123

1. Pull-down assay using a GST fusion protein 123
2. Results 125
3. Discussion 127

Chapter 5 General discussion and perspectives 129

1. The moss secretory pathway 129
2. Are RMRs vacuolar receptors? 131
3. Are RMRs E3 ubiquitin ligases? 133

Chapter 6 Material and methods.....137

A. Material 137

A.1 Plant material 137

A.2 Bacterial strains 138

B. Methods related to bacteria.....138

B.1 E. Coli Transformation by heat-shock 138

B.2 Preparation of XL-1 competent cells 138

B.3 Plasmid DNA extraction: miniprep 139

C. Methods related to plants.....140

C.1 Protoplasts isolation and transformation 140

Protoplasts isolation 140

Protoplasts transformation by PEG 140

C.2 Heat-shock on protonema for protein expression 141

C.3 Secretory pathway inhibitors treatment 141

C.4 Proteasome II inhibitor treatment 141

D. Molecular biology.....142

D.1 PCR 142

D.2 DNA digestion 142

D.3 DNA precipitation 142

D.4 Genomic DNA extraction 142

D.5 DNA electrophoresis 143
D.6 DNA extraction from agarose gel 143
D.7 DNA fragment ligation in a plasmid 143
D.8 Extraction of total RNA from *P. patens* 144
D.9 Reverse transcription: synthesis of cDNA 144
E. Methods related to proteins 144
E.1 Moss total proteins extraction in SB buffer 144
E.2 SDS-PAGE 144
E.3 Western blot 145
E.4 Colloidal Coomassie blue staining 146
E.5 Production of GST-RMR recombinant proteins in BL-21 strain 146
E.6 Pull-down assay 147
F. Microscopy 147
Confocal microscopy 147

Acknowledgements 149

Annexes 151
1. Primers 151
2. Vectors and constructs 153
2.a Cloning vectors 153
2.b Cloning strategies 153
3. Vector maps 154

References 161

Abstract

Plant vacuoles play a wide range of functions within the cell, from the maintenance of turgor pressure and rigidity, to the storage or degradation of various molecules. Two types of vacuoles with distinct pH can coexist in the same single cell. Acidic vacuoles can be considered as homologues to animal lysosomes while neutral vacuoles are involved in proteins and secondary metabolites storage. Targeting of proteins to the lytic vacuole has been extensively studied and the vacuolar receptors involved, the VSRs, are now well characterized in higher plants. However, less is known about the traffic of proteins to the neutral/storage vacuole. RMR proteins are thought to be vacuolar receptors for the neutral/storage vacuole. However, the complete deletion of the five RMR genes in *Physcomitrella patens* did not lead to any developmental phenotype. This work aimed to investigate the role of RMR proteins in the moss.

In the first chapter, we review the plant secretory pathway system and how proteins are targeted to vacuoles.

In the second chapter, we studied the moss secretory pathway by developing a fluorescent reporter library. Several mechanisms seem to be conserved between the moss and the flowering plants.

In the third chapter, we focused on the characterization of the single and quintuple knock-out RMR mutants. We finally obtained a trafficking phenotype: the fluorescent reporter *Citrine-Card* was mistargeted in the single, triple and quintuple KO mutants. Fluorescent signal was detected in endoplasmic reticulum in the mutants, while it was observed in the central vacuole in WT. Trafficking to vacuole of a protein carrying this ctVSD was RMR-dependent.

In the last part of this thesis, we identified some putative binding partners of the cytosolic part of *Pp*RMR2 by GST pull-down assay and mass spectrometry analysis.

Résumé

Chez les plantes, les vacuoles occupent un grand nombre de fonctions, allant du maintien de la pression de turgescence et de la rigidité cellulaire en passant par le stockage ou la dégradation de diverses molécules. Deux types de vacuoles ayant un pH distinct peuvent coexister au sein d'une même cellule. Les vacuoles acides sont considérées comme étant des homologues aux lysosomes présents dans les cellules animales, tandis que les vacuoles neutres sont impliquées dans le stockage de protéines et de métabolites secondaires. L'adressage des protéines à la vacuole lytique a été largement étudié et les récepteurs vacuolaires impliqués, les VSRs, sont des protéines bien caractérisées. À l'opposé, les connaissances sur l'adressage des protéines à la vacuole neutre ou de stockage sont moindres. Les protéines RMR sont très probablement les récepteurs vacuolaires impliqués, bien que la délétion des cinq gènes RMR chez *Physcomitrella patens* n'ait conduit à aucun phénotype visible. Ce travail a donc pour objectif l'élucidation du rôle des protéines RMR chez la mousse.

Dans le premier chapitre de cette thèse nous avons regroupé les principales données concernant le système sécrétoire et endomembranaire chez les plantes, et nous avons également documenté comment les protéines sont adressées aux vacuoles.

Dans le second chapitre, nous avons étudié le système sécrétoire de la mousse en développant une bibliothèque de marqueurs fluorescents. Différents mécanismes cellulaires semblent conservés entre les mousses et les plantes à fleurs.

Dans le troisième chapitre, nous nous sommes intéressés à la caractérisation des simples et quintuple knock-out mutants RMR. Nous avons finalement obtenu un phénotype de tri vacuolaire: un défaut d'adressage est observé avec le marqueur fluorescent *Citrine-Card* dans les simples, triple et quintuple KO mutants. Le signal fluorescent a été détecté dans le réticulum endoplasmique chez les mutants, tandis que la fluorescence est observée dans la vacuole centrale chez le WT. Cela montre que l'adressage à la vacuole d'une protéine comportant ce ctVSD est dépendant des RMRs.

Dans la dernière partie de ce travail, nous avons identifié des partenaires interagissant très probablement avec la partie cytosolique de *Pp*RMR2 par des analyses de GST pull-down et de spectrométrie de masse.

List of abbreviations

% (v/v)	mL / 100mL
% (w/v)	g / 100 mL
µg	microgram
µl	microliter
APs	Aspartic proteinases
ARF1	ADP-Ribosylation factor 1
ATP	Adenosine triphosphate
ATPase	Adenosine triphosphate hydrolase
A. thaliana	*Arabidopsis thaliana*
BFA	Brefeldin A
BiFC	Bimolecular fluorescence complementation
BiP	Binding immunoglobulin protein
BP-80	Binding protein of 80 kDa
CCV	Clathrin-coated vesicle
cDNA	Complementary DNA
CME	Clathrin-mediated endocytosis
COPI	Coat protein I
COPII	Coat protein II
CTPP	Carboxyl-terminal propeptide
ctVSD	C-terminal vacuolar sorting determinant
C-ter	C-terminal
DIP	Dark-induced protein
DMSO	Dimethyl sulfoxide
DNA	Deoxyribonucleic acid
DV	Dense vesicle
E. coli	*Escherichia coli*
EE	Early endosome
EDTA	Ethylenediaminetetraacetic acid
ER	Endoplasmic reticulum
ERAD	ER-associated protein degradation
ERES	ER-export sites
ESCRT	Endosomal sorting complex required for transport
GDP	Guanine diphosphate
GEF	Guanine exchange factor
GFP	Green fluorescent protein
Gly	Glycine
GRAIL	Gene related to anergy in lymphocytes
GREUL	Goliath Related E3 Ubiquitin Ligase 1
GST	Glutathione-S-transferase
GTP	Guanosine triphosphate
HECT	Homologous to the E6-AP carboxyl terminus
HR	Homologous recombination
HSP70	70 kilodalton Heat-shock protein
Ile	Isoleucine
IPTG	Isopropyl β-D-1-thiogalactopyranoside
IRT1	Iron regulated transporter 1

Kb	Kilobase
KDa	Kilodalton
KO	Knock-out
LE	Late endosome
Leu	Leucine
LSP	Leaderless secretory proteins
LV	Lytic vacuole
M	Molar
Mbp	Mega base pairs
mg	milligram
ml	milliliter
mM	milliMolar
mRNA	Messenger RNA
miRNA	Micro RNA
MVB	Multivesicular bodies
N. benthamiana	*Nicotiana benthamiana*
N. tabacum	*Nicotiana tabacum*
nm	Nanometer
nM	NanoMolar
NR	Neutral red
NV	Neutral vacuole
OD	Optical density
PA domain	Protease-associated domain
PAC	Precursor Accumulating Vesicles
PBS	Phosphate buffer saline
PCR	Polymerase chain reaction
PEG	Polyethylene glycol
PI3K	Phosphatidylinositol 3-kinases
PI4K	Phosphatidylinositol 4-kinases
PM	Plasma membrane
P. patens	*Physcomitrella patens*
PSI	Plant specific insert
PSV	Protein storage vacuole
psVSD	Physical structure vacuolar sorting determinant
PVC	Prevacuolar compartment
Rab	Ras-related in brain
RFP	Red fluorescent protein
RING	Really interesting new gene
RMR	Receptor-like membrane RING-H2
RNA	Ribonucleic acid
RNAse	Ribonuclease
siRNA	Small interfering RNA
RFN13	RING finger protein 13
SCAMP1	Secretory carrier membrane protein 1
SDS	Sodium dodecyl sulfate
SDS-PAGE	SDS-Polyacrylamide gel electrophoresis
SNARE	Soluble N-ethylmaleimide sensitive factor adaptor protein receptor
SP	Signal peptide
ssVSD	Sequence-specific vacuolar sorting determinant
SRP	Signal recognition particle
UPR	Unfolded protein response
TEMED	N, N, N’, N’-tetrramethylethylenediamine

TGN	*Trans*-Golgi network
TIP	Tonoplast intrinsic protein
TM	Transmembrane domain
UV	Ultraviolet
VAMP	Vesicle associated membrane protein
VSD	Vacuolar sorting determinant
VSR	Vacuolar sorting receptor
WT	Wild type
YFP	Yellow fluorescent protein

Chapter 1
General Introduction

A. Generalities about the plant secretory pathway and the endomembrane system

The plant endomembrane system consists of different organelles: the nuclear envelope, the endoplasmic reticulum (ER), the Golgi apparatus, the *trans*-Golgi Network (TGN), the pre-vacuolar compartment, the endosomes, the vacuoles and the plasma membrane. Some are directly connected by a maturation process while others are connected by trafficking vesicles. These different components collaborate for cargo molecule processing, packaging, transport and delivery to their residence site within the cell. Proteins are transported from the ER through the Golgi apparatus and then are directed to their final destination (plasma membrane, vacuole…) (Figure 1.1). The maintenance of this cellular compartmentation is primordial for the function of the plant cell. The secretory pathway plays a major role for the cell, because it is involved in cell interaction, differentiation and division, but also in various biotic and abiotic stress responses.

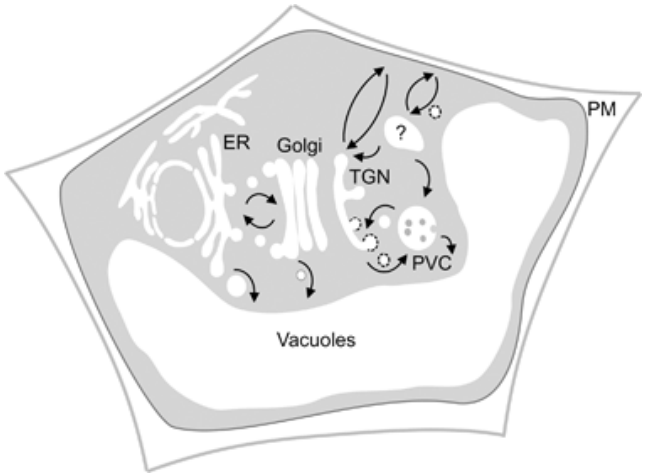

Figure 1.1 Simplified representation of the secretory pathway in plants (Foresti and Denecke, 2008)
Three routes of proteins trafficking to the vacuole have been described. First, via the classical route, proteins traffic through the ER, Golgi and TGN before reaching prevacuolar compartment. In the second route, cargoes bypass the Golgi and traffic to vacuole directly from the ER. The last route is a post-Golgi clathrin-mediated route from the TGN through the PVC.

A.1 Early secretory pathway

Endoplasmic Reticulum

Role of the ER

The endoplasmic reticulum (ER) is the first organelle in the secretory pathway and plays a central role in the cell. It is a multifunctional compartment, involved in protein synthesis and post-translational modifications, addition of N-linked oligosaccharides, formation of disulfide bonds, lipid biosynthesis but also in calcium storage (Hammond & Helenius, 1995). The traditional model of ER structure describes two main parts, both of which are present in all eukaryote cells: the rough ER (RER) and the smooth ER (SER). The RER membrane is associated with ribosomes and is partially continuous with the nuclear envelope whereas the smooth ER is composed of tubular structures without ribosomes. Recent studies showed the ER as a highly dynamic organelle, composed by a network of interconnected tubules. This structure can adapt in response to specific stimuli by morphological modifications and ER movements are driven by the cytoskeleton (Sparkes *et* al., 2011; Sparkes 2013). In plants, ER forms a continuous compartment between adjacent cells through plasmodesmata (Sparkes 2013) and it is closely associated with the actin cytoskeleton (Sparkes *et* al., 2009).

Translocon and Signal peptide

The entry of secretory proteins into the ER is usually linked with the presence of a signal peptide (SP) at the N-terminus of the protein. Import of soluble and membrane resident proteins into the ER occurs with the association of ribosomes and a protein pore called translocon. The SP is recognized and bound by a signal recognition particle (SRP), which interacts with the rough ER membrane, allowing the translocation of the polypeptide across the membrane through the translocon (Lütcke 1995; Hamman et al., 1998). Translocons form structurally and functionally dynamic aqueous pores in the ER membrane, and play a major role in the maintenance of the membrane permeability. The co-translational translocation of a nascent protein starts when the latest is still bound to the ribosome. The SRP binds at the same time the SP of the nascent protein and the 60S ribosome unit, causing a pause of the translocation process. This complex interacts then with the SRP receptor localized on the ER membrane, triggering the transfer of the peptide to the translocon. During the further translation and transfer to the ER lumen, the growing polypeptide is protected from cytosol exposition through the ribosome's alignment with the translocon pore (Lodish *et* al., 2008). The pore is open only when a peptide is being translocated, preventing ionic leakage between the cytosol and the ER lumen.

Removal of the SP occurs while the protein is translocated through the membrane and it is a major step contributing to correct folding of the protein (Nielsen et al, 1997; Vitale and Denecke 1999). The signal peptide is cleaved by a signal peptidase, a transmembrane protein associated with the translocon. Cleavage of the SP allows the protein release from the membrane and then its proper folding in the ER lumen (reviewed by Auclair *et* al., 2011).

ER quality control

Proteins are folded in the lumen of ER where glycosylation can also occur. At this step, the ER plays an important role in quality control whereby misfolded proteins are recognized and retained within the ER or directed to a degradation pathway (Hammond and Helenius 1995, Vitale and Denecke 1999). This quality control is primordial for the cell because it is involved in various stress responses and thus in plant adaptation to the environment (reviewed by Liu and Howell, 2010).

A misfolded protein can have three fates. Firstly, it may accumulate or aggregate in the lumen; secondly it may be targeted to the vacuole or the lysosome (in animals), where protein degradation occurs and thirdly it may be degraded in the cytosol by the proteasome machinery after re-exportation to the cytosolic face of the ER (Brodsky and McCracken 1999; Vashist and Ng 2004). How the cell determines which process to use and how misfolded protein are recognized is still unclear. In fact, a large percentage of ER-synthesized proteins are misfolded or unfolded, justifying the major role of the ER quality control: to avoid the dispatching of non-properly matured proteins to their final cellular compartments. Misfolded proteins are detected by various sensors, including the molecular chaperones. The main chaperone families of the ER are heat shock proteins (Hsp) including BiP (HSP70), the peptidyl-prolyl isomerases, the thiol-disulfide oxidoreductases, calnexin and calreticulin (reviewed by Ellgaard and Helenius, 2003).

ER Associated Degradation system (ERAD)

ERAD is a quality control system of the ER which clears the misfolded proteins from the ER through ubiquitylation. This cellular pathway plays an important role in cell homeostasis (reviewed by Ruggiano 2014). To date, most knowledge of this mechanism came from studies in yeast and mammals. Less is known about the plant ERAD system. This system involves an ubiquitin-proteasome system, where the substrate is ubiquitylated before degradation in the cytoplasm (Müller *et* al., 2005; reviewed by Liu and Li, 2014). Brandizzi *et* al. (2003) visualized a putative ERAD pathway using a GFP fusion protein recognized as misfolded by the cell, which was degraded after a retrograde translocation back to the cytosol. The ERAD system has also been shown to play a major role during salt stress in *Arabidopsis.* Ubiquitylated proteins are more abundant under these conditions. Consequently, an

Arabidopsis mutant line with a defective ERAD system (hrd3-a mutant) is more sensitive to salt stress than the wild-type line: seedlings are smaller and weaker (Liu *et* al., 2011).

Unfolded Protein Response

The Unfolded Protein Response (UPR) is an adaptive response from the cell to environmental and internal stresses. This intracellular signaling pathway is an essential part of the ER quality control and helps to reduce the misfolded and unfolded proteins accumulation (Liu and Kaufman 2003). UPR allows the re-establishment of cell homeostasis in order to decrease the ER stress, caused by various factors such as luminal calcium luminal depletion, hypoxia, pathogen infection or genetic mutation. This pathway involves different mechanisms that will cooperate to deal with the stress such as the induction of UPR genes, the decrease of global protein synthesis and the activation of the ERAD system (Fanata *et* al., 2013). Extended activation of the UPR pathway can lead to apoptotic cell death.

From the ER to the Golgi apparatus

Two classes of coat proteins, COPI and COPII, are involved in the transfer of proteins between the ER and the Golgi apparatus. This vesiculation is highly conserved within the eukaryotic domain. Proteins destined to the Golgi apparatus are exported from the ER by COPII-coated vesicles. The COPII vesicles bud off from specific sites of the ER membrane, the ER-exit sites (ERES; Barlowe *et* al., 1994; reviewed by Viotti, 2014). In the reverse direction, COPI-coated vesicles mediate a retrograde transport that selectively recycles mistargeted proteins (*e.g.* KDEL targeted proteins) from the **cis**-Golgi complex back to the ER (reviewed by Duden 2003).

COP vesicles

COPII: anterograde traffic

COPII vesicles mediate the transport of cargo from the ER to the *cis*-Golgi (Robinson *et* al., 2007). Their formation requires ER export sites (ERES) where the packaging of cargo into vesicles occurs. COPII complex formation occurs in several steps with protein interactions (Figure 1.2). First, the ER-membrane-resident GEF (guanine nucleotide exchange factor) protein Sec12 catalyzes the activation of the small GTPase Sar1, helping it to release GDP and to bind GTP. Once Sar1 is activated, it anchors into the ER membrane by insertion of its amphipathic N-terminal tail. Sar1 GTP drives the assembly of the cytosolic COPII subunits. The coat is formed by Sec23/Sec24 dimers forming an internal layer and completed with Sec13/Sec31 for the external scaffold layer. When the coat is achieved, the vesicle buds and is released from the ER donor membrane. Finally, the hydrolysis of Sar1-GTP is

triggered by Sec23, which leads to the disassembly of the COPII coat (Jürgen 2004; Hanton *et* al., 2009; Hwang and Robinson 2009; reviewed by Tang *et* al., 2005; Hugues and Stephens 2008).

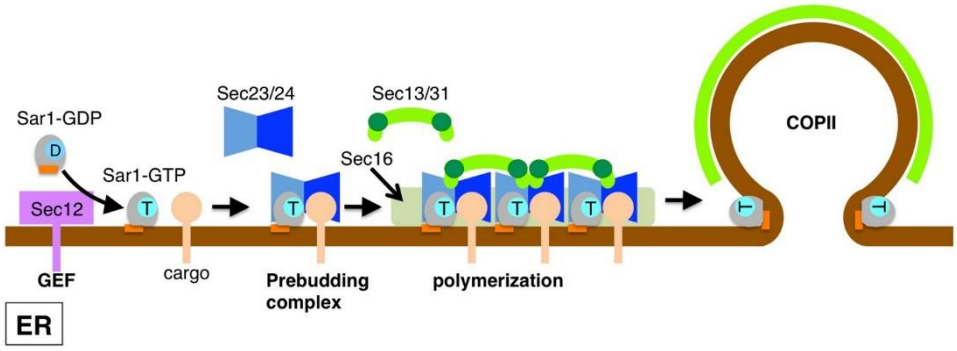

Figure 1.2 Mechanism of COPII coat assembly (adapted from Yorimitsu *et* al., 2014).
Vesicle formation starts upon the recruitment of Sar1 to the ER membrane. Then ER integral membrane protein Sec12 exchanges GDP for GTP bound to Sar1 through its GEF activity. Membrane-associated GTP-bound Sar1 recruits the inner coat Sec23/24 complex and then assembles along with cargo protein into the pre-budding complex. Outer coat Sec13/31 complexes are recruited to the pre-budding complexes and self-assembled. The polymerization of Sec13/31 by self-assembly drives membrane curvature to form a spherically shaped vesicle.

Mutations in gene coding for COPII components leads to developmental deficiencies in plants (reviewed by Chung *et* al., 2016) and interruption of the COPII-mediated transport has severe effects on protein traffic which can lead to cell death (Hanton *et* al., 2009).

COPI: retrograde traffic

COPI vesicles mediates recycling of proteins from Golgi to ER, in order to capture escaped ER resident proteins, and retrograde transport within the Golgi (from *trans* to *cis* cisternae; Pimpl *et* al., 2000). First studied in mammalian cells, they have been described in yeast and plant cells (reviewed by Hanton, 2005). They require a seven-subunit coat (named coatomer) and the GTPase ARF1 (Jürgens 2004). Assembly of the coat begins with the activation of ARF1 by the released of GDP and the binding of GTP catalyzed by an ARF-GEF (Figure 1.3). This activation leads to a direct interaction of ARF1 with the Golgi membrane. Activated and membrane-anchored ARF1 recruits the seven coatomer subunits from the cytosol. These subunits can be separated in two layers: the inner layer involved in cargo binding and membrane attachment, including ɣ, δ, ξ and βCOP; and the outer scaffold including α, β' and εCOP. The formation of the coat contributes to the capture of the cargo proteins and causes the curvature of the membrane. When the coat is totally formed, the vesicle buds. The uncoating of COPI

vesicle starts with GTP hydrolysis which triggers the dissociation of ARF1 from the vesicle membrane (Kirchhausen 2000; Beck 2009 and Barlowe 2013).

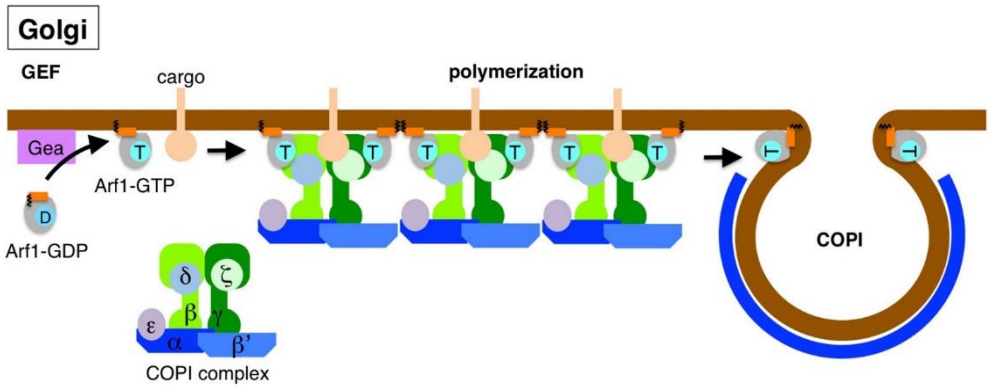

Figure 1.3 Mechanism of COPI coat assembly (adapted from Yorimitsu *et* al., 2014).
COPI vesicle formation is also initiated by GTP-GDP exchange on ARF1 through the action of the GEF Gea protein (Gea1 or Gea2), which is peripherally located on the Golgi membrane. GTP-bound ARF1 stably binds to the membrane by a myristoylated amphipathic helix. The heptamer complex of the COPI coat is recruited en bloc and associates with cargo as well as two ARF1 molecules though the inner layer coat complex (β/γ/δ/ζ-COP). As in COPII, vesicles are formed upon polymerization of the outercoat (α/β'/ε-COP). The amphipathic helix of ARF1 has some role in the scission of budded vesicles.

ER exit sites (ERES)

ERES are the sites of export for proteins to the Golgi, where COPII vesicles are forming. Their physical structure is still unclear but they have been described to be a sort of membrane microdomains. Little is known about ERES in plant because most studies come from animal cells and the features of ERES can be different depending on the cell type and between kingdoms (DaSilva *et* al., 2004; review by Tang *et* al., 2005). It was proposed to define them as sites where nascent COPII membrane and COPII vesicles in transit can be found (DaSilva *et* al., 2004). In tobacco cells, ERES and Golgi bodies were observed moving together and are probably closely associated. Even if the reason needs to be elucidated, ERES and cisternal Golgi stacks are physically close (DaSilva *et* al., 2004; Budnik and Stephens, 2009). It has been shown that Golgi stacks do not associate with only one ERES but can be bound to several ERES at the same time (Yang *et* al., 2005).

ER retention signal

ER resident proteins carry a retention signal. For soluble proteins most of the time this signal is a tetrapeptide KDEL, HDEL or RDEL found in C-terminal position. A substitution of one amino acid in

this tetrapeptide is enough to disrupt the retention of the protein (Denecke *et* al., 1992). Different studies have shown that secreted proteins fused with KDEL sequence in C-terminal position were then retained in the ER (reviewed by Pagny *et* al., 1999). This mechanism of retention is highly specific and mostly conserved between mammals and plants (Denecke *et* al., 1992; reviewed by Pagny *et* al., 1999).

Traffic from ER to Golgi

As described previously, ER proteins are packaged in vesicles and exported to the Golgi at ERES sites. Because ER and Golgi bodies are highly dynamic structures, different models of protein trafficking from ER to Golgi in plants have been proposed (Figure 1.4; Hanton *et* al., 2005). The first model called "vacuum cleaner model" is based on the Golgi bodies' movements along the ER. Golgi stacks collect vesicles at ERES in order to obtain their cargoes. The second model is called "stop and go". Here the Golgi bodies stop at ERES, obtain cargoes, move along the actin filaments, then stop at another ERES and collect more cargoes. This model suggests the involvement of a specific signal on ERES causing a transitory association between Golgi and ERES. Then last model is the "ERES mobile model" where Golgi and ERES together are highly mobile along the ER. This model describes a continuous transport of cargoes between these two compartments. However, the connections between Golgi and ER are still unclear and the mechanisms of interaction need to be elucidated (Hanton *et* al., 2005).

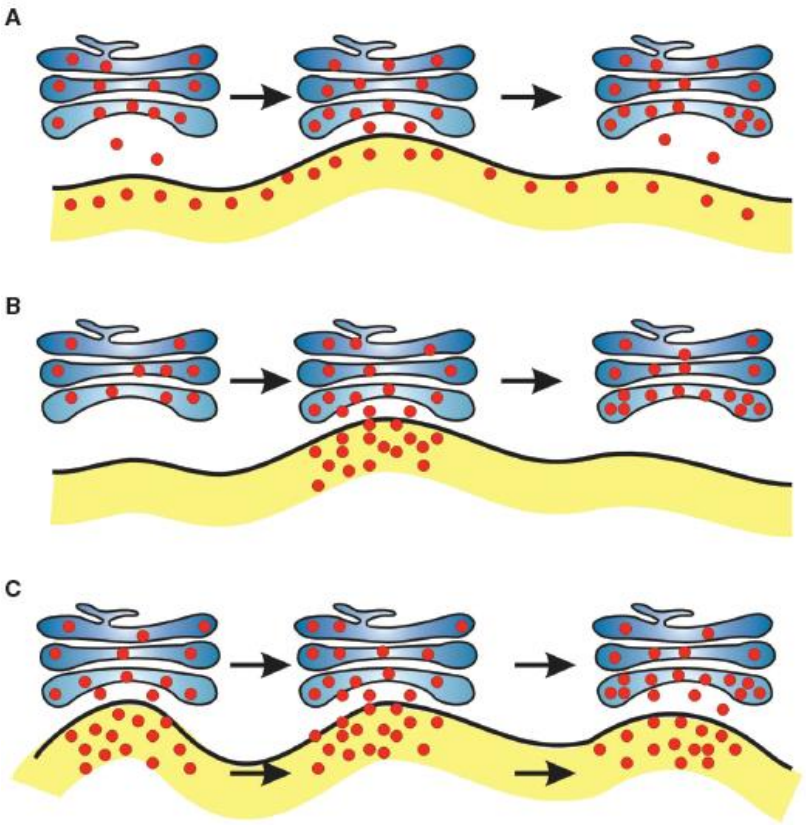

Figure 1.4 Models for proteins transport from ER to Golgi (Hanton *et* al., 2005).
A: The vacuum cleaner model. Golgi bodies move along the ER surface, picking up cargo. The entire ER is capable of exporting proteins. B: The stop-and-go model. Golgi bodies move along the ER and stop at fixed ERES, where protein transport takes place. After transfer of cargo from ER to Golgi, the Golgi body moves to the next site and collect more cargo. C: The mobile ERES model. Golgi bodies and ERES move together, allowing continual protein transport between the two organelles.

ER exit bypassing Golgi

Multiple export pathways from the ER have been described in plants. The classical export pathway from ER to the Golgi is sensitive to Brefeldin A (BFA), a fungal metabolite which can reversibly block the retrograde traffic by inhibiting the formation of COPI vesicles and consequently also block the anterograde traffic. Other BFA-insensitive pathways have been described but it is possible that most of them exist only in seeds (Vitale and Denecke 1999). It has been shown that some storage proteins may bypass the Golgi and traffic to the vacuole via precursor-accumulating vesicles (PAC) *e.g.* in maturing pumpkin seeds. Aggregates of storage proteins were visible within the ER by immunocytochemical staining (Hara-Nishimura *et* al., 1998). Toyooka *et* al. (2000) highlighted the transport of a vacuolar cysteine proteinase (SH-EP) from the ER to the protein storage vacuole (PSV)

bypassing the Golgi. This SH-EP has a C-terminal KDEL ER-retention signal. The proform of the enzyme has been observed accumulating at the edges of ER, in vesicles budding from it and in large vesicles distinct from PSV but not in the Golgi. Others studies support the hypothesis of a direct pathway from ER to lytic vacuoles. Originally discovered in yeast, a route from the cytosol to the lytic vacuole involving autophagy was also proposed in plants. Structures similar to autophagosomes containing vacuolar proteins like seed storage proteins were detected by electron microscopy (Michaeli *et* al., 2014). In 2013, Viotti *et* al., proposed a Golgi-bypassing route in *Arabidopsis*, where the ER membrane contributes to lytic vacuole biogenesis. Indeed, the tonoplast intrinsic protein α-TIP was able to reach the vacuole even after treatment with Brefeldin A in mesophyll protoplasts of tobacco plants (Gomez and Chrispeels 1993).

Golgi apparatus

The Golgi apparatus is a major organelle consisting of different stacked polarized cisternae, which can be divided in three main compartments: *cis*, *medial* and *trans*-Golgi which are functionally distinct (Staehelin and Moore 1995). The Golgi apparatus processes proteins arriving by vesicles from the ER at the *cis*-Golgi face and sends them from the *trans*-Golgi face to various locations in the cell (lysosomes, plasma membrane…) or out of the cell (secretory vesicle). Unlike mammalian cells which have one large Golgi apparatus next to the nucleus, numerous (up to one hundred) mobile Golgi stacks can be found in the cytoplasm of plant cells (DaSilva *et* al., 2004). Different major functions of the Golgi in the plant cell have been described. It can be considered as the glycan factory of the cell because it synthetizes and exports complex polysaccharides for the cell wall but also glycolipids for the plasma membrane and storage glycoproteins (Staehelin and Moore 1995). Golgi resident enzymes are single pass transmembrane proteins which are found in distinct cisternae depending on their function. The two main families of enzymes are the glycosidases and the glycosyltransferases, which are involved in the production of glycans and the modifications of N-or O-linked carbohydrates, attached to proteins and lipids (Saint-Jore-Dupas *et* al., 2004). After these modifications and maturations (glyco-) proteins are packaged in transport vesicles in the *trans*-Golgi and sent to their specific destinations in the cell (Driouich *et* al., 1993; Dupree and Sherrier 1998).

Plant Golgi bodies are highly motile because they are physically and mechanically bound to the actin cytoskeleton. In tobacco epidermal cells expressing a GFP fused to the actin-binding domain of talin, Golgi bodies were observed moving along the ER in an actin-dependent way but they did not interact with the microtubules (Brandizzi *et* al., 2002). Previous studies also showed a close link between Golgi stacks moving along actin cables and the ER, by expressing a Golgi protein fused to GFP (Boevink *et* al., 1998).

Two models of protein transport across the Golgi stacks have been proposed. The first one is based on the protein transport between the Golgi cisternae by vesicles budding from one cisterna and fusing with the next, in both anterograde and retrograde directions. The Golgi is here considered as a static organelle with small vesicles moving between compartments (Orci *et* al., 1998).

The second model proposes that proteins and lipids are transported in the *cis*-to-*trans* direction through cisternal maturation; while retrograde transport of Golgi-resident proteins is mediated by COPI vesicles (Glick *et* al., 1997; Allan and Balch 1999; Alberts *et* al., 2008). This model implies a dynamic organization of Golgi apparatus with the *trans*-cisternae being consumed while a new *cis*-cisternae forms. It is now the more generally accepted model. Transport of Golgi-resident proteins by COPI vesicles was also demonstrated (Orci *et* al., 1997).

A.2 Late secretory pathway

Trans-Golgi Network (TGN)

Initially thought to be part of the Golgi apparatus as in animal cells, the TGN was shown in plants to be an independent and separate organelle (Hawes and Satiat-Jeunemaitre 2005). Uemura *et* al. (2004) characterized in *Arabidopsis* protoplasts fluorescent plant TGN markers that localized in structures distinct from Golgi bodies. Foresti and Denecke (2008) also showed in tobacco leaf epidermis cells that fluorescent markers of plant TGN do not colocalize with Golgi markers.

The TGN has been described as a dynamic organelle, with a role in the exocytosis and endocytosis pathways (Foresti and Denecke 2008; Kang *et* al., 2011). However the definition of plant TGN is still unclear, it has been suggested to function as an early endosome while in animal cells these are two separate compartments (Lam *et* al., 2007; Viotti *et* al., 2010; reviewed by Uemura and Nakano 2013). One of the first studies used a rice secretory carrier membrane protein 1 (SCAMP1), known to be a post-Golgi proteins involved in endocytosis in animals, which was fused to YFP and expressed in tobacco BY-2 cells. The localization was observed in plasma membrane (PM) and mobile cytosolic organelles. These highly motile organelles are BFA-sensitive and form aggregates after treatment. Confocal immunofluorescence with SCAMP1 antibodies confirm that these organelles are distinct from Golgi and multivesicular bodies (MVB) and act as early endosomes (Lam *et* al., 2007). Viotti *et* al. (2010) observed in *Arabidopsis* that secretory proteins passed through the TGN before reaching their final destination, by studying the route of a brassinosteroid receptor BRI1 and a boron exporter BOR1, both localized in the PM. Using a secreted version of GFP, a YFP fusion of these membrane proteins and the endocytic tracer FM4-64, their work also allowed to distinguish the TGN and MVB as two distinct

compartments. The TGN was described as a highly mobile organelle which temporarily associates with the Golgi.

The size of the TGN may vary according to the cell function or specialization, but also depending on the number and type of vesicles that bud from it (Marty 1999; reviewed by Gendre *et* al., 2015). Three type of vesicles associated with the TGN have been described: the clathrin-coated vesicles (CCV), the COPI vesicles and the secretory vesicles (reviewed by Gendre *et* al., 2015). Proteins trafficking through the TGN can be directed to the plasma membrane or to the vacuole or lysosome in animal cells. At this point, targeting to the vacuole require a vacuolar sorting determinant, while targeting to the plasma membrane can be considered as the default pathway (Sanderfoot and Raikhel 1999).

Endosomes

Plants endosomes are highly dynamic membrane structures, considered as an intermediate compartment, which take part in endocytosis and biosynthesis pathways by receiving vesicles from the TGN or the plasma membrane. Endosomes are part of the late secretory system and are involved in the recycling or degradation of plasma membrane proteins and in the traffic of secreted proteins targeted to the vacuole or lysosomes (Geldner 2004; Otegui and Spitzer 2008). Endosomes also play a role in diverse cellular mechanisms such as polar tip growth, cell polarity, auxin mediated cell-cell communication and gravitropism (Geldner 2004; Samaj *et* al., 2005). With these numerous implications endosomes are important players in trafficking pathways signaling and regulation (Reyes *et* al., 2011). In yeast and mammals, different types of endosomes have been described. The early endosomes (EE) receive endocytic cargo vesicles from the plasma membrane. At this point, material can also be return to the PM via recycling endosomes. EE are considered as an important sorting station for vesicles in the endocytic and secretory pathway. Late endosomes (LE) are derived by maturation form the EE; they are also called multivesicular bodies (MVB) because they are formed by the invagination of the endosome membrane itself. They are involved in the degradation of membrane proteins by fusion with lysosomes or act in their recycling to the TGN (Otegui and Spitzer, 2008). The endosome system in plants differs from the other eukaryotes. Two main compartments have been described in literature: the TGN, which acts as early or recycling endosomes, and the MVB, considered as a late endosome (Otegui and Reyes, 2010; Contento and Bassham, 2012). These two compartments have been highlighted using the fluorescent dye FM4-64, which labels first the PM. This dye allows to study the endocytic pathway as it labels also very quickly the early endosomes and later the vacuole (Contento and Bassham, 2012; Bolte *et* al., 2004).

Early endosomes were not observed in plants while MVB were described to be active transport carriers for vacuolar proteins. Indeed, mutation in Rab5-like GTPase, a MVB localized protein, leads to vacuolar transport perturbation (reviewed by Otegui and Spitzer, 2008). Plant endosomes play a major role in endocytosis and more precisely in protein recycling, protein degradation and receptor-mediated signaling. Recycling of vacuolar cargo receptors via endosomes to the TGN needs a complex of proteins called retromer. This complex is conserved through eukaryote kingdom, localized in EE and it is involved in the recruitment of the cargoes (Seaman 2012). Some proteins were observed to be continually cycling between the PM and the EE, like the auxin carrier PIN1 (Otegui and Reyes 2010). Endosomes are also involved in degradation of membrane proteins via lysosomes or vacuoles. Membrane proteins that will be degraded are marked by an ubiquitin tag which causes their internalization into the MVB. Different protein complexes, called Endosomal Sorting Complex Required for Transport (ESCRT-0-I-II and III), are involved in this mechanism. ESCRT complexes differ in different organisms. The ESCRT-0 does not exist in plants while it is essential in animals, another unrelated complex replaces it. Endosomes play also a role in receptor-mediated signaling. In this process, activated receptors at the PM can be internalized by endocytosis into endosomes and then interacting with other downstream factors, in the endosomes membrane (Otegui and Spitzer 2008; Otegui and Reyes, 2010).

Vacuoles

Vacuoles are an endpoint of the secretory system in plants. They are dynamic organelles and important compartments for plant cell metabolism and life (Wink 1993). In general, a plant cell contains one large vacuole, which can occupy more than 90% of the total cell volume. Vacuole function depends of the cell type. They participate in homeostasis, cell turgor, growth and storage of metabolic products. They also have a hydrolytic role and can sequester toxic compounds. The size, number and function of vacuoles within a single cell depend on the kind of tissue and the cell type (reviewed by Marty 1999). These different functions can occur in the same compartment but a cell can also contain two different types of vacuoles (Paris *et* al., 1996).

A.3 Vesicular traffic

In the plant secretory pathway, vesicles mediate the transport of cargo proteins from an organelle to the next, until they reach their final destination. Vesicles move through the cytosol by interaction with cytoskeleton elements. The basis of this essential mechanism consists of the vesicle budding from a donor compartment, which contains cargo proteins, to the fusion of this vesicle to an

acceptor compartment where the cargo is released (Bonifacino and Glick 2004). This active process requires the recruitment of coat proteins and the intervention of small GTPases (Jürgens 2004). First studied in mammalian cells and yeast, the three major types of coated vesicles COPI, COPII and CCV are also found in plants (Figure 1.5). This classical model for vesicle transport requires different steps, from the formation of coated bud in the donor compartment, the vesicle formation and transport, to the coat protein release and fusion of the vesicle with the target membrane in order to discharge its content (Jürgens and Geldner 2002; Hwang and Robinson 2009).

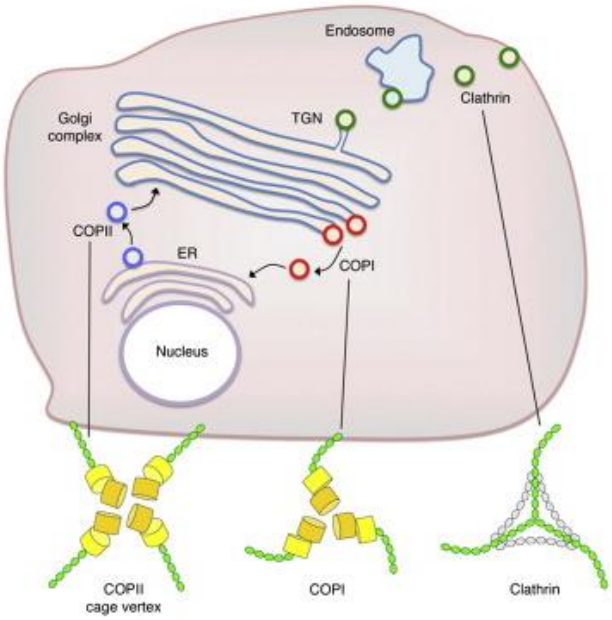

Figure 1.5 The three type of coated vesicles and their localization in the cell (from Hughson 2010)
In the early secretory pathway, newly synthetized proteins are transported by COPII and COPI coated vesicles between the ER and the Golgi. From the TGN, cargo proteins traffic to the plasma membrane or recycling endosomes by clathrin coated vesicles.

Clathrin-coated vesicles

Clathrin-coated vesicles (CCV) consist of a two-layered coat: the outer layer of clathrin structural proteins and the inner layer of adaptor protein (AP) complexes. The clathrin molecule is composed of heavy and light polypeptide chains. Three heavy chains and three light chains assemble to form a structural unit called a triskelion, which assembles to form the clathrin lattice. AP complexes play a major role in vesicle formation. They mediate the clathrin lattice recognition and assembly of the cargo proteins (Schmid 1997). Different AP complexes have been identified (AP1 to AP4) in

eukaryotic cells, which are involved in different pathways (reviewed by McMahon and Gills 2004). The coat assembly is also controlled by the ARF1-GTPase. Protein sorting at the TGN and endosome is mediated by AP1 complex which recognize the luminal domain of the cargo protein, while AP2 mediates CCV formation at the PM. Other adaptor proteins have been identified in animal cells but have not been found in plants. CCV have been localized at the TGN and the plasma membrane in animal cells as well as in plant cells (Sanderfoot and Raikhel 1999; Jürgens and Geldner 2002).

Mechanism of membrane fusion

Vesicle and target membrane interact first via tethering proteins recruited by Rab proteins. Rab proteins are a large family of GTPases proteins, involved in the regulation of membrane trafficking and vesicles formation. They are key regulatory factors in docking of vesicles on target membranes (Hutagalung and Novick, 2011). The fusion of the transport vesicle with the acceptor compartment involves the action of SNAREs (soluble NSF attachment protein receptors): a v-SNARE in the vesicle membrane and t-SNAREs in the target membrane. This primes the interaction of the v-SNARE protein on the vesicle surface with the cytosolic domain of t-SNAREs localized on the target membrane. Then a SNARE complex is formed by four SNAREs, forming a bundle which brings the membranes close enough for fusion, where the vesicle releases the cargo to the acceptor compartment (Sanderfoot and Raikhel 1999). The dissociation of the SNARE complex is an ATP-dependent reaction, mediating by α-SNAP (soluble NSF attachment protein) and NSF proteins. (Hutagalung and Novick 2011) (Figure 1.6).

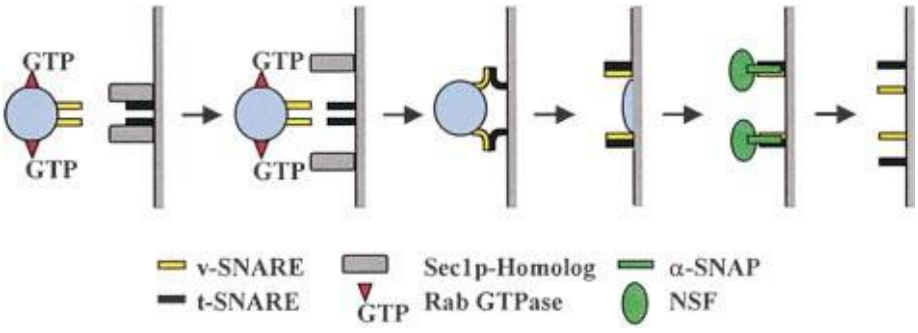

Figure 1.6 The SNARE mechanism of vesicle fusion (from Sanderfoot and Raikhel, 1999).
On the vesicular membrane, the v-SNARE and the Rab-type GTPase recognize on the target membrane the t-SNARE and Sec1 p-Homolog. After this docking event, Sec1 p-Homolog is removed and the formation of the SNARE complex allows the vesicle fusion with the target membrane. Finally, α-SNAP and NSF mediate the dissociation of the SNARE complex, allowing the retrograde recycling of the v-SNARE.

A.4 Endocytosis

Endocytosis general mechanisms

Endocytosis is a mechanism of internalization of material and protein cargoes into plasma membrane transport vesicles. This process plays a crucial part in numerous cellular mechanisms as turnover of proteins or hormone transport, but also in various responses to environmental signals like responses to pathogens or cell signaling (Otegui and Spitzer 2008; Reyes *et* al., 2011; Contento and Bassham 2012). It is the principal way for membrane and extracellular proteins to enter the cell (reviewed by Fan *et* al., 2015) (figure 1.7). In animals, three types of endocytosis have been described: phagocytosis, pinocytosis and receptor-mediated endocytosis (Alberts *et* al., 2008). Phagocytosis is the ingestion of large particles via vesicles called "phagosomes". This process takes place in the immune response and in clearance of dead cells. Pinocytosis represents the internalization of fluid and solutes (proteins and polysaccharides) via small vesicles, formed from coated pits of the plasma membrane. This mechanism is involved in cellular metabolism and signaling. Receptor-mediated endocytosis, also described in plants, occurs for specific molecules transport (proteins and lipids) and implicates clathrin-coated vesicles. It plays a role in various cellular functions, from the turn-over of membrane proteins, the uptake of extracellular molecules, to the activation of signaling pathways (McMahon and Boucrot 2011).

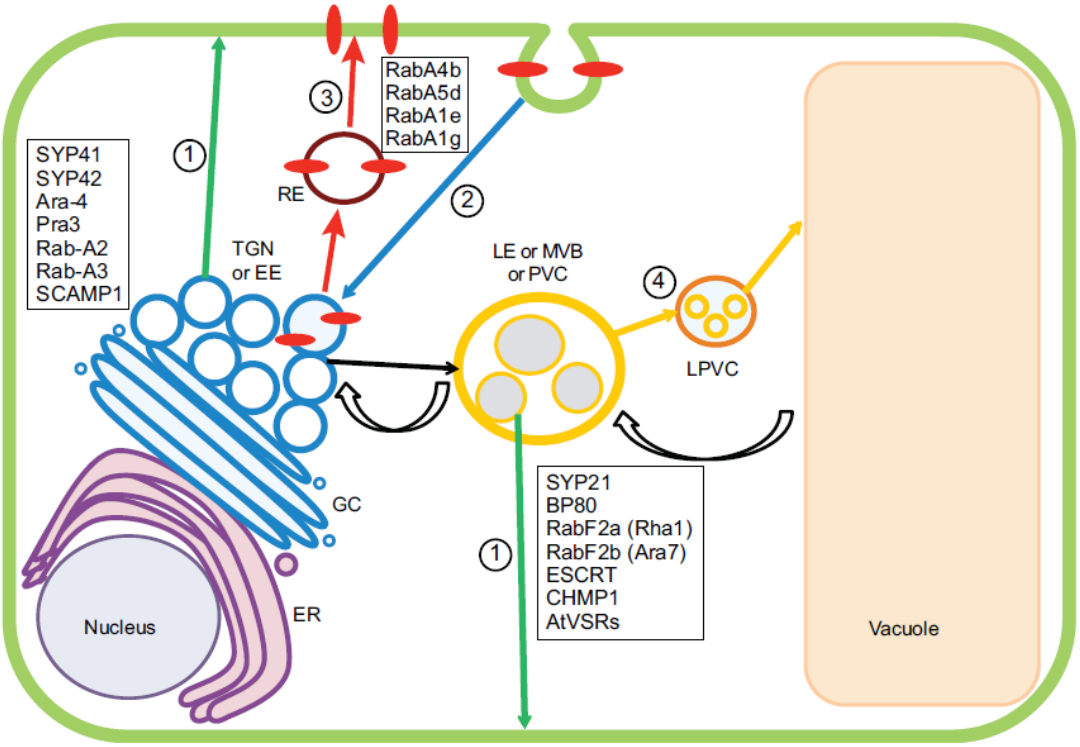

Figure 1.7 The endocytic pathway in plants (Contento and Bassham 2012)

Components of the endocytic pathway are involved in biosynthetic, degradative and recycling transport. The trans-Golgi network and early endosomes act as the point of organization for these three pathways. This diagram displays the organelles involved in endomembrane trafficking: nucleus, endoplasmic reticulum (ER), Golgi complex (GC), trans-Golgi network (TGN) / early endosome (EE), late endosome (LE) or multivesicular body (MVB) or prevacuolar compartment (PVC), late prevacuolar compartment (LPVC), vacuole surrounded by the tonoplast, recycling endosome (RE). The colored arrows designate potential traffic between organelles. The green arrows indicate pathway 1, the biosynthetic transport route to the plasma membrane that passes through the TGN and sometimes the MVB. The blue arrow shows a pathway (2) that is taken by plasma membrane components (red ovals) as they are internalized into endocytic vesicles and move through the TGN. Proteins associated with the TGN are listed. The thick, red arrows represent a recycling pathway (3), by which plasma membrane components might be returned to the plasma membrane through a specialized RE. Proteins associated with the RE are shown. The orange arrows designate the transport pathway (4) for newly synthesized vacuolar components, as well as cellular materials destined for degradation in the vacuole. Proteins associated with MVBs are shown. Transport from the TGN to MVBs is designated by a black arrow. Retrograde transport from the VAC to the MVB is represented by curved black arrows.

Clathrin mediated endocytosis in plants (CME)

In plants, the endocytic pathway is involved in various essential functions, as cell growth, nutrients uptake, hormonal signaling, detection of environmental signals and defense against pathogens. The main endocytic process is dependent on clathrin coated vesicles that pinch off from PM, where the cargoes are recognized, then packaged and incorporated into CCV. After the scission, newly formed CCV can fuse with the early endosomes, from where cargoes can continue to their final destination (Chen *et* al., 2011). CCV are also a main way for membrane protein retrieval and membrane receptor down regulation. Two major kinds of proteins are involved in plant CME. The first group includes the sub-units of the clathrin coat, the adaptor (AP) complexes. The second group is formed by various cytosolic proteins, playing a role in budding and fission events (Holstein 2002). Cargo selection requires adaptor complexes that recognize different motifs or post-translational modifications such as phosphorylation or ubiquitylation. The recognition of specific motifs is a mechanisms well studied in animals but still unclear in plants. The role of CME in plant development was highlighted by studies on the PIN proteins. These proteins were the first identified cargoes of CME, allowing to establish a link between endocytosis and auxin-mediated development (reviewed by Chen *et* al., 2011). CME was also described to be involved in the regulation of plant defense response against pathogens, specifically against bacterial and fungal elicitors. Pathogen attack could trigger plant immune response by regulating some membrane receptors via endocytosis. It is the case of the *Arabidopsis* FLS2 receptor, which recognizes the bacterial flagellin and is taken up from the PM into CCV (reviewed by Fan *et* al., 2015). CME plays also a role in uptake of nutrients such as metallic ions. The receptors IRT1 and BOR1, for iron and boron respectively, have been described to cycle from PM to endosomes. When needed, these proteins are sorted into vacuoles for downregulation in order to avoid metallic ion toxicity (Chen *et* al., 2011).

Clathrin-independent endocytic routes in plants

Alternatives endocytic pathways have been described in plants. One of these involves membrane microdomains also called lipids rafts. Microdomains are well studied in yeast and mammals but less is known in plants. These dynamic platforms, insoluble in some detergents, are implicated in the concentration of some receptors and in the assembly of certain signal transduction machineries. Membrane microdomains play a role in the amplification or the attenuation of various cellular signaling cascades (Puri *et* al., 2004). In *Arabidopsis*, flotillin1 (flot1) was the first membrane protein identified which form microdomains, acting in an independent clathrin-endocytic pathway. This protein involved in seedling development was localized in plasma membrane and in intra-cellular vesicles. Flot1 was also observed to partially colocalize with the endocytic marker FM4-64 (Li *et* al., 2012; reviewed by Fan *et* al., 2015).

Ubiquitylation mediated plant endocytosis

One of the well-known roles of ubiquitin tag is the marking of proteins for degradation by the 26S proteasome. However, ubiquitin is also involved in protein trafficking to the vacuole / lysosome by endocytosis. This pathway was first observed in yeast and mammals but today evidence is accumulating in plants. In *Arabidopsis*, it was observed in the study of the iron transporter ITR1. This transporter was described in the TGN/ EE of root hair cells and it is responsible for the iron uptake from the soil. IRT1 needs to be monoubiquitylated to enter the endocytic route for vacuolar degradation. Mutations in the two key lysines, sites of ubiquitination, increases its stability. IRT1 has been described to cycle between the PM and the early endosomes, depending on its monoubiquitylation (reviewed by Tian and Xie, 2013).

A.5. Protein secretion

Unconventional protein secretion

Proteins trafficking through the "classical" protein secretion pathway are transiting from the ER via the Golgi/TGN to their final destination. By default, soluble proteins are secreted at the plasma membrane. Cell secretion plays a role in cell to cell communication and pathogen defense, which can be constitutive of induced by internal or external stimuli (Krause *et* al., 2013). Uptake in the ER is determined by the presence of a Signal Peptide at the N-terminal end of the newly synthesized polypeptide. There are also some secreted proteins lacking this SP. These Leaderless Secretory Proteins (LSP) do not follow the ER/Golgi classic route but are trafficking through an "unconventional secretion pathway" and are directly secreted from the cytosol into the extracellular matrix (Agrawal *et* al., 2010; Ding *et* al., 2012; Krause *et* al., 2013). First identified in mammalian and yeast cells, data for unconventional secretion studies in plants are now accumulating (Drakakaki and Dandekar 2013).

Plant secretome studies

The term secretome was firstly defined by Tjalsma *et* al. (2000) after their work on protein transport in *Bacillus subtilis*. It was including the protein secretion machinery and the secreted proteins. Nowadays, the term secretome has evolved and has be defined for plants by Agrawal *et* al. (2010) as "the global group of secreted proteins into the extracellular space by a cell, tissue, organ or organism at any given time and conditions through known and unknown secretory mechanisms involving constitutive and regulated secretory organelles" (reviewed by Krause *et* al., 2013). Previous studies showed that LSPs can represent more than 50% of the identified secretome and suggested that LSP may play a role in stress responses and defense against pathogen (Agrawal *et* al., 2010). Early work

on the plant secretome was performed with cultured cells but it has been shown that these do not reflect natural conditions. Recent studies propose alternatives to cell cultures, allowing *in planta* work, such as gravity extraction from leaves or vacuum infiltration methods (Alexandersson *et* al., 2013; Krause *et* al., 2013).

B. Vacuole types and protein targeting to vacuole

B.1 Vacuole types

Plant cells can contain different vacuole types with different functions, depending of the cell type and the developmental stage. The distinction between Lytic Vacuole (LV) and Protein Storage Vacuole (PSV) and their presence within a single cell were demonstrated by different studies (Hoh *et* al., 1995; Paris *et* al., 1996; Vitale and Raikhel 1999). Epimashko *et* al. (2004) demonstrated that mesophyll cells of *Mesembryanthemum crystallinum L.* under salt stress conditions have two functionally different vacuoles, an acidic and a non-acidic. This allows the plant to compartmentalize salt storing and malate accumulation/mobilization.

The three kinds of vacuoles described in literature are the following:
Lytic Vacuole: it is an acidic compartment which can be compared to the lysosome in animal cells. This lytic vacuole contains hydrolytic enzymes and plays an important role to maintain cell turgor. This type of vacuole develops in vegetative organs in plants. Acidic vacuoles were shown to accumulate the pH-sensitive dye Neutral Red (NR) (Di Sansebastiano *et* al., 2001).
Neutral vacuole: it has been described in vegetative tissues and did not accumulate NR in contrast to the lytic vacuole (Di Sansebastiano *et* al., 2001).
Protein Storage Vacuole: involved in the accumulation of proteins, this type of vacuole is found in storage tissues of seeds and developing seeds.

According to the classical model, after trafficking through the ER and Golgi, vacuolar proteins are targeted to their final destination. Protein targeting to vacuoles is dependent on a signal, which can be found at different locations in the protein structure: at the N- or C-terminus or internal to the protein. The first model for the biogenesis of distinct vacuolar type was based on the localization of aquaporin Tonoplast Intrinsic Protein (TIP) isoforms and proposed an organelle-specific localization. Based on immunolocalization, these first studies showed that α-TIP are present in Protein Storage Vacuole (PSV) whereas γ-TIP are found in Lytic vacuole (LV) (Paris *et* al., 1996; Neuhaus and Roger,

1998; Jauh *et* al., 1998) and δ-TIP in vacuole accumulating pigments and vegetative storage proteins (Jauh *et* al., 1999). More recent studies on *A. thaliana* demonstrated that TIP isoforms distribution and expression are regulated during development (Hunter *et* al., 2007; Gattolin *et* al., 2010). TIP isoforms distribution is tissue specific and depends on the developmental stage: γ and δ-TIP are found in vegetative tissues (but not in root tip) whereas α-TIP predominates during seed maturation but decreases after germination (Hunter *et* al., 2007). In Soybean, the reversible functional switch from vegetative storage to lytic vacuole in paraveinal mesophyll is accompanied by a replacement of δ-TIP by γ-TIP (Murphy 2005).

B.2.Vacuolar sorting determinants

Soluble vacuolar proteins are sorted to the vacuoles by cargo receptors, which bind a specific component: a vacuolar sorting determinant (VSD). This sorting signal is found in the vacuolar protein precursor and it is mostly removed during maturation after vacuolar sorting. In plant cells, three vacuolar sorting determinants have been distinguished: sequence specific VSDs (ssVSD), C-terminal VSDs (ctVSD) and protein-structure-dependent VSDs (psVSD). Each determinant is structurally and functionally distinct (Neuhaus and Roger 1998) (Figure 1.8).

- *ssVSDs*: they address proteins to the lytic vacuole. SsVSDs were first characterized in sweet potato prosporamin and in barley proaleurain (Matsuoka and Nakamura 1991; Koide *et* al., 1997; Holwerda *et* al., 1992). In mutants lacking the propeptide, sporamin was secreted, proving the presence of vacuolar sorting determinant in the propeptide (Matsuoka and Nakamura 1991). An ssVSD can be located in an N-terminal or C-terminal propeptide or in an internal propeptide, e.g. in castor bean ricin (Frigerio *et* al., 2001). In the case of sporamin and aleurain, the N-terminal propeptide contains a NPIR motif. Mutational analysis indicates that an Ile or Leu is critical for the function of the VSD, as well as less conserved amino acids around it (Matsuoka and Nakamura 1999).

- *ctVSDs*: they were first characterized at the C-terminal region of barley lectin (Bednarek *et* al., 1990; Bednarek and Raikhel 1991), tobacco chitinase A (Neuhaus *et* al., 1991) and phaseolin (Frigerio *et* al., 1998). All three proteins are missorted if they are synthesized without their carboxyl-terminal propeptide (CTPP). The function could also be blocked by replacement of the C-terminal amino acid by a Gly (Neuhaus *et* al., 1991) or by the addition of two Gly or a C-

terminal N-glycan (Bednarek *et* al, 1990), indicating C-terminal binding by the putative receptor. There is no other conserved motif.

- *psVSD*: this determinant is a feature of some seed storage proteins, which aggregate in the ER or in the Golgi. Vacuolar sorting could be caused by this aggregation. Castelli and Vitale showed that phaseolin forms membrane associated aggregates which are sorted to the vacuole while mutated phaseolin did not aggregate and was secreted (Castelli and Vitale 2005; Frigerio *et* al., 1998).

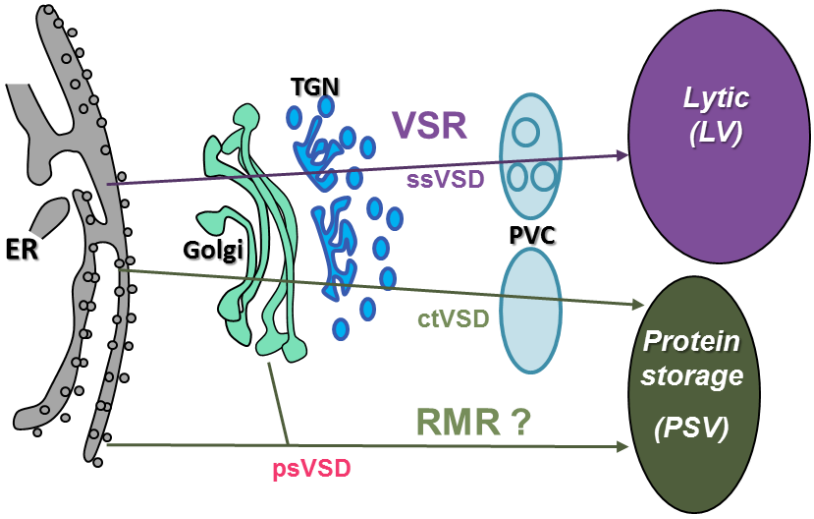

Figure 1.8 Proteins targeting to vacuole, current model. Different routes have been described, involving two cargo receptors. The first route involves a sequence specific VSD which target the protein to the lytic vacuole. The second route involves a C-terminal VSD which target the protein to the PSV. The third route involves a protein structure VSD forms aggregates in the ER or in the Golgi and go to the PSV.

B.3 Vacuolar sorting receptors in plant cells

Two families of vacuolar receptor are thought to be involved in protein trafficking to vacuoles: the VSR (Vacuolar Sorting Receptor) and the RMR (Receptor Membrane Ring-H2) families.

The VSR family

The VSR receptor was first identified as the BP-80 protein and isolated from pea clathrin-coated vesicles (Kirsch *et* al., 1994; Paris et al, 1997; Paris and Neuhaus, 2002). VSR are type I membrane proteins, constituted of an N-terminal luminal domain which includes a Protease-

Associated domain (PA), a large VSR specific domain, three Cys-Rich EGF Repeats (Epidermal Growth Factor) a single transmembrane domain, and a short cytosolic tail (Figure 1.9).

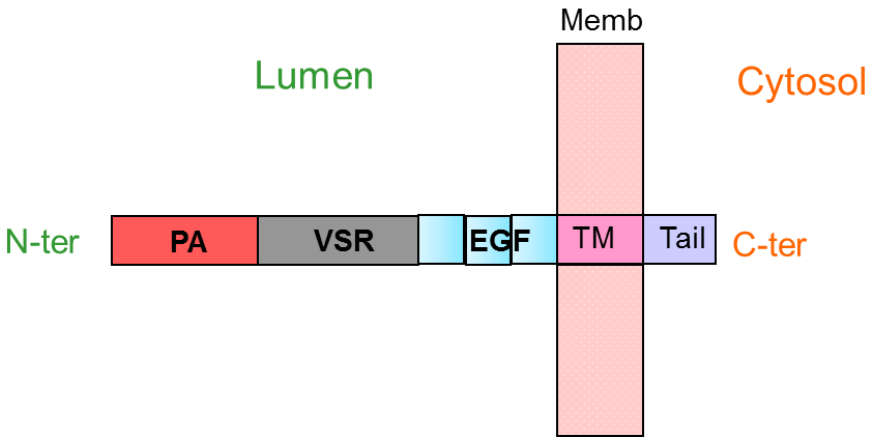

Figure 1.9 Schematic VSR structure (not to scale). N-ter: N-terminus; PA: Protease-associated domain; VSR: VSR domain; EGF: Epidermal Growth Factor domain (3 repeat); MP: plasma membrane; TM: Trans-membrane domain; C-ter: C-terminus

Kirsch *et* al. (1994) demonstrated that BP-80 binds *in vitro* the ssVSD of barley proaleurain, but showed no affinity for the pea prolectin and the barley prolectin, the latter carrying an already characterized ctVSD signal. Several publications have shown the involvement of VSR in the transport of vacuolar soluble proteins to the LV (Jiang and Rogers 1998; DaSilva *et* al., 2006; Zouhar *et* al., 2010). BP-80 was described by immunocytochemistry to localize in the *trans*-cisternae of the Golgi, in the TGN, and in the prevacuolar compartment (Paris *et* al., 1997). The current model suggests that BP-80 is a pH-dependent ligand binder. Cargo proteins are bound in the Golgi. Recycling of BP-80, from the prevacuolar compartment to the Golgi after cargo release, is a strongly supported hypothesis (DaSilva *et* al., 2006). However, an alternative model implying ER to TGN traffic has been proposed (Niemes 2010; Robinson 2013). Reviewed by Robinson and Neuhaus (2016), this second model proposes that VSRs interact with their ligands earlier in the secretory pathway, in ER or in *cis*-Golgi. It also brings evidence that the dissociation of the ligand-receptor complex cannot occur in a pH-dependent way, because of the similarity of pH value between the two compartments.

VSR proteins are encoded by seven genes in *A. thaliana* (AtVSR1 to AtVSR7). Homologous receptors have been identified in all land plants including lycophytes and mosses, where eight VSR genes have been found.

The RMR family

RMR proteins were identified by their homology to the PA domain of VSR proteins (Cao *et* al., 2000; reviewed by Wang *et* al., 2010). For this reason, RMRs were thought to be involved in ligand binding as vacuolar receptors. RMR structure consists of an N-terminal luminal domain, the Protease-associated domain, a single transmembrane domain and a cytosolic tail with a RING-H2 domain (Really Interesting New Gene, with two Histidines) (Figure 1.10). RING domains are cysteine-rich, zinc-binding domains and are known as protein-interaction domains. They consist of a pattern of conserved cysteine and histidine residues binding two zinc ions (Borden 2000; Kosarev *et* al., 2002). RING domains are involved in various cellular mechanisms in eukaryotes, such as signal transduction, transcription and protein-protein interactions (Borden and Freemont 1996). RMRs belong to the PA-TM-RING protein family, which combine PA, transmembrane domain and RING domains, and has been identified in many organisms: in plants, mammals (GRAIL; Seroogy *et* al., 2004), *Xenopus* (GREUL1; Borchers *et* al., 2002) and *Drosophila* (Goliath; Bouchard and Cote 1993) but not in yeast (Bocock *et* al., 2009). In plants, many RMRs include a C-terminal serine rich region (Jiang *et* al., 2000).

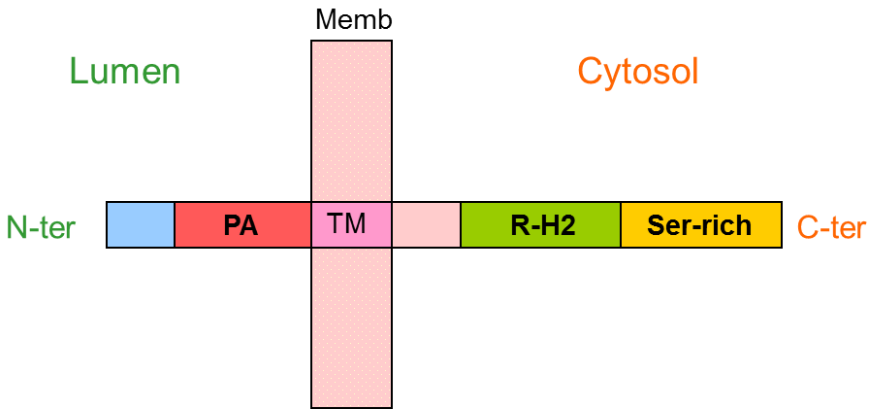

Figure 1.10 Schematic RMR structure (not to scale). N-ter : N-terminus ; PA : Protease-associated domain ; P : plasma membrane ; TM : Trans-membrane domain ; RING-H2 : RING H2 domain, Serine rich : Serine rich cytosolic tail; C-ter: C-terminus. Furthermore, in Arabidopsis thaliana RMR 1, 3 and 4 include a C-terminal serine rich region (Jiang *et* al., 2000).

In tobacco and tomato cells, RMR proteins were localized in organelles also labelled with anti-DIP antibodies: the PSV crystalloid (Jiang *et* al., 2000). DIP (dark-induced tonoplast intrinsic protein) is an isoform of TIP, found in the crystalloid bodies, precursors of the PSV during seed development. Jiang *et* al. (2000) proposed that DIP-positive organelle might function as PVC and fuse to form the PSV. Park *et* al. (2005) described localization of *At*RMR1 in the prevacuolar compartment of PSV and in the Golgi. In *Arabidopsis* protoplasts, *At*RMR1 colocalizes with DIP-positive organelles. *In vitro* binding assays

showed an interaction of the luminal domain of *At*RMR1 with the ctVSD of phaseolin. These results strongly suggest that AtRMR1 may act as a cargo receptor for proteins with ctVSD targeting to the PSV. However, in both tobacco leaves and *Arabidopsis* protoplasts, Occhialini (2011) found *At*RMR2 mostly localized in the TGN while *At*RMR1 localized in ER structures. Occhialini also described by BiFC (Bimolecular Fluorescence Complementation) that *At*RMR2 can form homodimers and can also form heterodimers with AtRMR1, both localizing in the TGN. In rice, *Os*RMR1 was localized by immunogold labelling in Golgi apparatus, in TGN and in an electron-dense organelle similar but distinct from the MVB (Shen *et* al., 2011). This organelle was proposed to act as a PVC for the PSV pathway in rice. Moreover, Scabone *et* al. (2011) showed that transmembrane (TM) and C-terminal domain (CT) of *At*RMR1 fused to a RFP construct was localized in the lumen of central vacuole, in leaves, roots and embryos of *A. thaliana* transgenic plants. These results highlight the involvement of the TM-CT of *At*RMR1 in protein targeting to vacuole.

RMR proteins are encoded by six genes in *Arabidopsis* (AtRMR1 to 6) and by five genes in *Physcomitrella patens*. RMR proteins form two distinct subfamilies in Angiosperms and Gymnosperms. Single and double mutants in *At*RMR genes had no detectable phenotypes (Stigliano, PhD thesis; E. Rojo, personal communication). *At*RMR1 belongs to the subfamily 1 while the five other *At*RMRs belong to the subfamily 2. Moss RMRs form a clearly separate clade from Angiosperms and are represented by two subfamilies, the first one including RMR1 and 2, and the second one including RMR3, 4 and 5 (figure 1.11).

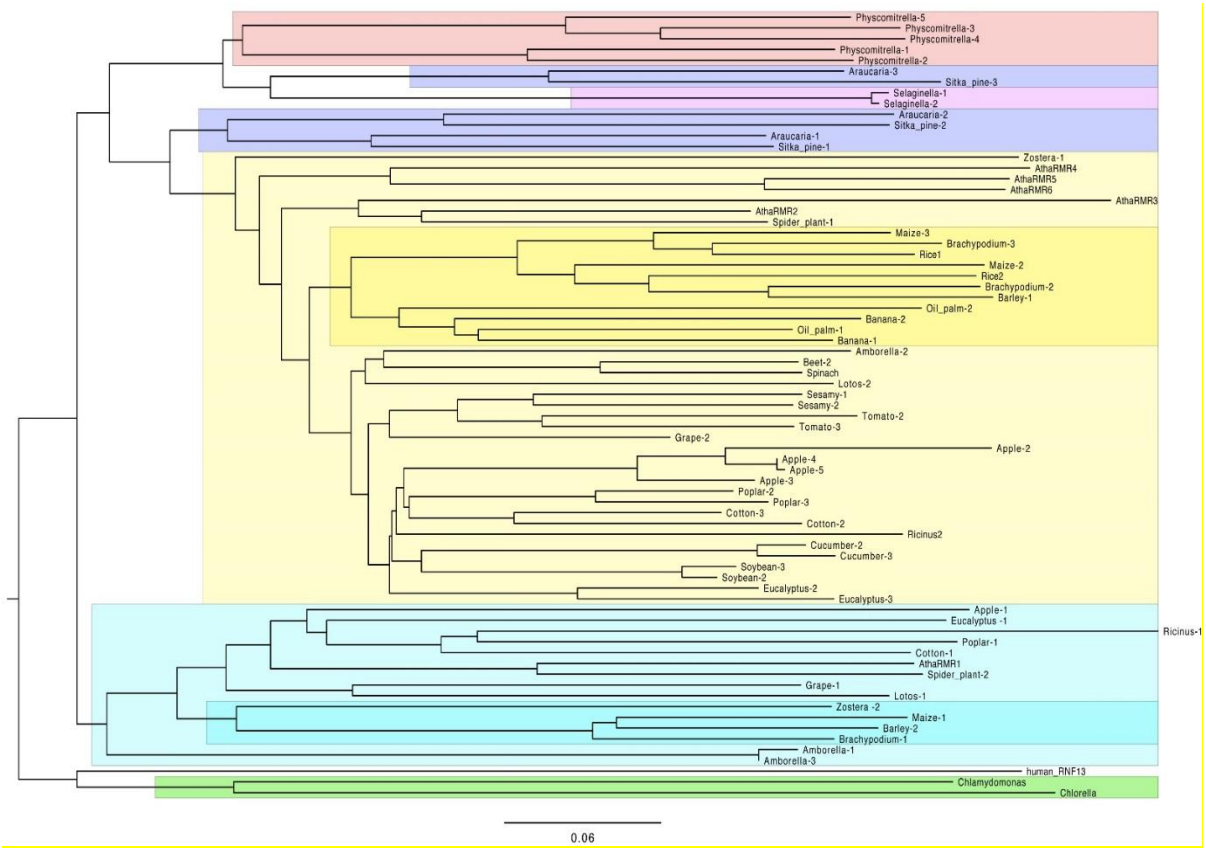

Figure 1.11 Phylogenic tree of plant RMRs. The majority of Angiosperms have two types of RMRs, *e.g. Arabidopsis*. Two sub-families of RMRs have been identified in moss.

Protease-Associated domain

VSR and RMR have in common a PA domain. It was first found as an insert in several classes of animal proteases but also in an animal hormone receptor. The PA domain is thought to serve as a regulatory domain in non-catalytic regions of protein and could form protein-protein interactions. In VSRs and RMRs the PA domain is thought to be involved in ligand binding in the lumen of the secretory pathway but its role is still unclear (Mahon and Bateman 2000; Luo and Hofman 2001). Features of PA domain were discussed more recently in different studies. It was described to play a role in prodomain processing and secretion of tomato subtilase 3; mutants in which some amino acids of the PA domain were deleted, were unable to cleave the prodomain of the enzyme (Cedzich *et* al., 2009). Luo *et* al. (2004) presented a model of how the luminal region of VSRs recognizes their cargo. In this work, the crystal structure of the PA domain of *At*VSR was determined alone and coupled with the barley aleurain VSD sequence. Conserved among various VSRs, its role in cargo recognition appears to require a highly conserved cargo binding loop. Because this loop is also present in RMRs structure, it is consistent to think that the function is also conserved. Another part of this work showed that sequence preceding

the NPIR motif of VSD is recognized by the PA domain of *At*VSR. Finally, several role of the PA domain have been proposed, as the involvement in protein/protein interaction and specifically in ligand/substrate binding or the regulation of substrate access to active site (Cao *et* al., 2000; Mahon and Bateman 2000; Luo and Hofmann 2001; Luo *et* al., 2014).

C. C-terminal VSD used in this work

C-terminal VSDs are small propeptide sequences found at the end of precursors of vacuolar proteins, which were described to be necessary and sufficient for the targeting to a vacuole. In the next section we describe in more details ctVSD previously confirmed in literature that were used during this work.

C.1 Ct-VSD of tobacco Chitinase A

Plant chitinases hydrolase chitin and chitosan, a polymer of N-acetylglucosamin and glucosamine, structural components found in a wide variety of organisms like fungi or insects. There are numerous kinds of chitinases in plants, with specific cellular localization and activity (Punja and Zhang, 1993). These enzymes play a role in resistance against pathogens but are also involved in different physiological mechanisms such as stress responses or plant growth (reviewed by Grover 2012). They can be classified according to their biochemical and molecular characteristics. A classification according to their amino acids sequence leads to several families and classes (Neuhaus 1999). In 1991, Neuhaus *et al.* worked on tobacco cells expressing two different chitinases: a class I tobacco, the chitinase A which accumulates in vacuoles, and a secreted cucumber class III chitinase. Deletion of the C-terminal propeptide of tobacco chitinase A caused its secretion, while addition of this C-terminal propeptide to the cucumber chitinase caused its accumulation in vacuoles. These results showed that the C-terminal sequence of tobacco chitinase A is both necessary and sufficient for vacuolar targeting. A fluorescent marker was then developed: the C-terminal VSD of tobacco chitinase A was fused to the GFP reporter and fluorescence was accumulating in neutral vacuoles, i.e. those that do not accumulate the dye Neutral Red (Di Sansebastiano *et* al., 1998).

C.2 Ct-VSD of barley lectin (BL)

Lectins are carbohydrates binding proteins and are produced by a wide variety of plants. They bind their ligand without altering its structure (Peumans and Van Damme, 1998). Most plant lectins

localize in protein bodies of seed cotyledons. Numerous roles were proposed for them, such as defense against pathogens or involvement in plant-microbe symbiosis (reviewed by De Azevedo Moreira *et* al., 1991). Barley lectin accumulates in specific tissues such as adult root tips and root cap cells in seedlings (Lerner and Raikhel, 1989). The functional role of the C-terminal propeptide (CTPP) (15 amino acids) was investigated and it was found to be also a VSD. Bednarek *et* al. (1990) showed that barley lectin lacking the CTPP was secreted from the cells. The cucumber chitinase was addressed to the vacuole in tobacco protoplasts, when it was fused with the C-terminal propeptide of barley lectin, (Bednarek and Raikhel, 1991).

C.3 Ct-VSD of Phaseolin

Phaseolin is one of the major glycoproteins in common bean (*Phaseolus vulgaris* L.) seeds and can represent up to 50% of the total proteins in mature seeds (Slightom *et* al., 1983). It was described to accumulate in the PSV in developing cotyledons. Frigerio *et* al. (2001) generated a phaseolin mutant where the last four C-terminal amino acids AFVY were deleted. The mutant was secreted. They also showed that the truncated peptide coupled with the fluorescent reporter GFP was secreted in the apoplast. They concluded that the C-terminal tetrapeptide AFVY is necessary for the protein targeting to the vacuole, in transgenic tobacco and in *Arabidopsis* cells.

C.4. Ct-VSD and PSI of Cardosins

Cardoon flowers (*Cynara cardunculus* L.) are used in cheese manufacture. These milk-clotting properties are due to two plant aspartic proteinases: the cardosins A and B. They share a similar structure including a PSI (Plant Specific Insert) domain, which separates the two chains of the mature form (Vieira *et* al., 2001; Pissara *et* al., 2007). Although Cardosins A and B belong to the same family, their localization, trafficking in the cell and biological role are very different and not completely resolved.

Generalities about Aspartic proteinases (APs)

Aspartic proteinases are widely distributed in the living world. They can be found in animals, plants, yeast, fungi and viruses (reviewed by Simoes and Faro, 2004). This enzyme family is involved in a broad range of biological mechanisms such as protein maturation or degradation, stress responses,

programmed cell death and defense against pathogens (Mutlu and Gal, 1999; Simoes and Faro 2004). APs are classified in different families according to their amino acid composition.

Plant APs

Plant aspartic proteinases are found all across the plant kingdom, from gymnosperms (Salmia 1981) to monocotyledonous (rice, maize) and dicotyledonous plants (*Arabidopsis*, cardoon, tobacco). First identified from seeds, they were also found in leaves, flowers and petals (Mutlu and Gal 1999). They are synthetized as a single-chain precursor and the mature form is obtained after a proteolytic maturation. Most plant APs belong to the A1 family, also found in animals and microbes, which is active at acidic pH and inhibited by pepstatin A (a potent reversible inhibitor originally isolated from an actinomyces; Umezawa *et* al, 1970; Mutlu and Gal 1999). Plant APs are tissue specific but are primarily found in vacuoles and protein bodies. In mammalian cells, Aps mostly localize in lysosomes but can also be secreted (Simoes and Faro, 2004).

Plant AP domain structure

The closest non-plant AP is the lysosomal cathepsin D which can have up to 45% amino acids sequence similarity with plant APs. Plant APs have a common structure that can be divided into three domains: an N-terminal region, a PSI domain and a C-terminal region (reviewed by Mutlu and Gal 1999; Simoes and Faro 2004). The PSI is a sequence of about 100 amino acids, which is partially or entirely removed during the maturation process of the protein. Its function was not clearly identified, but an involvement in protein sorting to vacuoles was supposed. One of the best characterized plant AP is the barley grain phytepsin (Runenberg-Roos *et* al., 1991). Kervinen *et* al. (1999) determined its structure and suggested that the PSI domain is a membrane binding region involved in vacuolar targeting. Törmäkangas *et* al. (2001) worked on phytepsin trafficking in tobacco protoplasts and showed that the deletion of the PSI domain leads to the secretion of the protein. The implication of PSI in membrane destabilization has been proposed by Egas *et* al. (2000). This work shows the capacity of the PSI domain to interact with vesicles causing leakage of their content, under acidic pH conditions.

Cardosin A

The first well-characterized cardosin was the cardosin A, localized in the pistil and which mostly accumulates in protein storage vacuoles of the stigmatic papillae (Ramalho-Santos *et* al., 1997). It was also found in lower amounts in the vacuoles of epidermal cells. It was shown that two morphologically distinct vacuoles can coexist in the same cell of stigmatic papillae (Pissara *et* al., 2007). One of the hypothetical roles for cardosin A is in pollen recognition. Two further roles have been suggested: in

flower senescence as cardosin A accumulates in these mature organs, and in pathogen defense (Ramalho-Santos *et* al., 1997; Simoes and Faro 2004; Pissara *et* al., 2007). In 2008, Duarte, Pissara and Moore showed that cardosin A can be transiently expressed and addressed to the vacuole in heterologous species, i.e. in tobacco leaves and *Arabidopsis* seedlings. This work also suggested that an N-terminal segment of the PSI domain is cleaved during the maturation process, after exportation from the ER. More recently, the PSI sequence and/or the C-terminal sequence of cardosin A were described to be sufficient to target a fluorescent reporter to the vacuole (Pereira *et* al., 2013).

Cardosin B

Even though cardosin B has a similar amino-acid composition to cardosin A, its expression drastically differs and is developmentally regulated. It is localized in the extracellular matrix of pistil cells and young inflorescences and is secreted to the cell walls (Vieira *et* al., 2001). In contrast to cardosin A, the PSI domain of cardosin B is completely removed during the protein maturation. Figueiredo *et* al. (2006) showed that cardosin B is accumulated during the programmed cell death (PCD) of the nucellus and the maturation of the embryo sac. These results suggest the involvement of cardosin B in PCD events. A function in defense against pathogens has also been proposed (Vieira *et* al., 2001).

During her PhD thesis, C. Pereira worked on the expression on the cardoon aspartic proteinase (AP) cardosin A, in heterologous systems (*A. thaliana* and *N. tabacum*). The aim of her work was the study of the intracellular transport of cardosin A to its final destination: the LV and the PSV. Results showed that cardosin A has two VSDs: the PSI (Plant Specific Insert) domain and a C-terminal sequence (ctVSD). She also observed that the ctVSD mediates the transport by the classical secretory pathway whereas the PSI domain mediates the traffic to the vacuole via a route bypassing the Golgi (Pereira 2012).

C.5 Ct-VSD and PSI of moss Aspartic proteinase

As explained before, plant aspartic proteinases are mainly found in the vacuole or protein bodies and are involved in different mechanisms such as protein processing and degradation (Simoes and Faro, 2004). In *P. patens*, Schaaf *et* al. (2004) isolated a cDNA encoding an aspartic proteinase named *Pp*AP1. This cDNA was cloned to obtain a construct of AP1 with a C-terminal GFP fusion. This homologous reporter is a good tool to explore targeting to vacuole in a seedless plant. Results showed vacuolar fluorescence accumulating in transiently transformed moss protoplasts.

D. RMR homologues

PA-TM-RING proteins, which combine PA, transmembrane domain and RING domains, have been identified in several organisms such as mammals (GRAIL; Seroogy *et* al., 2004), *Xenopus* (GREUL1; Borchers *et* al., 2002) and *Drosophila* (Goliath; Bouchard and Cote, 1993) but not in yeast (Bocock *et* al., 2009) (Figure 1.12). These homologues of RMRs are involved in various cellular functions, *e.g.* protein quality control, cell proliferation, apoptosis, immune regulation or signaling (reviewed by Nakamura 2011). The majority of these PA-TM-RING proteins possess also an apparent N-terminal signal peptide and are E3 ubiquitin ligases. In mammals, different classes of E3 ligases have been described, according to their subcellular localization. The ER localized E3 ligases target substrates for proteasomal degradation. The mitochondrial class help to maintain the mitochondrial integrity while others E3 ligases act in endocytic compartments and are involved in endocytosis or lysosomal degradation. However, E3 ligases have been described to be quite unstable because of their self-ubiquitylation activity (Nakamura 2011). The expression level of PA-TM-RING proteins is very low in mammals, suggesting specific role as molecular regulators for organization, integrity or dynamics of membrane organelles (Erickson 2011; Nakamura 2011).

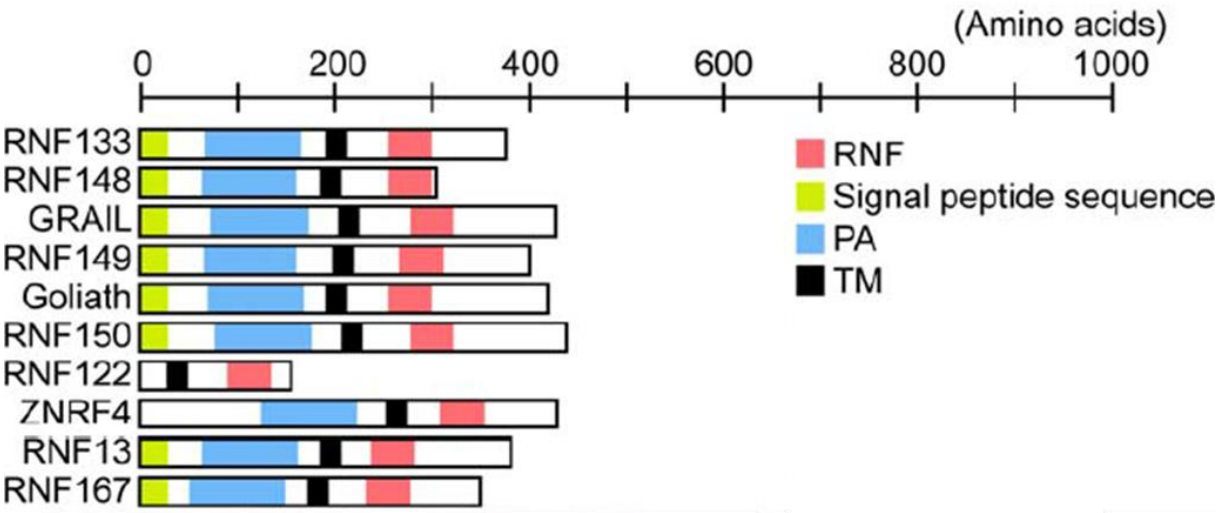

Figure 1.12 Comparison of the domain structures of various putative transmembrane RNF proteins (Nakamura 2011). PA, protease-associated domain; TM, putative transmembrane domain; RNF, Ring Finger

D.1 GRAIL (mammals)

The GRAIL protein (Gene Related to Anergy in Lymphocytes) also known as RNF128 (Ring Finger protein 128), is necessary for anergy induction (Seroogy *et* al., 2004) and is involved in primary T cells activation, survival and differentiation (Kriegel et al, 2009). Anergy is a mechanism in which the lymphocytes are functionally inactivated but remain alive (Schwartz 2003). It is an immunologic self-tolerance mechanism and is reversible. Anergic CD4 cells are unable to proliferate and their production of Interleukin 2 (IL2) is considerably diminished (Anandasabapathy *et* al., 2003). In this T cell unresponsiveness pathway, ubiquitylation and deubiquitylation are important triggering factors (reviewed by Whiting *et* al., 2011).

GRAIL is a PA-TM-RING protein composed of 428 amino acids and it is a type I transmembrane single sub-unit E3 ligase protein. It contains a highly conserved cytosolic RING-H2 finger. A mutation analysis demonstrated that an intact RING domain is essential for its E3 ligase activity. Indeed, mutation of both histidines in the RING domain, substituted by two asparagines, is enough to disturb this E3 activity (Anandasabapathy *et* al., 2003). GRAIL also has a luminal PA domain (Figure 1.13). The PA domain recognizes and captures on the luminal face of the membrane the substrate CD83, which is then ubiquitylated by the RING finger domain on the cytosolic face. As mentioned before, GRAIL expression is affected by ubiquitylation and deubiquitylation events but it is also regulated by autoubiquitylation with several K48-linked ubiquitins (Whiting *et* al., 2010).

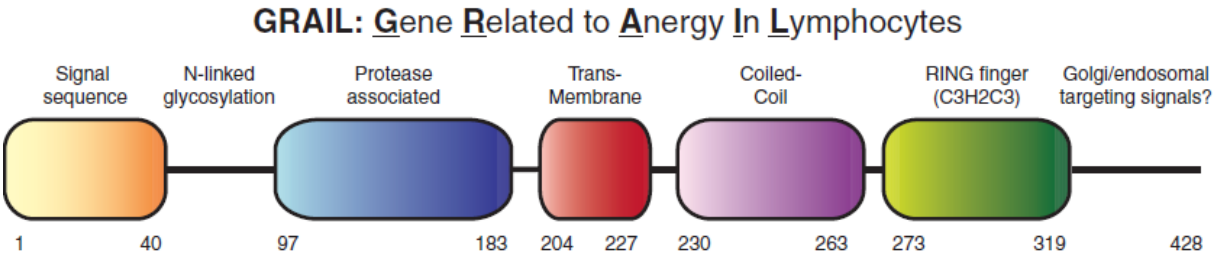

Figure 1.13 Schematic representation of the structural domains of GRAIL protein (Whiting *et* al., 2011). The RING finger domain is a RING-H2 type and functions as an ubiquitin E3 ligase. The Protease Associated domain captures transmembrane protein targets for ubiquitylation.

D.2 Goliath and Godzilla

The d-goliath was first characterized in *drosophila* as a protein with 2 zinc finger structures involved in the regulation of gene expression during mesoderm formation (Bouchard and Côté, 1993). Goliath homologues, such as m-goliath in mouse or h-goliath in human were later identified. Another member of the family, Godzilla, was also identified in *Drosophila*. Both proteins, have the PA-TM-RING domains (figure 1.14).

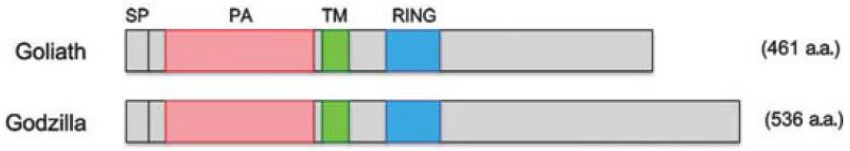

Figure 1.14 Schematic domain structure of Drosophila Goliath and Godzilla (Yamazaki *et* al., 2013): SP, signal peptide; PA, protease-associated domain; TM, transmembrane, and RING domain. Goliath and Godzilla encode endosome-localized PA-TM-RING E3 ligase

Goliath and Godzilla were localized in endosomal membrane. Goliath is specifically expressed in muscles while Godzilla shows a more general expression pattern in *Drosophila*. The high identity between their two RING domains (also conserved among the larger Goliath family) suggests conserved role and function. Yamazaki *et* al. (2013) demonstrated that mutation of the two key histidines to asparagines of the RING domain leads to the loss of ability to generate large endosome. This work highlights a role of Goliath and Godzilla in regulation of recycling endosome trafficking via ubiquitylation of target proteins. The main target of these proteins was identified as the SNARE receptor VAMP3 (Yamazaki *et* al., 2013). Furthermore E3 ligase activity was demonstrated by in vitro ubiquitylation tests (Guais *et* al., 2006).

D.3 RING Finger protein 13

RING Finger protein 13 (RFN13) was first identified in chicken (chicken RING zinc finger, C-RZF), as being over expressed in embryogenic brain cells, when growing with the addition of tenascin-C, an extracellular matrix glycoprotein (Tranque *et* al., 1996). This protein is another member of the PA-TM-RING family like GRAIL and Goliath (Figure 1.15). The RFN 13 gene is conserved in many organisms such as mammals (dog, cow) or insects (mosquito) (Jin *et* al., 2011). It is ubiquitously expressed in various

non-embryogenic tissues. In mouse, RFN13 was localized in the endosomal and lysosomal system and show to have an E3 ubiquitin ligase activity (Bocock *et* al., 2009). In other organisms, it has been found in the nucleus and/or membrane organelles like endosomes. RNF13 is one of the best known proteins of the goliath family and it may be involved in the regulation of cancer and tumor development, by ubiquitylation of various proteins. Its expression can be upregulated by myostatin and tenascin, two cellular factors associated with cell proliferation (reviewed by Jin *et* al., 2011). RFN13 has also a nuclear-localization signal and may traffic to the inner nuclear envelope in response to a signal (Bocock *et* al., 2009).

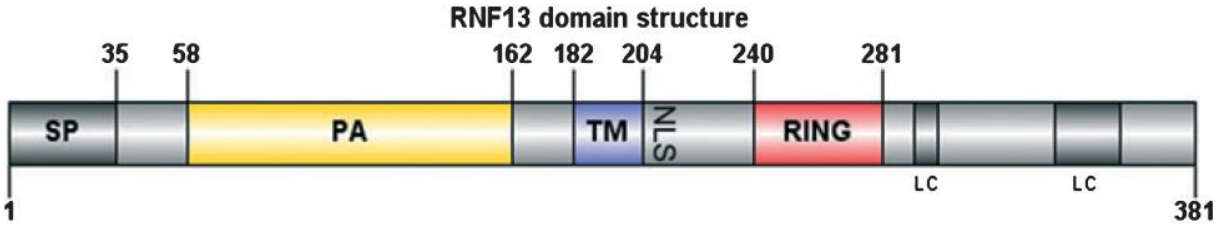

Figure 1.15: Schematic structure of RNF13 protein (Jin *et* al., 2010).
SP, signal peptide; PA, protease-associated domain; TM, transmembrane region; RING, RING finger domain; NLS, nuclear localization signal; LC, low complexity.

D.4 Other PA-TM-RING proteins

There are numerous other PA-TM-RING proteins, mainly identified in mammals, involved in various cellular functions, depending of their subcellular localization. Some are acting in proteins degradation mechanism in the ER, like RNF170 or RNF122, playing a role in ubiquitylation of ERAD substrate or calcium signaling and ubiquitylation, respectively. Other PA-TM-RING proteins were observed to be involved in apoptosis. RNF182 is a pro-apoptotic factor regulating pH homeostasis. RNF152 is a lysosomal E3 ligase with a pro-apoptotic and a self-ubiquitylation activities (reviewed by Nakamura 2011).

E. RMR proteins and ubiquitylation activity: a key role for the RING domain?

The ubiquitin system plays an important role in diverse cellular functions. Its best known implication is as label of proteins for the degradation pathway by proteasomes (Hershko 1988; Hershko and Ciechanover 1998). However, ubiquitin is also involved in non-proteolytic processes, such as proteins internalization into the endocytic pathway (Kölling and Hollenberg 1994), translocation of membrane proteins to the internal vesicles of late endosomes by the ESCRT system (reviewed by Reyes *et* al., 2011) or DNA repair and kinase activation in mammalian cells (reviewed by Hofmann 2009).

E.1 Ubiquitylation mechanism

Ubiquitin is a highly conserved protein of 76 amino acids, found in all eukaryotic organisms. Ubiquitylation consists of the covalent attachment by the C-terminus of one (or several) ubiquitin to the ε-amino group of a substrate lysine. Ubiquitylation is ATP-dependent and requires a cascade of three enzymes: E1, the ubiquitin activating enzyme; E2, the ubiquitin conjugating enzyme and E3, the ubiquitin ligase enzyme (reviewed by Varshavsky 1997; Guerra and Callis, 2012) (Figure 1.16). Firstly, E1 activates the ubiquitin by using ATP hydrolysis, to form a high-energy thioester bond between the C-terminal glycine of ubiquitin and a cysteine of the E1 enzyme. Activated ubiquitin is then transferred to a cysteine residue of an E2 enzyme by a transesterification reaction. The last step consists of the ubiquitin delivery by the E3 ligase to the protein substrate. The substrate is recruiting by the E3, which initiates the conjugation (reviewed by Varshavsky 1997; Vierstra 2003).

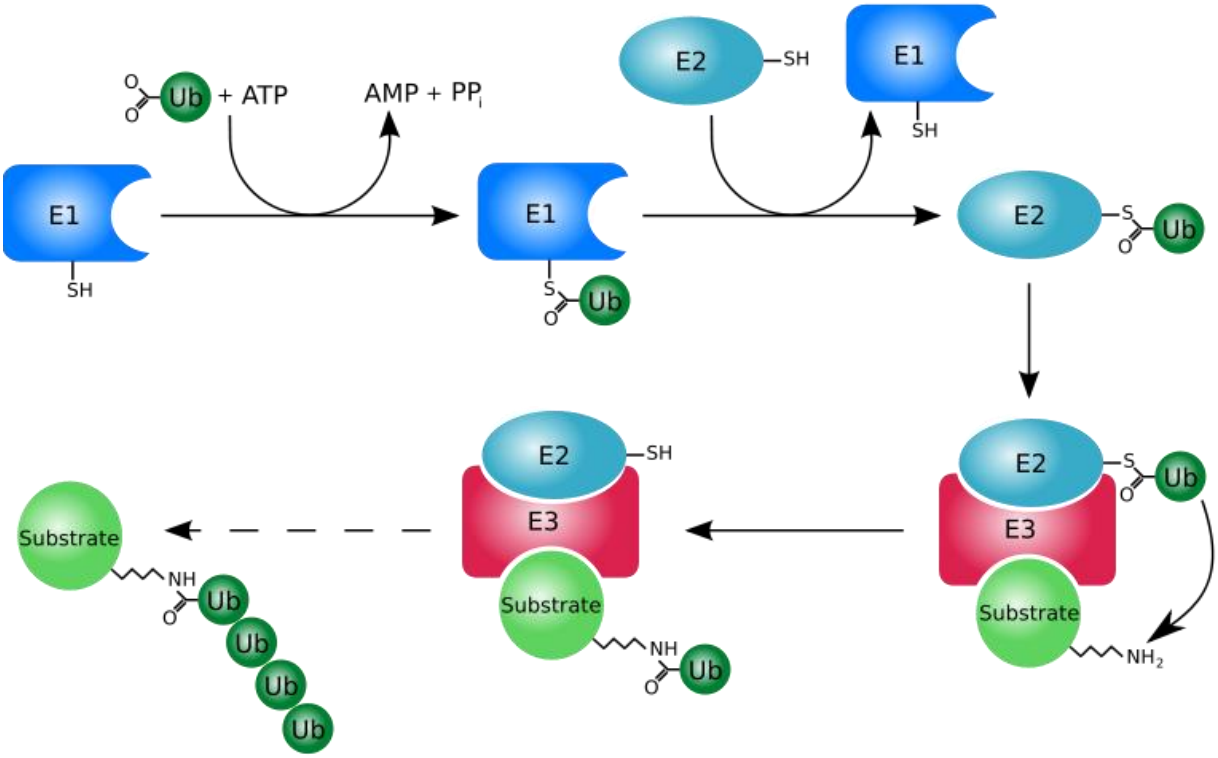

Figure 1.16 Schematic representation of the ubiquitylation enzyme cascade (from Ubiquitylation.svg and Guerra and Callis, 2012). E1 activates ubiquitin at the expense of two ATP equivalents by forming a high-energy thioester bond between the E1 active-site Cys and the C-terminus of ubiquitin. Ubiquitin is then passed to an active-site Cys on E2. Then, the ubiquitin-E2 thioester bond is brought into proximity of the desired protein target by the E3 ligase, which then transfers ubiquitin to a lysine. Many E3 can polyubiquitylate the substrate.

E.2 Different ubiquitin tags for diverse purposes

The number of linked ubiquitins and at which lysine they are linked to each other can vary. Three types of ubiquitin tags have been described: monoubiquitylation, multiubiquitylation and polyubiquitylation. These different tags target proteins to different pathways in the cell (Figure 1.17).

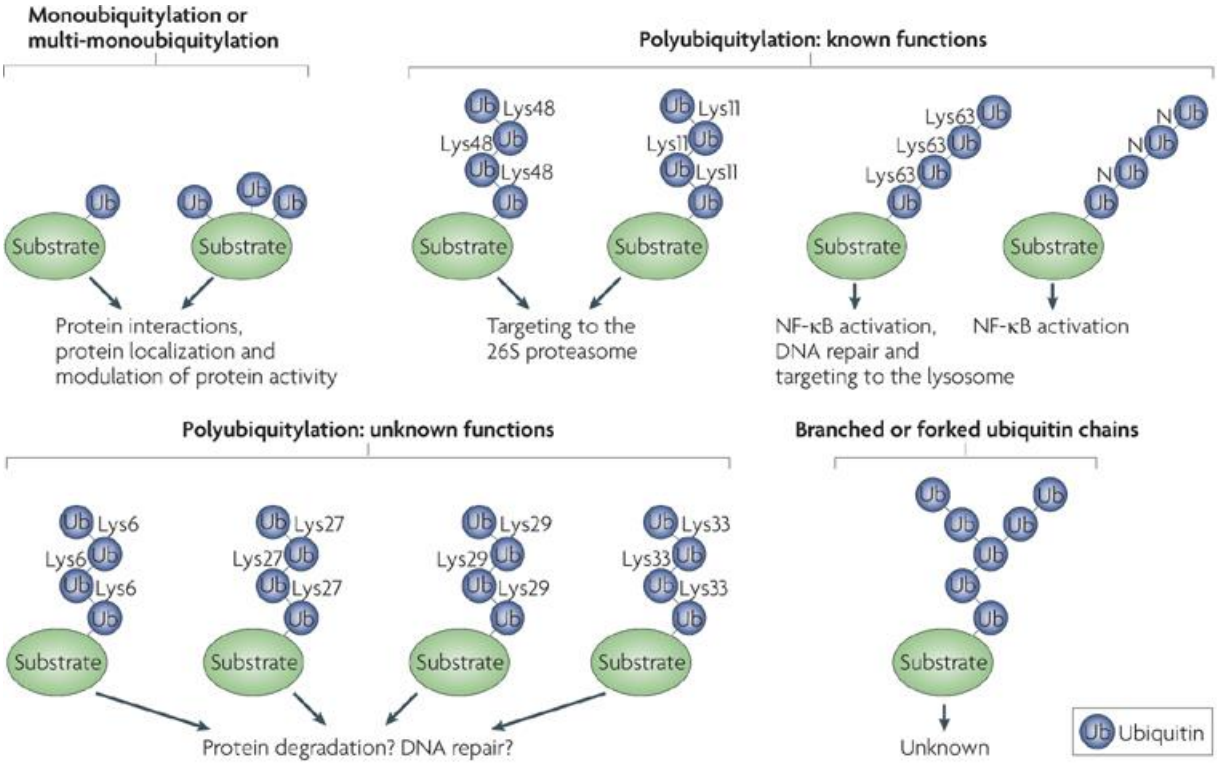

Figure 1.17 Different tags of ubiquitylation and outcome of marked proteins (Ye and Rape, 2009)

A pyramid of ubiquitylation allows specific regulated ubiquitylation of many different substrates. In *Arabidopsis*, ubiquitin is activated by two different E1, 37 different E2 and more than 1500 different E3 (Vierstra 2012). Polyubiquitin chains linked via Lys-48 and Lys-11 are the signal for proteasome degradation. Multiubiquitylation is a sorting signal for internalization into the endocytic pathway (Kölling and Hollenberg, 1994). Monoubiquitylation is a signal for the transfer of transmembrane proteins to internal vesicles within multivesicular bodies (MBV) (Katzmann et al, 2002). Polyubiquitylation via Lys-63 is a tag for endocytosis (Reviewed by Piper and Lehner 2011; Lauwers et al., 2010; Katzmann et al., 2002).

E.3 RING domain and ubiquitylation: the E3 ligases family

The ubiquitin tag is involved in broad and diverse roles in many cellular mechanisms. Numerous E3 ligases have been identified among eukaryotes providing the specificity of their function and mode of action. Three major families have been described in eukaryotes: the RING, the HECT and the U-box proteins.

RING E3 ligases

RING E3s are the largest E3 subfamily known to date. They can be considered as molecular scaffolds, helping other proteins to interact and transferring directly the ubiquitin tag from E2 to the substrate. RING domains bind the E2 enzyme through the loop region with zinc coordination and the central helix (Deshaies and Joazeiro 2009; Pickart 2001). This 70 amino acids RING domain is cysteine-rich, zinc-biding domain and can be considered as protein-interaction domain. A conserved pattern of cysteine and histidine residues coordinate two zinc ions (Borden 2000; Kosarev *et* al., 2002) (Figure 1.18).

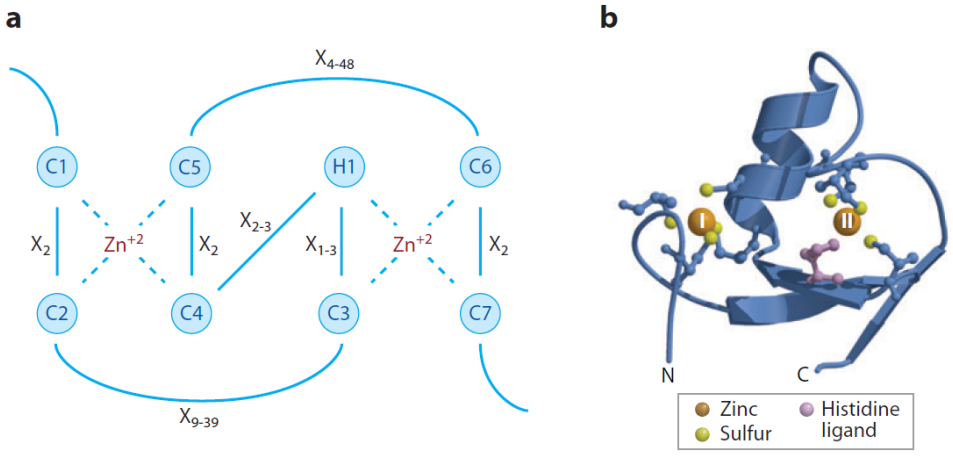

Figure 1.18 The RING finger domain (Deshaies and Joazeiro, 2009)

a. Primary sequence organization of the RING-HC domain. The first cysteine that coordinates zinc is labelled as C1, and so on. H1 denotes the histidine ligand. Xn refers to the number of amino acid residues in the spacer regions between zinc ligands.
b. Ribbon diagram of the three-dimensional crystal structure of the RING domain from protein c-Cbl. The zinc atoms sites I and II are numbered.

In sub-family RING-H2, the cysteine in position 5 is substituted by a histidine (Borden and Freemont 1996; Borden 2000). Many RING domains have intrinsic E3 activity, but some do not (Deshaies and Joazeiro, 2009). In other proteins, RING domains are also involved in various mechanisms, such as signal transduction, transcription and protein-protein interactions (Borden and Freemont, 1996). RING E3 ligases can function as oligomers and can multimerize to form heterodimers, like Mdm2-Mdmx, which interacts with tumor suppressor in mouse (reviewed by Deshaies and Joazeiro 2009; Linares *et* al., 2003). Different structural types of RING E3 ligases have been observed. Some are single subunit E3 like cCbl, which activates Tyrosine Kinase Receptor (*e.g.* EGF receptor). Deletion or mutation in the RING inhibits the EGF dependent-EGFR degradation. Others are multi sub-units E3 (*e.g.* APC), where the substrate recognition occurs by one of the separate subunit (reviewed by Deshaies and Joazeiro, 2009).

RING E3 ligases can be regulated in several ways. Substrate or E2/E3 modification by phosphorylation/dephosphorylation can directly enhance or decrease the ubiquitylation activity. Many RING E3 are ubiquitylated by autocatalytic processes but this down regulation could be also mediated by a distinct E3 ligase (Deshaies and Joazeiro, 2009).

HECT E3 ligases

The HECT domain, possessing an intrinsic catalytic activity, is composed of about 350 residues, and can be divided in two distinct sub-domains, the N-terminal and the C-terminal lobes. The larger N-ter lobe is the binding site of the E2 enzyme and is connected by a flexible region to the smaller C-ter lobe, where the active site cysteine residue is found (Bernassola *et* al., 2008). In mammals, the HECT family is composed of about 30 E3, and the first member identified was E6AP (also known as UBE3A), an enzyme involved in tumorigenesis and brain development (reviewed by Metzger *et* al., 2012). The best characterized sub-group of HECT enzyme is the C2-WW-HECT, conserved from yeast to mammals, containing a tryptophan-tryptophan domain and involved in the regulation of endocytosis and trafficking via polyubiquitylation. In general, HECT E3 may be implicated in oncogenic regulation because many already identified protein substrates are tumor suppressor molecules (Bernassola *et* al., 2008).

U-box E3 ligases

The U-box domain is a 70 amino acids sequence, found in yeast and mammals, with architecture similar to the RING domain, without metal ions. This molecular scaffold does not contain zinc binding zone but a network of hydrogen bonds and salt bridges instead. U-box domain possesses an E2 binding surface and some sites for chaperone binding (especially from heat-shock protein family). Deletion or mutation in this domain leads to the loss of ubiquitylation activity (Hatakeyama *et* al., 2001). The most studied U-box E3 ligase is CHIP (also known as STUB1), which is thought to take part in protein folding and degradation by ubiquitylation, and acts probably as a co-chaperone. Previous studies showed that CHIP is a mediator of cytosolic protein quality control, involved in ubiquitin-proteasome system degradation. It targets proteins for proteasomal degradation in combination with HSP70 and takes part in glucocorticoid receptor ubiquitylation when interacting with HSP90 (Hatakeyama *et* al., 2001; Metzger *et* al., 2012).

F. The moss *Physcomitrella patens*

F.1 *P. patens* as an experimental model

P. patens is a bryophyte and a member of the *Funariaceae* family. Its life cycle, significantly different from flowering plants, is characterized by an alternation of generations, where the haploid stage (the gametophyte) is dominant. *P. patens* is used as a model organism in plant biology, genetics and development. It has numerous advantages for biological studies because of its interesting phylogenetic position. More than four hundred millions years ago, mosses and vascular plants diverged but they still have genetic and biological mechanisms in common (Cove and Knight, 1993). The study of moss will allow understanding processes involved in the evolution between higher and lower plants. In this way, *P. patens* is an ideal tool for the comprehension of the development of flowering plants such as *Arabidopsis thaliana*.

Mosses and higher plants share many physiological and molecular mechanisms, e.g. the regulation of their development by similar hormones (auxins, cytokinins, abscisic acid; Cove 1997) or stress responses (Machuka *et* al., 1999). Therefore we can suppose that other processes are conserved, such as the functioning of the secretory system. We can postulate that cellular mechanisms involved in vacuolar targeting are also conserved between mosses and flowering plants. Moreover, *P. patens* can be quickly and easily grown with *in vitro* culture and the protonema stage allows studies at the single cell level. One of its biggest advantages for genetic studies is the high frequency of site-specific integration of a foreign DNA in its genome by means if homologous recombination. *P. patens* protoplasts have a high regenerative capacity and because of this, they are an excellent plant material for genetic transformation.

F.1.a Life cycle

The life cycle of *Physcomitrella patens* is dominated by the haploid gametophyte (Figure 1.19). The first tissue developing from the spore is the filamentous protonema. It is composed of two cell types:

- Chloronema cells, characterized by the presence of abundant chloroplasts and a cell wall between adjacent cells perpendicular to the filament axis.
- Caulonema cells, characterized by the presence of fewer chloroplasts and an oblique cell wall between adjacent cells (Cove and Knight 1997).

These two filament types grow by the extension and division of the apical cell. Caulonema cells grow rapidly and play an adventitious role, while chloronema cells develop more slowly and assume an assimilatory role for the plant (Cove 2005).

Study of chloronema growth has shown that the cells elongate by a polarized process called tip growth. In this case, growth occurs only at the tip of the cell. This mechanism is found in various walled cells such as pollen tubes or root hairs (Menand *et* al., 2007). Protonema cells are a very convenient biological material for studies which allow to easily isolated protoplasts for transiently genetic transformation. The initial meristem of the gametophore (also called bud) is formed by the development of one lateral sub-apical cell from the caulonema. It forms the different parts of the gametophore:

- basal pigmented cells called rhizoids, allowing mosses to anchor in the soil and to absorb nutrients and water.
- leafy moss shoots with both male (antheridia) and female (archegonia) reproductive organs.

The zygote formed by gamete fusion develops into a diploid sporophyte, including a capsule containing numerous haploid spores (up to 4000).

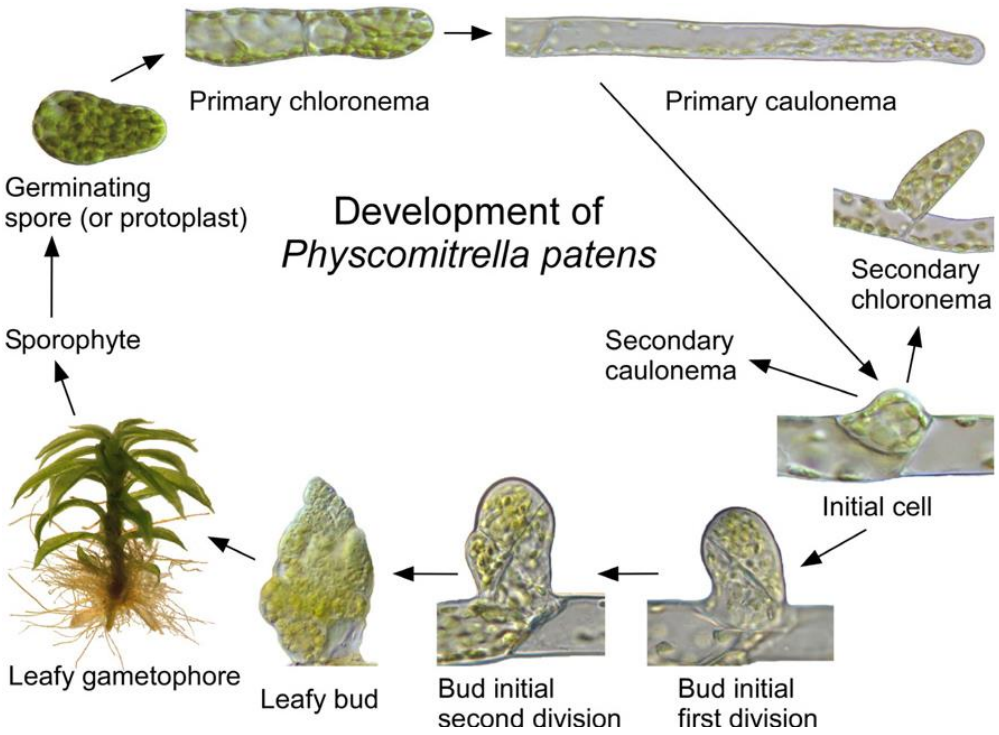

Figure 1.19 Development of *Physcomitrella patens* (Roberts *et* al., 2012).

A haploid spore or protoplast germinates to form a primary chloronema which subsequently differentiates into a more rapidly growing primary caulonema. The caulonema subapical cells divide to produce initials cells, which develop into lateral secondary chloronemata, secondary caulonemata (not shown), or buds. Buds develop into leafy gametophores, which produce apical gametangia. Fertilization of an egg by swimming sperm at the gametophore apex produces a zygote, which develops into a diploid sporophyte consisting of a stalk and sporangium (not shown). Meiotic divisions within the sporangium generate haploid spores.

The sporophyte is generally develops at the end of summer while spores appears overwinter. Antheridia and archegonia are found on the same shoot and self-fertilization is frequent (Cove 2005). Favorable conditions for gametogenesis are short days combined with a temperature lower than 18°C. *P. patens* can grow *in vitro* on a mineral media, under discontinuous light and at 25 degrees Celsius. The complete gametophyte development requires about 8 to 10 weeks and the production of spores 3 to 4 months (Cove 1997; Schaefer *et* al., 2001).

F.1.b Genome

Most laboratories working with *P. patens* use the wild-type (WT) strain *Grandsen* which originated from a single spore isolated in England (Schaefer 2002). *P. patens* has 27 small chromosomes per haploid genome and its genome size is about 480 Mbp (Reski 1994). It was

completely sequenced and published in 2008 (Rensing *et* al., 2008). Approximately 364 000 ESTs are available and 38 000 transcripts were predicted or mapped (www.cosmoss.org). Mosses diverged from the common ancestor with flowering plants about 400 million years ago. Phylogeny studies have shown that *P. patens* shares a homology of 66% of genes with *Arabidopsis* (Nishiyama *et* al., 2003). Mosses have an interesting phylogenic position and represent a major element to understand the early evolution of land plants. The three bryophytes lineages (liverworts, mosses and hornworts) diverged before the ancestral lineage of vascular plants. The common ancestor of land plant was proposed to be a leafless axial gametophyte with a simple sporophyte (Ligrone *et* al., 2012).

F.1.c Homologous recombination and gene targeting in *P. patens*

One of the major reason to use *Physcomitrella patens* as a genetic tool in our laboratory is the high gene targeting efficiency by homologous recombination (Schaefer 2001; Schaefer 2002; Kamisugi 2006). Gene targeting consists in the replacement of a specific sequence in a genome by a foreign DNA sequence (or part of a sequence) through homologous recombination (HR). This mechanism could be a Knock-out (deletion or mutation in the targeted gene leading to its inactivation) or a Knock-in (insertion of a foreign sequence). The most employed method to obtain stable transformants by HR in *Physcomitrella* is the PEG-mediated DNA transfer to protoplasts (reviewed by Hohe *et* al., 2003). HR requires genetic constructs to contain sequences homologous to the targeting locus in the moss genome (figure 1.20). Hohe *e*t al. (2003) showed that the use of a linear DNA is decisive to increase the proportion of stable transformants. Indeed, protoplasts transformation with circular DNA leads to a high number of unstable transformants. Illegitimate recombination can occur in *P. patens* genome but at a very low efficiency (reviewed by Schaefer 2002). Moreover, numerous copies of the transgene can be integrated during the same event of transformation (Kamisugi 2006).

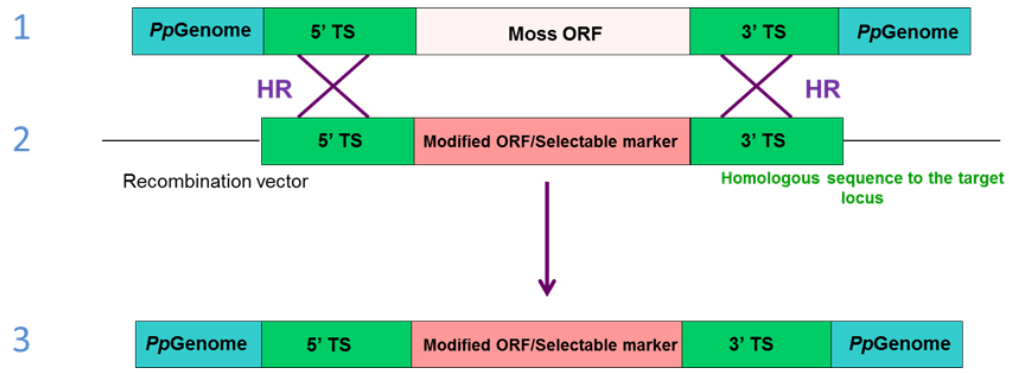

Figure 1.20 Principle of the homologous recombination in the moss genome via a recombination vector

1: The WT locus in the moss genome: with an Open Reading Frame and the 5' and 3' extremities

2: The replacement vector: with a modified ORF, a selectable marker and 5'/3' homologous sequences

3: After homologous recombination: replacement of the moss WT ORF by the modified ORF cassette

Cre/ Lox System

We will use the Cre/Lox system recombination for the elimination of the selectable marker. This system represents a very interesting tool in plant biotechnology, allowing specific mutations in the genome (Schaefer, 2002). The Cre/Lox system is composed by the Cre recombinase, the enzyme that catalyzes the recombination between two specific recognition sites, the LoxP sites (Nagy, 2000). Two LoxP sites flank the sequence that will be excised by the Cre recombinase. This Cre/Lox mechanism was discovered in the bacteriophage P1. In our working strategy of targeted mutagenesis, LoxP sites have to be integrated in our vector design. The Cre/Lox system allows also the elimination of multiples tandem insertions of the recombination cassette and of the selectable marker.

F.1.d RNAi in moss

Numerous endogenous siRNA (short interfering) and miRNA (micro interfering) are expressed in moss. These non-coding RNAs act as regulatory factors in the cell (Quatrano *et* al., 2007). Previous work underlined that gene targeting is sometimes ineffective when the gene of interest belongs to a large family because the function can be redundant with the other members. In this case, RNAi can be used as an efficient system to silence genes (Bezanilla *et* al., 2003). It has been shown in moss that multiple member gene of a family can be silenced at the same time. This tool to obtain moss mutants is an interesting way to study the effect of gene families, particularly when single gene mutations do not lead to a visible phenotype (Cove 2005; Bezanilla *et* al., 2003).

F.1.e Abiotic stress tolerance in moss

Gene targeting is an efficient strategy to investigate the abiotic stress tolerance in moss. Frank *et* al. (2005) showed that *Physcomitrella* displays a high degree of tolerance to salt, osmotic and dehydration stress, in comparison to *Arabidopsis*. The analysis of chlorophyll content after stress recovery indicates that *Physcomitrella* can tolerate up to 350mM NaCl while *Arabidopsis* is limited to 100mM. Mosses have also a high tolerance to severe water loss. Gametophytes and protonema are able to recover even after a loss up to 92% of their fresh weight. By a cDNA micro-array approach, it was found in *Physcomitrella* some genes related to stress responses, homologous to *Arabidopsis*. This work allows to confirm that some stress mechanisms are conserved between mosses and higher plants.

F.2 The moss vacuole

F.2.a Different kind of vacuoles

As described for higher plants, e.g. *Mimosa* or *Mesembryanthemum*, two kind of vacuole can coexist in the same cell (Epimashko *et* al., 2004). Observations of protonema cells after Neutral red (NR) staining show that this is also the case in *Physcomitrella patens*. Neutral red is a vital stain which was first observed to accumulate in lysosomes of animal cells. This dye is also a pH indicator, changing from yellow to red with lower pH. NR is able to diffuse through the PM and the tonoplast of living cells. It is protonated in acidic compartments such as the vacuolar lumen in plants, where it is then trapped. This dye is widely used in light microscopy (reviewed by Oparka, 1991; Dubrovsky *et* al., 2006). Acidic vacuoles are stained red while neutral vacuoles do not accumulate the dye. In apical cells of chloronema, these two type of vacuoles can be observed in the same cell (Figure 1.21).

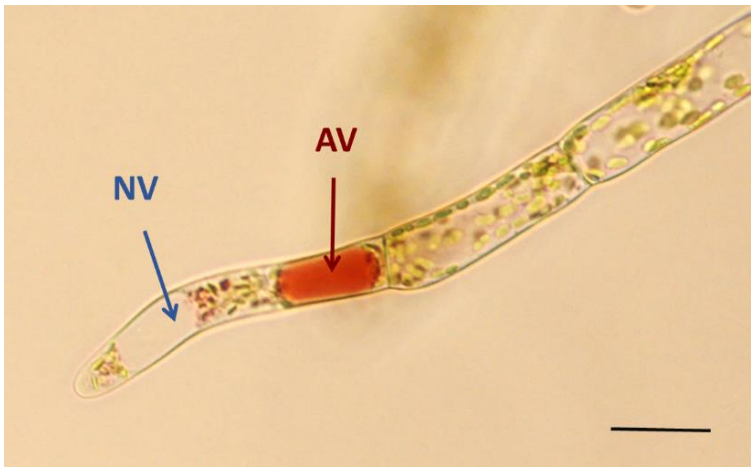

Figure 1.21 Two types of vacuoles can coexist in the same cell

Neutral (NV) and Acidic vacuole (AV). Neutral Red staining of protonema (chloronema) cells of *P. Patens*, observation in light microscope. Scale bar = 50µm

F.2.b Vacuole structure and dynamics

In animal cells, the distribution and the arrangement of some organelles, like the ER and the Golgi, have been observed to be regulated by the microtubules. In higher plants, this mechanism was described to be dependent on actin filaments. Oda *et* al. (2009) studied the vacuole organization in *P. patens* and more particularly the interaction between cytoskeletal structures and vacuolar membranes. They observed that moss vacuoles are dynamic structures, with inner sheets and tubular protrusions, especially in elongating cell tips. This worked demonstrated that contrary to flowering plants, microtubules were necessary to maintain vacuolar structures in moss. Visualization of tonoplast using fusion a construct expressing GFP and an *A. thaliana* t-SNARE AtVAM3, allowed to observed vacuolar membranes and other structures such as sheet-like and tubular components. In chloronema cells, observations showed that the vacuolar organization is simpler in sub-apical cells than in apical cells. Vacuoles of moss apical cells have a structure and a dynamics linked with their feature of tip growth. The close relationship between vacuoles and microtubules in moss emphasizes the evolutionary divergence, contrasting with the mechanisms observed in higher plants (Oda *et* al., 2009). Chloronema and caulonema cells display a different organelle composition, in accordance to their respective function. Chloronema cells present a high number of vacuoles and the organelles distribution is homogenous. On the opposite, most of the time caulonema cells show one basal vacuole and a different cytoplasmic repartition of organelles (Furt *et* al., 2012).

F.3 Quintuple RMR Knock-Out lines

In order to characterize the function of RMR proteins, single, multiple and quintuple RMR Knock-Out (KO) lines of *P. patens* have been generated by S. Ayachi during her PhD thesis (Ayachi 2012). Unfortunately, these mutants do not show any obvious phenotype (figure 1.22).

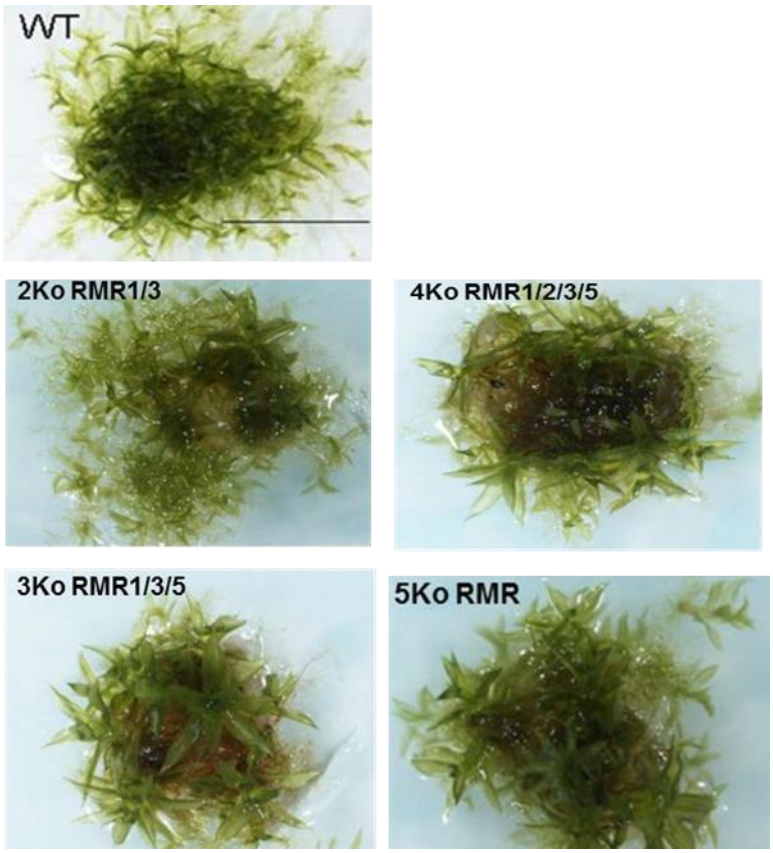

Figure1.22 WT and RMRs mutant lines (from Ayachi, 2012). Scale bar 5 mm. Light microscopy.

RMR locus deletions were done by gene targeting of each *Pp*RMR, eliminating the whole open reading frame (ORF). Replacement vectors carried a resistance cassette between two homologous sequences and two LoxP sites. Elimination of the resistance cassette was done using the Cre/Lox system, allowing to use it again for the next transformation.

S. Ayachi observed in 5 KO mutant lines that the pattern and the number of acidic vacuoles were not affected by the gene deletion (Ayachi 2012). The presence of neutral vacuoles was also observed in the mutants. 5KO mutant lines showed no abnormal developmental phenotype. In the following work, single KO *rmr2* or *rmr5*, triple *KO rmr2/rmr3/rmr5* and quintuple KO were used.

G. Aim of this thesis

Vacuoles are multifunctional organelles, essential for plant growth and development. They are involved in many cellular functions, from the maintenance of homeostasis to the storage of diverse molecules. Different kind of vacuoles can coexist in the same cell. Many studies concerning the role of the lytic/acidic vacuoles have been done but less is known about the traffic of proteins to the storage/neutral vacuole. So far, in higher plants, evidence are accumulating about implication of RMR proteins in vacuolar targeting but their mechanisms of action are still unclear.

The present research aims to elucidate the role of RMR proteins in the moss *Physcomitrella patens.* The deletion of the five genes coding for RMR proteins did not lead to any developmental phenotype. The first part of this thesis deals with the moss secretory pathway and the development of a fluorescent reporter library. Phenotypic analysis of transgenic lines will help us to understand some of the evolutionary mechanisms that occurred during plant land evolution. The second part of this work is focused on the characterization of the five Knock-out RMR mutants. Our work hypothesis is that RMRs may act as vacuolar receptors targeting proteins to the neutral/storage vacuole. Finally, to complete this investigation about RMRs function, we identified some putative partners of the cytosolic part of *Pp*RMR2.

Chapter 2
Study of the secretory system in moss: fluorescent reporters library

In plants, the secretory pathway consists of several organelles, from the ER to the vacuole, involved in the synthesis, maturation and targeting of proteins to their final destination within the cell. Vacuoles are considered as one of the endpoints of the secretory pathway. However, the majority of studies on this topic has been done in flowering plants and much less is known about seedless plants. *Physcomitrella patens* is a very suitable model for studying cellular mechanisms in lower plants and to better understand the evolutionary processes leading to current flowering and no-flowering plants. The highly efficient homologous recombination allows precise knock-out of genes, but also gene replacement, insertion of a reporter sequence into a gene to obtain a fusion protein of insertion of a reporter gene into a selected non-coding locus to obtain reproducible expression. Moreover, the filamentous structure of protonema is very appropriate for studies at the sub-cellular level. In fact, heterologous fluorescent markers can be expressed by insertion of the coding sequence, targeting non-coding loci (Schaefer 2001; Schaefer 2002; Kamisugi 2006). Filamentous cells of protonema facilitate the microscopic observations, allowing studies at single cell level.

Fluorescent reporters have already been generated by S. Ayachi (a previous PhD student) in order to visualize organelles of the secretory pathway in *P. patens.* Typical ER patterns showing reticulated structures and the nuclear envelope were observed with the P6-YFP marker. Golgi and TGN reporters (GONST1-YFP and Venus-SYP61) were also used, showing respectively punctate pattern and dynamics dots (Ayachi 2012). In this thesis, other fluorescent reporters were developed in order to supplement this library. A heat-shock promoter was used for all the new constructs. It facilitates the observation of protein transport within the cell. Moreover, all the constructs were addressed to the non-coding locus, called 108 in the moss genome (Schaefer and Zrÿd, 1997).

A. General secretory system markers

A.1 Reporter for the endoplasmic reticulum

As described previously, the ER reporter already available in our lab is a fusion protein of YFP and the P6 protein, which is anchored in the ER membrane, with a cytosolic domain (Peremyslov *et* al., 2004). To complete this work, we attached the C-terminal KDEL sequence to the fluorescent protein Citrine. This KDEL sequence is known to be sufficient to retain soluble proteins in the ER (Denecke *et* al., 1992; Pagny *et* al., 1999). Transgenic lines expressing the Citrine-KDEL fusion were generated. Confocal microscopic observations of protonema cells showed a reticular fluorescent pattern typical of ER, 24 hours after heat-shock induction. The nuclear envelope, which is continuous with the ER was also visible (figure 2.1).

Previously, Schaaf *et* al. (2004) also showed that a GFP-KDEL fusion was retained within the endomembrane system in transiently transformed moss protoplasts. We confirmed this pattern in our stable fluorescent line.

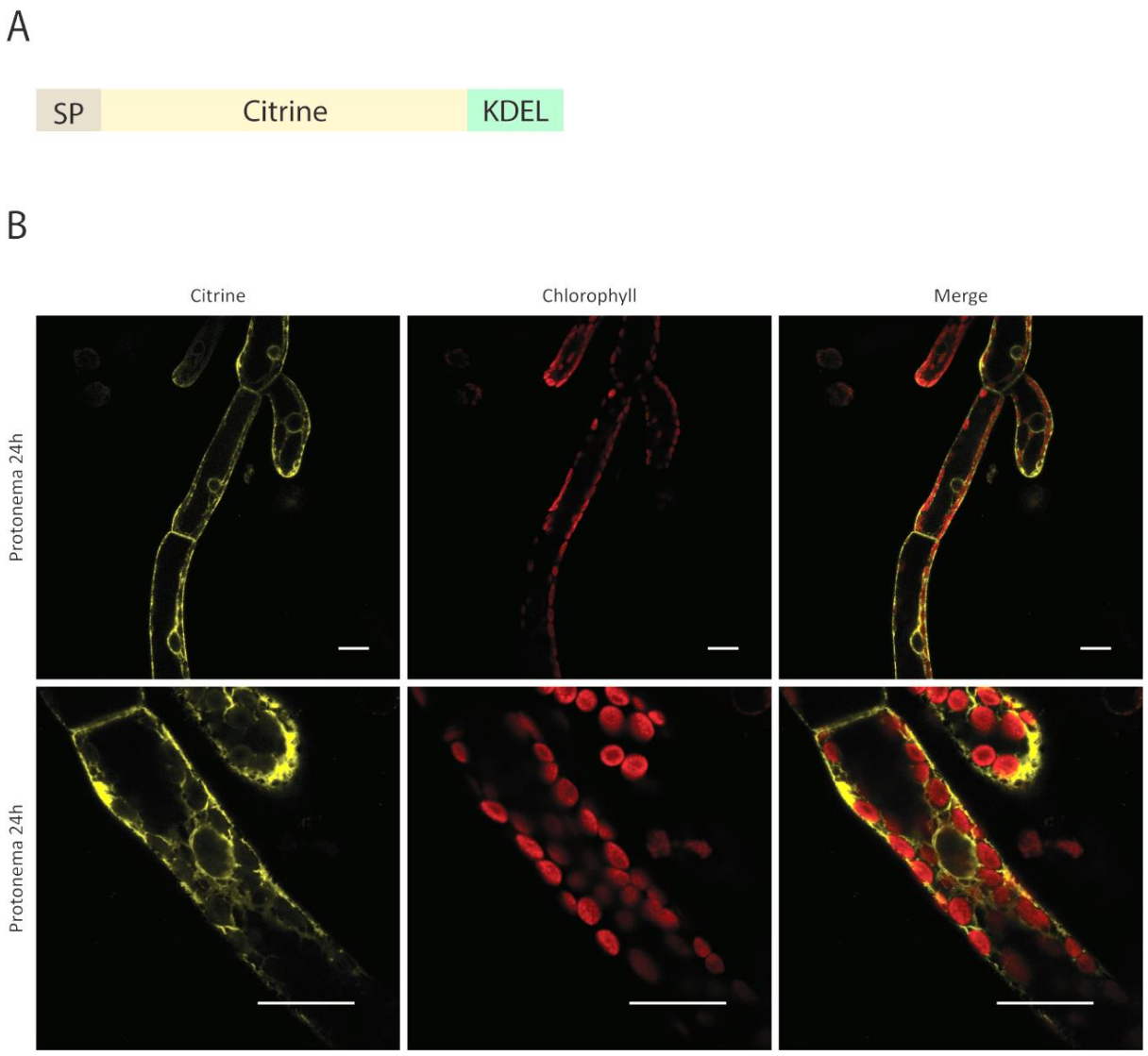

Figure 2.1 KDEL sequence is retained in the ER in *P. patens*

(A) Schematic representation of the Citrine-KDEL fusion construct. The KDEL sequence was fused to the C-terminus of the Citrine. The signal peptide came from the *A. thaliana* chitinase I.

(B) Fluorescence was observed in a typical ER pattern (left hand panel). Chloroplasts were visualized by the chlorophyll autofluorescence (center panel). The merged image shows the superposition of Citrine and chlorophyll (right hand panel). Observations were made on protonema 24 hours after heat-shock induction. Scale bar = 20 µm.

A.2 Reporter for the acidic vacuole

Many studies described the presence of different types of vacuole within a same cell (Hoh *et* al., 1995; Paris *et* al., 1996; Vitale and Raikhel 1999; Epimashko *et* al., 2004). Acidic and neutral vacuoles were observed using Neutral Red staining, in flowering plants but also in moss. Cathepsin H, a lysosomal enzyme in mammalian cells, has a high degree of similarity with aleurain (Rogers *et* al., 1985). Barley aleurain is a thiol protease found in acidic vacuoles and involved in the mobilization of reserves during seed germination (Holwerda and Rogers, 1993). This enzyme is synthetized as a proenzyme which is processed in two steps to it mature form, and which passes through the Golgi before reaching its final destination, the so-called aleurain-containing vacuole (Holwerda *et* al., 1990). Barley aleurain contains an ssVSD within its N-terminal propeptide, causing its sorting to the acidic vacuole. Exchange of this propeptide with the propeptide of another secreted thiol-protease (EP-B), caused secretion of aleurain and vacuolar targeting of EP-B (Holwerda and Rogers, 1992). *A. thaliana* Aleurain (*At*Aleurain) also has a similar ssVSD within its propeptide and is also addressed to the acidic vacuole (Zouhar and Rojo, 2009).

A transgenic moss line expressing *At*Aleurain-GFP showed a central vacuole labelling, correlated with the large vacuole stained by neutral red (Ayachi 2012). In this thesis, transgenic lines expressing *AtAleurain-Citrine* were generated. To confirm the vacuolar targeting previously described by other studies, the fluorescent protein Citrine (a variant of YFP) was chosen because of its better tolerance to an acidic environment. Confocal observations of protonema cells 24 hours after heat-shock induction indeed showed a vacuolar labeling. The same pattern was observed in leaves (Figure 2.3).

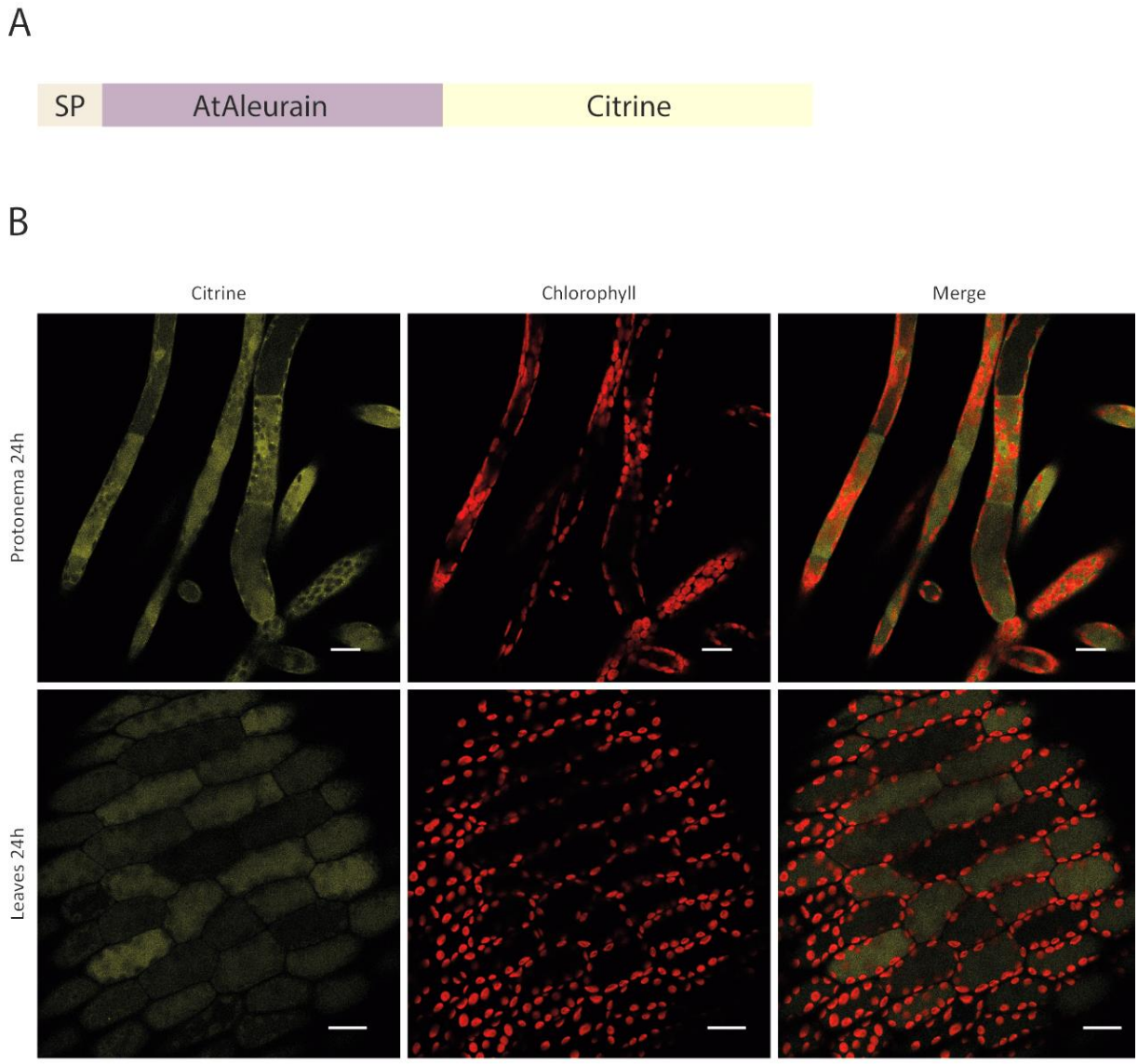

Figure 2.3 *At*Aleurain fused to Citrine is targeted to the central vacuole

(A) Schematic representation of the *At*Aleurain-Citrine fusion construct. The *At*Aleurain sequence was fused to the N-terminus of the Citrine.

(B) Fluorescence was observed in a typical vacuolar pattern (left hand panel). Chloroplasts were visualized by the chlorophyll autofluorescence (center panel). The merged image shows the superposition of Citrine and chlorophyll (right hand panel). Observations were made on protonema and leaves 24 hours after heat-shock induction. Scale bar = 20 µm.

A.3 Secreted reporter

A.3.a Citrine with just a signal peptide

Signal peptides (SP) are additional sequences found at the N-terminal side of most proteins, in order to enter the secretory pathway at the ER and to be transported to the final location within the cell. Most of the time, SP are removed from the mature protein (Von Heijne, 1990). Denecke *et* al. (1990) showed in plants, that protein entering the secretory pathway with an added signal peptide can be secreted via a default pathway. In order to obtain transgenic line expressing a secreted fluorescent protein, the SP of *At*Chitinase I was fused to the N-terminus of Citrine. Synthesis into the ER then secretion out of the cell was the expected result for this fusion. Protonema and leaf observations by confocal microscopy, 24 hours after heat-shock induction, showed unexpectedly a strong vacuolar fluorescence, in both protonema cells and in leaves (figure 2.4). Schaaf et al. (2004) had described (but not commented) an ER pattern for an *SP-GFP*, in transformed moss protoplasts. We considered this pattern due to slow exit from the ER before secretion.

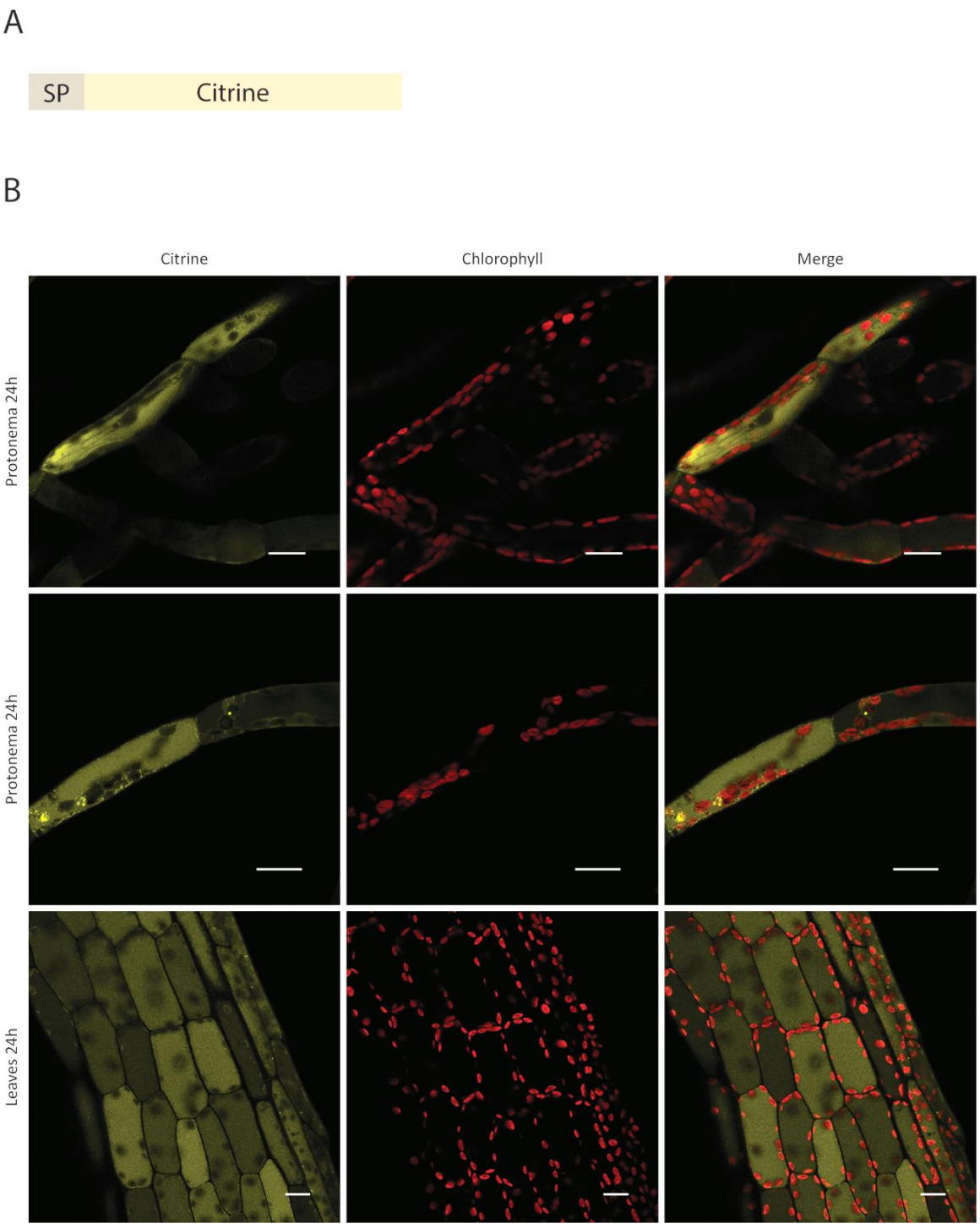

Figure 2.4 *SP-Citrine* entering the secretory pathway without any additional targeting sequence is addressed to the vacuole.

(A) Schematic representation of the SP-Citrin fusion construct. The signal peptide came from the *A. thaliana* chitinase I. The SP sequence of *At*Chitinase I was fused to the N-terminus of the Citrine.

(B) Fluorescence was observed in a typical vacuolar pattern (left panel). Chloroplasts are visualized by the chlorophyll autofluorescence (center panel). The merged image shows the superposition of Citrine and chlorophyll (right panel). Observations were made on protonema and leaves 24 hours after heat-shock induction. Scale bar = 20 µm.

A.3.b Secreted chitinase from *P. patens*

The unexpected vacuolar localization of a presumptive secreted reporter forced us to adopt a different approach, using an endogenous secreted protein. In order to obtain a vacuolar reporter, S. Ayachi (2009) has inserted the coding sequence of GFP in translational fusion into the gene encoding a presumptive vacuolar chitinase of *P. patens*. Unexpectedly, a fluorescent labelling was observed in the cell wall and not in the vacuole. Because so far little is known about the secretion of proteins in moss, we tried another candidate and we chose to create a fluorescent reporter by fusing Citrine at the N-terminus of a secreted chitinase identified in an analysis of the *P. patens* secretome (Lehtonen *et* al., 2013). In this study, a class I chitinase was identified. Chitinases are enzymes that degrade chitin, the second most abundant polysaccharide on earth. Plant chitinases are pathogenesis-related proteins involved in plant defense. Different isoforms concentrate in vacuoles and extracellular spaces of infected tissues after pathogen attack (Neuhaus, 1999; reviewed by Hamid *et* al., 2013).

Transgenic lines expressing the moss chitinase I fused to the C-terminal part of the Citrine were obtained. Accumulation of fluorescence in cell wall was observed from 24 hours after heat-shock induction, both in leaves and in protonema cells. An ER pattern was also observed at 24h hours after heat-shock induction, attesting of the entry of the construction in the secretory pathway. At 48h, only cell wall fluorescence was observed in leaves, confirming the secretion of the construct (figure 2.5).

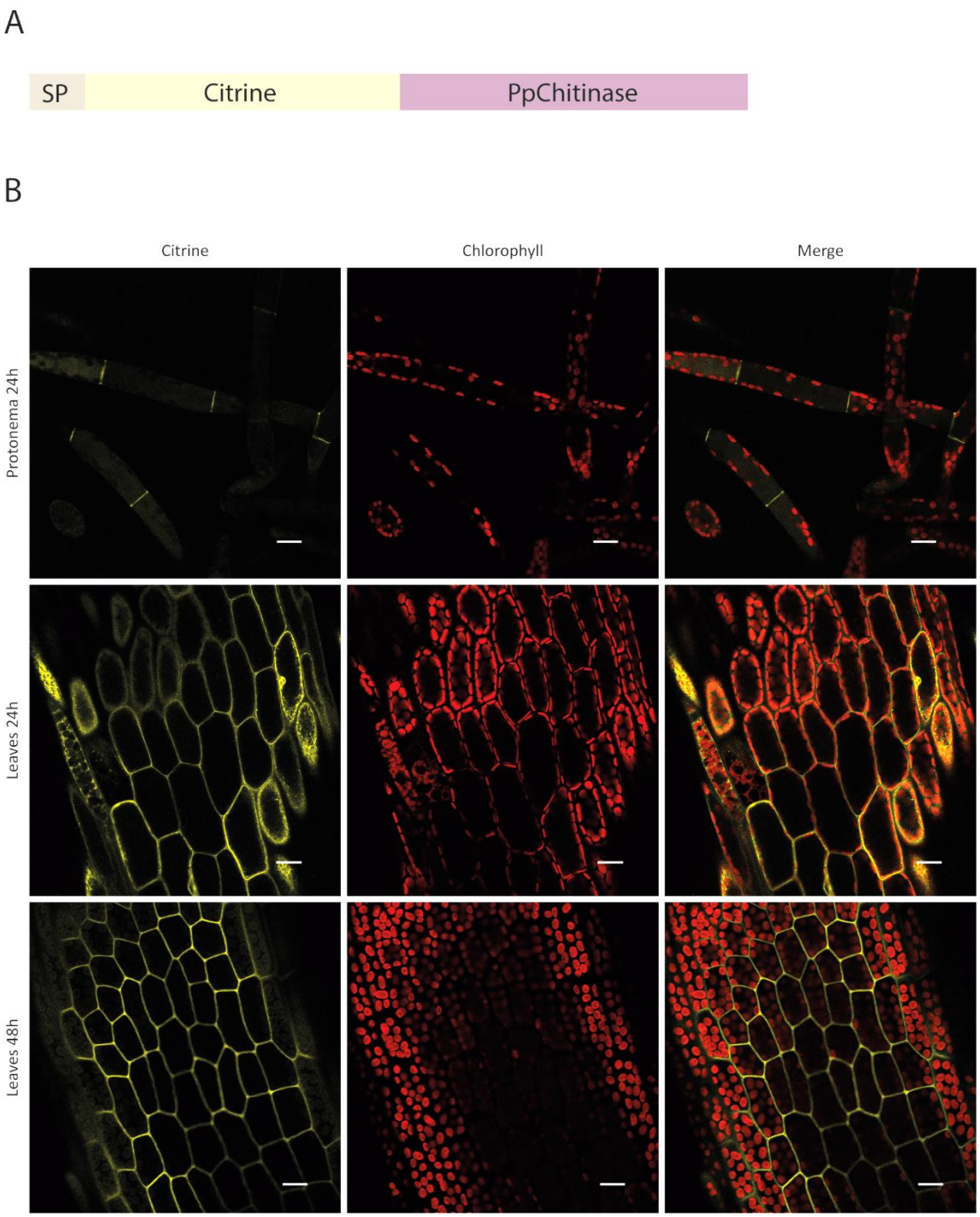

Figure 2.5 The fusion Citrine-*Pp*Chitinase I is targeted to the cell wall

(A) Schematic representation of the SP-Citrine-*Pp*Chitinase construct. The signal peptide used is the endogenous SP of the *Pp*Chitinase I. The rest of the sequence of *Pp*Chitinase I was fused to the C-terminus of Citrine.

(B) Fluorescence was observed in a typical cell wall pattern (left panel). Chloroplasts were visualized by the chlorophyll autofluorescence (center panel). The merged image shows the superposition of Citrine and chlorophyll (right panel). Observations were made on protonema cells and leaves 24 hours and 48 hours after heat-shock induction. Scale bar = 20 µm.

B. Reporters for the neutral vacuole (ctVSD)

B.1 CtVSD of tobacco chitinase A

The C-terminal propeptide of tobacco chitinase A was shown to be both necessary and sufficient for vacuolar targeting of a reporter protein in flowering plants (Neuhaus *et* al., 1991). Di Sansebastiano (1998) showed neutral vacuole labeling in tobacco protoplasts when expressing GFP with fused at its C-terminus the CtVSD of tobacco chitinase A. This was also observed in transgenic *A. thaliana* (Flückiger *et* al., 2003). Preliminary results had indicated that this reporter was also vacuolar in *P. patens* protoplasts (Maxime Quebatte, diploma thesis 1999). Consequently, we also made a vacuolar reporter using this ctVSD for the moss. As mentioned before, Citrine was used instead of GFP because this fluorescent reporter has been described to be more resistant to acidic pH and photobleaching. As expected, a strong vacuolar pattern was observed in protonema cells 24 hours after heat-shock (figure 2.6).

B.2 CtVSD of cardosin A

Cardosin A is a protease targeted to the protein storage vacuole of the stigmatic papillae of cardoon (Ramalho-Santos *et* al., 1997). Study of the intracellular transport of cardosin A allowed to identified a ctVSD, involved in the transport to the vacuole by the classical route (Pereira 2012). This ctVSD was fused to the C-terminus of the Citrine. The fusion construct was expressed in stable transgenic lines. Confocal microscopy confirmed the expected vacuolar pattern. Central fluorescent vacuoles were observed from 24 to 48 hours after heat shock induction, in both protonema cells (figure 2.7) and in leaves (figure 2.8).

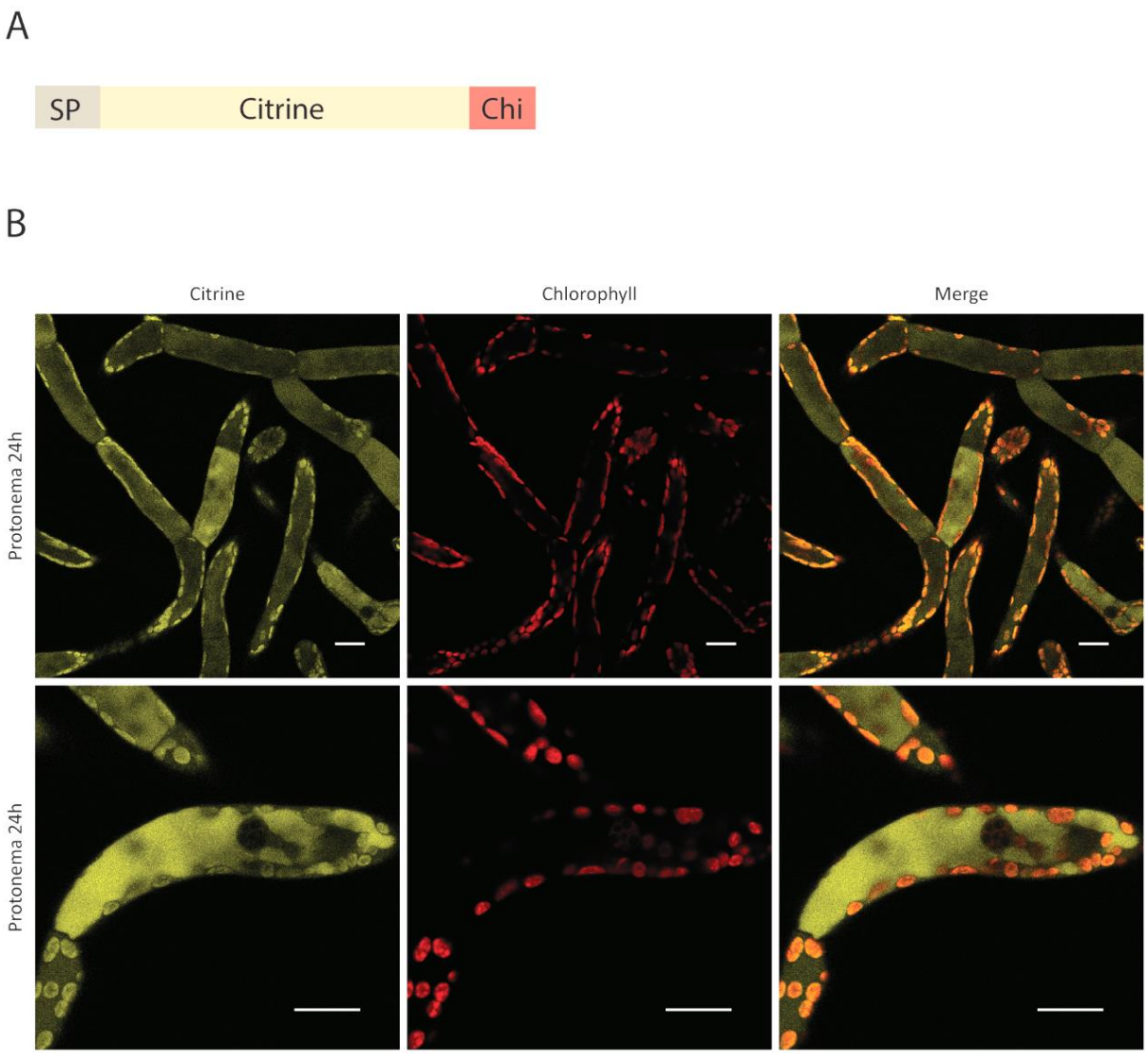

Figure 2.6 The ctVSD of tobacco chitinase A targets Citrine to the central vacuole of moss

(A) Schematic representation of the *Citrine-Chi* construct. The signal peptide used is the SP of the *A. thaliana* chitinase I. The ctVSD of tobacco Chitinase A was fused to the C-terminus of the Citrine.

(B) Fluorescence was observed in a vacuolar pattern (left panel). Chloroplasts were visualized by the chlorophyll autofluorescence (center panel). The merged image shows the superposition of Citrine and chlorophyll (right panel). Observations were made on protonema 24 hours after heat-shock induction. Scale bar = 20 µm.

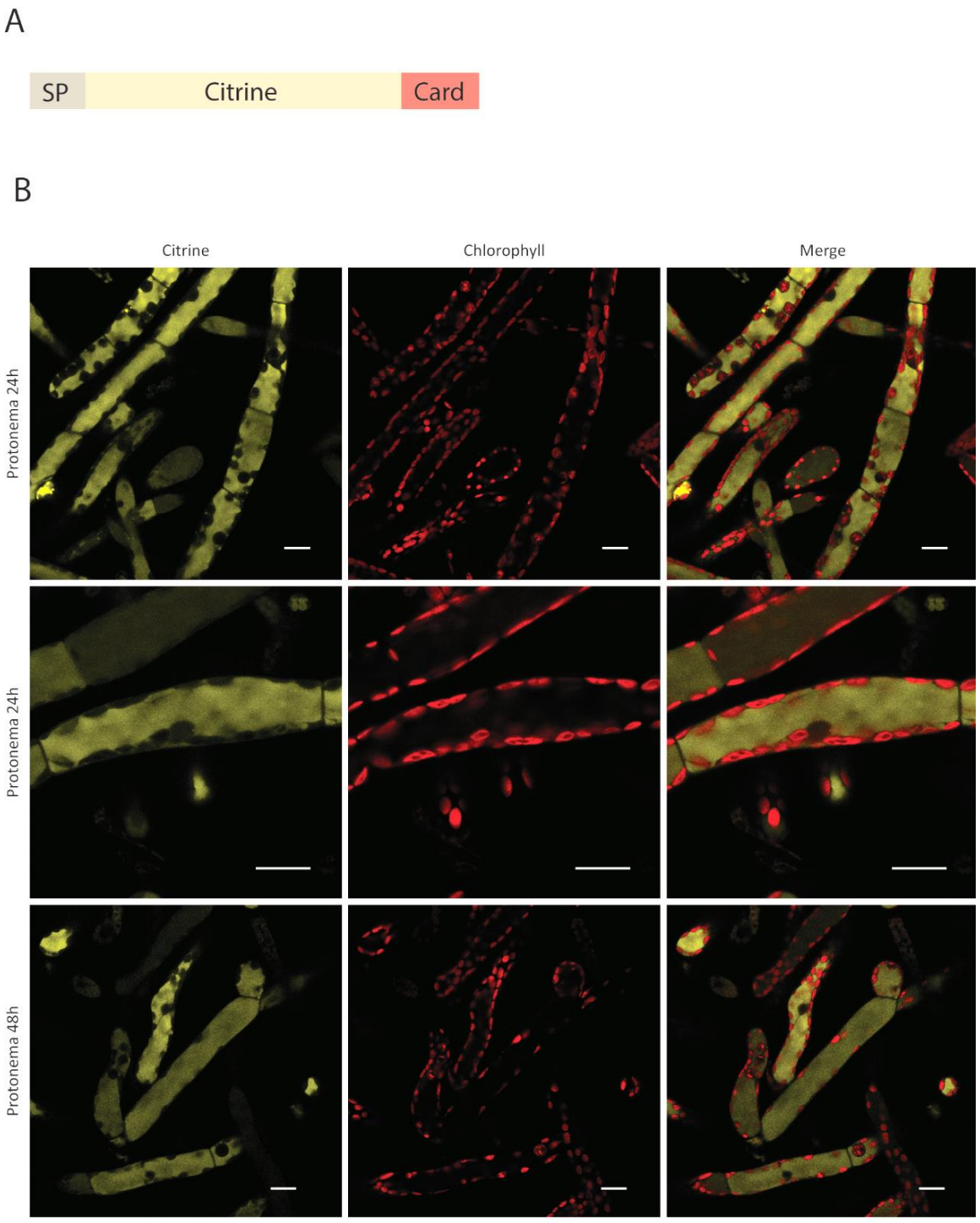

Figure 2.7 The ctVSD of cardosin A targets Citrine to the central vacuole of moss protonema cells

(A) Schematic representation of the Citrine-Card construct. The signal peptide used is the SP of the *A. thaliana* chitinase I. The ctVSD of cardosin A was fused to the C-terminus of the Citrine.

(B) Fluorescence was observed in a vacuolar pattern (left panel). Chloroplasts are visualized by the chlorophyll autofluorescence (center panel). The merged image shows the superposition of Citrine and chlorophyll (right panel). Observations were made on protonema 24 hours and 48 hours after heat-shock induction. Scale bar = 20 µm.

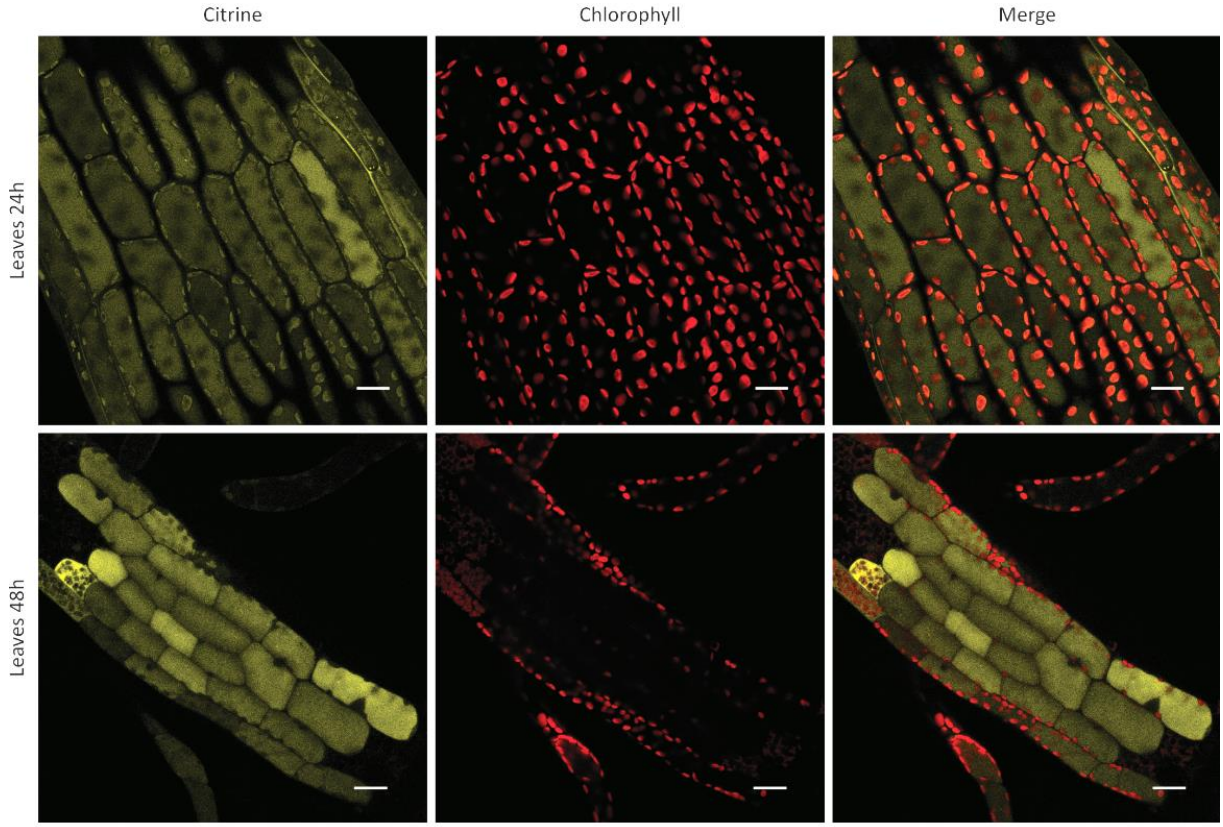

Figure 2.8 The CtVSD of cardosin A targets Citrine to the central vacuole in moss leaves

Fluorescence was observed in a vacuolar pattern (left panel). Chloroplasts were visualized by the chlorophyll autofluorescence (center panel). The merged image shows the superposition of Citrine and chlorophyll (right panel). Observations were made on leaves 24 hours and 48 hours after heat-shock induction. Scale bar = 20 µm.

B.3 CtVSD of moss aspartic proteinase 1

Aspartic proteinases are enzymes involved in proteolytic processes and are found in a wide range of organisms, from bacteria to mammals. In moss, *Pp*AP1 was identified to be an aspartic proteinase targeted to the vacuole (Schaaf *et* al., 2004). However, Schaaf *et* al. worked only on transiently infected protoplasts with the fusion GFP-*Pp*Ap1 and did not generate stable lines. In order to confirm their results and to test an endogenous ctVSD, the C-terminal sequence of *Pp*AP1 was fused to the C-terminus of Citrine. *Pp*AP1 is homologous to cardosins. The ctVSD of *Pp*AP1 was identified by analogy. Because this ctVSD sequence is very similar to the ctVSD of cardosin A, a vacuolar labeling was also expected in transgenic lines. Microscopic observations indeed showed fluorescent vacuoles in protonema cells, from 24 hours after heat-shock (figure 2.9).

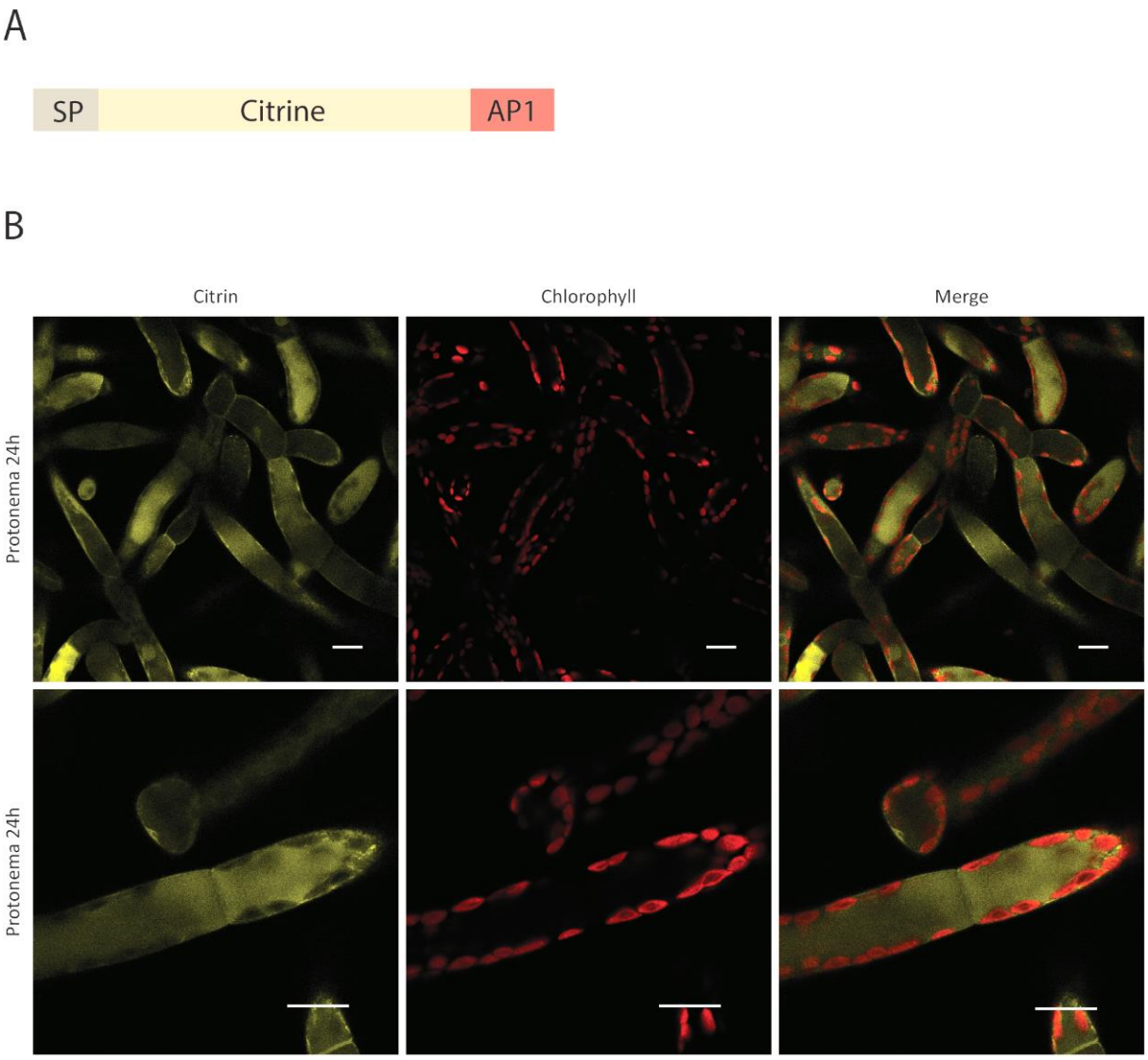

Figure 2.9 The CtVSD of *Pp*AP1 targets Citrine to the central vacuole of moss protonema cells

(A) Schematic representation of the Citrine-AP1 construct. The signal peptide used is the SP of the *A. thaliana* chitinase I. The CtVSD of *Pp*AP1 was fused to the C-terminus of the Citrine.

(B) Fluorescence was observed in a vacuolar pattern (left panel). Chloroplasts are visualized by the chlorophyll autofluorescence (center panel). The merged image shows the superposition of Citrine and chlorophyll (right panel). Observations were made on protonema 24 hours after heat-shock induction. Scale bar = 20 µm.

C. Plant Specific Insert reporters

PSI domains are exclusively found in plant aspartic proteases. The physiological role of these saposin-like domains is still unclear but they are involved in pathogen resistance and vacuolar targeting (Törmäkangas *et* al., 2001; Bryksa *et* al., 2011). PSI domains interact with membranes. Deletion of the PSI domain of barley phytepsin lead to its secretion instead of its vacuolar targeting in tobacco protoplasts (Törmäkangas *et* al., 2001). Both cardosin A and B contain a PSI domain but their biological properties and cellular localizations differ. Despite a high amino acid sequence similarity, cardosin A is vacuolar while cardosin B is secreted in the extracellular matrix of the floral transmitting tissue of cardoon; but to vacuoles in agroinfiltrated tobacco leaves (Vieira *et* al., 2001; Pereira 2012). For this reason, PSI domains of cardosin A and B are interesting tools to understand vacuolar targeting.

C.1 PSI domain from Cardosin A

The PSI domain of cardosin A (PSI-A) was fused to the N-terminus of Citrine. A fluorescence signal was expected in the central vacuole. Confocal observations 24 hours and 48 hours after heat-shock revealed a vacuolar labeling in protonema cells (figure 2.10). ER was also visible at both times, in some cells.

C.2 PSI domain of the cardosin B

The PSI domain of cardosin B (PSI-B) was fused to the N-terminus of Citrine. By analogy to what is observed in flowering plants, secretion of the fusion protein is expected so extracellular spaces should be labeled. Confocal observations 24 hours after heat-shock revealed an ER and nucleus pattern for most cells. A light vacuolar labeling could also be observed in few cells. 48 hours after induction, vacuolar labeling was stronger but the nuclear envelope was still visible for a majority of cells (figure 2.11).

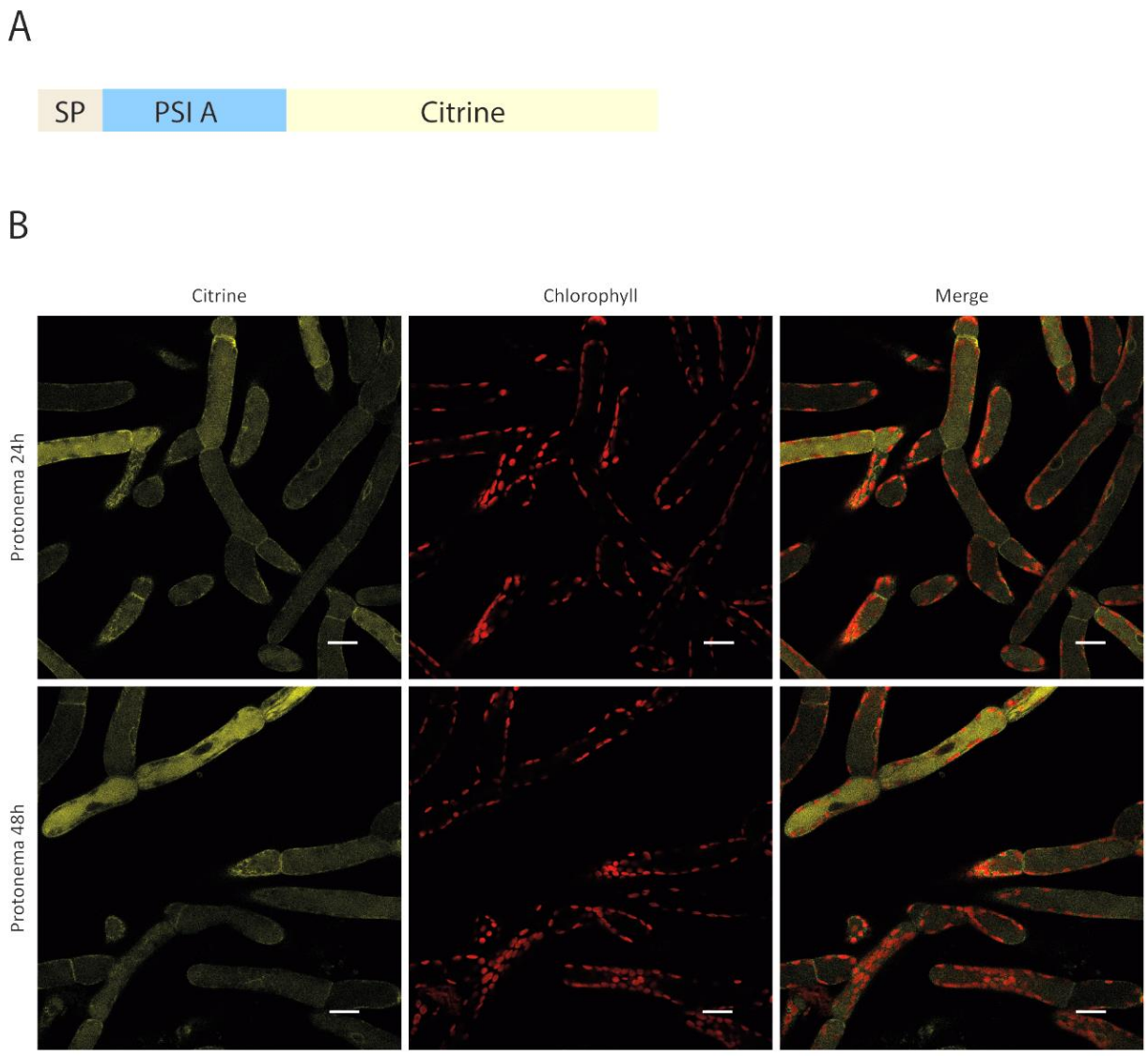

Figure 2.10 The PSI domain of cardosin A targets Citrine to the central vacuole of protonema cells

(A) Schematic representation of the SP-*PSIA*-Citrine construct. The signal peptide came from the *P. patens* chitinase I. The PSI domain of cardosin A was fused to the N-terminus of Citrine.

(B) Fluorescence was observed in a vacuolar pattern (left panel). Chloroplasts were visualized by the chlorophyll autofluorescence (center panel). The merged image shows the superposition of Citrine and chlorophyll (right panel). Observations were made on protonema 24 hours and 48 hours after heat-shock induction. Scale bar = 20 µm.

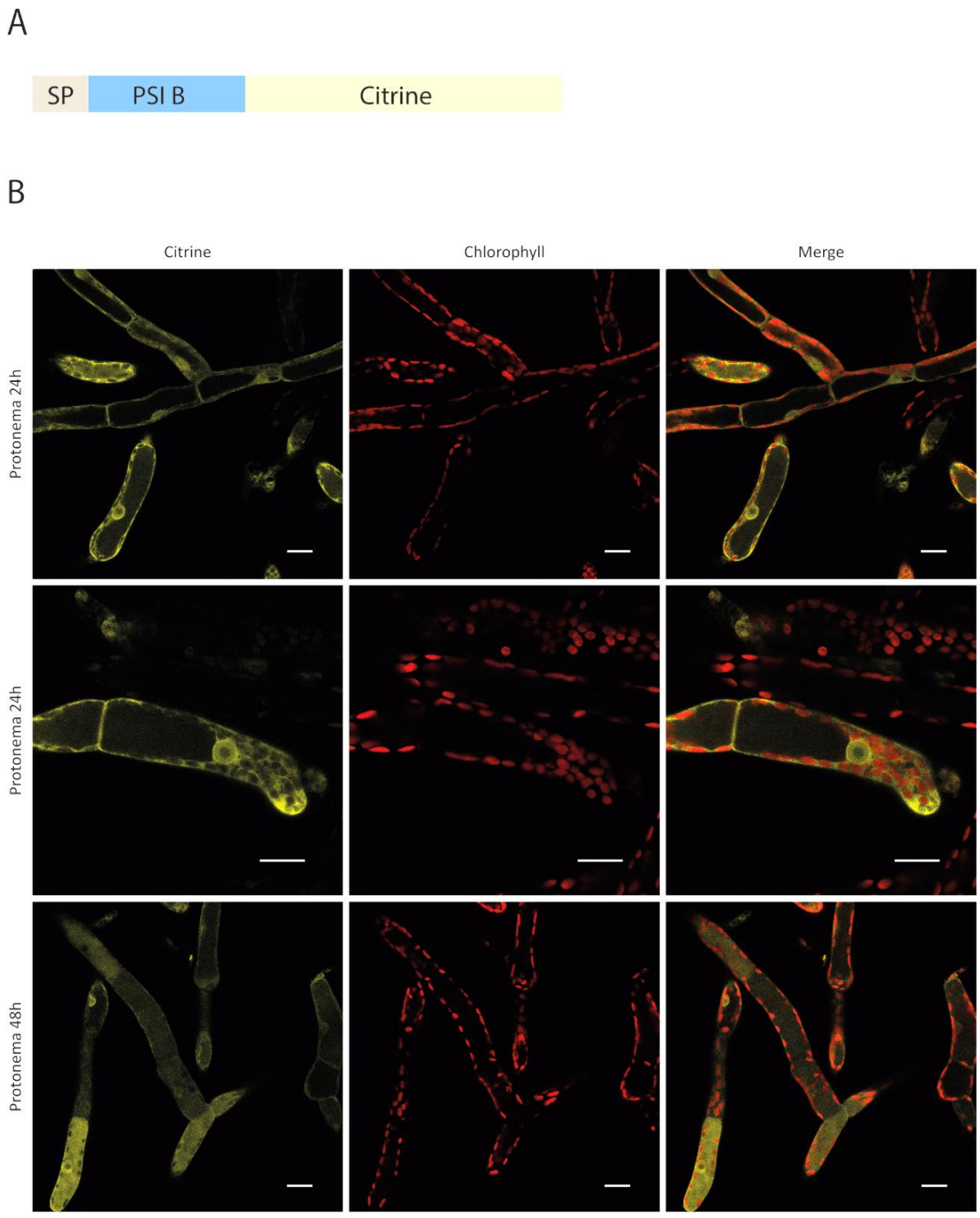

Figure 2.11 The PSI domain of cardosin B targets Citrine to the central vacuole of protonema cells

(A) Schematic representation of the SP-*PSIB*-citrin construct. The signal peptide used came from the *P. patens* chitinase I. The PSI domain of cardosin B was fused to the N-terminus of Citrine.

(B) Fluorescence was observed in a vacuolar pattern (left panel). Chloroplasts were visualized by the chlorophyll autofluorescence (center panel). The merged image shows the superposition of citrin and chlorophyll (right panel). Observations were made on protonema 24 hours and 48 hours after heat-shock induction. Scale bar = 20 µm.

D. Discussion

So far, little is known about the moss secretory pathway. In our laboratory, a first set of fluorescent markers was established by a previous PhD student in order to study the organelles involved in the secretory pathway (Ayachi 2012). To complete this collection and to extend our knowledge about the secretory pathway in seedless plants, we developed further fluorescent markers, in particular several vacuolar reporters.

Our results showed that general secretory system reporters like ER-retained marker or acidic vacuole marker were targeted to the expected destination in the moss cell, as in flowering plants. The ssVSD of barley and *Arabidopsis* aleurain have been found to direct the protein to the lytic vacuole (Holwerda and Rogers, 1993; Zouhar and Rojo, 2009). Our results showed that the ssVSD of *At*Aleurain directed the fluorescent reporter to the central vacuole. In plants as in animals, proteins with a KDEL sequence at their C-terminus were retained in the ER (reviewed by Pagny *et* al., 1999). In our case, the KDEL sequence was apparently sufficient to retain the *SP-Citrine* construct in the ER. Schaaf *et* al. (2004) worked on moss protoplasts and observed a similar pattern of fluorescent ER in transfected moss protoplasts expressing a *SP-GFP-KDEL* construct. Transgenic lines expressing the *Citrine-Ppchitinase* showed an accumulation of fluorescence in the cell wall of protonema and leaves.

Proteins having a ctVSD were described to be directed to the neutral/storage vacuole. The three characterized ctVSD of tobacco chitinase, cardosin A and *Pp*AP1 were tested in moss. These constructs were targeted to the central vacuole, as predicted. Our results showed that ctVSD already validated in flowering plants, are also recognized and well processed in the moss.

The PSI domains, found exclusively in plant APs, were described to play a role in proteins trafficking. Indeed the PSI from cardosin A is involved in vacuolar targeting (Pereira 2012). In cardoon, the PSI domain from cardosin B seems to play a role in the secretion of the protein in the floral transmitting tissue, destined to the extracellular matrix. In tobacco cells, cardosin A and B are vacuolar (Pereira 2012). In this work we observed that transgenic moss expressing the PSI domain from cardosin A fused to Citrine, showed a vacuolar pattern, as expected. In protonema, expression of the PSI.B fused to Citrine, showed first an ER labeling (at 24 hours) then a central vacuolar fluorescence (at 48 hours). We did not observed that *PSIB-citrine* is secreted in *P. patens*.

In plants, it has been demonstrated that proteins entering the secretory pathway by the ER with only a signal peptide can be secreted via a default pathway (Denecke *et* al., 1990). A conflicting result was obtained for the *SP-Citrine* construct, which was supposed to be secreted, as was the case in angiosperms. *SP-Citrine* was instead addressed to the central vacuole in protonema cells. In moss, fluorescent reporters entering the secretory pathway with only a SP and no specific other targeting signal appears to be directed to the vacuole. Our results suggest that secretion mechanisms have evolved between seedless and flowering plants and a specific signal is maybe necessary for protein secretion in moss. Otherwise, we can also suppose that the Citrine contains a cryptic signal for vacuolar targeting, recognized in moss but not in flowering plants.

These fluorescent reporters highlight that there are cellular features involved in vacuolar targeting that are conserved between mosses and flowering plants. However, the question about different pathways existing to reach the same kind of vacuole remains non-answered. This topic was discussed in the following chapter with the used of secretory pathway inhibitors on mutants and WT transgenic lines.

Chapter 3
Characterization of RMR Knock-out mutants

Plants can contain different vacuole types within a same cell (Hoh *et* al., 1995; Paris *et* al., 1996). According to the classical secretory pathway model, luminal proteins reach the vacuole after trafficking through the ER and the Golgi apparatus. These proteins are sorted to their final destination by cargo receptors, which recognize and bind a specific component, a vacuolar sorting determinant (VSD). First identified, ssVSDs are NPIR-like motifs which target proteins to the lytic vacuole. VSRs are well characterized vacuolar receptors and their role in protein sorting to lytic vacuole is now admitted (Jiang and Rogers 1998; DaSilva *et* al., 2006; Zouhar *et* al., 2010). Identified by their homology to the PA domain of VSR proteins, RMR proteins are thought to be vacuolar receptors, targeting proteins to the PSV (Cao *et* al., 2000). However, the role of RMRs is still unclear and needs further investigations. RMRs and their homologues belong to the PA-TM-RING protein family. In animals, several of these proteins have been identified as E3 ubiquitin ligases, suggesting another interesting role for RMRs.

This part of our work was focused on the elucidation of the role of RMR proteins in *P. patens*, where five RMR genes have been identified. A previous PhD student generated single, multiple and quintuple Knock-Out (KO) lines of RMR in moss (Ayachi 2012). However, these mutants did not show any visible phenotype. Localization of ER and Golgi reporters was not different between WT and mutants (Ayachi 2012). In order to further characterize the RMR mutants, we tested several additional fluorescent reporters, treated the moss with secretory pathway inhibitors and stress conditions. The localization of RMR in moss was also addressed. The localization of RMR proteins can either support their role as vacuolar receptors or suggest new roles, such as involvement in an ubiquitylation mechanism.

A. Phenotypic characterization of RMR mutants with fluorescent reporters

As described in the previous chapter, fluorescent reporters were developed to study the moss secretory system. A HSP promoter was used for all the constructs because it allows to observe the protein's progression within the cell. All the constructs were inserted into the non-coding locus 108 in the moss genome (Schaefer and Zrÿd, 1997). In the following part, several markers described in the previous chapter were tested in RMR mutants, in order to detect a phenotypic difference between the WT and the mutant lines.

A.1 CtVSD reporters

CtVSD are found at the C-terminus of many proteins directed to the PSV. Because RMRs are possibly involved in the recognition of ctVSD, different ctVSD constructs were tested. In WT transgenic lines, several ctVSD constructs lead to a vacuolar fluorescent pattern. If RMRs play a role in this mechanism, protein mistargeting is expected in RMR mutants.

A.1.a CtVSD of tobacco chitinase I

This ctVSD has been used in our laboratory for a long time. In tobacco protoplasts, expression of the fluorescent protein GFP carrying the ctVSD of tobacco chitinase A, lead to a central vacuolar labeling (Di Sansebastiano *et* al., 1998). In tobacco protoplasts and *Arabidopsis* plants, this reporter labeled a different vacuole than another vacuolar reporter (Aleu-GFP6) targeted to acidic vacuoles (Di Sansebastiano *et* al., 2001; Flückiger *et* al., 2003). In this context, the construct *Citrine-Chi* was tested to study vacuolar targeting in moss. Two RMRs mutants were used, the triple Knock-out mutant where RMR 2 and 4 are remaining and the quintuple knock-out where all RMRs are missing. Transgenic lines were generated and analyzed by confocal microscopy. 24 hours after heat-shock induction, strong vacuolar fluorescence was observed in all lines. Unexpectedly, there was no phenotypic difference between the WT and the mutant lines (figure 3.1).

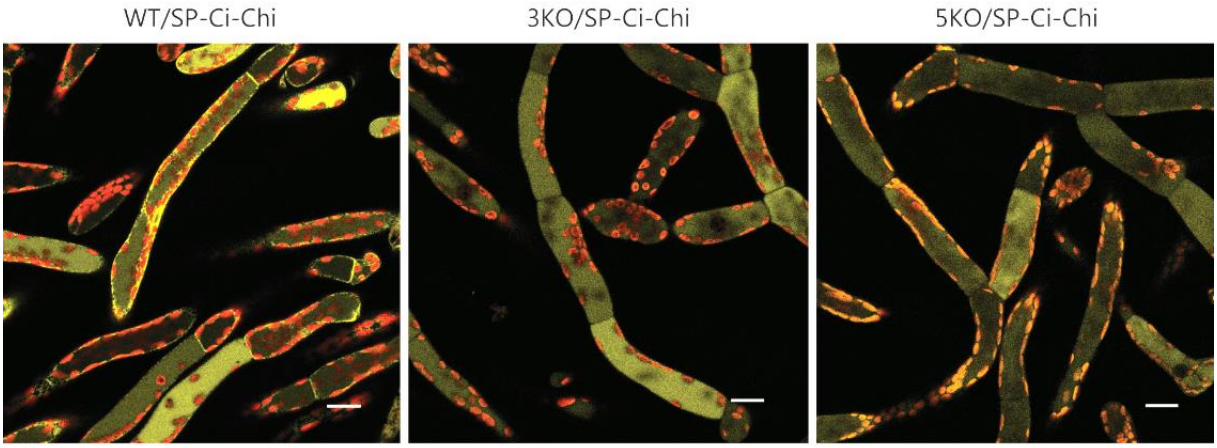

Figure 3.1 No targeting difference between the WT and the mutant lines expressing Citrine-Chi

Vacuolar fluorescence was observed in the three transgenic lines, WT (left panel), 3KO (center panel) and 5KO (right panel). Observations were made on protonema 24 hours after heat-shock induction. Scale bar = 20 µm.

A.1.b CtVSD of cardosin A

Cardosin was described to be accumulated in protein storage vacuoles of the stigmatic papillae of cardoon (Ramalho-Santos *et* al., 1997). The ctVSD of cardosin A was efficiently targeting a reporter to vacuole in tobacco. Because there was no targeting difference between WT and mutants expressing *Citrine-Chi*, Citrine with the ctVSD of cardosin (*Citrine-Card*) was tested in several RMR mutants. 5KO and 3KO (*rmr1,3,5*) transgenic lines were obtained. 24 hours after heat-shock induction, confocal microscopy showed a difference of fluorescent pattern in mutant lines. A typical ER pattern was observed in 3KO and 5KO mutants while it was strongly vacuolar in WT (figure 3.2). In mutants, the fusion protein was blocked in the ER, even 48 hours after heat-shock induction. In this typical ER pattern, the nuclear envelope is well visible.

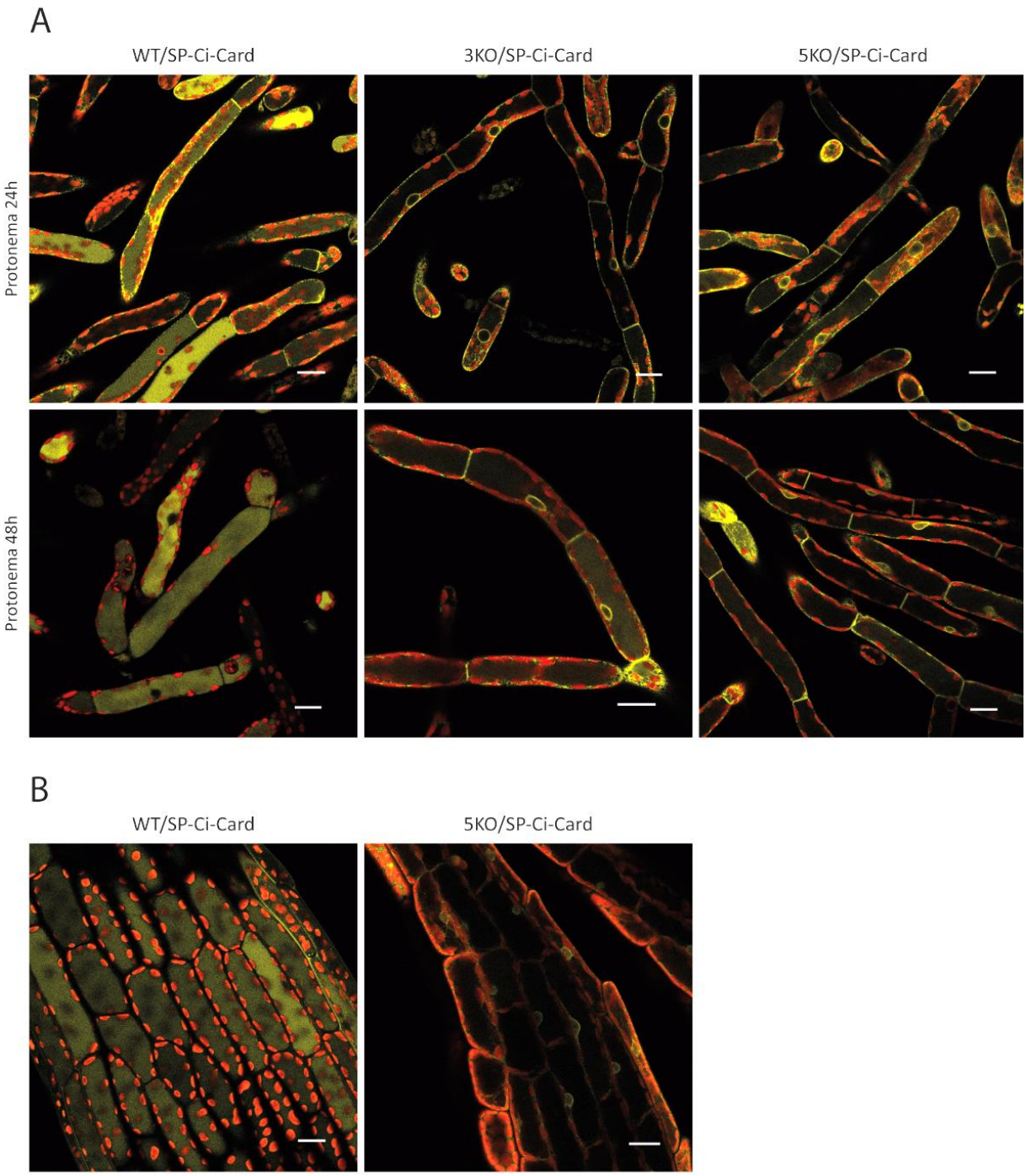

Figure 3.2 The Citrine-Card construct is mistargeted in RMR mutant lines

(A) Vacuolar fluorescence was observed in WT (left panel), but the fusion was mistargeted in the 3KO (center panel) and 5KO lines (right panel).

(B) Leaf cells expressing the Citrine-Card construct, vacuolar in WT ER retained in 5KO line

Observations were made 24 hours after heat -shock induction. Scale bar = 20 µm.

Moss RMRs can be separated into two sub-families, RMR1 and 2 in one, RMR3, 4 and 5 in the other one (figure 1.11). Since single RMR KO mutants were available in the lab, two mutants representing each subfamily were tested with the construction Citrine-Card: *rmr2* and *rmr5*. In both 1KO mutants, most of the fluorescence was retained in the ER in comparison with the WT line, 24 hours after heat-shock induction (figure 3.3). A faint vacuolar pattern could also be observed in some cells in the mutant lines. Despite being member of two distinct sub-families, mutants lacking RMR2 or RMR5 showed the same fluorescent pattern as the 5KO line.

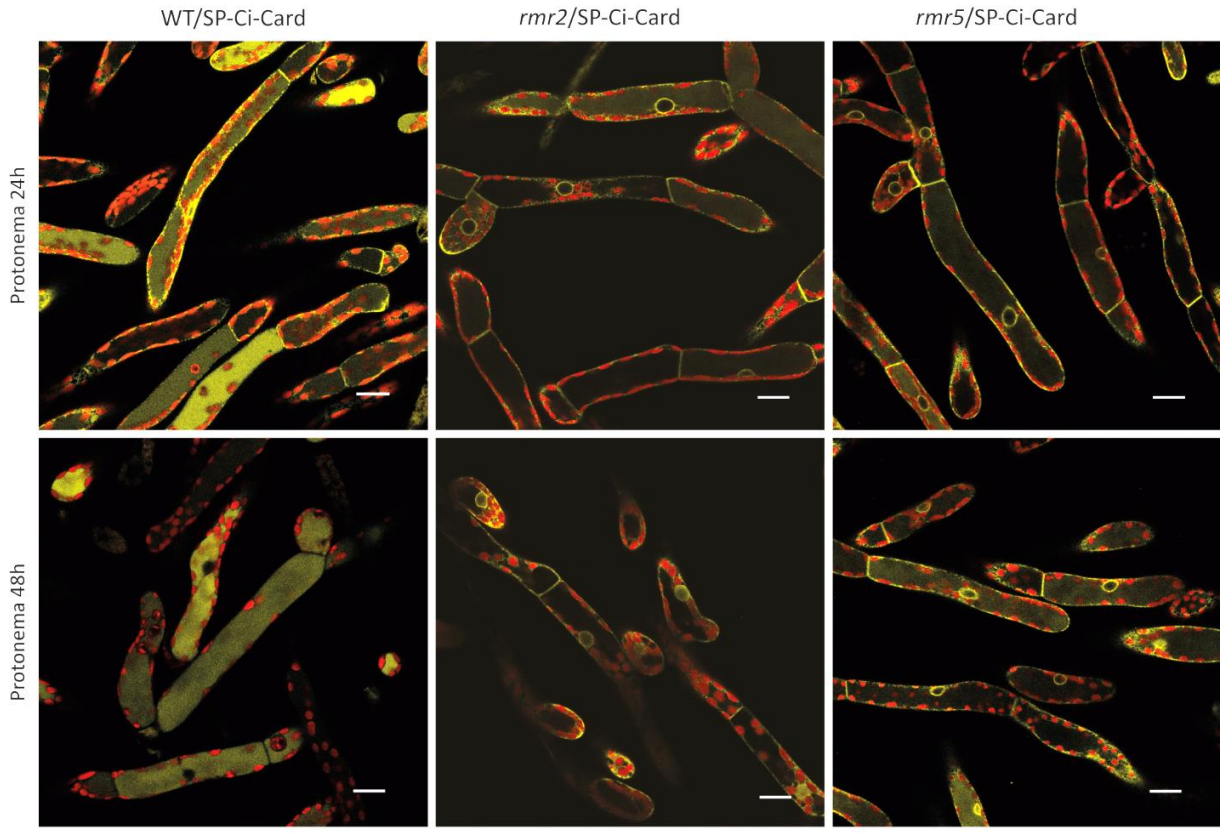

Figure 3.3 Citrine-Card is also mistargeted in single KO mutant lines

Vacuolar fluorescence was observed in WT (left panel), but the fusion was mistargeted in *rmr2* (center panel) and in *rmr5* (right panel). Observations were made on protonema 24 hours and 48 hours after heat-shock induction. Scale bar = 20 µm.

In WT expressing Citrine-Card, fluorescent vacuoles were observed. In all four mutant lines (1, 3 or 5KO), most of the fluorescence was ER-localized. In order to investigate this phenotypic difference, immunoblot analysis of Citrine in the different lines was performed (figure 3.4). Total proteins were extracted 24 hours after heat-shock induction. The fusion *Citrine-Card* was detected in all lines. However, additional bands are also visible in all samples. They show partial degradation products of the fluorescent reporter, probably due to the high level of expression induced by the heat-shock promotor.

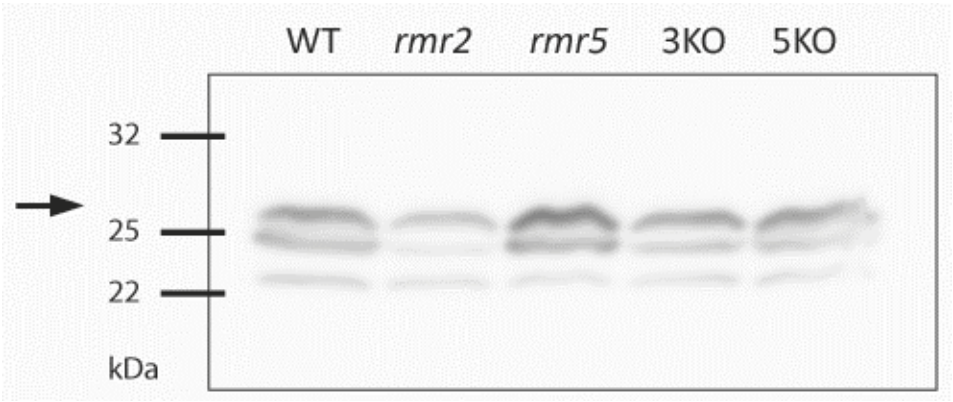

Figure 3.4 Western blot of proteins extracts from moss lines expressing Citrine-Card. All lines showed the same protein pattern.
Citrine has a molecular weight of 27 kDa (arrow), Citrine-card has a molecular weight of 27.7 kDa. Protonema was ground, 24 hours after heat-shock induction. Total soluble proteins were analyzed by SDS-PAGE followed by immunoblotting with anti-GFP to detect Citrine.

A.1.c CtVSD of PpAP1

Moss aspartic proteinase 1 was described to accumulate in the vacuole of protonema cells (Schaaf *et* al., 2004). Because the sequence of the ctVSD of AP1 (LGF AEAA KGEFV) is very similar to that one of cardosin (VGF AEAA), the same mistargeting that was observed with *Citrine-Card* was expected in mutants expressing *Citrine-AP1*. However, 24 hours after heat-shock induction the same vacuolar pattern in both WT and mutant was observed (figure 3.5). There was no difference of fluorescent pattern: contrary to *Citrine-Card*, *Citrine-AP1* was not retained in the ER in 5KO mutant.

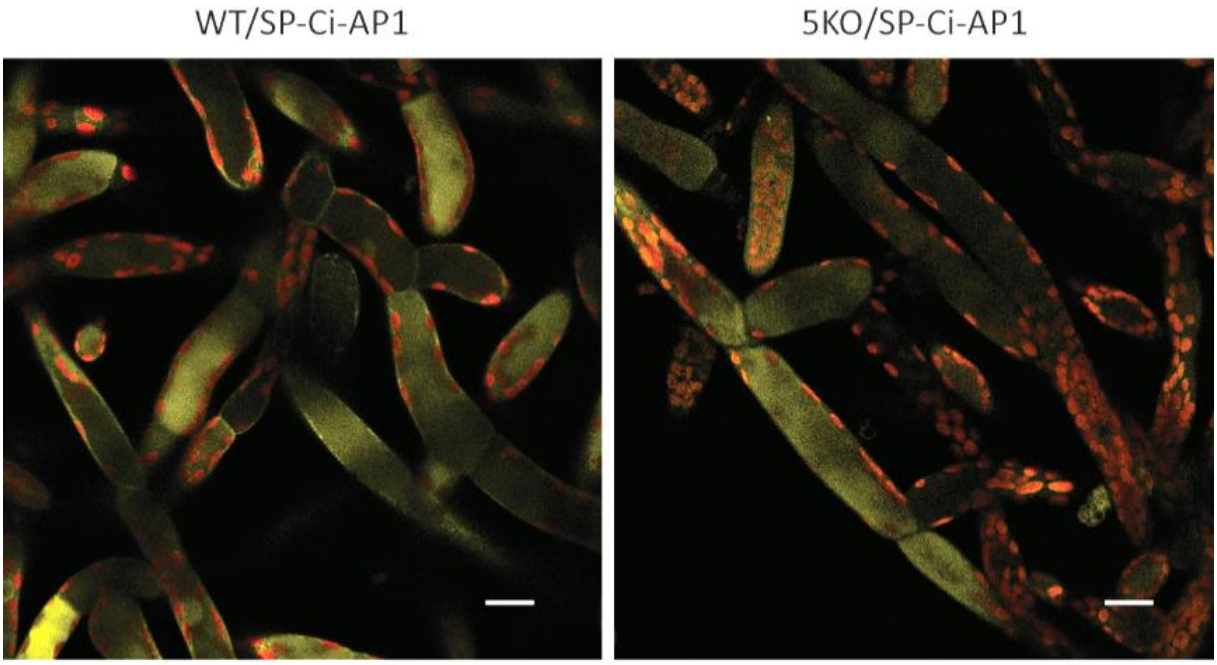

Figure 3.5 No targeting difference between the WT and the 5KO line expressing Citrine-AP1
Vacuolar fluorescence was observed in both transgenic lines, WT (left panel) and 5KO (right panel). Observations were made on protonema 24 hours after heat-shock induction. Scale bar = 20 µm.

A.2 PSI reporters

Exclusively found in plant aspartic proteases, PSI domains are involved in protein-membrane interactions. Little is known about their specific cellular role but there is evidence implicating them in vacuolar targeting (Törmäkangas *et* al., 2001; Bryksa *et* al., 2011). In cardoon flowers, cardosin A is targeted to the vacuole while cardosin B is secreted to the extracellular matrix. In tobacco Agroinfiltrated leaves however, both cardosins are vacuolar. Both ctVSD and PSI domains of cardosin A and B targeted mCherry to vacuoles, but the PSI domains of cardosin A and B are differently affected by dominant-negative mutants of rabD2 or Sar1 (Pereira 2013). Therefore we tested the PSI domains of both cardosin A and B in 5KO RMR line. If RMRs are involved in their trafficking to vacuoles, we expected a mistargeting of the fluorescent signal in the mutants.

A.2.a PSI from cardosin A

WT and 5KO transgenic line expressing the PSI domain of cardosin A fused to Citrine showed a mixed ER and vacuolar labeling, 24 hours and 48 hours after heat-shock induction (figure 3.6). No difference was observed between the WT and the 5KO line.

A.2.b PSI domain from cardosin B

The PSI domain of cardosin B was found to target mCherry to the vacuoles in the agroinfiltrated tobacco (Pereira 2012). In WT transgenic protonema cells, the fusion *PSIB-Citrine* was targeted to the central vacuole. In the 5KO line, fluorescent ER was visible 24 hours after heat-shock induction. However, after at 48 hours a vacuolar fluorescence was observed, similar to the WT line (figure 3.7).

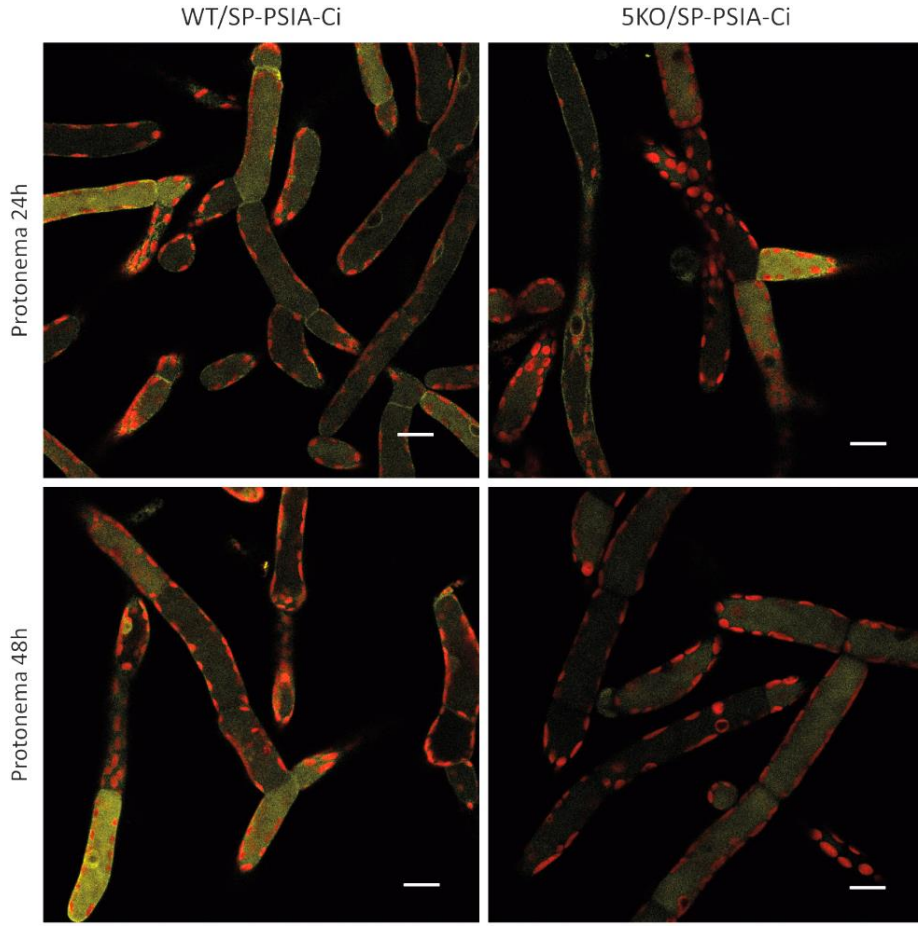

Figure 3.6 No targeting difference between the WT and the 5KO line expressing PSIA-Citrine

Vacuolar fluorescence was observed in both transgenic lines, WT (left panel) and 5KO (right panel). Observations were made on protonema 24 hours and 48 hours after heat-shock induction. Scale bar = 20 µm.

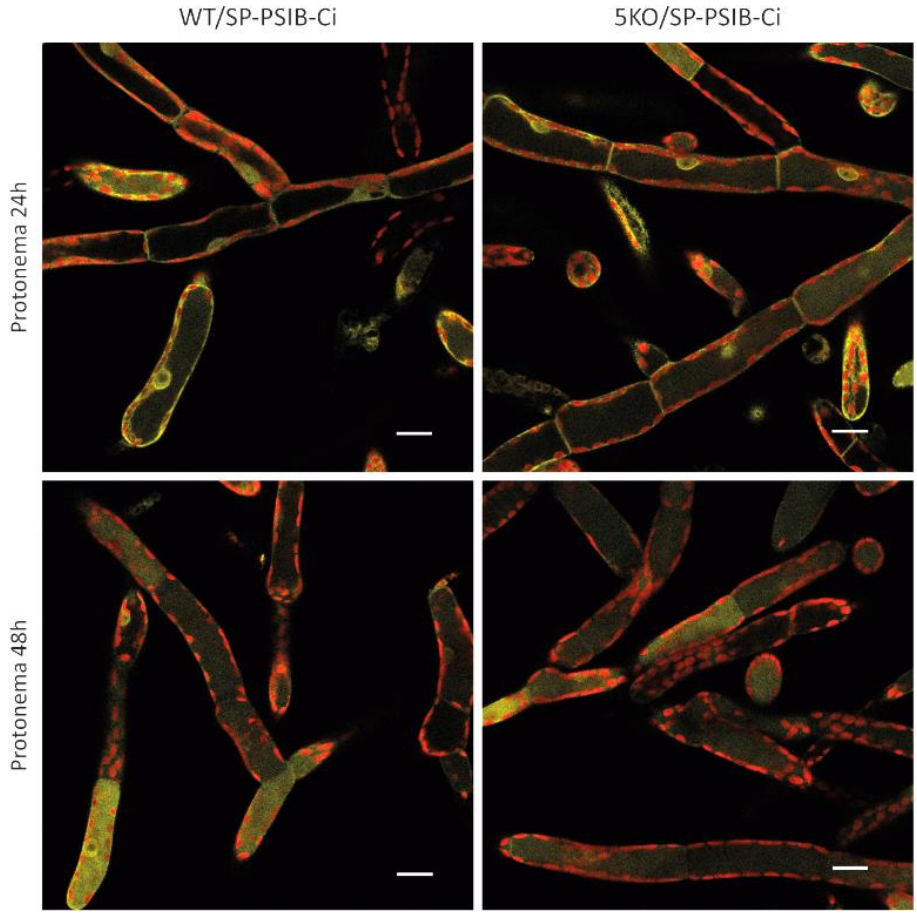

Figure 3.7 No difference of targeting is observed between the WT and the 5KO line expressing PSIB-Citrine Vacuolar fluorescence was observed in both transgenic lines, WT (left panels) and 5KO (right panels) 48 after heat-shock induction. Observations were made on protonema cells. Scale bar = 20 µm.

A.3 Further vacuolar markers

A.3.a Secreted Citrine (*SP-Citrine*)

In flowering plants, expression of a fluorescent protein targeted to the secretory pathway via the ER (by a signal peptide) leads to its secretion. In contrast, in moss, a WT transgenic line expressing the *SP-Citrine* construct showed a strong vacuolar fluorescence. This construct was also tested in 5KO and 1KO lines, to see if this unexpected vacuolar targeting was affected in RMR mutants. 24 hours after heat-shock induction, the typical vacuolar pattern was observed in both mutant lines (figure 3.8).

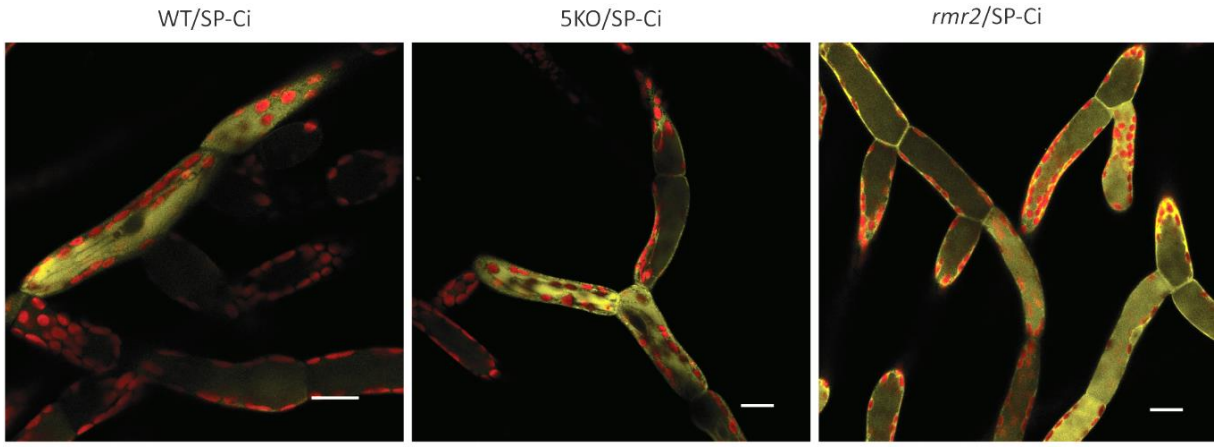

Figure 3.8 No difference of targeting was observed between the WT and the mutant lines expressing *SP-Citrine* Vacuolar fluorescence was observed in all transgenic lines: WT (left panel), 5KO (center panel) and *rmr2* (right panel) 24 hours after heat-shock induction. Observations were made on protonema cells. Scale bar = 20 µm.

A.3.b Acidic vacuole reporter

Neutral red coloration of protonema showed an acidic central vacuole accumulating the dye for most part of cells. This vacuole is also labeled in transgenic plants expressing the *At*Aleurain-GFP (Ayachi 2012) and the *AtAleurain-Citrine* constructions. Barley Aleurain and *Arabidopsis* contain an ssVSD sequence responsible for the targeting to the acidic vacuole (Holwerda et Rogers, 1993; Zouhar *et* al., 2009). RMRs are not expected to be involved in this type of vacuolar targeting. 5KO line expressing the *AtAleurain-Citrine* construction was nevertheless tested. Observations 24 hours after heat-shock induction showed a vacuolar fluorescent pattern for a majority of the protonema cells (figure 3.10). As expected, the fluorescent pattern was the same as the WT transgenic line, and no difference was found.

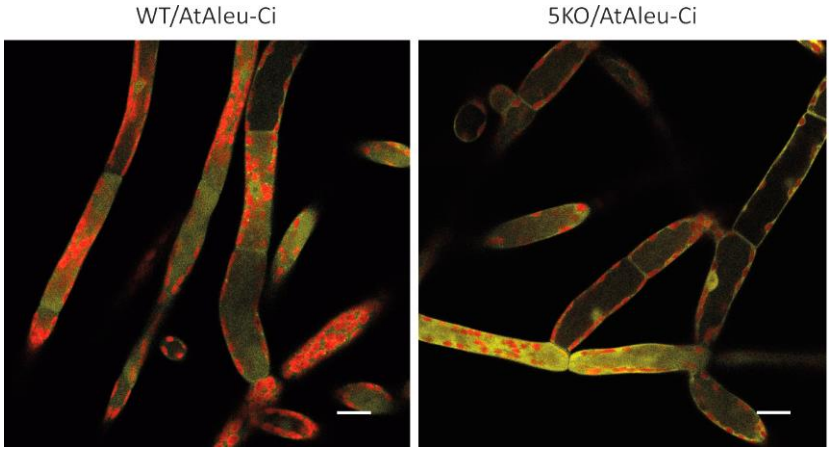

Figure 3.10 No difference of targeting was observed between the WT and the 5KO line expressing *AtAleurain-Citrine*

Fluorescence localized in the central vacuole was observed in both transgenic lines, WT (left panel) and 5KO (right panel) 24 hours after heat-shock induction. Observations were made on protonema cells. Scale bar = 20 µm.

A.3.c Secreted moss chitinase

A WT transgenic moss line expressing a fluorescent secreted chitinase was generated and the fluorescence was localized in cell wall. Although no difference of pattern was expected between the mutant and the WT, this construction was also tested on 5KO line. Confocal microscopy showed the same pattern as the WT line. The fluorescence signal was localized in cell wall 24 hours after heat-shock induction, in protonema cells but also in leaves (figure 3.9).

A.3.d ER-retained reporter

The KDEL sequence is known to be a signal for ER retention. Tested in WT line expressing the *Citrine-KDEL* fusion, a typical ER labeling was observed in protonema cells. In a 5KO line, the same fluorescent pattern was expected. Confocal observations confirmed this expectation, the mutant line showed a strong ER labeling, with the well visible nuclear envelope (figure 3.11).

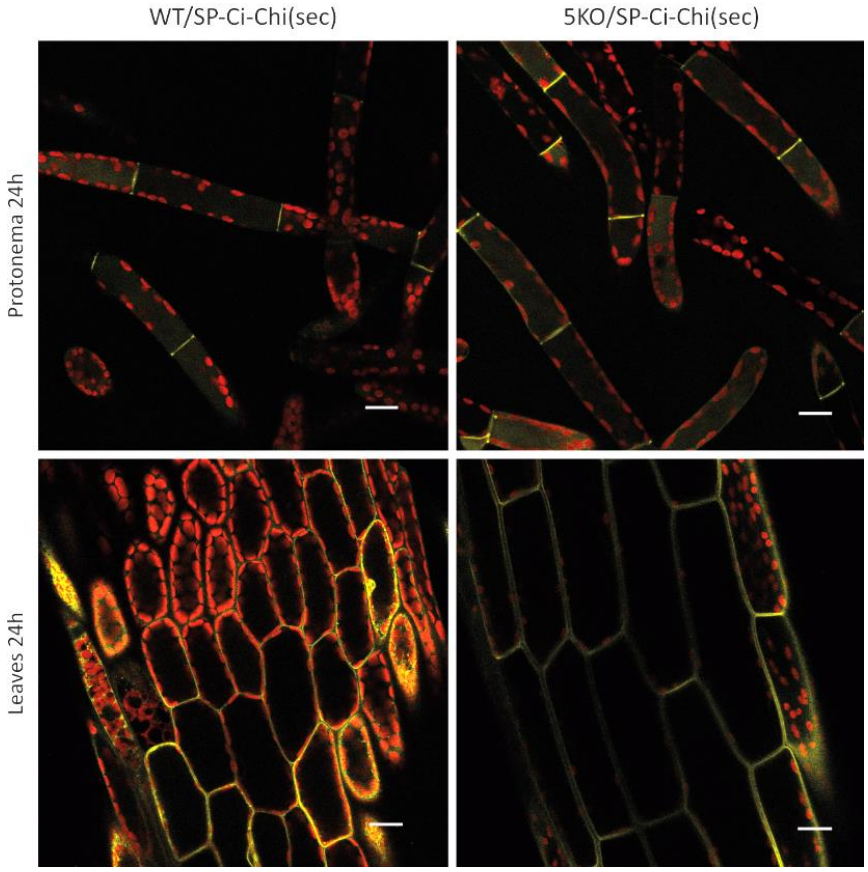

Figure 3.9 No difference of targeting is observed between the WT and the 5KO line expressing the fluorescent secreted *Pp*chitinase

Fluorescence localized in the cell wall was observed in both transgenic lines, WT (left panels) and 5KO (right panels) 24 hours after heat-shock induction. Observations were made on protonema cells and leaves. Scale bar = 20 µm.

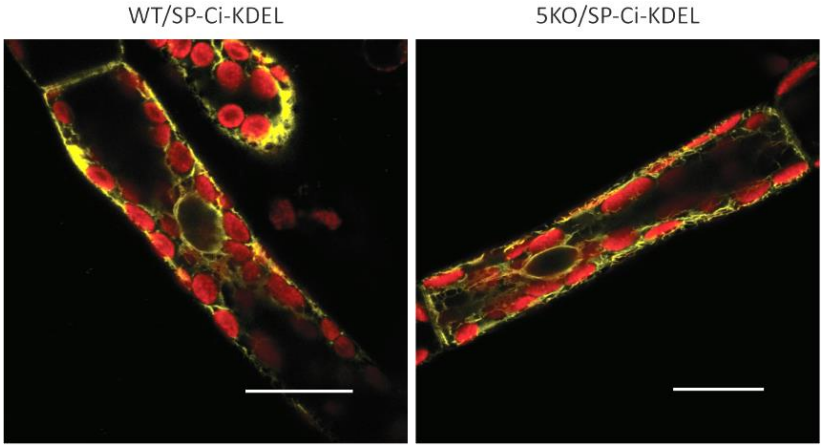

Figure 3.11 No difference of labeling was observed between the WT and the 5KO line expressing the ER-retained signal.

Fluorescence was observed in a typical ER pattern in the WT transgenic line (left panel) and in the 5KO mutant line (right panel). Observations were made on protonema 24 hours after heat-shock induction. Scale bar = 20 µm.

A.4 Discussion

Because RMRs are thought to be involved in protein targeting to neutral/storage vacuole, several construct with ctVSD already characterized in angiosperms were tested in WT and KO mutant lines. Mistargeting of the reporter in the mutant line would indicate the involvement of RMR proteins in vacuolar targeting. The ctVSD of tobacco chitinase A was shown to be both necessary and sufficient for vacuolar targeting of a reporter protein and has been used since many times as a standard (Neuhaus *et* al., 1991; Stigliano *et* al., 2014).Moreover, Park and coworkers (2006) observed that the luminal part of *At*RMR binds *in vitro* the ctVSD of tobacco chitinase. Moss protoplasts transiently expressing the whole *Pp*AP1 sequence fused to GFP showed vacuolar fluorescence (Schaaf *et* al., 2004). The ctVSD of *Pp*AP1 was sufficient to target Citrine to the moss vacuole. In our work, no striking difference of fluorescent pattern between WT and mutant lines were observed for these two ctVSD, as a vacuolar pattern was also observed in the mutant lines. The absence of RMRs did not have any effect on the vacuolar targeting of these reporters in moss. If RMRs are vacuolar receptors, these two proteins do not belong to cargoes recognized by moss RMRs.

At last we detected an obvious difference of targeting for the ctVSD of cardosin A. In angiosperms, the C-terminal peptide of cardosin A was shown to be sufficient to target a reporter to the vacuole (Pereira *et* al., 2013). In our WT transgenic lines expressing Citrine with the ctVSD of cardosin A, a strong vacuolar fluorescent pattern was observed as expected, while fluorescence was retained in the ER in the 5KO, 3 KO and even two different 1KO mutants. Thus, when RMRs were absent, trafficking of this fluorescent reporter to the vacuole was inhibited. Moreover, it was enough to delete a single RMR gene (*Pp*RMR2 or *Pp*RMR5) to disrupt trafficking to the central vacuole. The same phenotype of the two single KO mutants excludes a differential function of the two subfamilies and could suggest a dosage effect. Indeed, we are still struggling to detect RMRs in *P. patens* and they could be very short lived. The ctVSD of *Pp*Ap1 differs from the ctVSD of cardosin A by only five additional amino acids and is unaffected. CtVSDs are inactivated when their very C-terminus is blocked by a bulky N-glycan or terminal Gly (Neuhaus *et* al., 1994; Bednarek *et* al., 1991). The addition of Glycine residues at the C-terminus of *Citrine-Card* could clarify the situation as it would prevent its interaction with RMRs and thus its vacuolar targeting.

PSI domains are only found in plants. They have been described to be signals for protein targeting to the vacuole (Pereira 2013). Differential sensitivity to dominant-negative Rab or Sar1 mutants underlined the existence of several pathways to reach the central vacuole. In moss, the PSI from cardosin A or B were both sufficient to target a reporter to the vacuole. There was no difference

between the WT and the 5KO line expressing either *PSIA-Citrine* or *PSIB-Citrine*, in both cases, fluorescence was vacuolar. Furthermore, we cannot decide yet if PSI A and B are taking the same route to reach the central vacuole in moss.

General secretory system reporters like ER-retained marker or secreted markers were not expected to be mistargeted in mutant lines. In both WT and 5KO lines expressing *Citrine-Ppchitinase*, fluorescence was localized in cell wall, as expected. In mutants, the ER-retained marker showed the same typical ER labeling than the WT. RMRs probably do not play a part in these cellular processes.

We confirmed that the ssVSD of *At*Aleurain targets the fluorescent reporter Citrine to the central vacuole in moss and did not observe any difference between the WT and the mutant lines. In flowering plants, the ssVSD of aleurain is known to target the protein to the lytic vacuole by interacting with a VSR (Holwerda and Rogers, 1993). Our results confirm that RMRs are not involved in the recognition of ssVSD and in proteins trafficking to the acidic vacuole. Nevertheless, even though two types of vacuole (acidic/non acidic) have been observed in *Physcomitrella patens* with neutral red staining, there is no evidence for the existence of storage vacuoles in moss.

Regarding the *SP-Citrine* construct, which was first designed to obtain a secreted pattern, the fluorescent reporter was targeted to the central vacuole, both in WT and in 5KO lines. As discussed in the previous chapter, the fluorescent reporter Citrine could contain a cryptic signal for vacuolar targeting, which would be not recognized in flowering plant. Further studies like the addition of Glycine residues at the C-terminus of SP-Citrine, could also prevent the recognition of a potential cryptic ctVSD, and would help to clarify this mechanism. Another hypothesis that we considered was a default vacuolar targeting because of the overexpression due to the strong HSP promoter. Proteins could formed aggregates in the ER and directly go to the vacuole for degradation. This route bypassing the Golgi was described for some vacuolar storage proteins in seeds (Vitale and Galili, 2001). However, we did not observed any aggregates in the ER by confocal microscopy that should support this hypothesis.

B. Vacuolar routes studies: secretory pathway inhibitors effects

In flowering plants, several different pathways to reach the vacuoles have been described. Generally, vacuolar proteins following the classical route are trafficking from the ER to Golgi/TGN, and to their final destination via multivesicular bodies or PVC compartments. This is the case for numerous soluble vacuolar cargoes such as aleurain, phaseolin or 12S globulin. However, proteins can also bypass the Golgi to directly reach the vacuole (reviewed by Uemura and Ueda, 2014). These routes were generally described in seeds for storage proteins, which may be packed into dense vesicles in the ER itself, before reaching the PSV (Vitale *et* al., 1999). In 2013, Stigliano *et* al. showed that two glycosylated vacuolar GFPs present a differential ENDO-H sensitivity and may thus follow distinct pathways. Analysis of the glycosylation pattern strongly suggested that one reporter transited through the Golgi and not the other one. Pereira *et* al. (2014) suggest a model where the several vacuolar routes depend on the cell type and environmental conditions. Secretory pathway inhibitors are efficient tools for studying proteins trafficking within the plant cell and Brefeldin A and Wortmannin are frequently used to block trafficking pathways.

Brefeldin A (BFA)

Initially discovered as an antibiotic, Brefeldin A is a fungal metabolite which reversibly and indirectly perturbs anterograde transport from the ER to the Golgi. Its targets are Sec7-type GEFs, necessary for Arf1 (ADP ribosylation factor 1 protein) activation, which plays a central role in Golgi transport. In many eukaryotes, BFA blocks the recruitment of COPI proteins, resulting in fusion of Golgi cisternae with ER (reviewed by Nebenführ *et* al., 2002). In plants, BFA induces changes in various organelles such as ER, Golgi and endosomal compartments. Tse *et* al. (2007) observed Golgi and PVC aggregates after BFA treatment in transgenic tobacco BY2 cells, expressing Golgi or PVC fluorescent reporter. However, they described a differential sensitivity to BFA of Golgi and PVC compartments. Not all Arf-GEF are BFA-sensitive in plants and this sensitivity can differ in different species (Geldner *et* al., 2003). *P. patens* Arf-GEF are expected to be BFA-sensitive, based on the critical amino acids in the Sec7 domain.

Wortmannin

Wortmannin is another fungal metabolite, which has been demonstrated to irreversibly inhibit phosphatidylinositol 3-kinases (PI3K) and phosphatidylinositol 4-kinases (PI4K) (Ui *et* al., 1995). PI3K catalyzes the production of phosphatidylinositol 3-phosphate (PI3P), an important lipid found in specific membranes of the secretory pathway. Wortmannin is known to perturb the secretory pathway and in plants specially the traffic to the lytic vacuole. It is generally used to study endosomal

organization and cellular trafficking. Previous studies demonstrated that Wortmannin interferes with protein trafficking to the acidic vacuole by blocking transport to the TGN. In plants, several routes addressing proteins to the vacuole have been described, and they do not show the same sensitivity to Wortmannin. It was shown that barley lectin and class I chitinases transit trough the Wortmannin-sensitive vacuolar route in tobacco cells (Matsuoka *et* al., 1995). Wang *et* al. (2009) described that Wortmannin induces homotypic fusion of prevacuolar compartments as well as TGN in transgenic tobacco cells expressing GFP-BP80. More generally in plants, Wortmannin treatment leads to fusion of MVB and formation of abnormal vacuolar structures (reviewed by Foissner *et* al., 2016). In *Arabidopsis* root cells, Wortmannin causes clustering, fusion and swelling of TGN and MVB, affecting the recycling of the vacuolar receptor BP-80 and indirectly the vesicular transport to the vacuole (Takác *et* al., 2012).

Study of inhibitors effects could help to distinguish the vacuolar routes followed by our different markers in moss. It may also give some clues about the involvement of RMRs in this trafficking protonema cells of transgenic lines were thus treated with Brefeldin A and Wortmannin. Localization of the fluorescent signal was then monitored by confocal microscopy.

B.1 Results

In the following work, protonema was treated overnight with 50µM of Brefeldin A or 30 µM of Wortmannin, following the heat-shock induction. Confocal observations were made the next day, 20 hours after induction of protein expression.

Transgenic lines (WT and 5KO) expressing *AtAleurain-Citrine*, usually showed a central vacuolar fluorescence. After Brefeldin A treatment, central vacuoles were not fluorescent anymore in either line (Figure 3.12). The fluorescent signal was visible in nuclear envelopes and in other ER structures. Protein transport to the Golgi was thus blocked by Brefeldin A. With Wortmannin, a different pattern was observed. Trafficking of *At*Aleurain to the vacuole was also blocked but the non-fluorescent central vacuole appeared swollen. Because of this, it was difficult to distinguish exactly where the fluorescent reporter was accumulated. Again no differences were noticed between the WT and the 5 KO line.

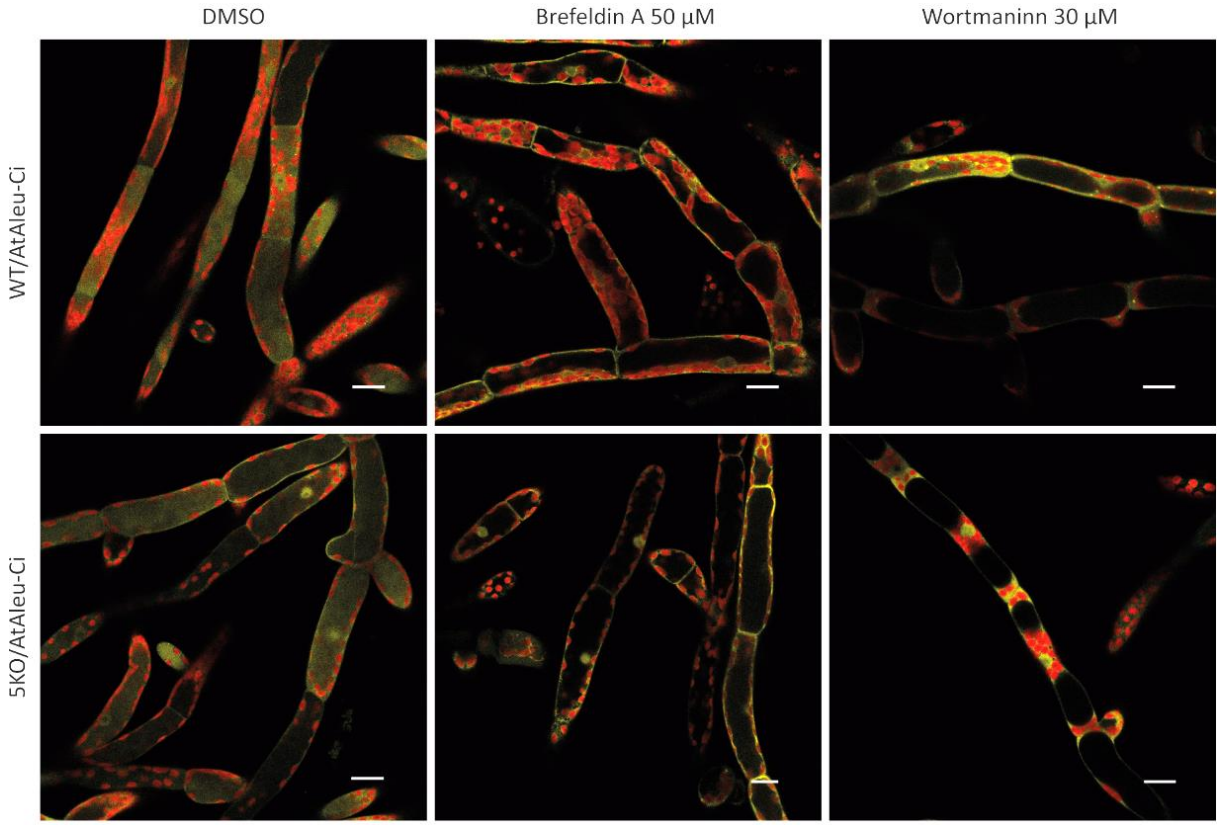

Figure 3.12 Vacuolar trafficking is inhibited by the secretory pathway inhibitors in protonema cells of transgenic lines expressing *AtAleurain-Citrine*.

Protonema cells were treated with 50 µM Brefeldin A (center panel) or 30 µM Wortmannin (right panel) overnight, just after heat-shock. DMSO was used as control (left panel). Confocal observations were made 20 hours after heat-shock. Scale bar = 20 µm.

To investigate the mechanism of the vacuolar targeting of *SP-Citrine*, a WT and a 5KO transgenic line expressing it were also treated with BFA and Wortmannin. Vacuolar trafficking was again blocked after treatment with either inhibitor (Figure 3.13). Again, BFA treatment lead to a fluorescent ER-like pattern, with easily observed nuclear envelopes. A very similar pattern was observed after Wortmannin treatment but again the central vacuole was swollen. This vacuolar route was again inhibited in both WT and 5KO lines. The RMR-independent vacuolar targeting of both reporters was thus BFA-and Wortmannin-sensitive.

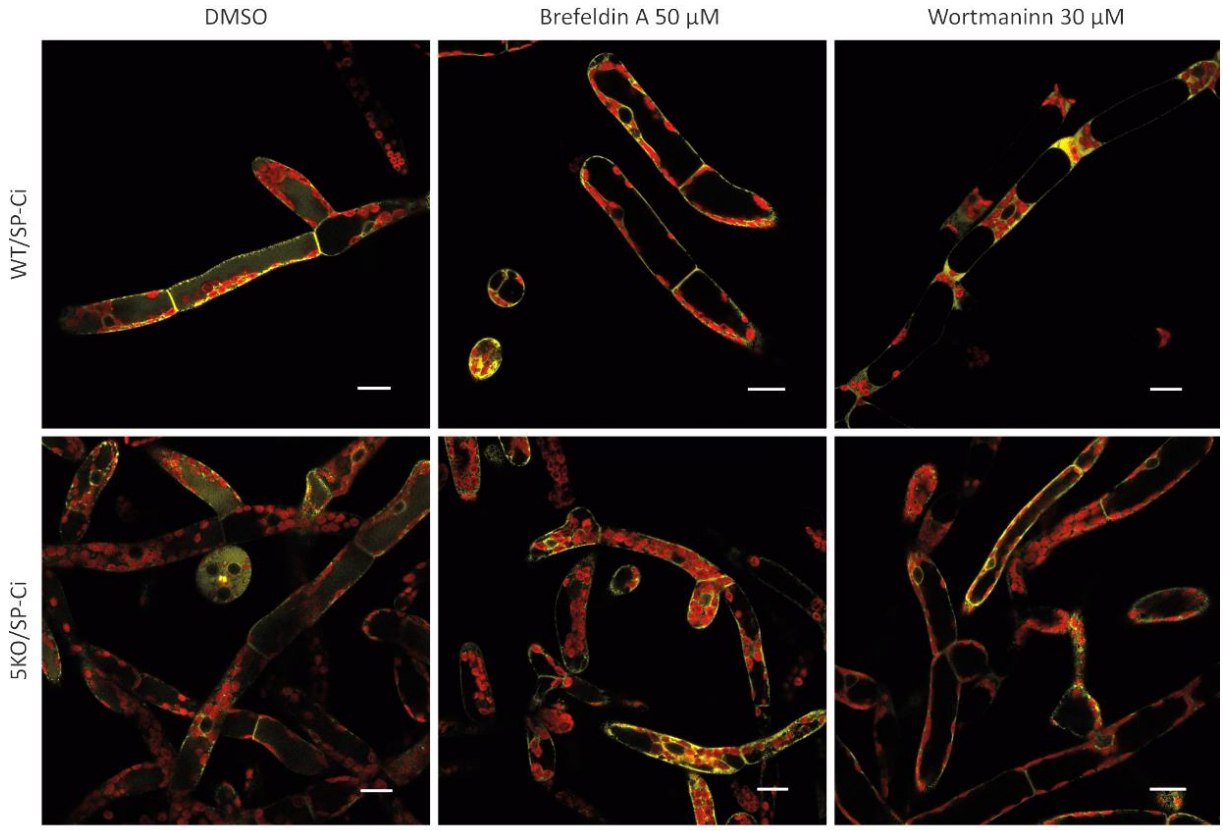

Figure 3.13 Vacuolar trafficking of *SP-Citrine* is inhibited by the secretory pathway inhibitors in protonema cells Protonema cells were treated with 50 µM Brefeldin A (center panel) or 30 µM Wortmannin (right panel) overnight, just after heat-shock. DMSO was used as control (left panel). Confocal observations were made 20 hours after heat-shock. Scale bar = 20 µm

We then tested the effect of these inhibitors on the lines expressing Citrine with the ctVSD of cardosin (*Citrine-card*) which has an RMR-dependent vacuolar localization: fluorescent vacuoles were observed in WT transgenic line while ER structures were visible in 1KO, 3KO and 5KO lines. In all three lines, treated cells showed an inhibition of vacuolar targeting of the fluorescent reporter (figure 3.14). *Citrine-Card* thus also follows a BFA-and-Wortmannin-sensitive pathway to vacuoles. After treatment with BFA, ER and nuclear envelope were visible in WT and 5KO lines. Cells treated with Wortmannin showed again swollen central vacuoles and fluorescent ER structures.

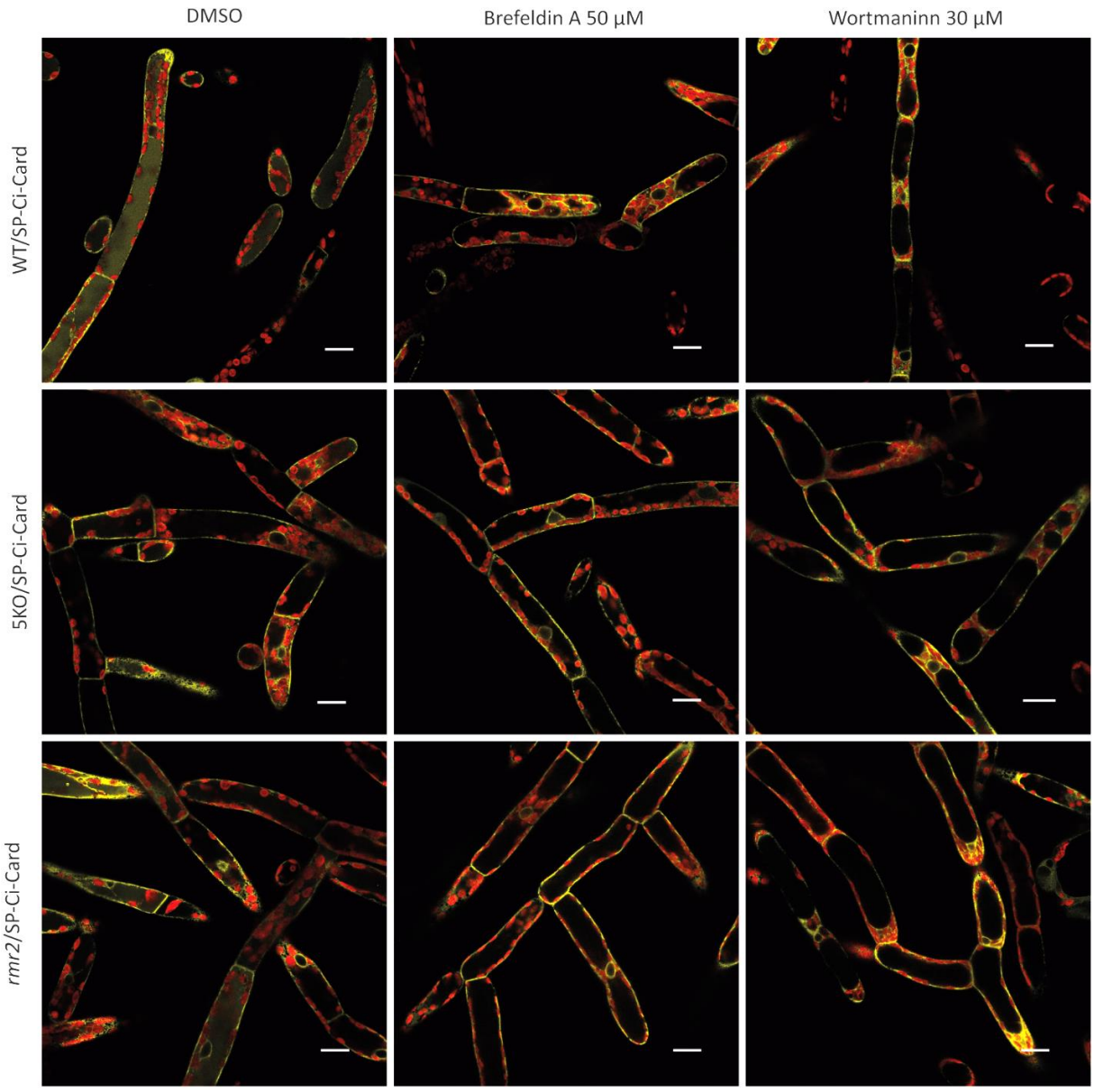

Figure 3.14 Vacuolar trafficking of *Citrine-Card* is inhibited by the secretory pathway inhibitors in protonema cells.

Protonema cells were treated with 50 µM Brefeldin A (center panel) or 30 µM Wortmannin (right panel) overnight, just after heat-shock. DMSO was used as control (left panel). Confocal observations were made 20 hours after heat-shock on three different lines: WT/SP-Ci-Card, 5KO/SP-Ci-Card and *rmr2*/SP-Ci-Card. Scale bar = 20 µm

The ctVSDs of cardosin A and of tobacco chitinase A were thought to direct the reporter to the vacuole by the same pathway. However we observed a different targeting in 5KO line expressing these constructs. Citrine coupled with the ctVSD of cardosin A was predominantly retained in the ER while ctVSD of chitinase was directed to the vacuole. WT and 5KO line expressing the ctVSD of tobacco chitinase were treated with BFA and Wortmannin. Confocal observations revealed that the vacuolar route was also blocked after treatment with both inhibitors (figure 3.15), while in controls, most cells showed a strong vacuolar fluorescence. After inhibitor treatment, trafficking to the vacuole was mostly inhibited by BFA or Wortmannin. *Citrine-Card* took a BFA–and-Wortmannin-sensitive route, as all other constructs tested in this work.

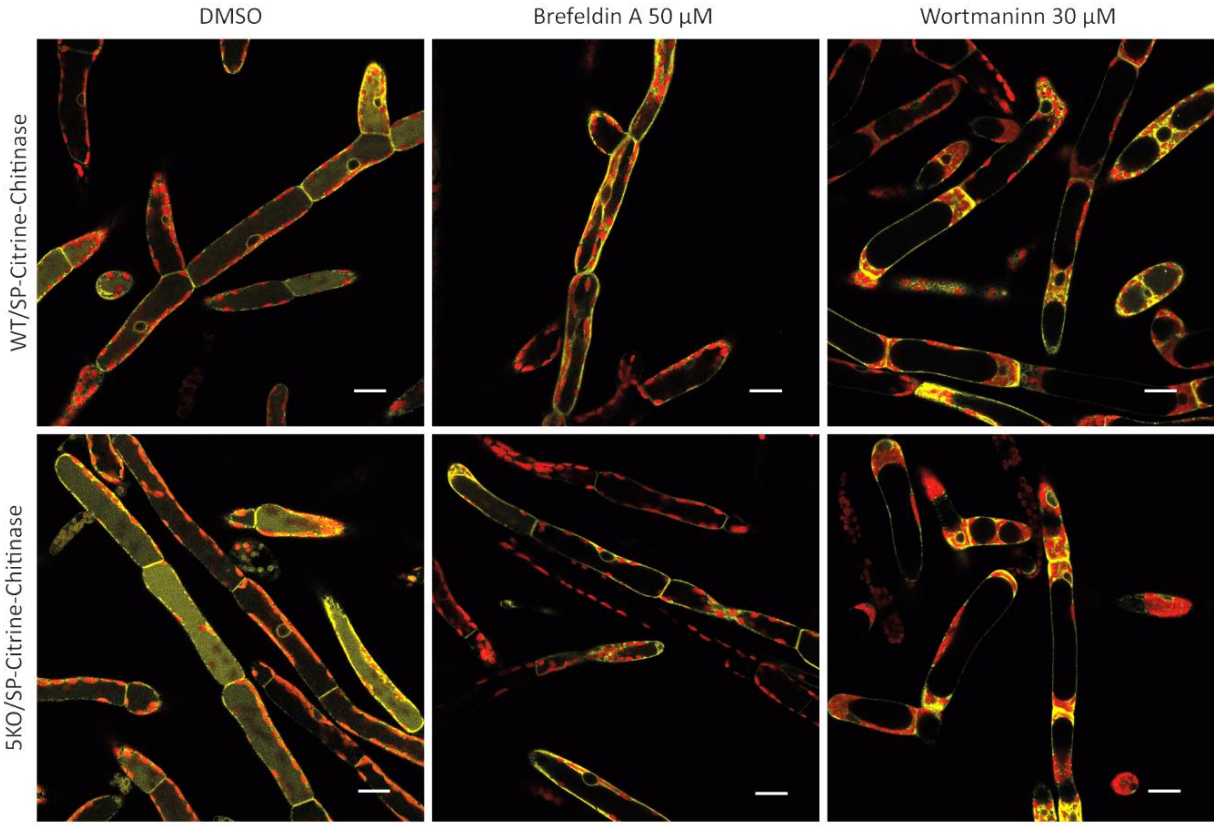

Figure 3.15 Vacuolar trafficking of *Citrine-Chi* is inhibited by the secretory pathway inhibitors in protonema cells. Protonema cells were treated with 50 µM Brefeldin A (center panel) or 30 µM Wortmannin (right panel) overnight, just after heat-shock. DMSO was used as control (left panel). Confocal observations were made 20 hours after heat-shock. Scale bar = 20 µm

B.2 Discussion

In flowering plants, different pathways to the vacuole were observed and characterized by the use of secretory pathway inhibitors like BFA and Wortmannin. Two post-Golgi routes were identified, involving two kind of vacuolar receptors. In one side, ssVSD were described to be recognized by VSR receptors and to target proteins to the acidic vacuole (Jiang and Rogers 1998; DaSilva *et* al., 2006; Zouhar *et* al., 2010). On the other side, ctVSD were shown to direct proteins to the neutral/storage vacuole and RMRs could play the role of receptors in this mechanism. The distinct routes to the vacuole were defined by different sensitivity to secretory pathway inhibitors. Cardosin A contains two VSDs, a ctVSD and a PSI domain, acting in distinct vacuolar route. Wortmannin treatment allowed to differentiate these routes: the ctVSD was guiding reporters to the central vacuole via a Wortmannin-sensitive route, while reporters with the PSI domains trafficked via a Golgi/PVC-independent route, not affected by Wortmannin (Pereira, 2012). Stigliano *et* al. (2013) observed a differential effect of BFA on two vacuolar glycosylated GFPs, GFP-gl133-Chi and Aleu-GFP-gl133 (with a ctVSD and an ssVSD respectively), corroborating other evidence about the two distinct routes taken by these reporters to the vacuoles. GFP-gl133-Chi seems to transit from ER to vacuole by an independent-Golgi route.

BFA has an effect earlier in the secretory pathway because it blocks the formation of COPI vesicles and indirectly affects the transport between ER and Golgi. The majority of Golgi enzymes are found in ER compartment after a BFA treatment (reviewed by Nebenführ *et* al., 2002). Cis-Golgi cisternae disappear progressively during BFA treatment in tobacco BY2 cells (Ritzenthaler *et* al., 2002). Wortmannin prevents vesicular transport later in the secretory pathway. It was described to inhibit the recycling of TGN vesicles in plants because it blocks the enzyme necessary for the production of endosomal membrane lipids. Wortmannin is known to induce fusion of PVC in tobacco BY2 cells but also in mung bean seeds (Wang *et* al., 2009). Fusion of TGN with PVC was also described after Wortmannin treatment.

We chose to block trafficking pathway of some of our transgenic lines with BFA and Wortmannin in order to test for the existence of distinct vacuolar routes in moss. We selected lines expressing different kind of reporters, and supposed to take different routes to the vacuole. All lines targeting the reporter to the vacuole were equally affected by BFA and Wortmannin. This confirms that these drugs have similar targets in moss as in angiosperms. However, it does not indicate any difference in the transport pathway to vacuoles in moss. Further investigations could be done by testing the BFA and Wortmannin sensitivity of our other fluorescent line. Testing the line expressing *Citrine-PpChitinase*, could bring answers about common secretory compartments between proteins targeting to vacuoles and secreted proteins in seedless plants. As previously mentioned, PSI domain

from cardosin A traffics to vacuole via a Wortmannin-non-sensitive route (Pereira, 2012). Testing our PSIA and B fluorescent lines could also give information about these unconventional vacuolar determinants.

C. Localization of *Pp*RMR2

Several studies already investigated the localization of RMRs in higher plants. The first publication described the presence of RMRs in the PSV crystalloid in tomato cells (Jiang *et* al., 2000). Later, *At*RMR1 was localized in Golgi and in prevacuolar compartment of PSV (Park *et* al., 2005). More recently, *At*RMR2 was described to localize mainly in the TGN while *At*RMR1 was mainly in ER structures of tobacco leaves and *Arabidopsis* protoplasts (Occhialini 2011). In rice, *Os*RMR1 was localized in Golgi apparatus, in TGN and in PVC-like organelles (Shen *et* al., 2011). RMR proteins were first thought to be involved in vacuolar targeting because of their common PA domain with the well-known vacuolar receptors VSR. The PA domain plays a role in protein-protein interactions. However, it was also found that in *Arabidopsis* the TM and the C-terminal domain of *At*RMR1 localized in central vacuole when fused with the fluorescent reporter RFP (Scabone *et* al., 2011). This result could indicate that RMRs may act as receptors for cargoes trafficking all the way to the vacuoles.

In *P. patens*, the five RMR genes are generally expressed at the same low level but not in the same proportions in all tissues and organs. RMR1, 3 and 5 are more expressed in sporophytes and spores while the expression level of RMR2 is higher in protonema and gametophores. RMR4 is the only one to be equally expressed in all type of organs (figure 3.16). As described before, a phenotypic difference between the WT and the KO lines was observed only when the fluorescent construct *SP-Citrine-Card* was expressed. No differences were observed for the other ctVSD tested. The logical question that need to be answered is *are RMR directly involved in this phenotype or is it an indirect effect of the lack of these proteins?* Localization of RMRs in moss may help to investigate the cellular processes leading to this phenotype. *Pp*RMRs have never been localized. Assays of *Pp*RMRs immunodetection were done with antibodies raised against RMR2 and RMR4. Unfortunately, we did not detect the protein in moss extract. Immunolocalization was not possible as no antibody against *Arabidopsis* or rice RMR detected anything in western blot of moss extracts. Despite these antibodies were able to detect the recombinant RMR proteins produced in *E. coli*, we could not detect the moss proteins.

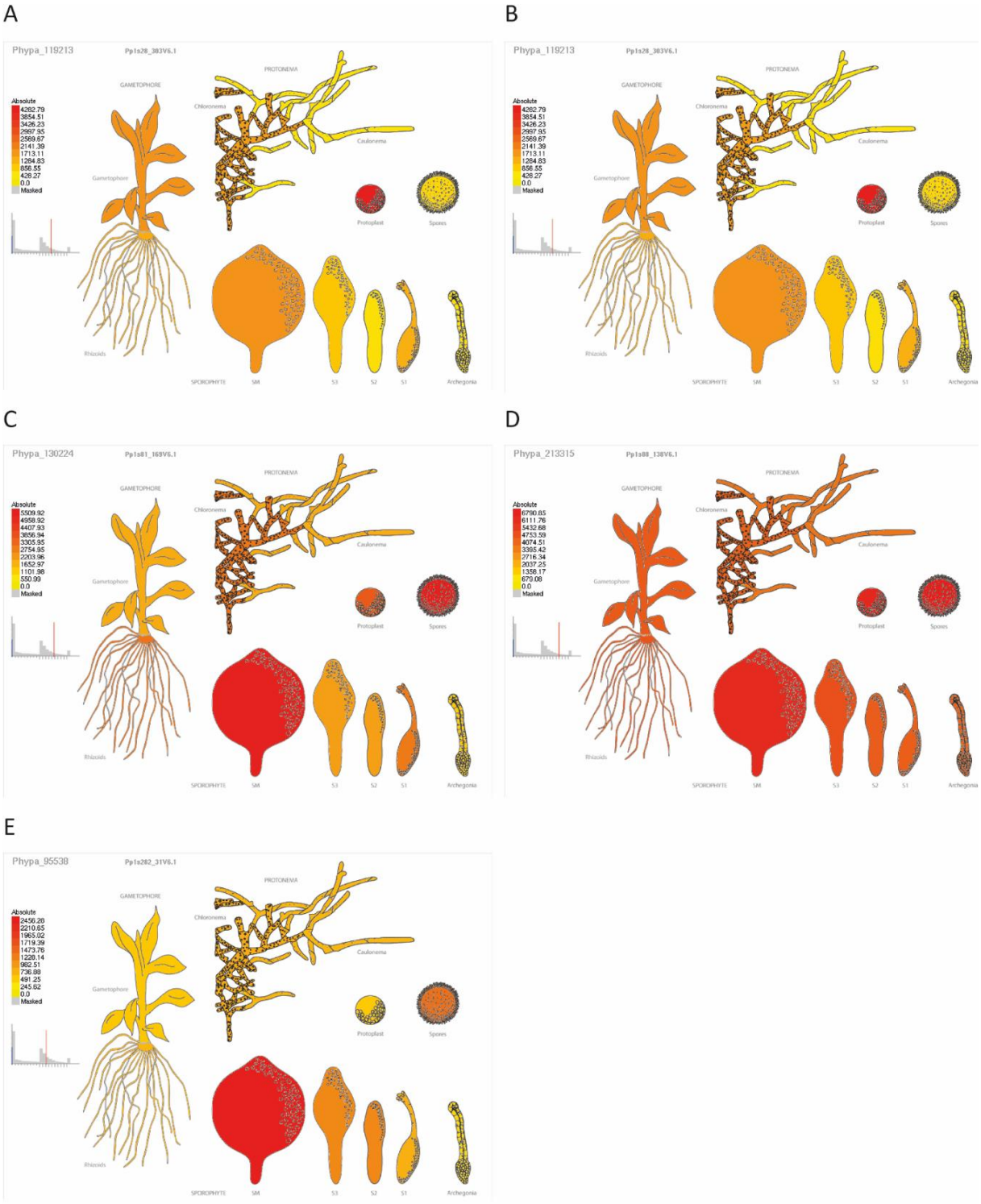

Figure 3.16 Expression profile of RMR1 and 2 according to the different moss organs (from Physcomitrella eFP browser). (A) RMR1 is more expressed in gametophore, sporophyte and chloronema

(B) RMR2 is more expressed gametophore, sporophyte and chloronema

(C) RMR3 is more expressed in gametophore, sporophyte and chloronema

(D) RMR4 is quite expressed at the same level in all organs

(E) RMR5 is more expressed in sporophyte and spore

C.1 *Pp*RMR2 localization in *Physcomitrella patens*

We decided to overexpress one *Pp*RMR fused to the fluorescent reporter Cerulean, a blue variant of GFP. From the five *Pp*RMRs, we chose to work with *Pp*RMR2. It is shown to be more expressed in chloronema and gametophores than in caulonema or spores.

A 1KO mutant of *Pp*RMR2 (*rmr2*) was generated by S. Ayachi (2012) and a transgenic line expressing the fluorescent construct *SP-Citrine-Card* was developed from this mutant (see section A of this chapter). In this transgenic line, the fluorescent pattern observed was very similar to the pattern observed in 5KO/*SP-Citrine-Card* line: the fluorescence was predominantly found in the ER. The trafficking to central vacuole was thus disrupted. Another PhD student is in the process of testing complementation of the mutant lines with various mutated versions of *Pp*RMR2.

A construct with the full sequence of *Pp*RMR2 cDNA C-terminally fused with the fluorescent reporter Cerulean was assembled with a HSP promoter. This construct was targeted to the non-coding PIG locus in the genome of *P. patens* WT. Stable lines were observed by confocal microscopy after heat-shock induction.

C.1.a Preliminary observations

Four transgenic lines *PpRMR2-Cerulean* were observed by confocal microscopy but unfortunately, no fluorescent signal was detected, 24 hours after heat-shock induction in any line (figure 3.17).

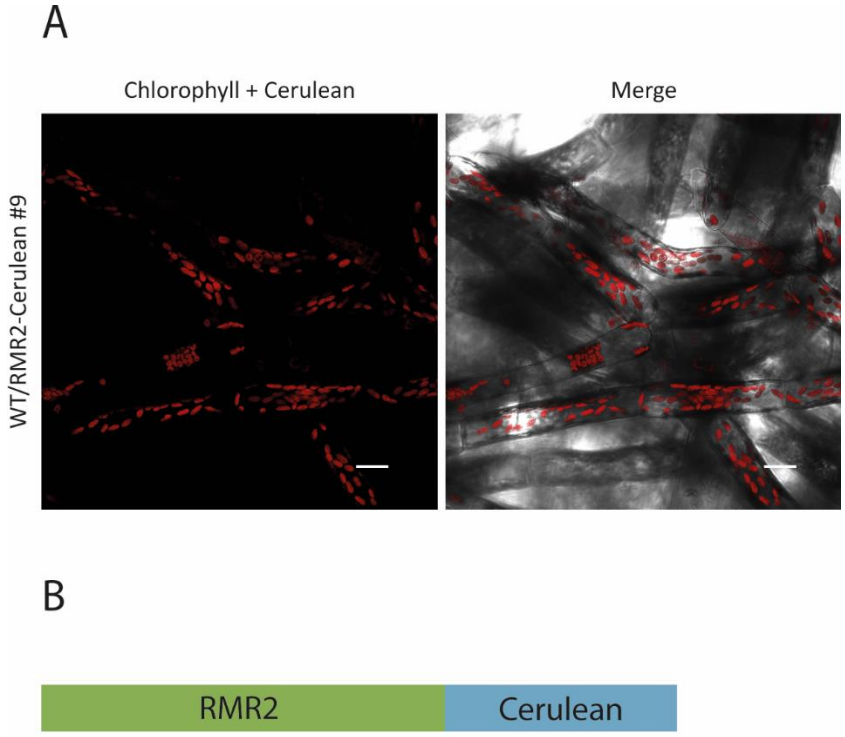

Figure 3.17 No fluorescent signal was detected in the transgenic line containing the RMR2-Cerulean construct. (A) The full length cDNA sequence of *Pp*RMR2 was fused to the N-terminus part of the Cerulean. Protonema was observed 24 hours after heat-shock induction. No Cerulean signal was detected. Chloroplasts were visualized by the chlorophyll autofluorescence (left). The right image shows the superposition of chlorophyll and bright field. Scale bar = 20 µm.
(B) Schematic representation of the *Pp*RMR2-Cerulean construct.

C.1.b Control of transgene insertion and expression

To explain the absence of detectable fluorescent signal, we performed several controls on the selected transgenic lines. Firstly, a western blot of total proteins from these lines, obtained 24 hours after heat-shock was done. Unfortunately we failed to detect any Cerulean, using anti-GFP antibodies (Figure 3.18). As a control we used a line expressing *Citrine-Card* under the same promoter and induced in the same manner.

Then we performed PCR on genomic DNA (genotyping) to assert proper insertion of the foreign DNA to the moss chromosome (figure 3.18). The whole construct was correctly detected in clones #2 and #9. On the contrary, the insert was not properly detected in clones #1 and #3, explaining why we did not observe any fluorescent signal in these two clones.

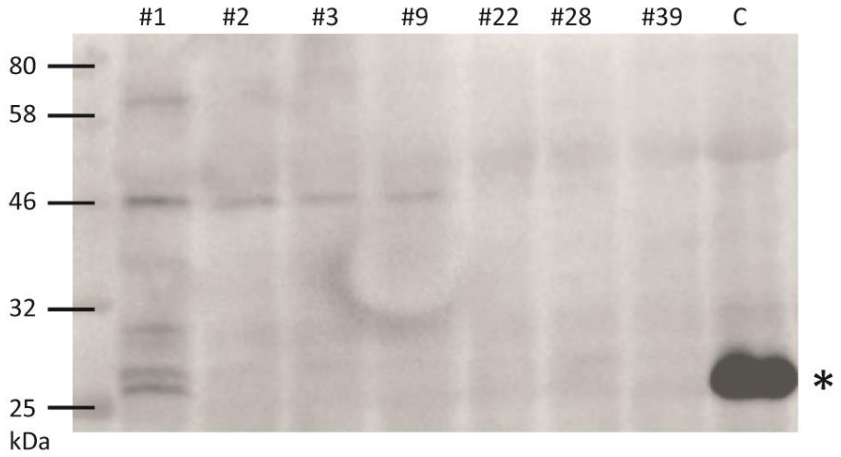

Figure 3.18 Western blot analysis of protonema trangenic lines WT/RMR2-Cerulean

The fusion protein RMR2-Cerulean has a predicted MW of 68 kDa. No signal was detected in the different lines. Equal amount of proteins extracted from protonema, 24 hours after heat-shock induction, were separated by SDS-PAGE and immunoblotted with anti-GFP antibodies. #1 to #39: transgenic lines WT/RMR2-Cerulean; C: positive control line expressing *Citrine-Card* (27kDa, black star).

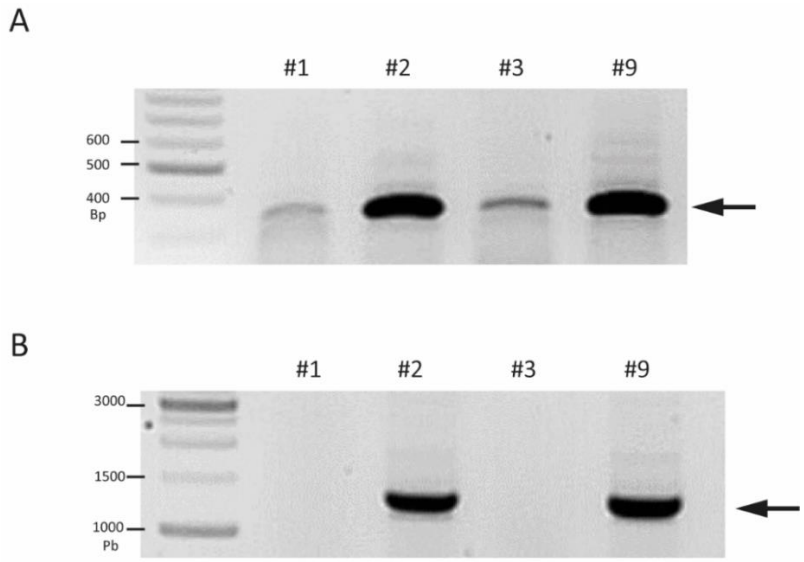

Figure 3.19 Genotyping of transgenic lines transformed with *RMR2-Cerulean*

Genomic DNA was extracted and PCR amplification were made with two couples of primers (A) Primers flanking the fluorescent reporter were used. The expected size (black arrow) is 320 bp (B) Primers flanking the whole construct were used. The expected size (black arrow) is 1290 bp

We also controled the expression of *RMR2-Cerulean* by PCR on cDNA. Unfortunately, despite numerous amplifications assays with several couples of primers, results were too ambigous to conclude whether gene silencing was involved. It has been described that RMRs proteins are probably very instable. If *RMR2-Cerulean* is properly expressed in protonema, this could be a reason why we did not succed to detect the fluorescent protein even if the genomic insertion is confirmed.

C.2 Proteasome inhibitors

If *Pp*RMR2 is not detected because of its low stability or its fast turn-over within the cell, treatment with proteasome inhibitors, could help to stabilize it and increase the probability of detection. Proteasome inhibitors are very helpful tools to study cellular processes. The proteasome represents the main system for proteins degradation. Inhibition of this mechanism will lead to stabilization of proteins by blocking the most important degradation pathway of the cell. In eukaryotes, the cytosolic proteasome also degrades unfolded membrane and secretory proteins reexported from the ER (reviewed by Lee and Goldberg, 1998). Treatment with proteasome inhibitors quickly reduces protein breakdown and causes an accumulation of ubiquitin-tagged proteins in the cell. Even though there are multiple active sites inside the proteasome structure, protein breakdown efficiently reduced even if not all sites are inhibited.

The proteasome inhibitor II (Santa Cruz Biotechnology) was used in attempt to stabilize *Cerulean-RMR2* in protonema *of P. patens*. Treatment was applied overnight at low concentration (100nM), after heat-shock induction. Observations were made as usual, 24 hours after the induction of proteins expression. Unfortunately, proteasome inhibitor treatment did not improve the detection of the Cerulean signal (figure 3.20). The fluorescent signal of Cerulean was not detected in any lines.

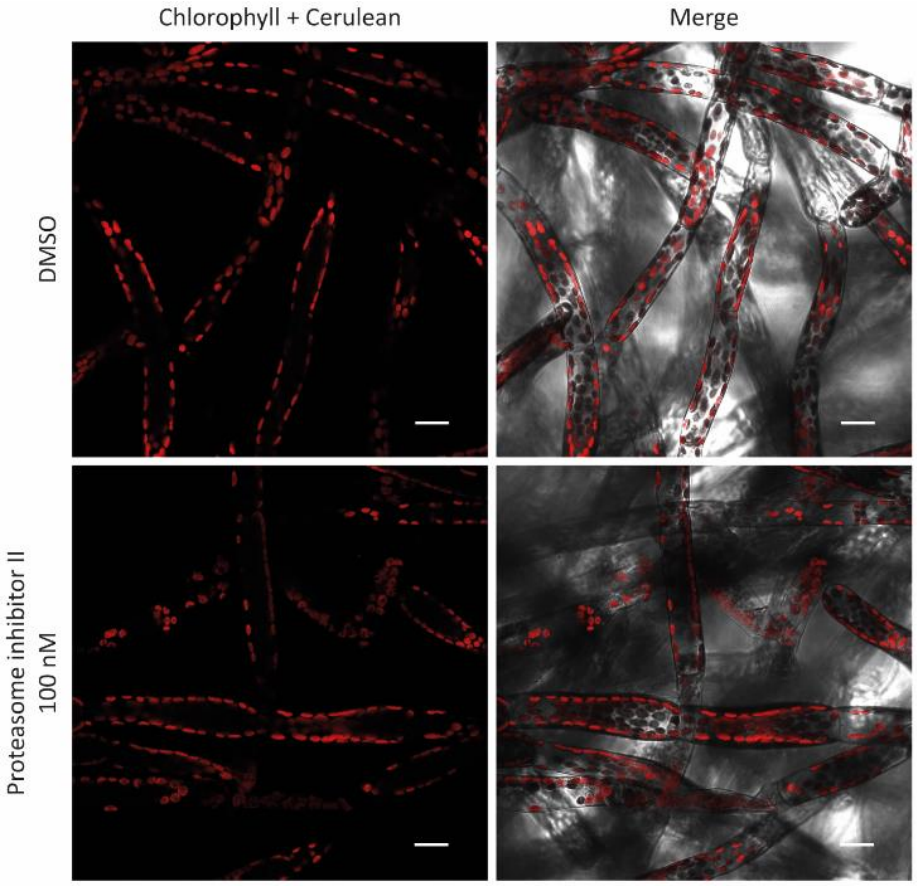

Figure 3.20 No fluorescent signal was detected in the transgenic line #9 expressing *RMR2-Cerulean* even after proteasome inhibitor II treatment.

Observations were made 24 hours after heat-shock induction and proteasome inhibitor II overnight treatment (100 nM) on protonema cells. No Cerulean signal was detected. Chloroplasts are visualized by the chlorophyll autofluorescence (left panel). The merged image shows the superposition of chlorophyll and bright field (right panel). Scale bar = 20 µm.

C.3 Discussion

Localization of *Pp*RMRs would help to understand their role in moss. However, we could not detect *RMR2-Cerulean* by confocal microscopy. A previous collaborator already described the difficulty to localize *At*RMR1 and 2 in *Arabidopsis* transgenic lines (Occhialini 2011). In his work, *At*RMR1-YFP and *At*RMR2-YFP were expressed under the control of the 35S promoter in different systems. *At*RMR2-YFP was localized in ER structures in *N. benthamiana* leaves and colocalization with the P6 reporter (an ER marker) was also confirmed. However, in transgenic *Arabidopsis* plants, *At*RMR2-YFP was very difficult to detect and a very faint signal in ER was observed, despite the strong 35S promoter. In *N. benthamiana* leaves, *At*RMR1-YFP was localized in dot structures and colocalization with the TGN marker SYP61 was confirmed. But in coexpression by agroinfiltration in *N. benthamiana*, the *At*RMR1-YFP fusion was not detectable without a preliminary treatment with a silencing inhibitor (p19) (Occhialini 2011).

We identified two clones with proper insertion of *Cerulean-RMR2* to the chromosome. If the heat-shock was done properly and if no post-translational modifications or regulations occurred, fluorescence should be detected in these two lines. However, we did not detect the Cerulean by PCR on cDNA. Detection of the fusion protein by western blot was no more successful. Results were too ambiguous to conclude if RNA silencing leading to a rapid degradation of the mRNA occurred, or if the problem was protein stability.

Because the main objective of this thesis was the characterization of the 5KO RMR mutants, we did not go further to explain this result. One possibility would be to test *e.g. Pp*RMR3 or *Pp*RMR4. A truncated version of PpRMR2 could also be used. In *N. benthamiana*, truncated *At*RMR1 or 2 tagged with YFP still labeled the same compartment than the full length protein, but the fluorescence was more intense (Occhialini *et* al., 2016). Other kinds of proteasome inhibitors could be used in order to increase the stability of the fusion construct and help its detection.

D. Phenotypic study of RMR mutants

Plants are sessile organisms and must permanently adapt to a changing environment. They have to adjust their cellular functions depending of various stresses, in order to counterbalance the negative impacts on their development. Numerous studies described the correlation between the ubiquitin-proteasome system (UPS) and plant stress tolerance. The ubiquitination mechanism plays a major role in the response to environmental stresses, such as drought, cold or salinity. UPS regulates the level and the stability of proteins within the cell. The adaptation to abiotic stresses requires the degradation of stress signaling molecules (reviewed by Lee and Kim, 2011). Evidence of the relationship between E3 ligases and stress signaling are accumulating (reviewed by Lyzenga and Stone, 2011). In hot pepper (*Capsicum annuum*) the protein Rma1H1 (Ring membrane anchor E3 ligase homologue of Human) was described to increase the tolerance to drought stress by inhibiting the targeting of the aquaporin PIP2;1 to the PM (reviewed by Lee and Kim, 2011). More recently, the correlation between salt stress and UPS highlighted the role of the protein STRF1 (Salt tolerance RING Finger 1), a membrane trafficking-related E3 ligase in *Arabidopsis* (Tian *et* al., 2015). RMR proteins are sharing a RING domain with a major group of E3 ligases, suggesting they could have an E3 ubiquitin ligase activity as well. Study of the impact of abiotic stresses on the RMR mutants could help us to characterize the function of these proteins. Because a relationship between sever water loss and E3 ligase activity had already been described, a previous PhD student investigated the effect of drought stress on 5KO mutants (Ayachi, 2012). However, the mutants recovered as well as the WT line after drought stress and no drought sensitivity was observed in the 5KO line. We decided to further investigate the impact of a salt stress.

D.1 Results

A previous study on *P. patens* showed a relationship between small heat shock proteins (sHSPs) and abiotic stress tolerance, especially in heat, salt and osmotic stress recovery (Ruibal *et* al., 2013). We decided to apply the same salt concentration (500mM NaCl) to stress our WT and 5KO mutant lines. Discs of three week old protonema were cut and put on medium supplemented with 500mM NaCl. Unexpectedly, a phenotypic difference was observed between the WT and the mutant after 4 weeks on regular NH4 medium, before applying salt stress (figure 3.21). The mutant line developed many more leafy gametophores than the WT. In WT, protonema represented the majority of the colony and only few gametophores were observed.

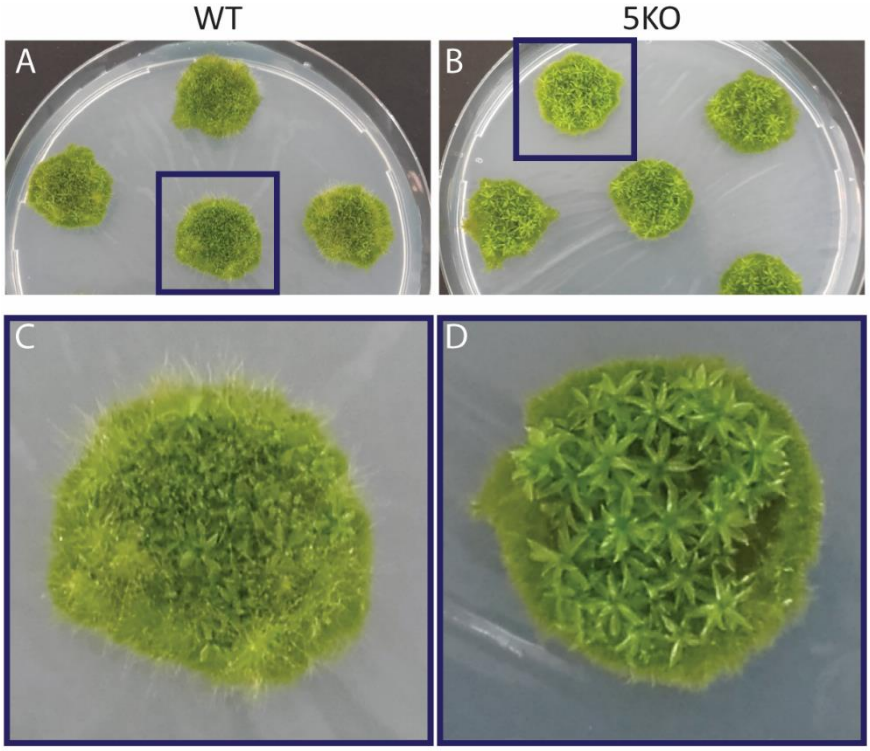

Figure 3.21 A phenotypic difference was observed between the WT and the 5KO mutant line after 4 weeks on NH4 medium (no treatment). (A) and (C) WT; (B) and (D) 5KO

Protonema was grown on NH4 medium for 3 weeks. Protonema discs were cut and grown on NH4 medium for 1 more week.

Despite the phenotypic difference observed before applying salt stress, the protonema discs were placed on NH4 medium supplemented with 500 mM of NaCl for two days. After two days of recovery in NH4 medium, both lines were drastically affected, protonema and leafy gametophores were yellowed. We did not observe any difference between the WT and the 5KO (data not shown). Two days of salt stress were too long because plants did not recovered and stayed yellowed. No difference in salt stress sensitivity was detected between mutant and WT. However, the important formation of gametophore in 5KO after 4 weeks on NH4 medium was unexpected. To confirm this difference, repetitions were done and 3KO and 1KO lines were also tested (figure 3.22). The same phenotype was observed in other mutant lines. All mutants developed many more leafy gametophores than the WT after 4 weeks on NH4 medium.

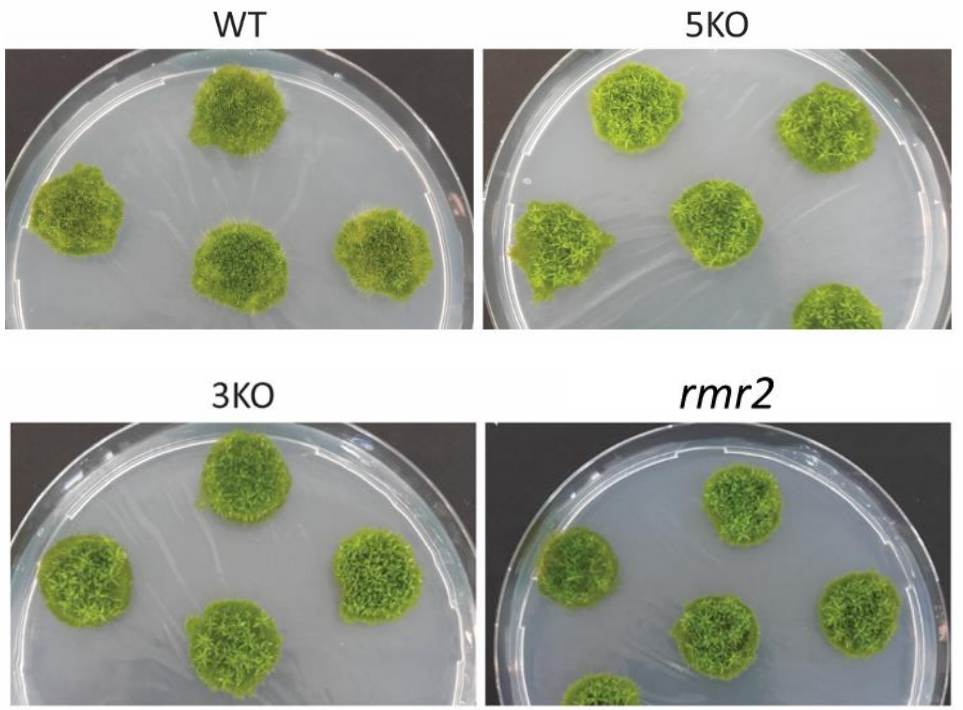

Figure 3.22 A phenotypic difference was observed between the WT, the 3KO, *rmr2* and the 5KO mutant line after 4 weeks on NH4 medium

Protonema was grown on NH4 medium for 3 weeks. Protonema discs were cut and grown on NH4 medium for 1 more week.

D.2 Discussion

In plants, numerous studies suggested a relationship between abiotic stress responses and E3 ligases activity. As members of the PA-TM-RING family and particularly because of their cytosolic RING domain, RMRs are probably ubiquitin ligases as well. *Pp*RMR mutants did not show any difference of sensitivity to drought stress but they could be involved in response to other abiotic stresses (Ayachi 2012). To test this hypothesis, salt stress (500 mM NaCl) was applied on RMR deletion mutants. No difference of sensitivity and recovery was observed between mutants and WT lines. However, a surprising phenotypic difference was observed in controls (non-stressed colonies). The RMR mutants developed many more leafy gametophores than the WT line. Colonies were grown on NH4 medium, in which the nitrogen source is ammonium tartrate. Ammonium tartrate plays a role in moss development and cell cycle and more specifically in the formation of caulonema cells. Indeed, ammonium tartrate supplementation blocks the development of *Physcomitrella* at the chloronema state (Schween *et* al., 2003).

Despite having a clear correlation between the phenotype observed on NH4 medium and the presence or absence of RMRs, the mechanism involved here remain to be elucidate. Replications and further investigations will be needed, *e.g.* testing different ammonium tartrate concentrations. Other abiotic stresses could also be tested such as heat, cold or dark stress.

Chapter 4
Identification of RMR2 partners: clues to the role of RMRs in moss?

RMR proteins are thought to be vacuolar receptors, playing a role in the trafficking of cargoes to the neutral or storage vacuole. So far, experimental evidence supporting this hypothesis is limited. In the previous chapter, a trafficking difference between the WT line and mutant lines (1KO, 3KO or 5KO) was observed, but only for the Citrine tagged with the ctVSD of cardosin A. In WT, the fluorescent protein was localized in the central vacuole, while in mutants, it was predominantly retained in the ER. Surprisingly, even a single RMR missing was enough to disrupt the traffic to the vacuole. Even though this result supports an involvement of RMRs in vacuolar targeting, it does not prove about a direct role. As a complementary approach, identification of putative partners of *Pp*RMR2 appeared essential. Moreover, independently of a role of RMRs in vacuolar targeting, an involvement in ubiquitylation is strongly suggested by the presence of the RING-H2 domain. RMRs are members of the PA-TM-RING family, which in animals have been found to act as E3 ubiquitin ligases (*e.g.* GRAIL in mammals) but without a role in trafficking. Based on this hypothesis, we decided to look for binding partners of the luminal domain, including the putative E3 ligase, and a pull-down assay using a Glutathione-S-Transferase (GST) protein fusion was selected.

1. Pull-down assay using a GST fusion protein

GSTs are enzymes, involved in detoxification processes by conjugating reduced glutathione (GSH) with a wide range of xenobiotic compounds (Townsend and Twe, 2003). They also play a role in protection against oxidative stresses. A 26 kDa GST is now used as an efficient tag for the synthesis and recovery of recombinant proteins in bacteria. Purification of GST-fusion proteins using a GSH-coupled affinity matrix is widely used to study these proteins by activity tests, crystallography and affinity tests. A GST-fusion protein bound to such a matrix (as GSH coupled to agarose/sepharose beads) can be used to identify and characterize proteins interacting with the probe protein (Harper and Speicher, 2011).

We expressed the cytosolic part of *Pp*RMR2 fused to GST in an expression vector (pGEX) where its expression is inducible by IPTG. This pGEX-GST system is efficient for the production of soluble recombinant proteins, avoiding the sequestration of proteins in inclusion bodies (Harper and Speicher,

2011). *Pp*RMR2-GST was then bound to GSH-coupled agarose beads, and used to capture putative binding partners of *Pp*RMR2 from total proteins contained in moss lysates. The prey proteins were eluted from the beads and separated by SDS-PAGE before their identification by mass spectrometry (figure 4.1).

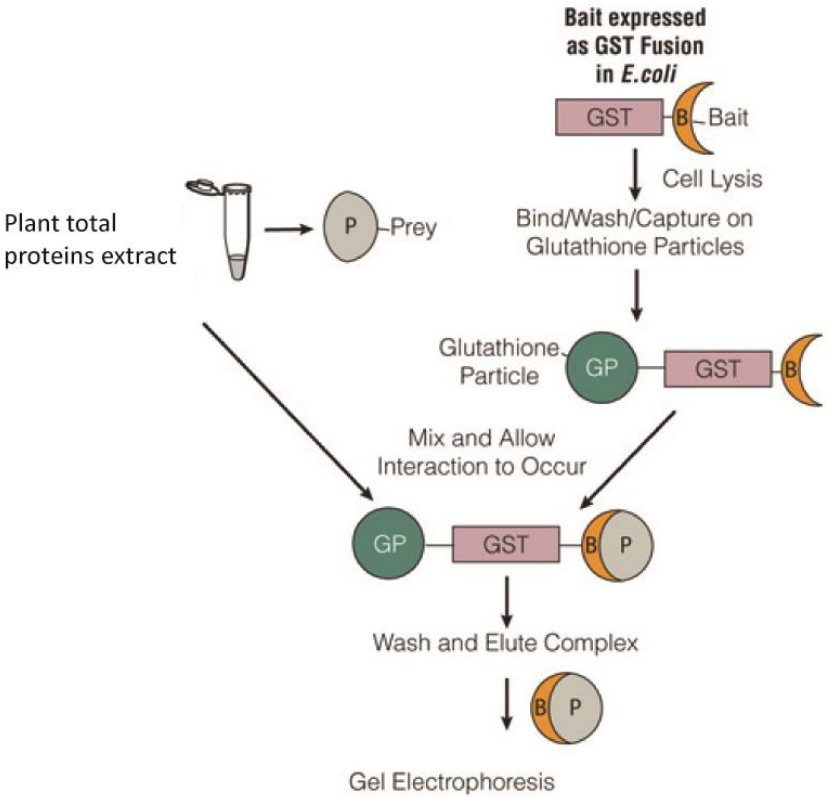

Figure 4.1 GST pull-down system (adapted from biotechniques.com)

The bait protein (cytosolic part of RMR2 fused to GST) is immobilized on agarose beads and incubated with a moss cell lysate containing putative target proteins. After washing steps, protein complexes are analyzed by SDS-PAGE and identified by mass spectrometry.

The C-terminal part of RMR2 was chosen for this experiment because this cytosolic part comprises the RING domain, which is a protein/protein interaction domain involved in a wide range of cellular processes. It is conserved in all animal homologues of RMRs - the PA-TM-RING protein group - (*e.g.* GRAIL, Goliath or RFN13), and plays an important role in their function as E3 ubiquitin ligases. We hope thus to identify among other binding partners substrates of the RMR E3 ligases.

2. Results

For the GST pull-down assay, the GST-*Pp*RMR2 fusion was purified and incubated overnight with total protein extracts from WT or 5KO line. After washing steps, proteins were separated by SDS-PAGE and visualized by colloidal Coomassie blue staining (figure 4.2). The GST protein alone was used as control.

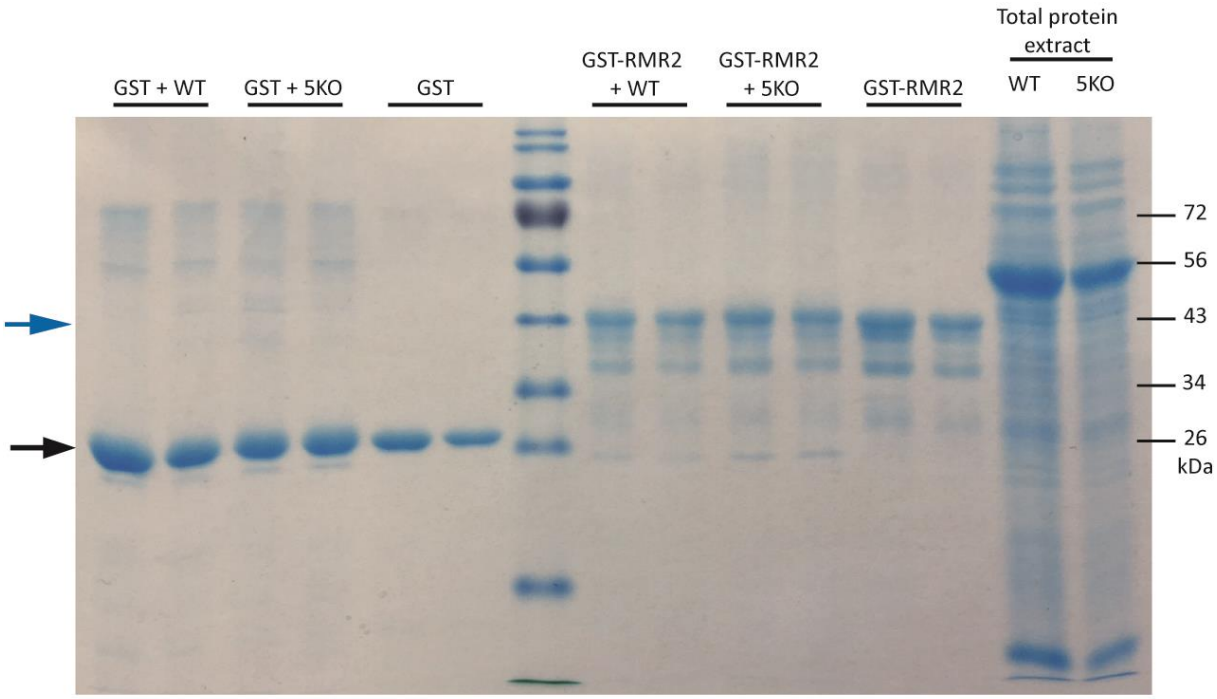

Figure 4.2 Pull down assay. Proteins were eluted from the GSH beads after overnight incubation with total protein extracts from WT or 5KO moss, using either GST or GST-RMR2 as a bait.

GST+WT: GST protein incubated with WT protein extract

GST+5KO: GST protein incubated with 5KO protein extract

GST-RMR2 + WT: GST-RMR2 fusion incubated with WT protein extract

GST-RMR2 +5KO: GST-RMR2 fusion incubated with 5KO protein extract

GST is 26 kDa (black arrow). The GST-RMR2 Fusion is 42 kDa (blue arrow).

After separation, pulled-down target-proteins were analyzed by mass spectrometry. The experiment was performed twice. Proteins identified two times or more in both repetitions are summarized in the following table (table I).

Table I Putative partners of the cytosolic part of *Pp*RMR2, identified by mass spectrometry

Protein	Pathway involved	Accession number	Protein extract used
Ubiquitin protein ligase HUWE1	Target to proteasome ?	PP1S138_130V6.1	WT + 5KO
Ubiquitin protein ligase UBR4	Modulation of protein activity ?	PP1S31_210V6.1	WT + 5KO
Ubiquitin activating enzyme E1		PP1S74_65V6.1	5KO
26S proteasome regulatory subunit T5	Protein degradation	PP1S218_133V6.1	5KO
26S proteasome regulatory subunit N9		PP1S131_74V6.1	5KO
26S proteasome regulatory subunit N3		PP1S65_153V6.1	5KO
Heat shock protein 70kDa	Chaperone proteins Quality control cell signaling ?	PP1S181_3V6.1	WT + 5KO
Heat shock protein 90kDa beta		PP1S118_219V6.1	5KO
Molecular chaperone HtpG (htpG, HSP90A)		PP1S83_80V6.1	5KO
Coatomer subunit beta	Coated transport vesicles	PP1S61_1V6.1 and PP1S42_100V6.1	WT + 5KO
Coatomer subunit gamma		PP1S276_96V6.1	5KO
Coatomer subunit alpha		PP1S135_34V6.1	WT

Proteins involved in four distinct cellular pathways were found as potential partners of the cytosolic part of *Pp*RMR2. The first proteins are involved in some ubiquitin pathway. The second proteins are regulatory subunits of the proteasome, involved in the binding of ubiquitylated proteins. The third proteins are chaperone proteins involved in the quality control. In the last group, the proteins are subunits of the coatomer, forming the coat of COPI vesicles, which mediate retrograde transport within the Golgi apparatus and from there to the ER.

3. Discussion

Among the different putative partners, some appear more coherent with the results presented in chapter three. In flowering plants, RMRs were localized at different places in the cells. In rice, *Os*RMR1 was observed in the Golgi, TGN and PVC-like organelle (Shen et al., 2011). In *A. thaliana, At*RMR1 was detected in the Golgi, PVC (Park *et* al., 2005) but also in ER structures, while *At*RMR2 was localized in the TGN (Occhialini 2011). We found that the reporter *Citrine-Card* was affected by the loss of RMRs. In the different mutants, targeting to the vacuole was disrupted and most fluorescent signal was retained in the ER. Thus, one hypothesis is that RMRs already bind their cargo proteins in the ER and help them to exit from there. In this case, the coatomer would be involved in including RMRs into COPI vesicles, for their retrograde transport within the Golgi and/or from Golgi to ER, after RMRs have released their cargo in a later compartment of the secretory pathway. This function would be independent of an E3 ubiquitin ligase activity. In animal and yeast cells, a role of COPI vesicles in endosomal trafficking has also been detected (Gabriely *et* al., 2007; Huotari and Helenius 2001). Although such a role has not been identified so far in plants (Heard *et* al., 2015), COPI may play a role in post-Golgi trafficking of RMRs.

Since *in vitro* ubiquitylation tests with the cytosolic part of *Pp*RMR2 showed an E3 ubiquitin ligase activity (C. Coppola, unpublished results), RMRs could also play an indirect role in the formation of vesicles by ubiquitylating coatomer subunits.

Regarding the two E3 ubiquitin ligases identified as probable partners, we found that their homologues in human are acting in distinct pathways. Firstly, the HUWE1 E3 ligase, which has an HECT domain, plays a role in apoptosis and cellular proliferation by targeting proteins for proteasomal degradation. Secondly, the UBR4 E3 ligase, which has a zinc finger domain, is involved in chromatin scaffolding in the nucleus and interacts with calcium-bound calmodulin in the cytoplasm. These E3 ligases may be regulated by ubiquitylation before ubiquitylating their own targets. They could be ubiquitylated by RMR2. Alternatively, RMRs may be ubiquitylated by either of these E3 ligases.

Proteasome subunits would make sense because the best known fate for ubiquitylated proteins is proteasomal degradation. RMRs could also be targeted for degradation by the proteasome, which could explain an apparent low stability or fast turn-over. However, in this pathway, E3 ligases and proteasome do not need to interact directly.

The next steps will be to confirm the putative partners, by studying their interactions with RMRs, *in vitro* and *in vivo*. Pull down assays using GST-RMR2 as the bait protein and the putative

partner fused to a His-tag as the target could be done. Interaction would be validated by immunodetection with antibodies against GST and His-tag. This approach could also be performed in the other way around, with partner as bait protein, trying to catch GST-RMRs. *In vitro* ubiquitylation tests using these partners as target for the cytosolic part of RMR2 (acting as an E3 ligase) could be another approach. Putative partners could be also cloned and expressed in transgenic moss lines already expressing *Pp*RMR2 tagged with a fluorescent reporter, if we manage to obtain a visible signal.

Chapter 5
General discussion and perspectives

1. The moss secretory pathway

The first part of this thesis aimed to develop a fluorescent reporter library to study the secretory pathway of *P. patens* and extend our knowledge about the evolution since seedless and flowering plants split. We developed several fluorescent markers and followed their localization in WT transgenic lines. General secretory system reporters were targeted at the expected localization, as well as vacuolar reporters including ctVSDs already characterized in angiosperms.

However, the construct *SP-Citrine*, expected to be secreted into the apoplast, as in flowering plants, was unexpectedly addressed to the central vacuole. The mechanism remains unclear and further investigations need to be done. We suspect that Citrine could contain a cryptic signal for vacuolar targeting in moss. The amino acid sequences of GFP and Citrine are almost identical and differ by only few amino acids. Alignment of sequences and modeling shows that apart from amino acid difference in direct contact with the internal fluorophore, Citrine and YFP differ in two amino acids, localized at the surface of the protein and which could affect the protein configuration and could be recognized as a vacuolar signal (figure 5.1). However, since we did not try to secrete GFP (as *SP-GFP*) we do not know if these differences are relevant. One the other hand, the C-terminal sequence of Citrine - or GFP - which extends away from the β-barrel could also be identified as a ctVSD by a moss receptor, with a specificity differing from its homologues in angiosperms. It would have been hidden in our other constructs with C-terminal extensions by ctVSDs or the whole chitinase sequences.

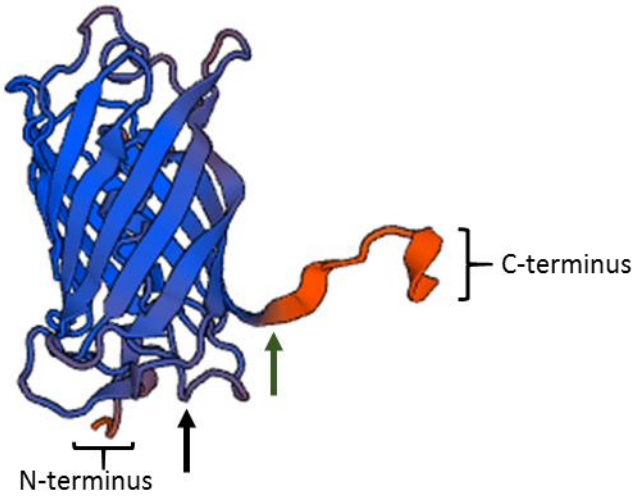

Figure 5.1 Model of Citrine structure (SWISS-MODEL.expasy.org)
The two amino acids at the surface of Citrine that differ from GFP are indicated by the arrows: Glutamine (back arrow) and Leucine (green arrow). The more mobile N-terminal and C-terminal extensions are highlighted in red.

If this assumption is correct, some of our conclusions will need to be reconsidered: the vacuolar targeting of our PSI constructs could be an artefact due to this C-terminus of Citrine and not to the PSI domain itself. However, other hypothesis should be considered. The vacuolar targeting observed for *SP-Citrine* could be a default targeting occurring in seedless plants. It could also be an overexpression effect due to the strong HSP promoter: an excess of fluorescent cargoes would be targeted to the vacuole for degradation.

Many aspects of the secretory pathway seem to be conserved between mosses and flowering plants. In *P. patens* vacuolar trafficking is also sensitive to BFA and Wortmannin. The HSP promoter is very convenient for protein transport monitoring but longer observations (*i.e.* 72 hours after induction) could complete this study, for some reporters that are very slow to exit the ER and reach their final destination.

2. Are RMRs vacuolar receptors?

The chapter three discussed the main topic of this thesis: the characterization of the quintuple RMR mutants. Our starting hypothesis was that RMRs are vacuolar receptors, targeting cargo proteins carrying a ctVSD to the neutral or protein storage vacuole. Our collection of fluorescent markers was tested in quintuple KO mutants. Trafficking of general secretory system reporters was not affected in the mutants, validating our hypothesis that RMRs are not involved in these mechanisms. We finally obtained a trafficking phenotype in mutant lines expressing one ctVSD reporter: *Citrine-Card*. This reporter was vacuolar in WT moss but dependent on RMRs to exit the ER. We also observed that the loss of even a single RMR was enough to perturb this vacuolar targeting. It could be a dosage effect, meaning that the total amount of *Pp*RMRs is just sufficient for proper trafficking or that the particular mutated RMR is necessary. A dosage effect of RMRs suggests that in single KO mutants the quantity of RMRs is already too low in comparison with the quantity of cargoes. Considering the low expression level of RMRs, an excess of cargo proteins should be visible as well in WT line expressing *Citrine-Card*.

Since we observed the same trafficking phenotype in two different single KO mutants of genes belonging to the two sub-families, it is unlikely that these two sub-families have distinct functions. Occhialini *et* al. (2016) showed that *At*RMR2 can make homodimers and can also form heterodimers with *At*RMR1. Dimerization of *Pp*RMRs could be necessary for their localization and consequently for their correct function. Accordingly, *Pp*RMRs could require to interact or to form heterodimers, explaining the phenotype observed when only one RMR is deleted (1KO, *rmr2*).

We did not detect any mistargeting of the other reporters containing other ctVSDs, all of which had been tested and confirmed in angiosperms. Even if these sequences were not recognized by *Pp*RMRs it does not mean that RMRs are not vacuolar receptors.

Pereira *et* al. (2013) showed that cardosin A has two VSDs, a ctVSD and an unconventional PSI signal. In agroinfiltrated tobacco cells, reporters with these two VSDs took different routes to the vacuole. In moss, different pathways to vacuoles have not yet been described. We treated our transgenic lines (WT and 5KO) with BFA or Wortmannin; both treatments lead to the interruption of vacuolar targeting. In WT lines, these results were expected because these reporters are supposed to traffic from the ER to the vacuole, passing through the Golgi. The classical model for VSRs as sorting receptors for soluble proteins like aleurain, is that VSRs are trafficking from the TGN via CCVs to an intermediate compartment before reaching the lytic vacuole. VSRs were described to recycle between PVC and TGN and can be considered as PVC markers (Jiang and Rogers, 1998; Miao *et* al., 2006). Very

recently, a new model about VSRs and their interaction with their ligands was proposed (Robinson and Neuhaus, 2016). It proposes that VSRs interact with cargoes earlier in the secretory pathway and binding already occurs in the *cis*-Golgi. It also proposes that VSRs release their cargoes already in the TGN and in a pH-independent way, in contrast to the classical model where the ligand dissociation was thought to be pH-dependent. The new model did not address the trafficking of RMRs. Our results showed that trafficking of the ssVSD reporter *Citrine-AtAleurain* to the vacuole in moss was inhibited by BFA and Wortmannin treatment, which is consistent with both VSR models.

Disruption of the vacuolar targeting of the ctVSD reporters is consistent with the hypothesis that RMRs act like VSRs as vacuolar receptors. Even though at this time the localization of RMRs is not known in moss, they will be probably found in the ER, Golgi or TGN, compartments that expected to be affected by BFA and Wortmannin. Moreover, after inhibitor treatment we did not observe a phenotypic difference between the WT and the 5KO.

We cannot conclude yet if *Pp*RMRs are directly involved in vacuolar targeting of if they are acting as regulators of some other receptor in this pathway. We cannot decide if there are distinct routes to central vacuole in *P. patens*. To go further in this study, treatment of all our lines (*e.g. PSI-Citrine* or *Citrine-Ppchitinase*) by BFA and Wortmannin need to be done and could extend our knowledge.

Localization of *Pp*RMRs is an important point that still needs to be achieved. Our strategy was to overexpress *Pp*RMR2 fused to Cerulean in WT. This fluorescent reporter was chosen because we also wanted to use this construct for a colocalization study with the line expressing *Citrine-Card*. We were not able to visualize *Cerulean-PpRMR2*. It is not possible yet to conclude if we had co-suppression (silencing) issues, if *Pp*RMR2 is a very short lived protein or if it is very little expressed. To avoid silencing, transformation of the 5KO line with *Cerulean-PpRMR2* could be done. Exchange of Cerulean for Citrine or GFP should also be considered.

3. Are RMRs E3 ubiquitin ligases?

The last part of this work was focused on the identification of *Pp*RMR2 partners. Our hypothesis was that as members of the PA-TM-RING family RMRs have very probably an ubiquitin ligase activity like their animal homologues, which are however not known to be involved in intracellular trafficking.

GRAIL is such a human homologue of RMR and is involved in polyubiquitylation during anergy induction in T cells. GRAIL recognizes and binds its substrate CD83 on the luminal side of the membrane, via its PA domain, and then ubiquitylates the cytosolic domain of CD83 via the RING-H2 domain (figure 5.2). If the cargoes bound by RMRs in plants are soluble luminal proteins, what will be the cytosolic substrate of its RING-H2 E3 ligase domain?

Indeed, an E3 ligase activity of the cytosolic part of *Pp*RMR2 was detected in our laboratory by an *in vitro* ubiquitylation test (C. Coppola, unpublished results). From the candidate interacting partners, some seem to be more coherent with our working hypothesis and the results of the chapter three. The coatomer subunits identified as *Pp*RMR2 partners are involved in intracellular trafficking between Golgi and ER, but endosomes might also use COPI trafficking as in animal and yeast. Regulatory subunits of the proteasome suggest a role of RMRs in regulating protein degradation. The two E3 ligases are more intriguing, suggesting cross-regulation between different E3s.

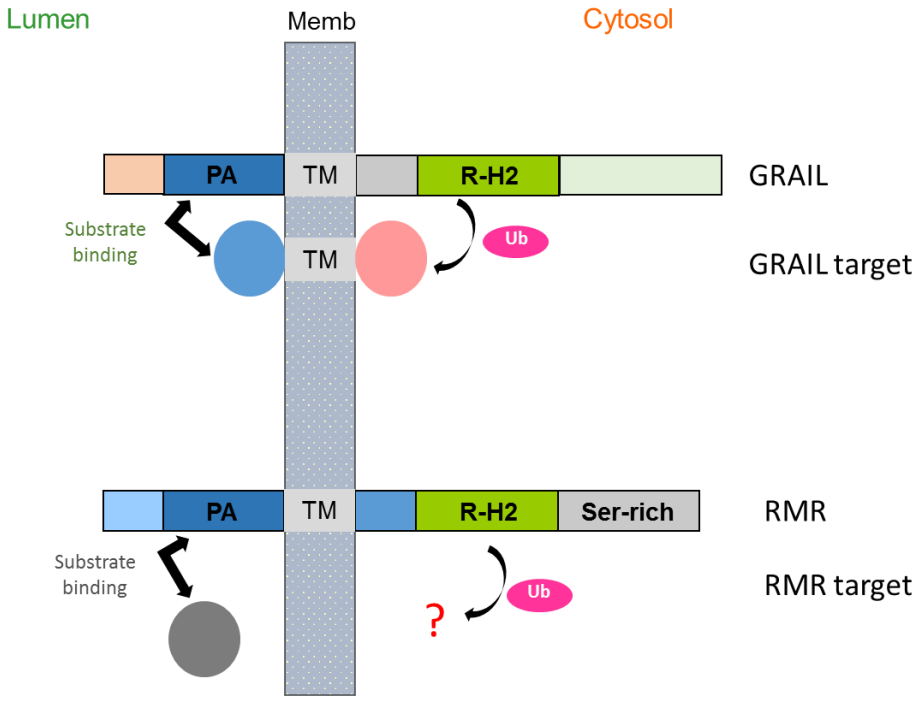

Figure 5.2 Schematic representation of the mechanism of GRAIL and the possible mechanism of RMRs (not to scale). The GRAIL target CD83 is a transmembrane protein. Binding of its luminal domain by the PA domain of GRAIL causes the ubiquitylation of CD83's cytosolic domain by the RING-H2 E3 ubiquitin ligase. What is the cytosolic substrate of the RING-H2 of RMR? TM, Transmembrane domain; PA, protease-associated domain; R-H2, RING-H2 domain; Ser-rich, serine-rich domain; Ub, ubiquitin

The identification of putative partners is just a first step and will need to be confirmed. To this end, GST pull-down with supposed partners as bait and *Pp*MR2 as prey protein could be performed. Interaction would be confirmed if RMRs are then bound. *In vitro* ubiquitylation tests of putative partners would be an additional approach to validate them. Moreover, overexpression of putative partners fused to a fluorescent reporter in WT and 5KO lines could lead to a visible phenotype such as accumulation of the protein in the mutant, due to the lacking ubiquitylation by RMRs, which could induce a slower turn-over.

Even if the exact link between abiotic stresses signaling and E3 ligase activity is still unclear, evidence about important role of ubiquitylation in stress responses are accumulating (Lyzenga and Stone, 2011). Quintuple *Pp*RMR mutants did not show a different sensitivity to salt stress than WT. However, we observed an unexpected phenotype after several weeks of growth on the NH4 medium

as *Pp*RMR mutants developed many more leafy gametophores than WT. We cannot yet explain this phenotype. Further phenotypic studies need to be done.

Even though their involvement in intracellular trafficking still remains unclear, this thesis provides new insights in the function of RMRs proteins with the characterization of potential interaction partners. This work was also the opportunity to create an extensive library of intracellular markers available to the moss community to further study the secretory pathway in this model plant.

Chapter 6
Material and methods

A. Material

A.1 Plant material

Physcomitrella patens wild type *Grandsen* strain was obtained from Didier Schaefer.

Culture conditions

Protonema cultures were grown on 9 cm diameter Petri dishes, containing solid NH4-agar medium, at 22°c in discontinuous light, with a photoperiod of 16 hours per day. A cellophane disk is placed directly on the medium before plating. Every seven days, lines are subcultured: plant tissues are collected and fragmented with a Polytron, then resuspended in sterile water before re-plating on solid medium.
For some experiments BCD medium was used in order to induce the formation of leaves. To obtain leaves and gametophores, freshly ground protonema was grown on Jiffy-7C® during minimum 4 weeks.

$CaNO_3$, $4H_20$	800 mg
$MgSO_4$, $7H_20$	250 mg
$FeSO_4$, $7H_20$	12.5 mg
NH4 tartrate	500 mg
Micro elements (1000x)	1 ml
Phosphate buffer (1000x)	1 ml
H_20	Adjust to 1 liter
Agar	7 g

NH4 medium composition

$CaNO_3$, $4H_20$	150 mg
$MgSO_4$, $7H_20$	250 mg
$FeSO_4$, $7H_20$	12.5 mg
Micro elements (1000x)	1 ml
Phosphate buffer (1000x)	1 ml
H_20	Adjust to 1 liter
Agar	7 g

BDC medium composition

Culture on Jiffy-7C® substrate

One Jiffy-7C® disc is rehydrated with 50 ml of sterile distilled water for 20 minutes. Then it was put in a magenta box and sterilized by autoclave. 1.5 ml of grinded fresh protonema is added on the top of the Jiffy-7C® and grown under standard conditions for 4 weeks or until satisfactory quantity of gametophores.

A.2 Bacterial strains

Culture conditions

Escherichia coli XL-1 Blue (*rec*A1, *end*A1, *gyr*A96, *thi*-1 *hsd*R17 (rk-, mk+), *sup*E44, *rel*A1, *λ*-, *lac*-) were grown on 9 cm diameter Petri dishes, containing solid LB medium.

NaCl	0.5 % (w/v)
Yeast extract	0.5 % (w/v)
Bactotryptone	1 % (w/v)
In H_20	

LB medium composition

B. Methods related to bacteria

B.1 E. Coli Transformation by heat-shock

E. coli XL-1 blue competent cells (100 ml of suspension in Eppendorf tube 1.5 ml) are placed on ice before adding purified plasmid (1 to 10 ng) or ligation mixture (15 µl). Cells are incubated on ice for 15-20 minutes. Then heat-shock is done: tube is put at 42°c during 90 seconds, then immediately back on ice for 3 minutes. Bacterial suspension is plated on LB-agar medium containing selective antibiotic and grown overnight à 37°C.

B.2 Preparation of XL-1 competent cells

XL-1 cells are plated on LB agarose + tetracycline and grown overnight at 37°C. The next day, one colony is took off for an overnight culture with 10 ml of LB medium. The suspension is grown overnight at 28-29°C and 180-200 rpm. The day after, 50 µl of culture was taken and inoculated in 10 ml of LB medium. The OD at 600 nm of the suspension is measured, the culture was diluted if the OD is superior to 0.8 and grown overnight at 28°C. The next day, a volume of the overnight suspension is taken and diluted in LB medium in order to reach an OD of 0.1-0.05 at 600 nm, in a final volume of 10-20 ml. At the end of the day, the OD at 600 nm was measured and 250 ml of LB medium were inoculated with the

suspension to have a final OD of 0.025 maximum. Culture was grown overnight at 28°C. The next morning, the culture is diluted to an OD of 0.3 in 250ml of LB medium and grown at room temperature until the OD was 0.6. The suspension is put on ice for 20 minutes then transferred in sterile Sorvall bottles for centrifugation and put again 10 minutes on ice. Cells were pelleted at 2800 rpm (Sorvall centrifuge), 4°C for 10 minutes. Supernatant was eliminated and pellet was resuspended very gently in 80 ml of cold TB medium (composition below). Sorvall bottles are kept on ice for 20 minutes. Then the suspension is centrifuged at 2800 rpm (Sorvall centrifuge), 4°C for 10 minutes. After removal of the supernatant, the pellet was carefully dissolved in 10 ml of cold TB medium and 0.7 ml of DMSO was added drop by drop. Suspension was kept on ice 10 minutes. Then, bacterial cells are aliquoted by 100 µl in Eppendorf tubes and immediately froze in liquid nitrogen. Tubes were stored at -80°C.

PIPES	0.605 g
$CaCl_2$	0.441 g
KCl	3.7 g
pH	Adjust to 6.7 with KOH
$MnCl_2$	2.17 g
H_20	Qs 200 ml

Composition of TB medium

B.3 Plasmid DNA extraction: miniprep

LB medium with antibiotic is inoculated with a single bacteria colony, and incubated overnight at 37°C and 180 rpm shaking. The following day, 1.5 ml of bacterial suspension are centrifuged in an Eppendorf tube at 12 000 rpm in order to pellet the cells. Supernatant is removed and cells are resuspended in 150 µl buffer 1 (25mM Tris-HCL pH8, 50mM glucose and 10 mM EDTA pH8). Mixture is incubated 3 minutes at room temperature (RT). Then 200 µl buffer 2 is added (0.2M NaOH and 1% SDS). Mixture is homogenized and incubated 5 minutes on ice. Then 150 µl re-cooled buffer 3 is added (KOAc 3M and acetic acid 5M). Mix vigorously or vortex 5 seconds. Mixture is incubated 5 minutes on ice and centrifuged 5 minutes at 12000 rpm. Supernatant is collected in a new Eppendorf tube and 400 ml of chloroform is added. Solution is mixed vigorously and centrifuged 4 minutes at 12 000 rpm. The superior aqueous phase is carefully collected in a new Eppendorf tube and DNA is precipitated with 900 µl 100% ethanol. Solution is mixed by inversion, incubated at RT for 10 minutes and centrifuged 10 minutes at 14000 rpm. DNA pellet is washed by 800 µl 70% ethanol and centrifuged 5 minutes at 14000 rpm RT. The pellet is dried at 65°C for 5 minutes and resuspended in 40-50µl H_20 + RNAse. Plasmid DNA extraction for sequencing are performed using the Nucleospin plasmid kit (Macherey-Nagel) and quantified using Nano-drop spectrophotometer.

C. Methods related to plants

C.1 Protoplasts isolation and transformation

Protoplasts isolation

P. patens protoplasts are isolated from 6-7 days Protonema cultures, digested by 1% driselase in 0.48M mannitol, during 1 hour. The suspension is gentle mixed every 20 minutes. After digestion, the protoplast suspension is filtered through a 40 mesh stainless steel sieve and transferred to 12 ml sterile centrifuge tubes. Protoplasts are pelleted by centrifugation at 420 rpm for 7 minutes. The supernatant is carefully removed and fresh mannitol 0.48M is added in order to resuspend the cells. This washing step is repeated 2 times more.

Protoplasts transformation by PEG

After isolation as described below, protoplasts are resuspended in MMM solution. 10-15 µg of DNA (plasmid) are added, in a 12 ml centrifuge tube. Then, 300 µl of protoplast are added and gently mixed. 300 µl of PEG solution are added and gently mixed. Protoplast suspensions are placed at 45°C for a 5 minute heat-shock. Then they are left 10 minutes at room temperature. To finish, the sample is progressively diluted with NH4-mannitol-glucose media: 5 x 300 µl added every minute then 5 x 1 ml added every minute. Protoplast suspensions are left in the dark overnight. The next day, protoplasts for stable transformation are embedded in top layer and plated on NH4 medium petri dishes, 3 ml Top layer for 3 ml of protoplasts suspension. 2 ml are plated per Petri dish. They are transferred on selective media with antibiotic 7 days later. Protoplasts for transient transformation are cultured in liquid media. After overnight in the dark, they are placed under growth conditions in phytotron. The observations take place from 24h to 72 hours after transformation, depending of the type of protein expressed.

Mannitol 0.48M	9.8 ml
$MgCl_2$ 1.5M	100 µl
MES 0.5M	100 µl
pH	Adjust to 5.6 with KOH

MMM composition

Mannitol 7%, $CaNO_3$ 0.1M	10 ml
PEG 4000	4 g
pH	Adjust to 7.2 with Tris-HCl 0.1M, pH 8

PEG solution composition

$CaNO_3$, $4H_20$	800 mg
$MgSO_4$, $7H_20$	250 mg
$FeSO_4$, $7H_20$	12.5 mg
NH4 tartrate	500 mg
Micro elements (1000x)	1 ml
Phosphate buffer (1000x)	1 ml
Mannitol	66 g
Glucose	5 g
H_20	Adjust to 1 L
Agar	7 g

NH4-Mannitol-Glucose medium composition

Mannitol	8.5 % (W/V)
Agar	1.4 % (W/V)

Top Layer composition

C.2 Heat-shock on protonema for protein expression

24 hours before microscopy observations or protein extraction, one week old protonema was heat-shocked. Moss was collected in a sterile way and put in a 12 ml tube filled with water, previously heated at 45°C in bain-marie. Tubes were placed in bain-marie at 45°C for 5 minutes. Then, protonema was cooled in a sterile Petri dish containing sterile room temperature water. After 2 minutes, protonema was taken and placed on solid NH_4 medium for 24 hours.

C.3 Secretory pathway inhibitors treatment

Brefeldin A (Sigma) and Wortmannin (InvivoGen) were respectively used at a final concentration of 50 µM and 30 µM in NH_4 liquid medium. 24 hours before microscope observation or protein extraction, protonema was heat-shocked in order to induce the expression of the fluorescent marker, 5 minutes at 45°C. Then protonema was incubated overnight, at room temperature and in the dark, in the inhibitor solution.

C.4 Proteasome II inhibitor treatment

Proteasome II inhibitor (SantaCruz) was used at a final concentration of 200 and 500 nM in NH_4 liquid medium. 24 hours before microscope observation or protein extraction, protonema was heat-shocked in order to induce the expression of the fluorescent marker, 5 minutes at 45°C. Then protonema was incubated overnight, at room temperature and in the dark, in the inhibitor solution.

D. Molecular biology

D.1 PCR

PCR reactions were performed in PCR 0.2 ml tubes (VWR) mixing the following reagents: buffer (final concentration 1X), dNTP (final concentration 0.2 mM), primer forward and reverse (final concentration 0.5 µM), 1 unit of DNA polymerase (GoTaq® or Phusion®), 5 to 10 ng of DNA template and milliQ water to a final volume of 20 to 50 µl.

D.2 DNA digestion

Digestion of DNA by one or two restriction enzyme(s) was done in a 1.5 ml Eppendorf tube, mixing the following reagents: 0.5 to 40 µg of substrate DNA, a corresponding volume of restriction buffer (final concentration 1X) and 1 unit of enzyme per µg of substrate DNA. The volume was adjusted with milliQ water, from 20 to 200 µl depending of the quantity of substrate DNA. The digestion was performed for 1 to 4 hours at 37°C. If needed, enzymes are inactivated 20 minutes at 65°C.

D.3 DNA precipitation

DNA were precipitated in 1.7 ml centrifuge tube with 1/10th volume of 3M sodium acetate (pH5.5) and 3 volumes of 100% ethanol. The tube was mixing by inversion then centrifuged 20 minutes at 16 000 rpm (Eppendorf) and 4°C. Supernatant was carefully removed and pellet was washed with 3 volumes of 70% ethanol. Then the tube is centrifuged 10 minutes at 16 000 rpm (Eppendorf) and 16°C. Supernatant was carefully removed, pellet was dried 5 minutes at 37°C and resuspended in milliQ water.

D.4 Genomic DNA extraction

100 mg of protonema were grinded with a pestle adapted on polytron and 100 µl of extraction buffer (composition below) and quartz sand. The pestle was rinsed with 2x 100 µl of extraction buffer. Tubes were centrifuged 5 minutes at maximal speed (16 000 rpm Eppendorf centrifuge). Supernatant was transferred in a new tube and 1 volume of chloroform was added. Tubes were vortexed 5 to 10 seconds and centrifuged 5 minutes at maximal speed. The hydrophilic phase was transferred in a new tube and 200 µl of isopropanol were added. After mixing and waiting 10 minutes at room temperature, tubes were centrifuged 10 minutes at maximal speed. Supernatant was removed and pellets were washed with 600 µl of 70% ethanol and centrifuged 5 minutes at maximal speed. After elimination of supernatant, pellets were dried 2 minutes at 55°C and then resuspended in milliQ sterile water with

RNAse (20 µg/ml). Tubes were incubated at 55°C for 10 minutes and vortexed. One last centrifugation was done in order to eliminate insoluble particles. After DNA quantitative analysis by nanodrop, solutions were diluted to 10 ng/µl and tubes were stored at -20°C.

Reagent	Final concentration	Volume for 50 mL
Tris-HCl pH7.5	200 mM	10 mL
NaCl	250 mM	2.5 mL
EDTA	25 mM	2.5 mL
SDS	0.5 %	1.25 mL
B-mercaptoethanol	10 mM	0.5 mL
H_20	X	33.25 mL

Composition of extraction buffer

D.5 DNA electrophoresis

Migration of DNA in agarose gel (0.8 to 1.5% depending of the DNA size) were performed in Mupid®-One system with TBE 0.5X buffer (composition below). 0.02% of Midori green (v/v) were added to melted agarose as DNA stain. DNA samples were separated according to size at 100 V for 20-30 minutes. DNA bands were visualized under UV light using a Gel Doc E-Box.

Tris base	108 g
Boric Acid	55 g
EDTA 0.5M	40 mL
H_20	qs 1L

Composition of TBE 10x buffer

D.6 DNA extraction from agarose gel

The band corresponding at the right DNA size was cut from the gel with a scalpel. DNA was purified with the Wizard SV gel and PCR clean-up kit from Promega.

D.7 DNA fragment ligation in a plasmid

Ligation reactions are done for 1 hour at RT, or overnight at 4°C, in the dark. The following reagents are mixed in a 1.7ml Eppendorf tube: 200 ng of vector, the corresponding amount of insert(s), 2X ligation buffer, 1 unit of T4 DNA ligase (Promega) and milliQ water to a final volume of 10 to 15 µl.

D.8 Extraction of total RNA from *P. patens*

Protonema cultures aged 6 days are collected, water excess is removed with a Whatman paper and protonema is weighed. 100 mg per sample are collected and immediately frozen in liquid nitrogen. Pre-cooled mortar and pestle are used; samples are quickly ground and transferred into 1.5 ml Eppendorf tubes, placed in liquid nitrogen. RNA extraction is performed using the NucleoSpin RNA Plant kit from Macherey-Nagel. RNAs are quantified using Nano-drop spectrophotometer.

D.9 Reverse transcription: synthesis of cDNA

500 ng of RNA extract is needed per reaction. Takara “prime script RT reagent kit” was used.

E. Methods related to proteins

E.1 Moss total proteins extraction in SB buffer

Protonema was collected with a spatula and exceed water was removed by drying the protonema on Whatman® filter paper. Then protonema was weighted and 500µl of SB2x is added per 100 mg of fresh material. Protonema was grinded with quartz sand. Samples were kept on ice. When homogenized grinding was obtained, proteins were denatured 5 minutes at 92°C. The lysate was then centrifuged 15 minutes at 16000 rpm (Eppendorf centrifuge). Supernatant was stored in a new tube at -20°C.

Tris-HCL 2M pH6.8	1 mL
DTT	616.9 mg
SDS 20%	4 mL
Bromophenol blue	40 mg
Glycerin	4 mL

Composition of Sample Buffer 4x (SB) for 10 ml

E.2 SDS-PAGE

A mini Protean III apparatus (Bio-Rad) was used for the migration of a discontinuous gel with two parts, the stacking and the running gels. For the composition of the gels see the table below. Gel migration is done in a 1X running buffer (composition below), 20 minutes at 20mA then 40 minutes at 35 mA or until the blue dye reached the bottom of the gel.

	Running gel 12%	Stacking gel
H_20	1.185 mL	1.5 mL
30% Bis-Acryl	2 mL	670 µL
2M Tris-HCl pH 8.8	1.735 mL	X
0.5M Tris-HCl pH 6.8	X	1.25 mL
20% SDS	25 µL	25 µL
Temed	5 µL	5 µL
10% APS	50 µL	50 µL
Bromophenol Blue	X	20 µL

Composition of running and stacking gel for SDS-PAGE

Tris-base	30.28 g
Glycin	144.11 g
SDS	20 g
H_20	qs 1L

Composition of running buffer 10X

E.3 Western blot

After SDS-PAGE proteins were transferred to a MS® nitrocellulose membrane using a mini Protean III apparatus (Bio-Rad). The sandwich was assembled as following: thick filter paper, sponge, filter paper, gel, nitrocellulose membrane, filter paper, sponge, thick filter paper and placed in the transfer cassette. The transfer was performed in 1X transfer buffer (composition below) at 100 volts for 1.30 hour at 4°C.

Tris-base	30.27 g
Glycin	144 g
H_20	qs 1L

Composition of transfer buffer 10X

After transfer, the membrane was stained with amidoblack (ethanol 100 45% v/v, glacial acetic acid 10% v/v and amidoblack 0.1% w/v) for 5 minutes, then washed 5 and 10 minutes with destain solution (ethanol 100 40% v/v and glacial acetic acid 10% v/v). After washing with PBS1x and PBS1x + tween 0.05%, the membrane was blocked in a solution of PBS5% + milk5% for 1 hour minimum. After washing with PBS1X, the membrane was incubated with the primary antibody (diluted 1:6000) in a solution of PBS1X + milk 1% for minimum 2 hours. The membrane was then washed 2 times with PBS1X + 0.05% tween and 1 time with PBS1X. After, the membraned was incubated in a solution of PBS1X + milk1% + 0.05%tween with the secondary antibody (diluted 1:8000). To finish, the membrane was washed 2 times with PBS1X and the revelation of the secondary antibody was done with Western bright^{Tm} ECL detection kit (Advansta).

NaCl	81.8 g
KCl	2 g
Na_2HPO_4	17.8 g
KH_2PO_4	3.48 g
H_20	qs 1L

Composition of PBS 10X buffer

E.4 Colloidal Coomassie blue staining

The gel was fixed with 40% ethanol + 10% acetic acid for 15 minutes. Then it was washed with distilled water for 5 minutes. Colloidal Coomassie blue staining was done overnight with gentle agitation. The gel was destained in distilled water for 30 min to 1 hour until the background was clear.

E.5 Production of GST-RMR recombinant proteins in BL-21 strain

Culture growth

10 ml of LA medium were inoculated with 1 colony of BL21-GST-RMR and BL21-GST (control) and grown overnight at 37°C with shaking.

The next morning, 50 ml of LA medium were inoculated with 2.5 ml of the overnight cultures and grown at 37°C with shaking, until the OD_{600} reached 0.5-0.7 (approximately 30-60 min). When the OD_{600} was reached, 1ml of non-induced sample was taken as control, Pelleted and resuspended in 50µl SB buffer1x.

Protein expression was induced by adding IPTG to a final concentration of 1mM. The culture were grown for 4h at 37°C with shaking. After induction, 1ml of culture was taken as induced control and diluted to obtain an OD_{600} 0.5-0.7. The sample were pelleted and resuspended in 100µl SB buffer1x.

After induction, the culture was pelleted by centrifugation at 4000g for 20 min at 4°C. Then, the pellet was stored at -20°C for the night.

Protein extraction

The cell pellet was resuspended in 20-40 ml of lysis buffer for native purification. Cells were sonicated on ice 3x 40 seconds with 1 minute of pause. The lysate was centrifuged at 10 000 rpm (Sorvall) for 30min at 4°C in *Corex* tubes. The supernatant was kept on a new tube and stored on ice until use.

Interaction with agarose beads and purification of recombinant protein

The lysate was incubated with 200µL of glutathione-agarose beads (Sigma-Aldrich) for 2h under light shaking at 4°C (falcon tube). Cut tips were used. After incubation, beads were washed by centrifugation of the lysate + beads 5 min at 400 rpm, 4°C. The supernatant was then removed. Beads were washed 3 times with 5 ml PBS 1x (filtered). Supernatant was removed at each step. The last pellet was resuspended in 500µl of PBS1x.

E.6 Pull-down assay

Recombinant protein (GST-RMR) extract was incubated with a total moss proteins extract, overnight at 4°C, under light shaking.

The extraction of total moss protein was done freshly in Tris-HCl 100 mM pH 7.5. One old week protonema was grinded with sand quartz: 150 mg of Protonema for 500µl Tris-HCl. The lysate was then centrifuged 15min at 16 000 rpm (Eppendorf) at 4°C. Supernatant was taken and filtered on 22µm with syringe in order to eliminate chloroplasts. Filtrate was ultracentrifuged at 100 000g, 1 hour at 4°C. Then it was diluted with Tris-HCl pH 7.5 100 mM to obtain an appropriate volume (about 10 ml). Extract was stored on ice until use.

After the overnight incubation, protein extract + beads were centrifuged 5min at 400 rpm, 4°C. The supernatant was removed and the beads were washed with 5 ml Tris-HCl 100mM pH 7.5 (buffer used for the protein extraction). This step was repeated 2 or 3 times. The last wash was done in Eppendorf tube and cut tips were used. After the last centrifugation, the maximum of buffer was removed. The pellet was resuspended in SB 1x and samples were heated at 90°C for 5 minutes before SDS-PAGE analysis.

F. Microscopy

Confocal microscopy

Images were collected with a Leica TCS SP5 II confocal laser scanning microscope. Digital images were acquired using LAS AF (version 2.0.0) and processed using Adobe Illustrator (CC 2015). Fragment of protonema filaments were transferred to a microscope slide, a drop of water was added and a coverslip was added on the top. Samples were excited by a 488 nm argon laser and detected with a 524-546 nm band-pass filter for Citrine and Cerulean.

Acknowledgements

I could never have achieved this project without the help and support of many people.

Firstly, I would like to thank my thesis director Prof. Jean-marc Neuhaus for giving me the opportunity to follow this project in the Laboratory of Molecular and Cell Biology, where working conditions were so pleasant.

I would also like to acknowledge Sébastien Thomine and Shanmugabalaji Venkatasalam for accepting to serve in my thesis committee.

I thank Didier Schaefer for his help and the scientific discussions we had.

I am indebted to Guillaume Gouzerh for his scientific support and help. Thanks for all your advices, time and availability, and for teaching me confocal microscopy!

I would like to express my gratitude to Sophie Marc-Martin for her technical support, kindness and friendship. She was on my side from the first day I arrived.

Another special thanks goes to Patricia Rossetti who contributed so much to this work. These almost four years of hard work we spent together are priceless to me. I already miss the Pathou-Nono team.

I would like to thank my past and present lab members, for their precious friendship and encouragements, especially “the girls”: Andrea, Empar and Carla but also Sanaa, Sonia, Chantal, Livia, Alexandre, Gianni, Fares, Jonas, Ivan, Francesco and Mohammed.

Thanks also to all the nice people from the other labs, to Alex and the team M, and to my friends from the “French side”.

Finally I would like to thank my family, especially my parents and my brother who had always believed in me.

Annexes

1. Primers

HSP fw	GTGAAGGCATCGTTAGCAGTT
121 (ter 35S)	TGTAGAGAGAGACTGGTGATTTC
Not.SP.Nsi fw	GGCCGCGGGGATCCAAGGAGATATAACAATGAAGACTAATCTTTTTCTCTTTCTCATCTTTTCACTTCTCCTATCATTATCCTCGGCCATGCA
Not.SP.Nsi rv	TGGCCGAGGATAATGATAGGAGAAGTGAAAAGATGAGAAAGAGAAAAAGATTAGTCTTCATTGTTATATCTCCTTGGATCCCCGC
Nsi.Citrine fw	GCCATGCATGTGAGCAAGGGCGA
Nhe-Citrine fw	TGAGCTAGCGTGAGCAAGGGCGAGGAGCT
Citrine rv	ATGTCGACTTACTTGTACAGCTCGTCCATGCCG
Citrine-chi rv	ATGTCGACTTACATAGTATCCACCAACAGTCCCTTGTACAGCTCGTCCATGCCG
Citrine-card rv	ATGTCGACTTAAGCAGCCTCAGCGAATCCCACCTTGTACAGCTCGTCCATGCCG
Citrine-AP1 rv	ATGTCGACTTACACGAACTCTCCCTTAGCAGCCTCAGCGAATCCCAACTTGTACAGC
Ci-KDEL Q5 fw	TTGTGATCACTGCAGGCATGCCGCTGA
Ci-KDEL Q5 rv	CTCATCCTTCTTGTACAGCTCGTCCATGCC
Citrine Q5 fw	TCACTGCAGGCATGCCGCTGA
Citrine Q5 rv	TCACTTGTACAGCTCGTCCATGCC
PSIA fw	AGCATGCATGTCATGAACCAGCAATGCAAG
PSIB fw	AGCATGCATGTTTTAAACCAACAATGCAAAACATTGG
PSI rv	CTAGCTAGCACCACCTGCAGCACCACC
RMR1 fw	ATCCAGATGGTGGTGAG
RMR1 rv	GCATAATTTAGGATCCACCAGGTC
RMR2 fw	TGGCGAAAAGCTGAGGTTG
RMR2 rv	AGTAGTTTCGTCCGGTGAAGC

RMR3 fw	GCATAGATCAGTGGCTACTCACGCGGA
RMR3 rv	AAGTTAACACAGATCTTCTCCCGA
RMR4 fw	TAGAGGACTATGAGAGCGGACAA
RMR4 rv	AGAGCCTACAGGTGAGGTTTGAG
RMR5 fw	ATCTGAAGGCGATGATTGGAT
RMR5 rv	TGCGACTCTTACCTTGTCAGC
SP-chi-moss fw	CTAGGATCCATGGGTAGGGAAGTACTAATGG
SP-chi-moss rv	GACTGCAGCGCGCTCACGCCCACCACCAA
GST-RMR2 fw	CGCGGATCCGAACCCGCTGGAATGAGCG
GST-RMR2 rv	GCGCCTCGAGTTAGCAGAGATCTTCGGAACC
PIG.Q5 fw	GCGACTAGTAGCTTTCGTCCGTATCATC
PIG.Q5 rv	GCGGGATCCTCTTATCAGTCTTGTGTAAATATATTAG
RMR2.Bam fw	CCGGTCGACGTGAGCAAGGGCGAGGAG
RMR2.sal rv	ACCGTCGACTCCGCCTCCGCCTCCTCCGCAGAGATCTTCGGAACC
Cerul.Sal fw	CCGGTCGACGTGAGCAAGGGCGAGGAG
Cerul.HA.Spe rv	CGCACTAGTTTAAGCGTAATCTGGAACATCGTATGGGTACTTGTACAGCTCGTCCATGC
SP.Chi.Sec fw	CATGGATCCATGGGAAGAACTACAGGGAC
SP.Chi.sec rv	GCAGCTAGCAGACGCAACAAATCGGACC
Citrin.Chi.sec fw	CTAGCTAGCGTGAGCAAGGGCGAGGAGCT
Citrin.Chi.sec rv	GTACCCGGGCTTGTACAGCTCGTCCATGC
Chiti.sec fw	AGTCCCGGGCAAGGGGAGTTGTTCGGAATC
Chiti.sec rv	CAACTCGAGTCAGCACCGTAGGTCGGTGC
AtAleurain fw	CATGGATCCATGTCTGCGAAAACAATCC
AtAleurain rv	GCAGCTAGCAGCCACAACGGGGTATG

2. Vectors and constructs

2.a Cloning vectors

The pGEM®-T easy vector system from Promega, with Ampicillin resistance, was used for sub-cloning.

The plasmid pBNRF was used for all the fluorescent reporter library. It is a pBluescript with two loxP sites flanking a resistance cassette NTPP for Neomycin

The plasmid pBNRF-108-HSP-Ter35S is the pBNRF with 5'TS *Pp*108 locus and 3'TS *Pp*108 locus as targeting sequences cloned before and after the resistance cassette; upstream the resistance cassette were cloned the promoter HSP promoter and the terminator 35S.

Citrine was amplified from the plasmid pSCR::mCitrine called pJA004 (Ampicillin resistance) provided by N. Geldner.

The pIG-HCG vector was provided by M. Hasebe and harbored a Gateway cassette driven by an HSP promoter and TrbcS terminator. The targeting sequences are PIG1bR and PIG1bL for the PIG locus. The resistance for transgenic plants is Hygromycin.

2.b Cloning strategies

pBNR-Citrine-CardA; pBNR-Citrine-Chi; pBNR-Citrine-AP1

The *SP* fragment was amplified by PCR by the following primers: Not.SP.Nsi fw/Not.SP.Nsi rv and cloned separately in pGEM®-T easy vector. The fragment *Citrine* was amplified by PCR by the following primers: Nsi.Citrine fw / Citrine-card or Citrine-Chi or Citrine-Ap1 rv and cloned separately in pGEM®-T easy vector. *Citrine-VSD* fragment was cut by NsiI/SalI, *SP* fragment was cut by BamHI/NsiI and both were cloned in pBNRF-108-HSP-Ter35S linearized by BamHI/SalI. For moss protoplasts transformation, the vector was linearized by AvrII/PacI.

pBNR-PSIA-citrine; pBNR-PSIB-citrine

The *SP* fragment was assembled by annealing the following primers: SP-Chi.moss fw/ SP-Chi.moss rv and cloned separately in pGEM®-T easy vector. The *PSI* fragment was amplified by PCR by the following primers: PSIA fw/PSI rv or PSIB fw/PSI rv and cloned separately in pGEM®-T easy vector. The *citrine* fragment was amplified by PCR by the following primers: Nsi.citrine fw/ Nhe.Citrine rv and cloned separately in pGEM®-T easy vector. The *SP* fragment was cut by BamHI/NsiI, *PSI* fragment was cut by NsiI/NheI, Citrine fragment was cut NheI/SalI and there were all cloned in pBNRF-108-HSP-Ter35S linearized by BamHI/SalI. For moss protoplasts transformation, the vector was linearized by AvrII/PacI.

pBNR-Ci-KDEL; pBNR-Ci

These plasmids were obtained with the Q5®Site-directed mutagenesis kit from NewEnglandBiolab$_{inc}$. The couples of primers used were: Ci-KDEL Q5 fw/ Ci-KDEL Q5 rv or Citrine Q5 fw/ Citrine Q5 rv. Plasmid was totally amplified by PCR from the matrix plasmid pBNR-HSP-108-Ci-Card.

pIG-Q5

The plasmid was obtained with the Q5®Site-directed mutagenesis kit from NewEnglandBiolab$_{inc}$. The couples of primers used were: PIG-Q5 fw/ PIG-Q5 rv or Citrine Q5 fw/ Citrine Q5 rv. Plasmid was totally amplified by PCR from the matrix plasmid pIG-HCG.

pIG-RMR2-Cerulean

The *RMR2* fragment was amplified by PCR by the following primers: RMR2.Bam fw/RMR2.sal rv and cloned separately in pGEM®-T easy vector. The fragment *Cerulean* was amplified by PCR by the following primers: Cerul.sal fw / Cerul.HA.Spe rv and cloned separately in pGEM®-T easy vector. *RMR2* fragment was cut by BamHI/SalI, *Cerulean* fragment was cut by SalI/SpeI and both were cloned in piG-Q5 linearized by BamHI/SpeI. For moss protoplasts transformation, the vector was linearized by PmeI.

3. Vector maps

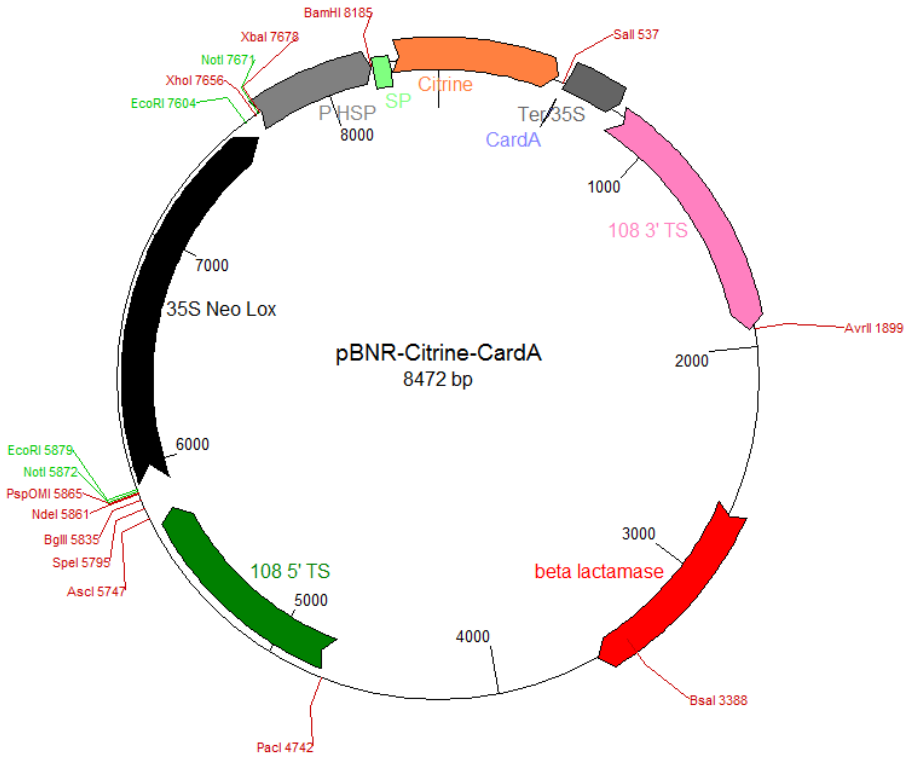

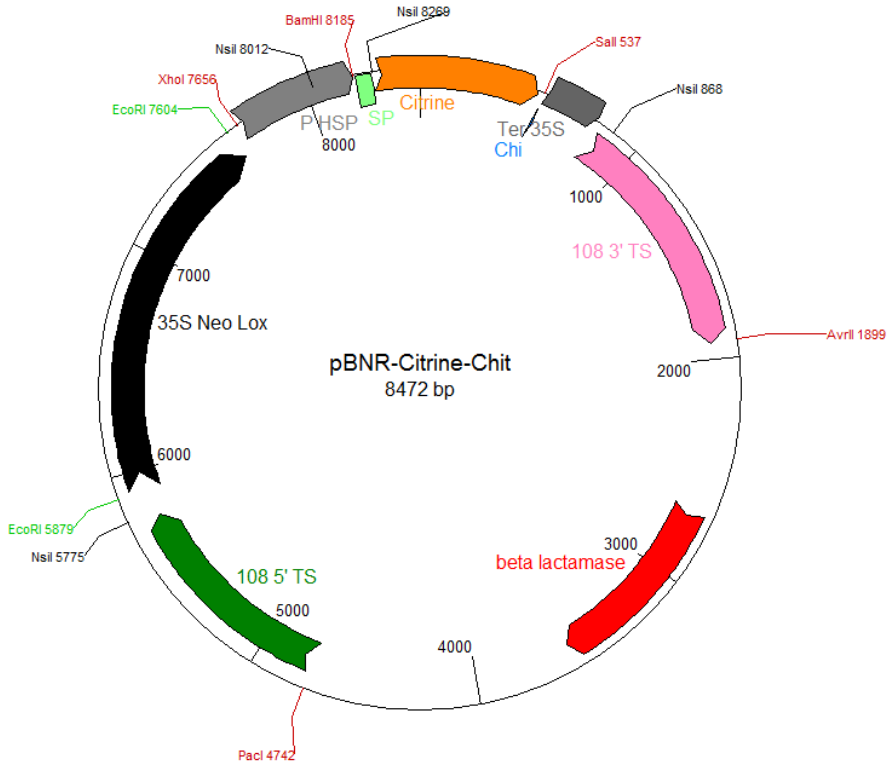
BamHI 8185
NsiI 8269
NsiI 8012
SalI 537
XhoI 7656
NsiI 868
EcoRI 7604
P HSP
SP
Citrine
Ter 35S
Chi
8000
1000
108 3' TS
7000
35S Neo Lox
AvrII 1899
pBNR-Citrine-Chit
8472 bp
2000
6000
EcoRI 5879
NsiI 5775
3000
beta lactamase
108 5' TS
5000
4000
PacI 4742

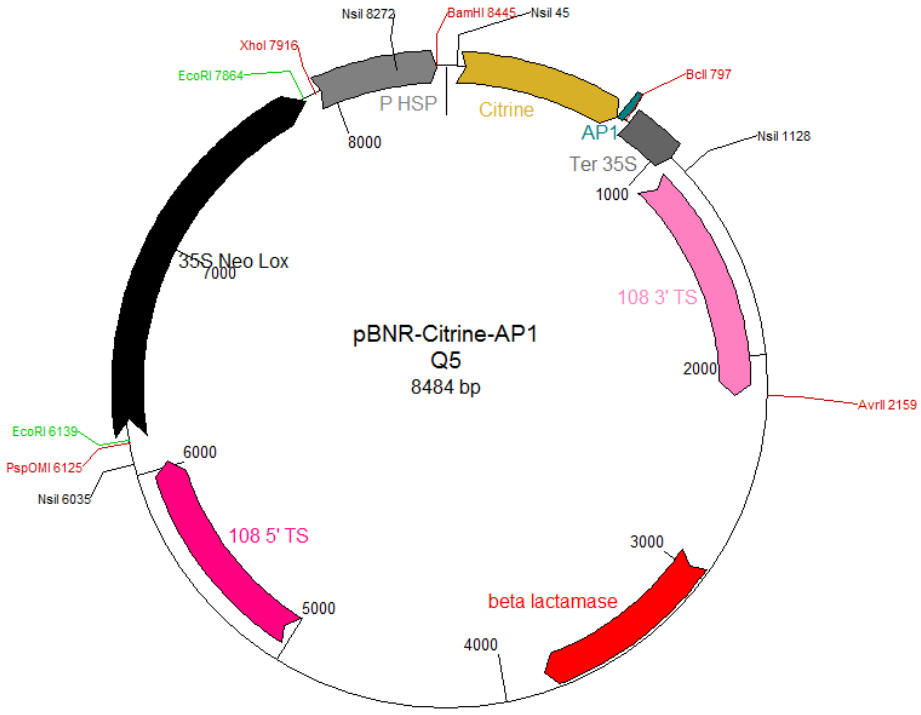
NsiI 8272
BamHI 8445
NsiI 45
XhoI 7916
EcoRI 7864
BclI 797
P HSP
Citrine
AP1
8000
NsiI 1128
Ter 35S
1000
35S Neo Lox
7000
108 3' TS
pBNR-Citrine-AP1
Q5
8484 bp
2000
AvrII 2159
EcoRI 6139
6000
PspOMI 6125
NsiI 6035
108 5' TS
3000
5000
beta lactamase
4000

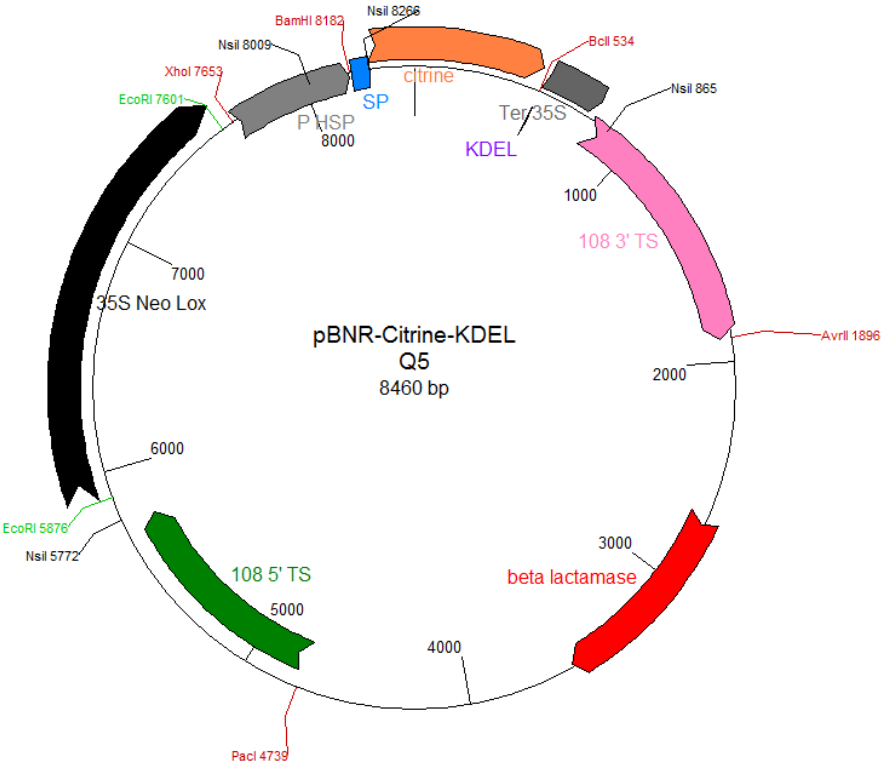
BamHI 8182
NsiI 8266
NsiI 8009
BclI 534
XhoI 7653
citrine
EcoRI 7601
SP
NsiI 865
P HSP
8000
Ter 35S
KDEL
1000
108 3' TS
7000
35S Neo Lox
pBNR-Citrine-KDEL
Q5
8460 bp
AvrII 1896
2000
6000
EcoRI 5876
NsiI 5772
3000
108 5' TS
beta lactamase
5000
4000
PacI 4739

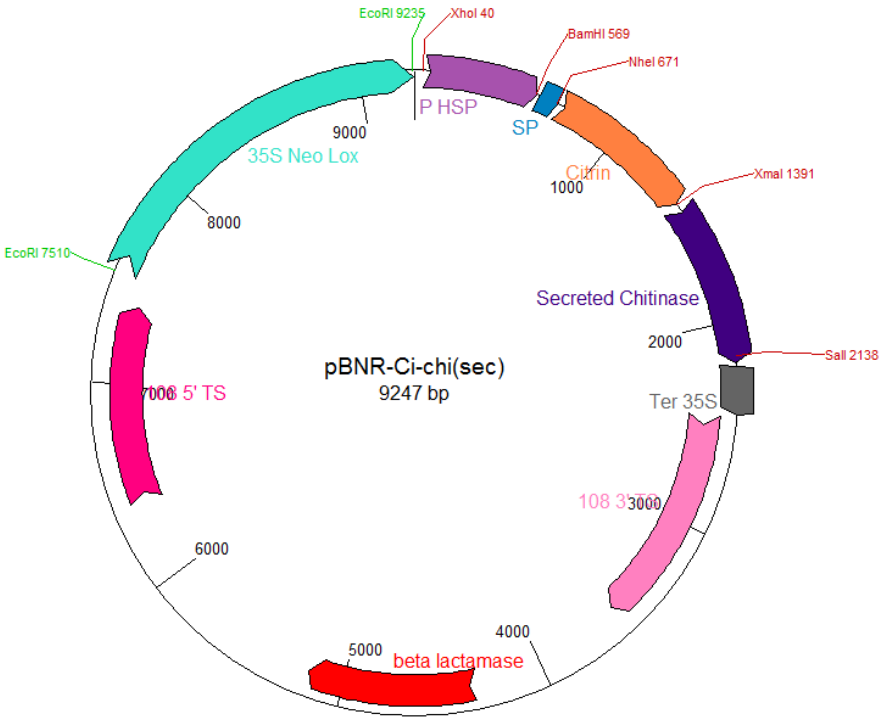
EcoRI 9235
XhoI 40
BamHI 569
NheI 671
P HSP
SP
9000
35S Neo Lox
Citrin
1000
XmaI 1391
8000
EcoRI 7510
Secreted Chitinase
2000
SalI 2138
pBNR-Ci-chi(sec)
9247 bp
108 5' TS
Ter 35S
3000
6000
4000
5000
beta lactamase

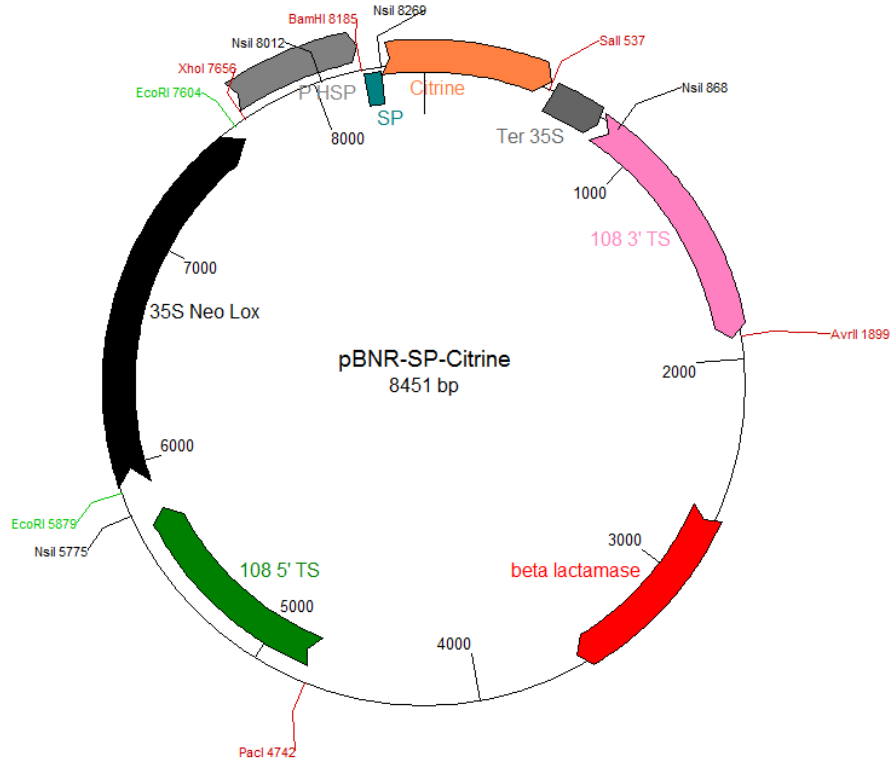
BamHI 8185
NsiI 8269
NsiI 8012
SalI 537
XhoI 7656
NsiI 868
EcoRI 7604
P HSP
Citrine
SP
8000
Ter 35S
1000
108 3' TS
7000
35S Neo Lox
AvrII 1899
pBNR-SP-Citrine
8451 bp
2000
6000
EcoRI 5879
NsiI 5775
3000
108 5' TS
beta lactamase
5000
4000
PacI 4742

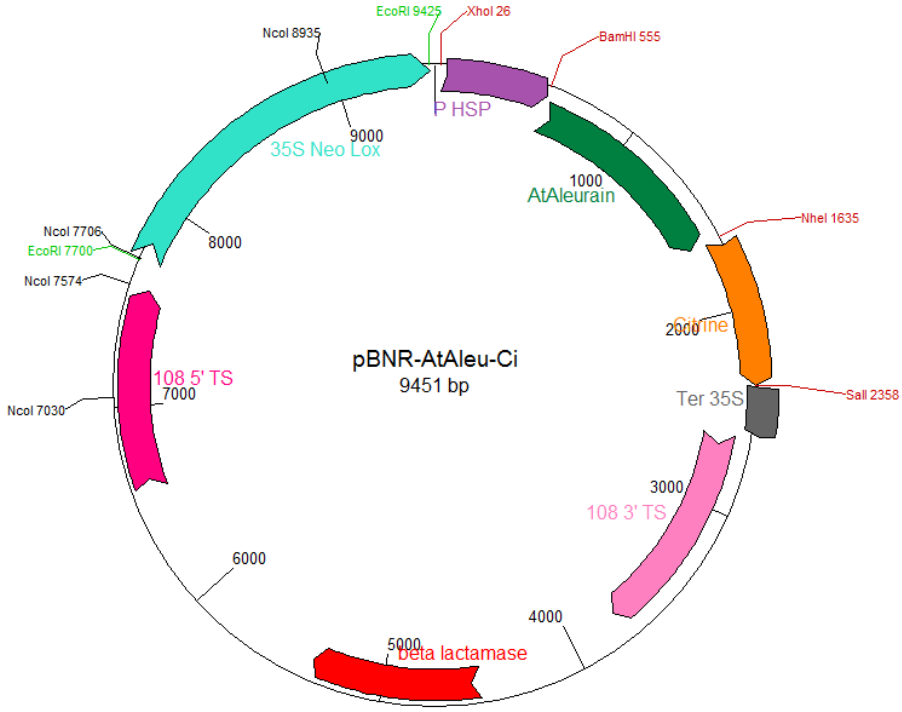
EcoRI 9425
XhoI 26
NcoI 8935
BamHI 555
P HSP
9000
35S Neo Lox
1000
AtAleurain
NheI 1635
NcoI 7706
8000
EcoRI 7700
NcoI 7574
2000
Citrine
pBNR-AtAleu-Ci
9451 bp
108 5' TS
7000
Ter 35S
SalI 2358
NcoI 7030
3000
108 3' TS
6000
4000
5000
beta lactamase

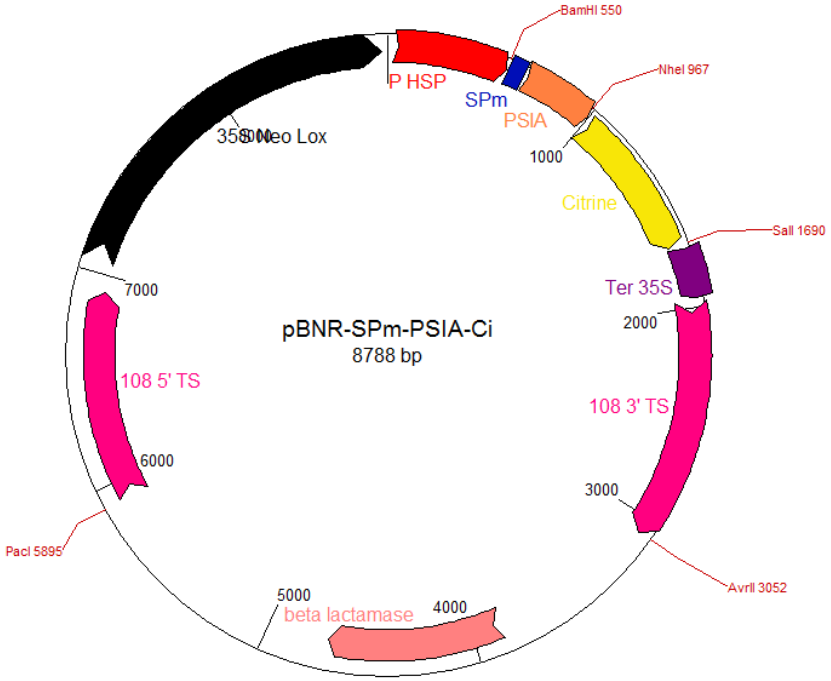
BamHI 550
Nhel 967
P HSP
SPm
PSIA
1000
Citrine
SalI 1690
Ter 35S
2000
108 3' TS
3000
AvrII 3052
5000
beta lactamase
4000
PacI 5895
6000
108 5' TS
7000
35S Neo Lox
pBNR-SPm-PSIA-Ci
8788 bp

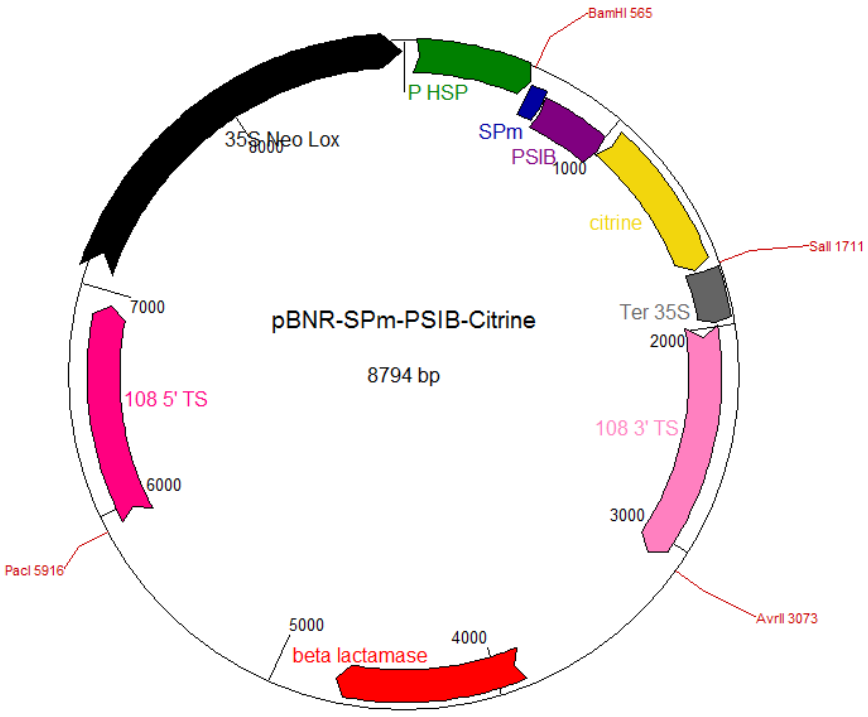
BamHI 565
P HSP
SPm
PSIB
1000
citrine
SalI 1711
Ter 35S
2000
108 3' TS
3000
AvrII 3073
5000
beta lactamase
4000
PacI 5916
6000
108 5' TS
7000
35S Neo Lox
8000
pBNR-SPm-PSIB-Citrine
8794 bp

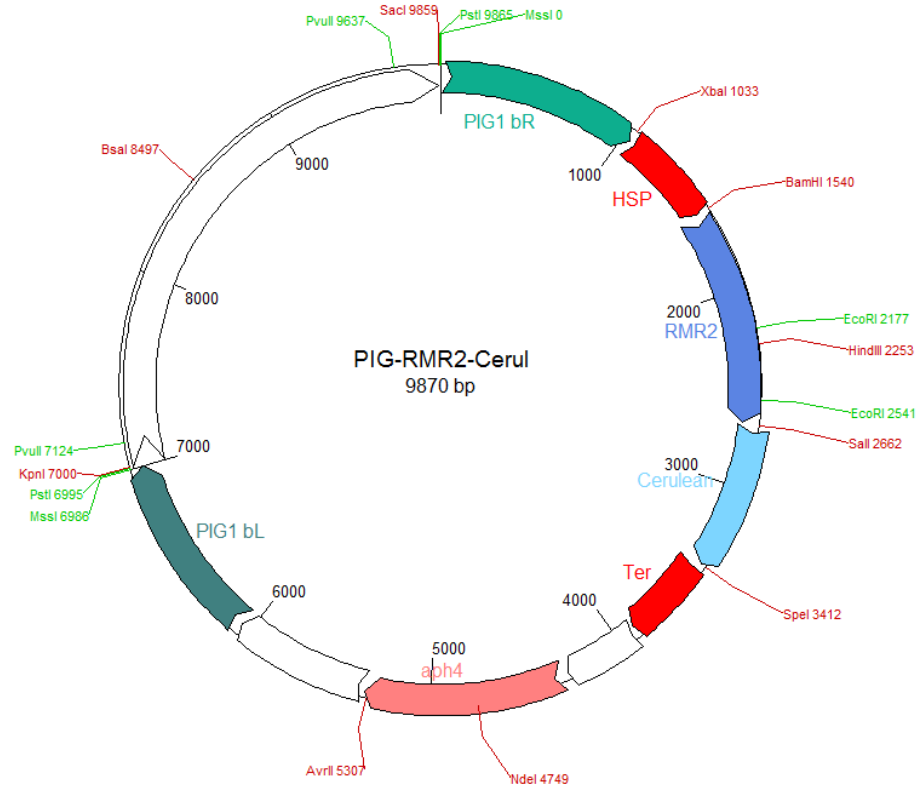
PIG-RMR2-CeruI
9870 bp
PIG1 bR
HSP
RMR2
Cerulean
Ter
aph4
PIG1 bL
SacI 9859
PstI 9865
MssI 0
XbaI 1033
BamHI 1540
EcoRI 2177
HindIII 2253
EcoRI 2541
SalI 2662
SpeI 3412
NdeI 4749
AvrII 5307
PvuII 7124
KpnI 7000
PstI 6995
MssI 6986
BsaI 8497
PvuII 9637
1000
2000
3000
4000
5000
6000
7000
8000
9000

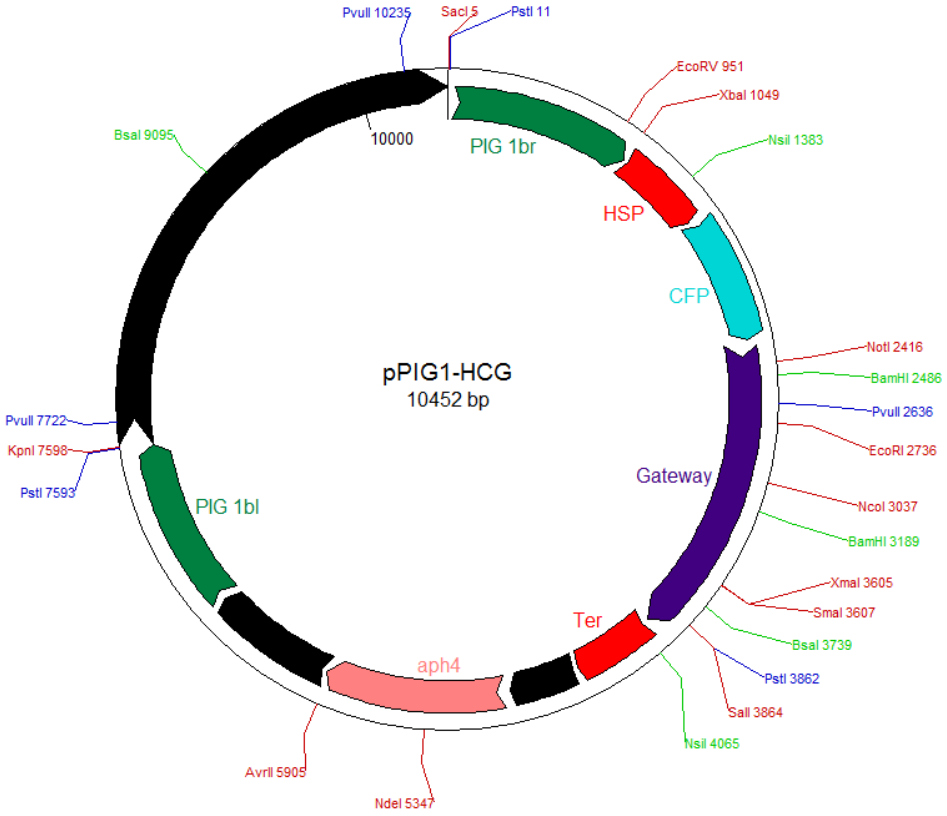
pPIG1-HCG
10452 bp
PIG 1br
HSP
CFP
Gateway
Ter
aph4
PIG 1bl
PvuII 10235
SacI 5
PstI 11
EcoRV 951
XbaI 1049
NsiI 1383
NotI 2416
BamHI 2486
PvuII 2636
EcoRI 2736
NcoI 3037
BamHI 3189
XmaI 3605
SmaI 3607
BsaI 3739
PstI 3862
SalI 3864
NsiI 4065
NdeI 5347
AvrII 5905
PvuII 7722
KpnI 7598
PstI 7593
BsaI 9095
10000

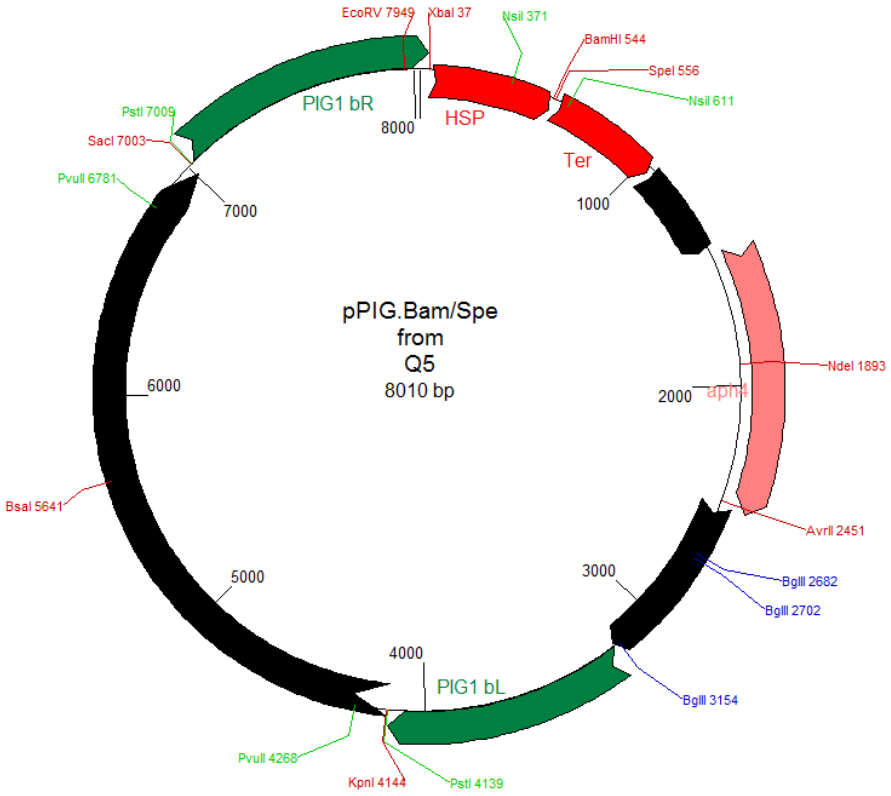
EcoRV 7949
XbaI 37
NsiI 371
BamHI 544
SpeI 556
NsiI 611
PIG1 bR
HSP
Ter
8000
1000
PstI 7009
SacI 7003
PvuII 6781
7000
pPIG.Bam/Spe
from
Q5
8010 bp
NdeI 1893
2000
aphA
6000
BsaI 5641
AvrII 2451
5000
3000
BglII 2682
BglII 2702
4000
PIG1 bL
BglII 3154
PvuII 4268
KpnI 4144
PstI 4139

References

Agrawal G.K., Jwa N-S., Lebrun M-H., Job D. and Rakwal R. (2010) Plant secretome: unlocking secrets of the secreted proteins. Proteomics 10: 799-827

Allan B.B. and Balch W.E. (1999) Protein sorting by directed maturation of Golgi compartments. Science 285: 63-66

Alexandersson E., Ali A., Resjö S. and Andreasson E. (2013) Plant secretome proteomics. Frontiers in Plant Science 4: 1-6

Alberts B., Johnson A., Lewis J., Raff M., Roberts K. and Walter P. (2008) Molecular Biology of the Cell. Fifth Edition. Garland Science, 1268p

Auclair S.M., Bhanu M.K. and Kendall D.A. (2011) Signal peptidase I: Cleaving the way to mature proteins. Protein Science 21: 13-25

Ayachi S. (2012) Study of moss vacuoles and functional characterization of the putative vacuolar receptors, the RMR proteins, PhD Thesis pp170

Barlowe C.K. and Miller E.A. (2013) Secretory Protein Biogenesis and Traffic in the Early Secretory Pathway. Genetics 193: 383–410

Barlowe C., Orci L., Yeung T., Hosobuchi M., Hamamoto S., Salama N., Rexach M.F., Ravazzola M., Amherdt M. and Schekman R. (1994) COPII: a membrane coat formed by Sec proteins that drive vesicle budding from the endoplasmic reticulum. Cell 77: 895-907

Beck R., Ravet M., Wieland F.T. and Cassel D. (2009) The COPI system: Molecular mechanisms and function. FEBS Letters 583: 2701–2709

Bednarek S.Y. and Raikhel N.V. (1991) The Barley Lectin Carboxyl-Terminal Propeptide is a Vacuolar Protein Sorting Determinant in Plants. The Plant Cell 3: 1195-1206

Bednarek S.Y., Wilkins T.A., Dombrowski J.E. and Raikhel N.V. (1990) A Carboxyl-Terminal Propeptide is Necessary for Proper Sorting of Barley Lectin to Vacuoles of Tobacco.
The Plant Cell 2: 1145-1 155

Bernassola F., Karin M., Ciechanover A. and Melino G. (2008) The HECT Family of E3 Ubiquitin Ligases: Multiple Players in Cancer Development. Cancer Cell 14

Bezanilla M., Pan A. and Quatrano R.S. (2003) RNA Interference in the Moss *Physcomitrella patens*. Plant Physiol. 133: 470-474

Bocock J.P., Carmicle S., Chhotani S., Ruffolo M.R., Chu H. and Erickson A.H. (2009) The PA-TM-RING protein RING finger protein 13 is an endosomal integral membrane E3 ubiquitin ligase whose RING finger domain is released to the cytoplasm by proteolysis. FEBS Journal 276: 1860–1877

Boevink P., Oparka K., Santa Cruz S., Martin B., Betteridge A., and Hawes H. (1998) Stacks on tracks: the plant Golgi apparatus traffics on an actin/ER network. The Plant Journal 15 (3): 441–447

Bolte S., Talbot C., Boutte Y., Catrice O., Read N.D. and Satiat-Jeunemaitre B. (2004) FM-dyes as experimental probes for dissecting vesicle trafficking in living plant cells. Journal of Microscopy 214 (2): 159–173

Bonifacino J.S. and Glick B.S. (2004) The mechanisms of vesicle budding and fusion. Cell 116: 153-166

Borden K.L.B. (2000) RING domains: Master builders of molecular scaffolds? J. Mol. Biol. 295: 1103-112

Borden K.L.B. and Freemont P.S. (1996) The RING finger domain: a recent example of a sequence-structure family. Current Opinion in Structural Biology 6: 395-401

Borchers A.G., Hufton A.L., Eldridge A.G., Jackson P.K., Harland R.M. and Baker J.C. (2002) The E3 ubiquitin ligase GREUL1 anteriorizes ectoderm during *Xenopus* development. Developmental biology 251: 395-408

Bouchard M.L. and Cote S. (1993) The *Drosophila melanogaster* developmental gene g1 encodes a variant zinc-finger-motif protein. Gene 125: 205-209

Brandizzi F., Hanton S., Pinto DaSilva L.L., Boevink P., Evans D., Oparka K., Denecke J. and Hawes C. (2003) ER quality control can lead to retrograde transport from the ER lumen to the cytosol and the nucleoplasm in plants. The Plant Journal 34: 269–281

Brandizzi F., Snapp E.L., Alison G., Roberts A.G., Jennifer Lippincott-Schwartz J. and Hawes C. (2002) Membrane Protein Transport between the Endoplasmic Reticulum and the Golgi in Tobacco Leaves Is Energy Dependent but Cytoskeleton Independent: Evidence from Selective Photobleaching. The Plant Cell 14: 1293–1309

Bryksa B.C., Bhaumik P., Magracheva E., De Moura D.C., Kurylowicz M., Zdanov A., Dutcher J.R., Wlodawer A. and Yada R.Y. (2011) Structure and Mechanism of the Saposin-like Domain of a Plant Aspartic Protease. The journal of biological chemistry 286 (32): 28265–28275

Brodsky J.L. and McCracken A. (1999) ER protein quality control and proteasome-mediated protein degradation. Cell & Developmental Biology 10: 507-513

Budnik A. and Stephens D.J. (2009) ER sites – localization and control of COPII vesicle formation. FEBS Letters 583: 3796-3803

Castelli S. and Vitale A. (2005) The phaseolin vacuolar sorting signal promotes transient, strong membrane association and aggregation of the bean storage protein in transgenic tobacco. J Exp Bot. 56 (415): 1379-87

Cao X., Rogers S.W., Butler J., Beevers L. and Rogers J.C. (2000) Structural requirements for ligand binding by a probable plant vacuolar sorting receptor. The Plant Cell 12: 493-506

Cedzich A., Huttenlocher F, Kuhn B.M., Pfannstiel J., Gabler L, Stintzi A. and Schaller A. (2009) The Protease-associated Domain and C-terminal Extension Are Required for Zymogen Processing, Sorting within the Secretory Pathway, and Activity of Tomato Subtilase 3 (SlSBT3). The journal of biological chemistry 284 (21): 1468-1478

Chen X., Irani N.G. and Friml J. (2011) Clathrin-mediated endocytosis: the gateway into plant cells. Current Opinion in Plant Biology 14: 674–682

Chung K.P., Yonglun Zeng Y. and Liwen Jiang L. (2016) COPII Paralogs in Plants: Functional Redundancy or Diversity? Trends in Plant Science 21 (9): 758-769

Contento A.L. and Bassham D.C. (2012) Structure and function of endosomes in plant cells. Journal of Cell Science 125: 3511–3518

Cove D.J., Knight C.D. and Lamparter T. (1997) Mosses as model systems. Trends in Plant Science 2: 99-105

DaSilva L.L.P., Snapp E.L., Denecke J., Lippincott-Schwartz J., Hawes C. and Brandizzi F. (2004) Endoplasmic reticulum export sites and Golgi bodies behave as single mobile secretory units in plant cells. The Plant Cell 16: 1753-1771

DaSilva L.L.P., Foresti O. and Denecke J. (2006) Targeting of the plant vacuolar sorting receptor BP80 is depedent on multiple sorting signals in the cytosolic tail. The Plant Cell 18: 1477-1497

De Azevedo Moreira R., Lima Ainouz I., Tadeu Abreu De Oliveira J. and Sousa Cavada B. (1991) Plant lectins, chemical and biological aspects. Mem. Inst. Oswaldo Cruz, Rio de Janeiro, 86(II): 221-218

Denecke J., De Rycke R. and Johan Botterman J. (1992) Plant and mammalian sorting signals for protein retention in the endoplasmic reticulum contain a conserved epitope. The EMBO Journal 11 (6): 2345-2355

Denecke J., Botterman J. and Deblaere R. (1990) Protein Secretion in Plant Cells Can Occur via a Default Pathway. The Plant Cell 2: 51-59

Deshaies R.J. and Joazeiro C.A.P. (2009) RING domain E3 ubiquitin ligases. Annual Review of Biochemistry 78: 399-434

Ding Y., Wang J., Wang Ju., Stierhof Y-D., Robinson D.G. and Jiang L. (2012) Unconventional protein secretion. Trends in Plant Science 17(10): 606-615

Di Sansebastiano G.P., Paris N., Marc-Martin S. and Neuhaus J.M. (1998) Specific accumulation of GFP in a non-acidic vacuolar compartment via a C-terminal propeptide-mediated sorting pathway. Plant J. 15: 571-582

Di Sansebastiano G.P., Paris N., Marc-Martin S. and Neuhaus J.M. (2001) Regeneration of a Lytic Central Vacuole and of Neutral Peripheral Vacuoles Can Be Visualized by Green Fluorescent Proteins Targeted to Either Type of Vacuoles. Plant Physiology 126: 78-86

Driouich A., Faye L. and Staehelin A. (1993) The plant Golgi apparatus: a factory for complex polysaccharides and glycoproteins. Trends in biochemical sciences 18: 210-214

Drakakaki G. and Dandekar A. (2013) Protein secretion: how many secertory routes does a plant cell have? Plant Science 203: 74-78

Duarte P., Pissara J. and Moore I. (2008) Processing and trafficking of a single isoform of the aspartic proteinase cardosin A on the vacuolar pathway. Planta 227: 1255-1268

Dubrovsky J.G., Guttenberger M., Saralegui A., Napsucialy-Mendivil S., Voigt B., Ek Balus F. and Menzel D. (2006) Neutral Red as a Probe for Confocal Laser Scanning Microscopy Studies of Plant Roots. Annals of Botany 97: 1127–1138

Duden R. (2003) ER-to-Golgi transport: COP I and COP II function. Molecular Membrane Biology 20: 197-207

Dupree P. and Sherrier D.J. (1998) The plant Golgi apparatus. Biochimica et Biophysica Acta 1404: 259-270

Egas C., Lavoura N., Resende R., Brito R.M.M., Pires E., Pedroso de Lima M.C. and Faro C. (2000) The saposin-like domain of the plant aspartic proteinase precursor is a potent inducer of vesicle leakage. The Journal of Biological Chemistry 275 (49): 38190-38196

Ellgaard L. and Helenius A. (2003) Quality control in the endoplasmic reticulum. Nature review molecular biology 4: 181-191

Epimashko S., Meckel T., Fischer-Schliebs E., Lüttge U. and Thiel G. (2004) Two functionally different vacuoles for static and dynamic purposes in one plant mesophyll leaf cell. The Plant Journal 37: 294-300

Erickson A.H. (2011) PA-TM-RING proteins: a new family of endosomal membrane proteins. FEBS Journal 278

Fan L., Li R., Pan J., Ding Z., and Lin J. (2015) Endocytosis and its regulation in plants. Trends in Plant Science 20 (6): 388-396

Fanata W.I.D., Lee S.Y. and Lee K.O. (2013) The unfolded protein response in plants: A fundamental adaptive cellular response to internal and external stresses. Journal of proteomics 93: 356-368

Figueiredo R., Duarte P., Pereira S. and Pissara J. (2006) The embryo sac of *Cynara cardunculus*: ultrastructure of the development and localization of the aspartic proteinase cardosin B. Sex Plant Reprod 19: 93-101

Flückiger R., De Caroli M., Piro G., Dalessandro G., Neuhaus J.M. and Di Sansebastiano G.P. (2003) Vacuolar system distribution in Arabidopsis tissues, visualized using GFP fusion proteins. J Exp Bot 54 (387): 1577-1584

Frigerio L., Foresti O., Hernandez Felipe D., Neuhaus J.M. and Vitale A. (2001) The C-terminal tetrapeptide of phaseolin is sufficient to target green fluorescent protein to the vacuole. J. Plant Physiol. 158: 499-503

Frigerio L., de Virgilio M., Prada A,. Faoro M. and Vitale A. (1998) Sorting of phaseolin to the vacuole is saturable and requires a short C-terminal peptide. The Plant Cell 10: 1031–1042

Frigerio L., Jolliffe N.A., Di Cola A., Hernández Felipe D., Paris N., Neuhaus J.M., Lord J.M., Ceriotti A. and Roberts L.M. (2001) The Internal Propeptide of the Ricin Precursor Carries a Sequence-Specific Determinant for Vacuolar Sorting. Plant Physiology 126: 167-175

Foissner I., Sommer A., Hoeftberger M., Hoepflingerand M.C. and Absolonova M. (2016) Is Wortmannin-Induced Reorganization of the trans-Golgi Network the Key to Explain Charasome Formation? Frontiers in Plant Science 7 (756)

Foresti O. and Denecke J. (2008) Intermediate organelles of the plant secretory pathway: identity and function. Traffic 9: 1599-1612

Frank W., Ratnadewi D. and Reski (2004*) Physcomitrella patens* is highly tolerant against drought, salt and osmotic stress. Planta 220: 384–394

Furt F., Lemoi K., Tüzel and Vidali L. (2012) Quantitative analysis of organelle distribution and dynamics in *Physcomitrella patens* protonemal cells. BMC Plant Biology 12 (70): 1471-2229

Gabriely G., Kama R. and Gerst J.E. (2007) Involvement of specific COPI subunits in protein sorting from the late endosome to the vacuole in yeast. Mol Cell Biol. 27(2): 526-40

Gattolin S., Sorieul M. and Frigerio L. (2010) Tonoplast intrinsic proteins and vacuolar identity. Biochemical Society Transactions 38: 769-773

Geldner N. (2004) The plant endosomal system – its structure and role in signal transduction and plant development. Planta 219: 547-560

Geldner N., Anders N., Wolters H., Keicher J., Kornberger W., Muller P., Delbarre A., Ueda T., Nakano A. and Jürgens G. (2003). The Arabidopsis GNOM ARF-GEF mediates endosomal recycling, auxin transport, and auxin-dependent plant growth. Cell 24; 112(2): 219-30

Gendre D., Jonsson K., Boutté Y. and Bhalerao R.P. (2015) Journey to the cell surface—the central role of the trans-Golgi network in plants. Protoplasma 252: 385–398

Glick B.S., Elston T. and Oster G. (1997) A cisternal maturation mechanism can explain the asymmetry of the Golgi stack. FEBS Letters 141: 177-181

Gomez L. and Chrispeels M.J. (1993) Tonoplast and soluble vacuolar proteins are targeted by different mechanisms. Plant Cell 5: 1113-1125

Grover A. (2012) Plant chitinases: genetic diversity and physiological roles. Critical Reviews in Plant Sciences 31: 57-73

Guais A., Siegrist S., Solhonne B., Jouault H., Guellaën G. and Bulle F. (2006) h-Goliath, paralog of GRAIL, is a new E3 ligase protein, expressed in human leukocytes. Gene 7: 112-120

Hamid R., Khan M. A., Ahmad M., Ahmad M.M., Abdin M.Z., Musarrat J. and Javed S. (2013). Chitinases: An update. Journal of Pharmacy & Bioallied Sciences 5(1): 21–29

Hamman B.D., Hendershot L.M. and Johnson A.E. (1998) BiP maintains the permeability barrier of the ER membrane by sealing the lumenal end of the translocon pore before and early in translocation. Cell 92: 747–758

Hammond C. and Helenius A. (1995) Quality control in the secretory pathway. Curr. Opin. Cell Biol. 7: 523–529

Hanton S.L., Matheson L.A., Chatre L. and Brandizzi F. (2009) Dynamic organization of COPII coat proteins at endoplasmic reticulum export sites in plant cells. The Plant Journal 57: 963-974

Hanton S.L., Bortolotti L.E., Renna L., Stefano G. and Brandizzi F. (2005) Crossing the divide – Transport between the endoplasmic reticulum and Golgi apparatus in plants. Traffic 6: 267-277

Hara-Nishimura I., Shimada T., Hatano K., Takeuchi Y. and Nishimura M. (1998) Transport of storage proteins to protein storage vacuoles is mediated by large precursor-accumulating vesicles. The Plant Cell 10: 825-836

Harper S. and Speicher D.W. (2011) Purification of proteins fused to glutathione S-transferase. Methods Mol Biol. 681: 259–280

Hatakeyama S., Yada M., Matsumoto M., Ishida N. and Nakayama K-I. (2001) U Box Proteins as a New Family of Ubiquitin-Protein Ligases. The Journal of Biological Biochemistry 276 (35): 33111–33120

Hawes C. and Satiat-Jeunemaitre B. (2005) The plant Golgi apparatus – going with the flow. Biochemica et Biophysica Acta 1744: 93-107

Heard W., Sklenář J., Tomé D.F., Robatzek S. and Jones A.M.(2015) Identification of Regulatory and Cargo Proteins of Endosomal and Secretory Pathways in *Arabidopsis thaliana* by Proteomic Dissection. Mol Cell Proteomics 14(7): 1796-813.

Hershko A., Ubiquitin-mediated Protein Degradation (1998) The Journal of Biological Chemistry 263: 15237-15240

Hershko A. and Ciechanover A, (1988) The ubiquitin system. Annu. Rev. biochem. 67: 425-479

Hofmann K. (2009) Ubiquitin-binding domains and their role in the DNA damage response. DNA Repair 8:544-556

Hohe A., Egener T., Lucht J.M., Holtorf H., Reinhard C., Schween G. and Reski R. (2003). An improved and highly standardised transformation procedure allows efficient production of single and multiple targeted gene-knockouts in a moss, Physcomitrella patens. Curr Genet 44: 339–347

Holstein S.E.H. (2002) Clathrin and Plant Endocytosis. Traffic 3: 614–620

Holwerda B.C. and Rogers J.C. (1993) Structure, functional properties and vascular targeting of the barley thiol protease, Aleurain. Journal of Experimental Botany 44: 321-329

Holwerda B.C., Padgett H.S. and Rogers J.C. (1992) Proaleurain vacuolar targeting is mediated by short contiguous peptide interactions. The Plant Cell 4: 307-318

Holwerda B., Galvin N.J., Baranski T.J. and Rogers J.C. (1990) In Vitro Processing of Aleurain, a Barley Vacuolar Thiol Protease. The Plant Cell 2: 1091-1106

Hughes H. and Stephens D.J. (2008) Assembly, organization, and function of the COPII coat. Histochem Cell Biol 129: 129–151

Hughson F.M. (2010) Copy coats: COPI mimics Clathrin and COPII. Cell 142(9): 19-21

Huotari J. and Helenius A. (2011) Endosome maturation. EMBO J. 30(17): 3481–3500

Hutagalung A.H. and Novick P.J. (2011) Role of Rab GTPases in membrane traffic and cell physiology. Physiol Rev. 91(1): 119-149

Hunter P.R., Craddock C.P., Di Benedetto S., Lynne M. Roberts L.M. and Frigerio L. (2007) Fluorescent Reporter Proteins for the Tonoplast and the Vacuolar Lumen Identify a Single Vacuolar Compartment in Arabidopsis Cells. Plant Physiology 145: 1371-1382

Hwang I. and Robinson D.G. (2009) Transport vesicle formation in plant cells. Current Opinion in Plant Biology 12: 660-669

Jauh G-Y., Fischer A.M., Grimes H.D. and Ryan C.A.Jr. (1998) δ-Tonoplast intrinsic protein defines unique plant vacuole functions. Proc. Natl. Acad. Sci. USA 95: 12995-12999

Jauh G.Y., Phillips T.E. and Rogers J.C. (1999) Tonoplast intrinsic protein isoforms as markers for vacuolar functions. Plant Cell 11: 1867-1882

Jiang L. and Rogers J.C. (1998) Integral Membrane Protein Sorting to Vacuoles in Plant Cells: Evidence for Two Pathways. The Journal of Cell Biology 143: 1183–1199

Jiang L., Phillips T.E., Rogers S.W. and Rogers J.C. (2000) Biogenesis of the protein storage vacuole crystalloid. The journal of Cell Biology 150: 755-76

Jin X., Cheng H., Chen J. and Zhu D. (2011) RNF13: an emerging RING finger ubiquitin ligase important in cell proliferation. FEBS J. 278:78-84

Jürgens G. (2004) Membrane trafficking in plants. Annu. Rev. Cell Dev. Biol. 20: 481-504

Kamisugi Y., Schlink K., Rensing S.A., Schween G., von Stackelberg M., Cuming A.C., Reski R. and Cove D.J. (2006) The mechanism of gene targeting in Physcomitrella patens: homologous recombination, concatenation and multiple integration. Nucleic Acids Res. 34: 6205–6214

Kang B-H., Nielsen E., Preuss M.L., Mastronarde D. and Staehelin L.A. (2011) Electron tomography of RabA4b- and PI-4Kβ1-labeled Trans Golgi Network compartments in *Arabidopsis*. Traffic 12:313-329

Katzmann D.J., Odorizzi G. and Emr S.D., (2002) Receptor downregulation and Multivesicular-Body sorting. Nat. Rev. Mol. Cell Biol. 3: 893-905

Kervinen J., Tobin G.J., Costa J., Waugh D.S., Wlodawer A. and Zdanov A. (1999) Crystal structure of plant aspartic proteinase prophytepsin: inactivation and vacuolar targeting. EMBO J. 23: 3497-3955

Kirsch T., Paris N., Butler J.M., Beevers L. and Rogers J.C. (1994) Purification and initial characterization of a potential plant vacuolar targeting receptor. Proceedings of the National Academy of Sciences 91: 3403–3407

Kirchhausen T. (2000) Three ways to make a vesicle. Nature Reviews Molecular Cell Biology 1: 187-198

Kisselev A.F. and Goldberg A.L. (2001) Proteasome inhibitors: from research tools to drug candidates. Chemistry & Biology 8: 739-758

Koide Y., Hirano H., Matsuoka K and Nakamura K. (1997) The N-terminal propeptide of the precursor to sporamin acts as a vacuole-targeting signal even at the C-terminus of the mature part in tobacco cells. Plant Physiol. 114: 863-870

Kölling R. and Hollenberg C.P. (1994) The ABC-transporter Ste6 accumulates in the plasma membrane in an ubiquitinated form in endocytosis mutants. The EMBO Journal 13: 3261 -3271

Kosarev P., Mayer K.F.X. and Hardtke C. (2002) Evaluation and classification of RING-finger domains encoded by the Arabidopsis genome. Genome Biology 3: 4

Krause C., Richter S., Knöll C. and Jürgens G. (2013) Plant secretome – from cellular to biological activity. Biochemica et Biophysica Acta 1934: 2429-2441

Lam S.K., Lung Siu C.H., Hillmer S., Jang S., An G., Robinson D.G. and Jiang L. (2007) Rice SCAMP1 Defines Clathrin-Coated, trans-Golgi–Located Tubular-Vesicular Structures as an Early Endosome in Tobacco BY-2 Cells. The Plant Cell 19: 296–319

Lauwers E., Erpapazoglou Z., Haguenauer-Tsapis R. and André B. (2010) The ubiquitin code of yeast permease trafficking. Trends Cell. Biol. 20: 196-204

Lee J.H and Kim W.T (2011) Regulation of Abiotic Stress Signal Transduction by E3 Ubiquitin Ligases in Arabidopsis. Mol. Cells 31: 201-208

Lee D.H. and Goldberg A.L. (1998) Proteasome inhibitors: valuable new tools for cell biologists. Trends in Cell Biology 8: 379-403

Lerner D.R. and Raikhel N.V. (1989) Cloning and Characterization of Root-Specific Barley Lectin. Plant Physiol. 91: 124–129

Lehtonen M.T., Takikawa Y., Rönnholm G., Akita M., Kalkkinen N., Ahola-Iivarinen E., Somervuo P., Varjosalo M. and Valkonen J.P.T. (2014) Protein secretome of moss plants (Physcomitrella patens) with emphasis on changes induced by a fungal elicitor. *J. Proteome Res.* 13: 447-459

Li R., Liu P., Wan Y., Chen T., Wang Q., Mettbach U., Baluška F., Samaj J., Fang X., Lucas W.J. and Lin J. (2012) A Membrane Microdomain-Associated Protein, Arabidopsis Flot1, Is Involved in a Clathrin-Independent Endocytic Pathway and Is Required for Seedling Development. The Plant Cell 24: 2105–2122

Ligrone R., Duckett J.G. and Renzaglia K.S. (2012) Major transitions in the evolution of early land plants: a bryological perspective. Annals of Botany 109: 851–871

Linares L., Hengstermann A., Ciechanover A., Müller S. and Scheffner M. (2003) HdmX stimulates Hdm2-mediated ubiquitination and degradation of p53. PNAS 100 (21): 12009–12014

Liu L., Cui F., Li Q., Yin B., Zhang H., Lin B., Wu Y., Xia R., Tang S. and Xie Q. (2011) The endoplasmic reticulum-associated degradation is necessary for plant salt tolerance. Cell Research 21: 957-969

Liu Y. and Li J. (2014) Endoplasmic reticulum-mediated protein quality control in *Arabidopsis*. Frontiers in Plant Science 5 (162)

Liu J.X. and Howell S.H. (2010) Endoplasmic reticulum protein quality control and its relationship to environmental stress responses in plants. The Plant Cell 22:2930-2942

Liu C.Y. and Kaufman R.J. (2003) The unfolded protein response. Cell Science at a Glance. Journal of Cell Science 116: 1861-1862

Lyzenga W.J. and Stone S.L. (2011) Abiotic stress tolerance mediated by protein ubiquitination. Journal of Experimental Botany 63(2): 599-616

Lodish H., Berk A., Kaiser C.A., Krieger M., Scott M.P., Bretscher A. and Ploegh H. (2008) Molecular biology. Sixth edition. W.H. Freeman and Company. 1150p

Luo X. and Hofmann K. (2001) The protease-associated domain: a homology domain associated with multiple classes of proteases. Trends in Biochemical Sciences 26: 147-148

Luo F., Fong Y.H., Zeng Y., Shen J., Jiang L., and Wong K.-B. (2014) How Vacuolar Sorting Receptor Proteins Interact with Their Cargo Proteins: Crystal Structures of Apo and Cargo-Bound Forms of the Protease Associated Domain from an Arabidopsis Vacuolar Sorting Receptor. The Plant Cell 26: 3693–3708

Lütcke H. (1995) Signal recognition particle (SRP), a ubiquitous initiator of protein translocation. Eur. J. Biochem. 228: 531 -550

Machuka J., Bashiardes S., Ruben E., Spooner K., Cuming A., Knight C. and Cove C. (1999) Sequence analysis of Expressed Sequence Tags from an ABA-Treated cDNA Library Identifies Stress Response Genes in the Moss Physcomitrella patens. Plant Cell Physiol 40: 378-387

Mahon P. and Bateman A. (2000) The PA domain: a protease-associated domain. Protein Science 9: 1930-1934

Marty F. (1999) Plant vacuoles. The Plant Cell 11: 587-599

McMahon H.T. and Boucrot E. (2011) Molecular mechanism and physiological functions of clathrin mediated endocytosis. Nature Reviews Molecular Cell Biology 12: 517-533

Matsuoka K. and Nakamura K. (1991) Propeptide of a precursor to a plant vacuolar protein required for vacuolar targeting. Proc Natl Acad Sci USA 88: 834-838

Matsuoka K. and Nakamura K. (1999) Large alkyl side-chain of isoleucine and leucine in the NPIRL region constitute the core of the vacuolar sorting determinant of sporamin precursor. Plant Mol. Biol. 41: 825-835

Matsuoka K., Bassham D.C., Raikhel N.V. and Nakamura K. (1995) Different sensitivity to Wortmannin of two vacuolar sorting signal indicates the presence of distinct sorting machineries in tobacco cells. The Journal Cell of Biology 130 (6): 1307-1318

Mauch F. and Staehelin L.A. (1989) Functional lmplications of the Subcellular Localization of Ethylene-lnduced Chitinase and & 1,3-Glucanase in Bean Leaves. Plant Cell 1: 447-457

Maurel C., Santoni V., Luu D.T., Wudick M.M., and Verdoucq L. (2009) The cellular dynamics of plant aquaporin expression and functions. Current Opinion in Plant Biology 12: 690–698

McMahon H.T. and Mills I.G. (2004) COP and clathrin-coated vesicle budding: different pathways, common approaches. Current Opinion in Cell Biology 16: 379-391

Menand B., Calder G. and Dolan L. (2007) Both chloronemal and caulonemal cells expand by tip growth in the moss *Physcomitrella patens*. Journal of Experimental Botany 58 (7): 1843–1849

Metzger M.B., Hristova V.A. and Weissman A.M. (2012) HECT and RING finger families of E3 ubiquitin ligases at a glance. Journal of Cell Science 125 (3): 531–537

Miao Y., Yan P.K., Kim H., Hwang I. and Jiang L. (2006) Localization of Green Fluorescent Protein Fusions with the Seven Arabidopsis Vacuolar Sorting Receptors to Prevacuolar Compartments in Tobacco BY-2 Cells. Plant Physiology 142: 945–962

Michaeli S., Avin-Wittenberg T. and Galili G. (2014) Ivolvement of autophagy in the direct ER to vacuole protein trafficking route in plants. Frontiers in Plant Science 5 (134)

Müller J., Pifanelli P., Devoto A., Miklis M., Eliott C., Ortmann B., Schulze-Lefert P. and Panstruga R. (2005) Conserved ERAD-like quality control of a plant polytopic membrane protein. The Plant Cell 17: 149-163

Murphy K.A., Kuhle R.A., Fischer A.M., Anterola A.M., Grimes A.D. (2005) The functional status of paraveinal mesophyll vacuoles changes in response to altered metabolic conditions in soybean leaves. Functionnal plant biology 22: 335-344

Mutlu A. and Gal S. (1999) Plant aspartic proteinases: enzymes on the way to a function. Physiologia Plantarum 105: 569-576

Nagy A. (2000) Cre Recombinase: the universal reagent for genome tailoring. Wiley-Liss, Inc. genesis 26: 99-109

Nakamura N. (2011) The Role of the Transmembrane RING Finger Proteins in Cellular and Organelle Function. Membranes 1: 354-393

Nebenführ A. (2002) Vesicle traffic in the endomembrane system: a tale of COPs, Rabs and SNAREs. Current Opinion in Plant Biology 5: 507-512

Nebenfür A., Ritzenthaler C. and Robinson D.G. (2002) Brefeldin A: deciphering an enigmatic inhibitor of secretion. Plant Physiol. 130(3): 1102-1108

Neuhaus J.M., Sticher L., Meins F. Jr, Boller T. (1991) A short C-terminal sequence is necessary and sufficient for the targeting of chitinases to the plant vacuole. Proc Natl Acad Sci 88: 362-366

Neuhaus J.M. and Roger JC. (1998) Sorting of proteins to vacuoles in plant cells. Plant Molecular Biology 38: 127-144

Neuhaus J.M. (1999) Plant chitinases (PR-3, PR-4, PR-8, PR-11). Pathogenesis-related proteins in plants CRC Press p77-105

Neuhaus J.M., Pietrzak M. and Boiler T. (1994) Mutation analysis of the C-terminal vacuolar targeting peptide of tobacco chitinase: low specificity of the sorting system, and gradual transition between intracellular retention and secretion into the extracellular space. The Plant Journal 5(1): 45-54

Nielsen H., Engelbrecht J., Brunak S. and von Heijne G. (1997) Identification of prokaryotic and eukaryotic signal peptides and prediction of their cleavage sites. Protein Engineering 10 (1): 1–6

Nishiyama T., Fujita T., Shin T., Seki M., Nishide H., Uchiyama I., Kamiya A., Carninci P., Hayashizaki Y., Shinozaki K., Kohara Y., and Hasebe M. (2003) Comparative genomics of *Physcomitrella patens*

gametophytic transcriptome and *Arabidopsis thaliana*: Implication for land plant evolution. PNAS 100 (13): 8007-8012

Occhialini A., Gouzerh G., Di Sansebastiano G.P., Neuhaus J.M. (2016) Dimerization of the Vacuolar Receptors AtRMR1 and -2 from Arabidopsis thaliana Contributes to Their Localization in the trans-Golgi Int J Mol Sci. 17(10)

Occhialini A. (2011) Localization and possible interaction between RMR receptors in plant cells. PhD thesis pp243

Oda Y., Hirata A., Sano T., Fujita T., Hiwatashi Y., Sato Y., Kadota A., Hasebe M. and Hazeawa S. (2009) Microtubules regulate dynamic organization of vacuoles in *Physcomitrella patens*. Plant Cell Physiol. 50 (4): 855-868

Orci L., Stamnes M., Ravazzola M., Amherdt M., Perrelet A., Söllner T.H. and Rothman J.E. (1997) Bidirectional transport by distinct populations of COPI-coated vesicles. Cell 90: 335-349

Orci L., Perrelet A. and Rothman J.E. (1998) Vesicles on strings: morphological evidence for processive transport within the Golgi stack. Proc. *Natl. Acad. Sci. USA* 95: 2279-2283

Oparka K.J. (1991) Uptake and Compartmentation of Fluorescent Probes by Plant Cells. Journal of Experimental Botany 42 (238): 565-579

Otegui M. and Spitzer C. (2008) Endosomal function in plants. Traffic 9: 1589-1598

Otegui M.S. and Reyes F.C. (2010) Endosomes in plants. Nature Education 3(9): 23

Pagny S., Lerouge P., Faye L. and Gomord V. (1999) Signals and mechanisms for protein retention in the endoplasmic reticulum. Journal of Experimental Botany 50 (331): 157–164

Paris N. and Neuhaus J.M. (2002) BP-80 as a vacuolar sorting receptor. Plant Molecular Biology 50: 903–914

Paris N., Rogers S.W., Jiang L., Kirsch T., Beevers L., Phillips T.E. and Rogers J.C. (1997) Molecular Cloning and Further Characterization of a Probable Plant Vacuolar Sorting Receptor. Plant Physiology 115: 29-39

Paris N., Stanley C.M., Jones R.L., Rogers J.C. (1996) Plant cells contains two functionally distinct vacuolar compartments. Cell 85: 563-572

Park M., Lee D. Lee G-L. and Hwang I. (2005) AtRMR1 functions as a cargo receptor for protein trafficking to the protein storage vacuole. The Journal of Cell Biology 170(5): 757-767

Pereira C., Pereira S. and Pissarra J. (2014) Delivering of proteins to the plant vacuole – an update. Int. J. Mol. Sci. 15: 7611-7623

Pereira C., Pereira S., Satiat-Jeunemaitre B. and Pissarra J. (2013) Cardosin A contains two vacuolar sorting signals using different vacuolar routes in tobacco epidermal cells. The Plant Journal 73: 87-100

Pereira C.S. (2012) Cardosin A molecular determinants and biosynthetic pathways, PhD Thesis 212p

Peremyslov V.V., Pan Y.W, and Dolja V.V. (2004) Movement Protein of a Closterovirus Is a Type III Integral Transmembrane Protein Localized to the Endoplasmic Reticulum. Journal of virology 78 (7): 3704–3709

Peumans W.J. and Van Damme E.J.M. (1998) Plant lectins: versatile proteins with important perspectives in biotechnology. Biotechnology and Genetic Engineering Reviews 15: 199-228

Pickart C.M. (2001) Mechanisms underlaying ubiquitination. Annu. Rev. Biochem. 70: 503–33

Pimpl P., Movafeghi A., Coughlan S., Denecke J., Hillmer S. and Robinson D.G. (2000) In situ localization and in vitro induction of plants COPI-coated vesicles. The Plant Cell 12: 2219-2235

Piper R.C. and Lehner P.J. (2011) Endosomal transport via ubiquitination. Trends Cell Biol 11: 647-655

Pissara J., Pereira C., Soares da Costa D., Figueiredo R., Durate P., Teixeira J. and Pereira S. (2007) From flower to seed germination in *Cynara cardunculus* : a role for aspartic proteinases. International Journal of Plant Developmental Biology (2): 274-281

Punja Z.K. and Zhang Y.Y. (1993) Plant chitinases and their roles in resistance to fungal diseases. Journal of Nematology 25(4): 526-540

Puri C., Tosoni D., Comai R., Rabellino A., Segat D., Caneva F., Luzzi P., Di Fiore PP. and Tacchetti C. (2004) Relationships between EGFR Signaling–competent and Endocytosis-competent Membrane Microdomains. Molecular Biology of the Cell 16: 2704–2718

Quatrano R.S., McDaniel S. F., Khandelwal A., Perroud P.-F. and Cove D.J. (2007) *Physcomitrella patens*: mosses enter the genomic age. Current Opinion in Plant Biology 10: 182–189

Ramalho-Santos M., Pissarra J., Verissimo P., Pereira S., Salema R., Pires E. and Faro C.J. (1997) Cardosin A, an abundant aspartic proteinase, accumulates in protein storage vacuoles in the stigmatic papillae of *Cynara cardunculus* L. Planta 203: 204-212

Rensing *et* al. (2008) The *Physcomitrella* Genome Reveals Evolutionary Insights into the Conquest of Land by Plants. Science 319: 64-69

Reyes F.C., Buomo R. and Otegui M.S. (2011) Plant endosomal trafficking pathways. Current Opinion in Plant Biology 14: 666-673

Ritzenthaler C., Nebenführ A., Movafeghi A., Stussi-Garaud C., Behnia L., Pimpl P., Staehelin A. and Robinson D.G (2002) Reevaluation of the effects of Brefeldin A on plant cells using tobacco Bright Yellow 2 cells expressing Golgi-targeted green fluorescent protein and COPI antisera. The Plant Cell 14: 237-261

Roberts A.W., Roberts E.M. and Haigler C.H. (2012) Moss cell walls: structure and biosynthesis. Front. Plant Sci.

Robinson D.G. and Neuhaus J.M (2016) Receptor-mediated sorting of soluble vacuolar proteins: myths, facts, and a new model. Journal of Experimental Botany 67 (15): 4435-4449

Robinson D.G., Herranz M-C., Bubeck S., Pepperkok R. and Ritzenthaler C. (2007) Membrane dynamics in the early secretory pathway. Critical review in Plant Sciences 26: 199-225

Rogers J.C., Dean D., Heck G.R. (1985) Aleurain: a barley thiol protease closely related to mammalian cathepsin H. Proc Natl Acad Sci U S A. 82(19): 6512–6516.

Ruggiano A., Foresti O. and Carvalho P. (2014) ER-associated degradation: Protein quality control and beyond. J. Cell Biol. Vol. 204 (6) 869–879

Ruibal C., Castro A., Carballo V., Szabados L. and Vidal S. (2013) Recovery from heat, salt and osmotic stress in *Physcomitrella patens* require a functional small heat shock protein PpHsp16.4. BMC Plant Biology 13: 174

Runeberg-Roos P.,Törmäkangas K. and Östman A. (1991) Primary structure of a barley-grain aspartic proteinase, a plant aspartic proteinase resembling mammalian cathepsin D. European Journal of Biochemistry 202 (3): 1021–1027

Saint-Jore-Dupas C., Gomord V.and Paris N. (2004) Protein localization in the plant Golgi apparatus and the *trans*-Golgi network. CMLS, Cell. Mol. Life Sci. 61: 159–171

Salmia M.A. (1981) Proteinase activities in resting and germinating seeds of Scots pine, *Pinus sylvestris*. Physiologia Plantarum 53(1): 39 – 47

Samaj J., Read N.D., Volkmann D., Menzel D. and Baluska F. (2005) The endocytic network in plants. TRENDS in Cell Biology 15(8): 425-433

Sanderfoot A.A. and Raikhel N. (1999) The specificity of vesicle trafficking: coat proteins and SNAREs. The Plant Cell 11: 629-641

Scabone C.M., Frigerio L. and Petruccelli S. (2011) A fluorescent reporter protein containing AtRMR1 domains is targeted to the storage and central vacuoles in *Arabidopsis thaliana* and tobacco leaf cells. Plant Cell Rep 30: 1823-1833

Seaman M. N. J. (2012) The retromer complex – endosomal protein recycling and beyond. Journal of Cell Science, 125(20), 4693–4702

Seroogy C.M., Soares L., Ranheim E.A., Su L., Holness C., Bloom D. and Fathman C.G. (2004) The Gene Related to Anergy in Lymphocytes, an E3 Ubiquitin Ligase, is Necessary for Anergy Induction in CD4 T Cells. The Journal of Immunology 173: 79-85

Schaaf A., Reski R. and Decker E.L., (2004) A novel aspartic proteinase is targeted to the secretory pathway and to the vacuole in the moss *Physcomitrella patens*. Eur J Cell Biol. 83: 145-152

Schaefer D.G. (2001) Gene targeting in *Physcomitrella patens*. Curr. Opin. Plant Biol. 4: 143–150

Schaefer D.G., Chakhparonian M. and Zrÿd J.P. (2001) *Physcomitrella patens*: un système expérimental modèle en génomique végétale. Ecole Thématique de Biologie Végétale

Schaefer D.G. and Zrÿd J.P. (1997) Efficient gene targeting in the moss Physcomitrella patens. Plant J. 11: 1195-1206

Schmid S.L. (1997) Clathrin-coated vesicle formation and protein sorting: an integrated process. *Annu. Rev. Biochem.* 66: 511-548

Seroogy C.M., Soares L., Ranheim E.A., SU L., Holness C., Bloom D. and Fathman C.G. (2004) The Gene Related to Anergy in Lymphocytes, an E3 Ubiquitin Ligase, is Necessary for Anergy Induction in CD4 T Cells. The Journal of Immunology 173: 79-85

Shen Y., Wang J., Ding Y., Gouzerh G., Neuhaus J-M. and Jiang L. (2011) The rice RMR1 associates with a distinct prevacuolar compartment for the protein storage vacuole pathway. Molecular Plant 4(5): 854-868

Simões I. and Faro C. (2004) Structure and function of plant aspartic proteinases. Eur. J. Biochem. 271: 2067-2075

Slightom J.L., Sun S.M. and Hall T.C. (1983) Complete nucleotide sequence of a French bean storage protein gene: Phaseolin. Proc. Natl. Acad. Sci. USA 80: 1897-1901

Sparkes I. A. (2013) Plant Endoplasmic Reticulum in: eLS. John Wiley & Sons, Ltd: Chichester

Sparkes I., Hawes C. and Frigerio L. (2011) FontiERs: movers and shapers of the higher plant cortical endoplasmic reticulum. Current Opinion in Plant Biology 14: 658-665

Sparkes I., Figerio L., Tolley N. and Hawes C. (2009) The plant endoplasmic reticulum: a wide web. Biochem. J. 423: 145-155

Staehelin L.A. and Moore I. (1995) The plant Golgi apparatus: structure, functional organization and trafficking mechanisms. Annu. Rev. Plant Physio. Plant Mol. Bio. 46: 261-288

Schween G., Gorr G., Hohe A. and Reski R. (2003) Unique tissue-specific cell cycle in *Physcomitrella*. Plant biol 5: 1-9

Stigliano E. (2011) The Role of Palmitoylation in the secretory pathway of plants. PhD thesis 181pp

Takáč T., Pechan T., Šamajová O., Ovečka M., Richter H., Eck C., Niehaus K. and Šamaj J. (2012) Wortmannin Treatment Induces Changes in Arabidopsis Root Proteome and Post-Golgi Compartments. J. Proteome Res. 11: 3127−3142

Tang B.L., Wang Y., Ong Y.S. and Hong W. (2005) COPII and exit from the endoplasmic reticulum. Biochemica et Biophysica Acta 1744: 293-303

Tian M., Lou L., Liu L., Yu F., Zhao Q., Zhang H., Wu Y., Tang S., Xia R., Zhu B., Serino G. and Xie Q. (2015) The RING finger E3 ligase STRF1 is involved in membrane trafficking and modulates salt-stress response in *Arabidopsis thaliana*. The Plant Journal 82: 81-92

Tian M. and Xie Q. (2013) Non-26S Proteasome Proteolytic Role of Ubiquitin in Plant Endocytosis and Endosomal Trafficking. Journal of Integrative Plant Biology 55 (1): 54–63

Tyers M. and Willems A.R. (1999) One ring to rule a superfamily of E3 ubiquitin ligases. Science 284: 603-604

Tjalsma H., Bolhuis A., Jongbloed J.D., Bron S. and van Dijl J.M. (2000) Signal peptide-dependent protein transport in *Bacillus subtilis*: a genome-based survey of the secretome. Microbiol. Mol. Biol. Rev. 64: 515-574

Törmäkangas K., Hadlington J.L., Pimpl P., Hillmer S., Brandizzi F., Teeri T.H. and Denecke J. (2001) A vacuolar sorting domain may also influence the way in which proteins leave the endoplasmic reticulum. Plant Cell 13: 2021-2032

Townsend D.M. and Tew K.D. (2003) The role of glutathione-S-transferase in anti-cancer drug resistance. Oncogene 22: 7369–7375

Toyooka K., Okamoto T. and Takao Minamikawa T. (2000) Mass Transport of Proform of a KDEL-tailed Cysteine Proteinase (SH-EP) to Protein Storage Vacuoles by Endoplasmic Reticulum–derived Vesicle Is Involved in Protein Mobilization in Germinating Seeds. The Journal of Cell Biology, 148 (3): 453–463

Tranque P., Crossin K.L., Cirelli C., Edelman G.M. and Mauro V.P. (1996) Identification and characterization of a RING zinc finger gene (C-RZF) expressed in chicken embryo cells. Proc Natl Acad Sci 93 (7): 3105-3109

Tse Y.C., Sheung Kwan Lam S.K. and Jiang L. (2007) Enigmatic Brefeldin A. Plant Signaling & Behavior 2(3): 199-202

Tyers M and Willems AR, One ring to rule a superfamily of E3 ubiquitin ligases. Science 284: 603-604

Uemura T. and Ueda T. (2014) Plant vacuolar trafficking driven by RAB and SNARE proteins. Current Opinion in Plant Biology 22:116–121

Uemura T. and Nakano A. (2013) Plants TGNs: dynamics and physiological functions. Histochem Cell Biol 140: 341-345

Uemura T., Ueda T., Ohniwa R.L., Nakano A., Takeyasu K. and Sato M.H. (2004) Systematic Analysis of SNARE Molecules in *Arabidopsis*: Dissection of the post-Golgi Network in Plant Cells. Cell Structure and Function 29: 49–65

Ui M., Okada T., Hazeki K. and Haseki O. (1995) Wortmannin as a unique probe for an intracellular signaling protein, phosphoinositide 3-kinase.Elsevier Science Ltd, TIBS 20: 302-307

Umezawa H., Aoyagi T., Morishima H., Matsuzaki M. and Hamada M (1970) Pepstatin a new pepsin inhibitor produced by Actinomycetes. The Journal of Antibiotics 23(5):259-262

Vashist S. and Ng D.T.W. (2004) Misfolded proteins are sorted by a sequential checkpoint mechanism of ER quality control. The Journal of Cell Biology 165 (1): 41-25

Varshavsky A. (1997) The ubiquitin system. Trend in Biochemical Sciences 22: 383-387

Vieira M., Pissara J., Verissimo P., Castanheira P., Costa Y., Pires E. and Faro C. (2001) Molecular cloning and characterization of cDNA encoding cardosin B, an aspartic proteinase accumulating extracellularly in the transmitting tissue of *Cynara cardunculus* L.. Plant Molecular Biology 45: 529-539

Vierstra R.D. (2012) The Expanding Universe of Ubiquitin and Ubiquitin-Like Modifiers. Plant Physiology 160: 2-14

Vierstra R.D. (2003) The ubiquitin/26S proteasome pathway, the complex last chapter in the life of many plant proteins. TRENDS in Plant Science 8: 135-142

Viotti C. (2014) ER and vacuoles: never been closer. Frontiers in Plant Science 5: 1-7

Viotti C., Krüger F., Krebs M., Neubert C., Fink F., Lupanga U. Scheuring D., Boutté Y., Frescatada-Rosa M., Wolfenstetter S., Sauer N., Hillmer S., Grebe M., Schumacher K. (2013) The endoplasmic reticulum is the main membrane source for biogenesis of the lytic vacuole in Arabidopsis. Plant Cell 25 (9): 3434-3449

Viotti C., Bubeck J., Stierhof Y.-D., Krebs M., Langhans M., van den Berg W., van Dongen W., Richter S., Geldner N., Takano J., Jürgens G., de Vries S., G. Robinson D.G. and Schumacher K. (2010) Endocytic and Secretory Traffic in Arabidopsis Merge in the Trans-Golgi Network/Early Endosome, an Independent and Highly Dynamic Organelle. The Plant Cell 22: 1344–1357

Vitale A. and Hinz G. (2005) Sorting of proteins to storage vacuoles: how many mechanisms? Trends in Plant Science 10: 316-323

Vitale A. and Galili G. (2001) The endomembrane system and the problem of protein sorting. Plant Physiol. 125(1): 115-8

Vitale A. and Denecke J. (1999) The Endoplasmic Reticulum-Gateway of the Secretory Pathway. The Plant Cell 11: 615-628

Vitale A. and Raikhel N. (1999) What do proteins need to reach different vacuoles? Trend in Plant Science 4 (4): 149-155

Von Heijne G. (1990) The signal peptide. J. Membrane Biol. 115: 195-201

Wang J., Cai Y., Miao Y., Kwan Lam S. and Jiang L. (2009) Wortmannin induces homotypic fusion of plant prevacuolar compartments. Journal of Experimental Botany 60(11): 3075-3083

Wang H., Rogers J.C. and Jiang L. (2010) Plant RMR proteins: unique vacuolar sorting receptors that couple ligand sorting with membrane. The FEBS journal 278: 59-68

Wink M. (1993) The plant vacuole: a multifunctional compartment. J Exp Bot 44: 231-246

Whiting C.C., Su L.L., Lin J.T. and Fathman C.G. (2011) GRAIL: a unique mediator of CD4 T-lymphocyte unresponsiveness. FEBS Journal 278: 47–58

Yamazaki Y., Christina Schönherr C., Varshney G.K., Dogru M., Hallberg B. and Palmer R.H. (2013) Goliath family E3 ligases regulate the recycling endosome pathway via VAMP3 ubiquitylation. The EMBO Journal 32: 524–537

Yang Y.D., Elamawi R., Bubeck J., Pepperkok R., Ritzenthaler C. and David G. Robinson D.G. (2005) Dynamics of COPII Vesicles and the Golgi Apparatus in Cultured Nicotiana tabacum BY-2 Cells Provides Evidence for Transient Association of Golgi Stacks with Endoplasmic Reticulum Exit Sites. The Plant Cell 17: 1513–1531

Ye Y. and Rape M. (2009) Building ubiquitin chains: E2 enzymes at work. Nature Reviews Molecular Cell Biology 10: 755-764

Yorimitsu T., Sato K. and Takeuchi M. (2014) Molecular mechanisms of Sar/Arf GTPases in vesicular trafficking in yeast and plants. Frontiers in Plant Science 5 (411)

Zouhar J., Muñoz A. and Rojo E. (2010) Functional specialization within the vacuolar sorting receptor family: VSR1, VSR3 and VSR4 sort vacuolar storage cargo in seeds and vegetative tissues. Plant J. 64: 577-588

Zouhar J. and Rojo E. (2009) Plant vacuoles: where did they come from and where are they heading? Curr Opin Plant Biol. 12(6): 677-84